Technische Universität München

Towards untangling Tau: Insights into Alzheimer's Disease Pathology and Novel Identification of Therapeutic Targets

Dissertation

Marie Neu

aus Ehringshausen

2025

Technische Universität München

TUM School of Medicine and Health

Towards untangling Tau: Insights into Alzheimer's Disease Pathology and Novel Identification of Therapeutic Targets

Marie Neu

Vollständiger Abdruck der von der TUM School of Medicine and Health der Technischen Universität München zur Erlangung einer

Doktorin der Naturwissenschaften (Dr. rer. nat.)

genehmigten Dissertation.

Vorsitz: Prof. Dr. Thomas Korn

Prüfende der Dissertation:

1. Prof. Dr. Stefan Lichtenthaler

2. Prof. Dr. Mikael Simons

Die Dissertation wurde am 22.05.2025 bei der Technischen Universität München eingereicht und durch die TUM School of Medicine and Health am 06.08.2025 angenommen.

I. List of figures

II. List of tables

III. List of contents

IV. Summary

Alzheimer's Disease (AD) is a progressive neurodegenerative disease, characterized by memory loss and cognitive decline. Hallmarks of the disease are, first, the formation of senile plaques, consisting of extracellular amyloid-ß peptide fibrils and, second, intracellular neurofibrillary tangles (NFT), consisting predominantly of aggregated and hyperphosphorylated Tau. Both factors result in the loss of neurons and synapses. NFT formation and in this regard the pathological Tau protein strongly correlates with cognitive decline and neuronal loss. The mechanisms of Tau aggregation, as well as the Tau-induced neurodegeneration, are not completely understood. Tau can propagate from cell to cell regardless of its isoform or possible mutations, however, the mechanism of intercellular transmission of Tau remains not fully understood. In disease states, it was shown that also pathological Tau, in forms of misfolded and aggregated Tau, can propagate from cell to cell. In AD, these prion-like particles are thought to be Tau seeds, containing aggregated Tau. The seeds are released into the extracellular space and can enter connected, naive cells, where a seeded templated aggregation of endogenous Tau occurs.

The first project objective aimed to identify proteins that differentially interact with physiological and pathological Tau in control or AD brain samples. In control brain tissue, Tau interactors were significantly enriched for ion transport proteins. Phospho-Tau antibodies preferentially co-precipitated proteins associated with RNA processing and splicing from both AD and control brains, suggesting that these interactions are preserved in the disease state, while ion transport functions are lost. Tau-seed induced aggregation can be modeled *in vitro* using iPS-derived neurons. A secondary interactome analysis was conducted that compares the interacting partners of Tau in seeded versus non-seeded induced pluripotent stem cell (iPS)-derived neurons and then examining the overlap of these findings with the human Tau interactome. This comparison revealed the robust interaction of Tau with RNA-processing/splicing and microtubule-associated proteins both *in vitro* and in postmortem brains.

The second project objective investigated proteomic and phosphoproteomic changes resulting from the seed-induced aggregation of endogenous Tau in human neurons derived from iPS cells. Results indicated only non-significant proteomic changes after seeding, while significant phospho-proteomic changes were observed after seed-induced Tau aggregation. Previously undescribed phosphorylation sites on the selective autophagy receptor NBR1 were discovered, which were significantly altered by Tau aggregation in vitro. Furthermore, it was shown that NBR1 directly interacts with phosphorylated Tau and Tau aggregates in various cell models. This interaction is associated with autophagic Tau degradation in HEK cells, and siRNA-mediated knockdown of NBR1 significantly increased Tau aggregate levels in iPS-derived neurons. Additionally, NBR1 specifically interacted with phospho-Tau in human AD brain, underscoring the relevance of our findings to the human disease. These insights provide a deeper understanding of the molecular interactions between autophagy receptors and Tau pathology in AD and reveal a role for NBR1 as an important receptor for pathological forms of Tau.

Overall, this PhD Thesis contributes to new mechanistic insights into AD pathology and may yield novel drug target candidates.

V. Zusammenfassung

Morbus Alzheimer ist eine fortschreitende neurodegenerative Erkrankung, die durch Gedächtnisverlust und kognitiven Abbau gekennzeichnet ist. Sie wird durch die Bildung von senilen Plaques aus Amyloid-ß-Peptidfibrillen und neurofibrillären „Bündeln“ (NFT), die vorwiegend aus aggregiertem und hyperphosphoryliertem Tau bestehen, charakterisiert. Diese führen zu einem Verlust von Neuronen und Synapsen. Die Bildung von NFTs und in diesem Zusammenhang die Präsenz des pathologischen Tau Proteins korreliert stark mit dem kognitiven Verfall und dem Verlust von Neuronen. Tau kann sich unabhängig von seiner Isoform oder möglichen Mutationen von Zelle zu Zelle ausbreiten, doch der Mechanismus der interzellulären Übertragung von Tau ist noch nicht vollständig geklärt. Bei der Alzheimer-Krankheit werden diese prionenähnlichen Partikel als Tau- Aggregationskeime angesehen, die aggregiertes Tau enthalten. Die Keime werden in den extrazellulären Raum freigesetzt und können in synaptisch verbundene, naive Zellen eindringen, wo es zu einer Aggregation von endogenem Tau kommt.

Das erste Projektziel bestand darin, Proteine zu identifizieren, die mit physiologischem und pathologischem Tau in Kontroll- und Alzheimer-Gehirnproben interagieren. Im Kontrollhirngewebe waren die mit Tau interagierenden Proteine signifikant mit Ionentransportproteinen angereichert. Phospho-Tau-Antikörper präzipitierten bevorzugt Proteine, die mit der RNA-Verarbeitung und dem Spleißen assoziiert sind, sowohl in AD- als auch in Kontrollgehirnen, was darauf hindeutet, dass diese Interaktionen im Krankheitszustand erhalten bleiben, während die Ionentransportfunktionen verloren gehen.

Die durch Tau induzierte Aggregation kann in vitro mit aus iPS-Zellen gewonnenen Neuronen modelliert werden. Um robuste Tau Interaktionen zu identifizieren und in vitro zu validieren, wurde eine weitere Studie durchgeführt, welche Tau-Interaktionspartner aus induzierbar pluripotenten Stammzellen (iPS) differenzierten Neuronen untersuchte. Dieser Vergleich zeigte die robuste Interaktion von Tau mit RNA-verarbeitenden/Splicing- und Mikrotubuli-assoziierten Proteinen sowohl in vitro als auch in postmortalen Gehirnen.

In einem zweiten Projektziel wurden die proteomischen und phosphoproteomischen Veränderungen untersucht, die sich aus der Tau-induzierten Aggregation in aus iPS-Zellen differenzierten Neuronen ergeben. Während keine signifikanten proteomischen Veränderungen identifiziert wurden, führte die Tau Aggregation zu einer signifikanten Veränderung auf phosphoproteomischer Ebene. Es wurden zudem bisher unbeschriebene Phosphorylierungsstellen des Autophagie Rezeptors NBR1 entdeckt, die durch die Tau-Aggregation signifikant verändert wurden. Die Ausschaltung von NBR1 führte zu einem Anstieg der Tau-Aggregate, was die Bedeutung von NBR1 im Tau-Abbau unterstreicht. Außerdem wurde gezeigt, dass NBR1 in verschiedenen Zellmodellen sowie im humanen Hirn direkt mit phosphoryliertem Tau und Tau-Aggregaten interagiert, was die Relevanz der Ergebnisse unterstreicht. Diese Erkenntnisse ermöglichen ein tieferes Verständnis der molekularen Wechselwirkungen zwischen Autophagie-Rezeptoren und der Tau-Pathologie bei Alzheimer und zeigen eine Rolle für NBR1 als wichtigen Rezeptor für pathologische Formen von Tau.

Insgesamt trägt diese Doktorarbeit zu neuen Erkenntnissen über die Mechanismen der Alzheimer-Pathologie bei und könnte neue Wirkstoffkandidaten hervorbringen.

1 Introduction

1.1 Neurodegenerative diseases

Neurodegenerative diseases encompass a range of incurable sporadic and familial disorders of the nervous system, characterized by progressive neuronal dysfunction and eventual neuronal loss. The most prevalent among these are Alzheimer's Disease (AD) and Parkinson's Disease (PD), with other notable examples including Amyotrophic Lateral Sclerosis (ALS), Frontotemporal Dementia (FTD), and Huntington's Disease (HD) (Rubinsztein, 2006). Age serves as the predominant risk factor for the onset of neurodegenerative diseases, which poses a significant concern in developed countries, where increased longevity and declining birthrates are contributing to a rapidly aging population (Heemels, 2016). Consequently, the prevalence of these age-dependent diseases is rising, and their impact is expected to impose a substantial financial burden on social and healthcare systems (Dorsey et al., 2013). Currently, available therapies for neurodegenerative disorders are primarily palliative, as they address symptoms but fail to halt disease progression or prevent onset. This highlights an urgent need for more effective treatments that target the underlying pathological mechanisms. A deeper understanding of these mechanisms will be crucial to developing novel therapeutics that can mitigate the impact of neurodegenerative diseases and improve outcomes for those affected by these debilitating conditions.

1.2 Alzheimer's Disease

AD is the leading cause of dementia, impacting over 35.6 million individuals globally. With the aging population, it is estimated that the number of people living with AD will double by 2030, reaching 65 million, and triple by 2050 to 115 million, assuming no significant advances in treatment (Wortmann, 2012; Yoshiyama et al., 2013). The disease affects more than 10% of those over the age of 65, resulting in substantial economic and societal costs (Aranda et al., 2021; Wimo et al., 2013). Although current treatments can temporarily alleviate symptoms or delay cognitive decline, they do not stop disease progression. Recently, Lecanemab, an FDA-approved monoclonal antibody that targets amyloid-β in early AD, represented a modest step forward in clinical care (Dyck et al., 2022), but it remains unclear whether antibody-based therapies will be capable of halting the disease process.

1.2.1 Hallmarks of AD

AD is a neurodegenerative condition marked by a gradual decline in memory and cognitive functions (Jahn, 2013; Morris et al., 2001). Two defining features of the disease are the accumulation of amyloid-β (Aβ) plaques, which consist of extracellular fibrils, and the formation of neurofibrillary tangles (NFTs) inside neurons, composed of hyperphosphorylated and aggregated Tau protein (Kosik et al., 1986; Mattson, 2004; Selkoe, 2001). Both of these pathological processes contribute to neuronal and synaptic loss (Cummings et al., 2015; Selkoe, 2002). AD can be categorized into familial and sporadic forms. Familial cases are associated with mutations in genes such as amyloid precursor protein (APP) and presenilin (PS1 and PS2), while sporadic AD results from a combination of genetic susceptibility and environmental factors (Lahiri et al., 2007; Tanzi and Bertram, 2005). NFTs are not only hallmarks of AD, but are also characteristic for primary tauopathies, including frontotemporal lobar degeneration with Tau pathology (FTLD), progressive supranuclear palsy (PSP) and

corticobasal degeneration (CBD) (Götz et al., 2018; McKee et al., 2009; Mori et al., 1994; Morris et al., 2003).

The amyloid hypothesis, which suggests that the accumulation of Aβ in the brain is the primary cause of AD-related neurodegeneration (Hardy and Selkoe, 2002; Hardy and Higgins, 1992), has evolved over time. It is now believed that Aβ-derived small oligomers are also toxic to neurons (Ferreira and Klein, 2011). Aß peptides are produced through the proteolytic processing of the amyloid precursor protein (APP), a transmembrane protein expressed abundantly in neurons (Haass and Selkoe, 1993; Zheng and Koo, 2011). The initial phase of Aβ production involves the cleavage of APP by β-secretase (BACE1) at its extracellular domain (Vassar et al., 1999), while the remaining membrane bound fragment gets cleaved by ϒ-secretase, consisting of presenilin (PSEN) 1 and 2 (Iwatsubo, 2004). After additional trimming by different secretases (Morishima-Kawashima, 2014), short Aß peptides of different lengths, mainly Aß40 and Aß42, are released into extracellular space (Steiner et al., 2018). Although generated in minor amounts, Aß42 is more prone to aggregation and was predominantly found deposited in senile plaques (Iwatsubo et al., 1994). Familial cases of AD are linked to pathogenic mutations in eg. APP and PSEN, which modify secretase processing, resulting in an overall increase in Aβ production or altering the ratio of Aß42/Aß40 (Müller et al., 2017; Steiner et al., 2018; Tanzi, 2012). Aß production is prevented in case of the alternative cleavage of APP by α-secretases, specifically by members of the a disintegrin and metalloprotease (ADAM) family (Lichtenthaler, 2010).

Interestingly, the presence of Aβ plaques does not correlate with cognitive decline, but NFTs, formed by pathological Tau protein, show a stronger connection to memory loss and neuronal damage (Bejanin et al., 2017; Digma et al., 2019; Giannakopoulos et al., 2003). Research indicates that Tau plays a crucial role in Aβ-induced toxicity (Roberson et al., 2007). Certain cases of AD patients with familial AD mutations are resistant to autosomal dominant AD due to other gene variants, like APOE Christchurch and Reelin-COLBOS (Arboleda-Velasquez et al., 2019; Llibre-Guerra et al., 2025). Notably, a patient with the presenilin 2 (PSEN2) p.Asn141Ile mutation showed Tau pathology, but exhibited no progression throughout the brain or cognitive decline, even with a high Aβ plaque load (Llibre-Guerra et al., 2025). This further underscores the potential of targeting Tau pathology as a therapeutic strategy.

In addition to the well-known Aß plaques and pathological Tau, AD is characterized by other pathological features that contribute to the complexity of the disease. Another hallmark is synapse loss and synaptic dysfunction, which closely follows Tau pathology and is one of the strongest correlations of cognitive decline in AD patients (DeKosky and Scheff, 1990). Furthermore, neuroinflammation plays a significant role in the progression of AD (Heneka et al., 2015). This inflammatory response is primarily mediated by microglia and astrocytes, which are brain immune cells (Kettenmann et al., 2011; Sofroniew and Vinters, 2010). Genome wide association studies revealed that especially microglia-related genes such as ApoE and TREM2 are high risk factors to develop familiar cases of AD (Bellenguez et al., 2022; Efthymiou and Goate, 2017). Besides the genetic evidence of microglia involvement in AD, there is evidence that Aß plaques are heavily surrounded by activated microglia (Stalder et al., 1999), which have the ability to reduce Aβ abundance likely through TREM2-mediated detection and phagocytosis of Aß aggregates (Lewcock et al., 2020; Lichtenthaler et al., 2022). Activated microglia can thus contribute to the pathology by releasing pro-inflammatory cytokines and reactive oxygen species, which may exacerbate neuronal injury and promote the aggregation of pathological proteins like Aβ and Tau (Heneka et al., 2015, 2014; Patel et al., 2005). Chronic

inflammation is therefore not merely a side effect of AD but an active participant in the disease's pathogenesis, potentially accelerating the cycles of neurodegenerative processes.

The progression of major AD pathophysiological events develops over time in accordance with the clinical course (Long and Holtzman, 2019): the disease initiates with a lengthy preclinical phase characterized by the early onset of amyloid deposition. Concurrently, early neuroinflammatory changes, such as microglial activation, take place. As the disease advances, Tau pathology extends throughout different brain regions. This spreading of Tau aggregates leads to synaptic dysfunction, synapse loss, and increased neurodegeneration. Cognitive impairment onset and its progression are associated with Tau accumulation and loss of hippocampal volume, rather than with amyloid deposition.

1.3 Tau

1.3.1 Physiological role of Tau

Tau is a microtubule-associated protein predominantly found in neurons (Binder et al., 1985), which is intrinsically disordered (Schweers et al., 1994). In healthy neurons, Tau is mainly located in axons, where it plays a critical role in stabilizing microtubules and facilitating their assembly (Weingarten et al., 1975). Its regulatory function extends to the dynamic instability of microtubules, allowing the cytoskeleton to adapt to cellular stress response (Feinstein and Wilson, 2005). Additionally, Tau interacts with motor proteins such as dynein and kinesin to regulate axonal transport (Stamer et al., 2002). Through competitive binding to microtubules, Tau modulates the velocity and efficiency of both anterograde and retrograde transport (Dixit et al., 2008; Hirokawa et al., 1988). Tau may also play a role in the formation of neurites, contributing to neuronal growth and maturation (Caceres and Kosik, 1990), as well as in synaptic plasticity and learning and memory related processes (Biundo et al., 2018).

In dendritic spines, Tau appears to influence synaptic plasticity, essential for learning and memory. The presence of Tau influences the function an structure of synapses, which might impact the neuronal network connectivity (Frandemiche et al., 2014; Ittner and Götz, 2011). Synaptic proteins were identified as interacting partners of Tau (Tracy et al., 2022), supporting the physiological role of Tau in synapses. Tau may also have a role in maintaining DNA integrity and regulating RNA levels within neurons (Sultan et al., 2011). There is evidence of Tau localizing and translocating into the nucleus (Candia et al., 2022; Portillo et al., 2021), where it might be involved in “nuclear maintenance” (Bravo et al., 2024b). Evidence of Tau potentially regulating RNA metabolism is supported by multiple studies consistently identifying RNA binding proteins as Tau interacting partners (Kavanagh et al., 2022). Furthermore, Tau impacts processes such as neuronal activity regulation, neurogenesis, and long-term depression, particularly in the hippocampus (DeVos et al., 2013; Hong et al., 2010; Kimura et al., 2014; Lei et al., 2012).

1.3.2 Gene structure and alternative splicing of Tau

The human Tau protein is encoded by the microtubule-associated protein Tau (MAPT) gene, which is located on chromosome 17q21 and comprises 16 exons (Andreadis et al., 1995; Neve et al., 1986).

In the human brain, six distinct isoforms of Tau are produced through alternative splicing of exons 2, 3, and 10 (Andreadis et al., 1995; Goedert et al., 1989a) (figure 1). Splicing in general is facilitated by the spliceosome, a complex made up of small nuclear RNA (snRNA) molecules

(U1-U6) and numerous proteins, which combine to small nuclear ribonucleoprotein particles (snRNP) (Love et al., 2015; Will and Lührmann, 2011). These snRNPs interact with pre-messenger RNA (mRNA) to excise introns and subsequently join the surrounding exons. Alternative splicing enables the generation of different mRNA variants from a single pre-mRNA. The inclusion or exclusion of the second repeat domain of Tau, determined by the alternative splicing of exon 10, results in either 3-repeat (3R) or 4-repeat (4R) Tau (Andreadis, 2005; Andreadis et al., 1992; Goedert et al., 1989b). This alternative splicing process is regulated by cis-acting elements, including both intronic and exonic splicing enhancer (ISE and ESE) and silencers (ISS and ESS), which can influence spliceosome assembly by either enhancing or inhibiting the binding of regulatory proteins (Ghigna et al., 2008). Additionally, trans-acting splicing factors modulate alternative splicing. These factors include heterogeneous nuclear ribonucleoproteins (hnRNPs) and serine/arginine (SR)-rich proteins (Dreyfuss et al., 2002; GRAVELEY, 2000). SR proteins can bind to various enhancer regions within the Tau gene, where they interact with and recruit components of the spliceosome. This assembly process determines whether exons are included or excluded (Kondo et al., 2004; Yu et al., 2004). Several SR family members have been shown to influence the alternative splicing of exon 10 (Qian and Liu, 2014). For instance, SRSF1 and SRSF2 promote the inclusion of exon 10, which increases the 4R Tau isoform (D'Souza and Schellenberg, 2005; Kondo et al., 2004), whereas SRSF7 modulates exon 10 exclusion, enhancing 3R Tau expression (Gao et al., 2007). SRSF11 was also identified as a regulator for exon 10 splicing (Wu et al., 2006).

The Tau isoforms are differentiated by the presence of zero, one, or two amino acid inserts of 29 or 58 residues (0N, 1N, 2N, respectively) at the N-terminal region, encoded by exons 2 and 3. Although the precise function of the N-terminal domain remains unclear, they may contribute to the attachment and spacing of Tau to microtubules and other cellular compartments (Chen et al., 1992). Additionally, this region could play a role in determining the cellular localization of Tau isoforms (Liu and Götz, 2013).

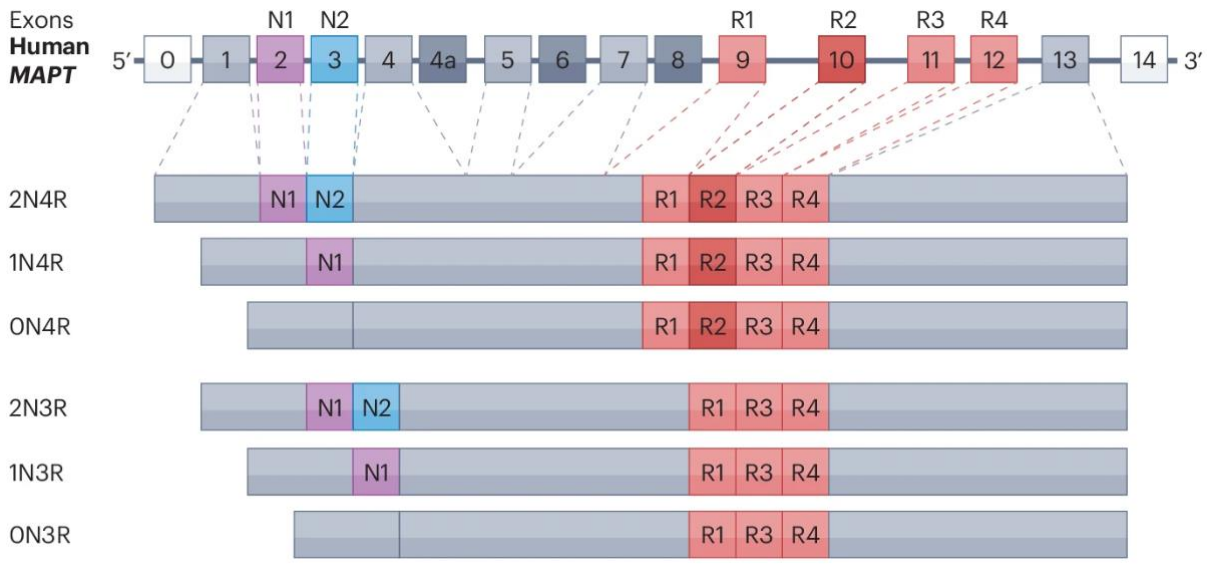

Figure 1: Gene structure and isoforms of Tau

The MAPT gene consists of 16 exons, which can be transcribed and translated into six distinct isoforms of the human Tau protein due to alternative splicing of exons 2, 3, and 10. These six isoforms differ in the presence or absence of one or two amino acid inserts in the N-terminus (0N, 1N, 2N, respectively), and by having either three or four carboxy-terminal repeat domains (3R or 4R) (adapted from (Bravo et al., 2024b)).

The expression of the different Tau isoforms correlates with the development of the human brain. In the fetal brain, only the 0N3R isoform is present, whereas the 4R isoform expression increases during the development. Both 3R and 4R isoforms are equally expressed in the adult brain (Andreadis, 2005; Spillantini and Goedert, 1998). The 0N, 1N and 2N isoform comprise ~54%, ~37% and ~9% of the total human Tau, respectively (Goedert and Jakes, 1990; Tanzi, 2012). Neurofibrillary tangles in AD contain both 3R and 4R Tau isoforms (Goedert, 2004; Sergeant et al., 1999). Aberrant splicing of exon 10 can result in an imbalance of the 3R:4R isoforms in the brain, leading to different tauopathies (Goedert et al., 1998). Isoforms are differentially expressed during development (Drubin et al., 1984), suggesting that they hold distinct physiological roles, such as contributing to unique aspects of neuronal growth, synapse formation, and cytoskeletal dynamics (Liu and Gong, 2008). Furthermore, the isoform expression and the splicing of the MAPT gene differs in subcellular location (Buchholz and Zempel, 2024) and each region of the human brain (Majounie et al., 2013). The MAPT mRNA expression as well as total Tau protein levels are higher in the neocortex (Trabzuni et al., 2012). This regional expression and protein level are compatible with the regional differences in the AD pathology and Tau pathology progression.

1.3.3 Pathological relevance of Tau splicing

Mutations in the MAPT gene can cause tauopathies such as Frontotemporal dementia (FTD) (Ghetti et al., 2015). Many of the mutations, such as the E10+14 and E10+16 mutations (figure 2) in intron 10, lead to an inclusion of exon 10, which results in an increased 4R-Tau isoform expression (Hutton et al., 1998). Mutations in exon 10, such as the N297K and P301L (figure 2), lead to an early onset and strong disease progression, and additionally to an increased level of 4R Tau (Delisle et al., 1999; Hutton et al., 1998). Tau binds to the microtubule through its repeat domain, hence 4R Tau binds microtubule more efficiently. An imbalanced 3R:4R ratio

can lead to a decreased Tau-microtubule interaction, thus impairing the axonal transport, which marks an early event in neurodegenerative disease (Stokin et al., 2005; Vos et al., 2008). It was shown that the imbalanced isoform ratio can lead to the impaired axonal transport of APP (Lacovich et al., 2017).

In AD and other tauopathies, missorting of Tau from axons into the somatodendritic compartment is an early pathological event, followed by synapse loss (Thies and Mandelkow, 2007). The retrograde and anterograde transport of Tau is regulated by an axon initial segment, which includes a Tau diffusion barrier. It was shown that the longest Tau isoforms (2N4R and 1N4R) are retained in the somatodendritic compartment, whereas shorter isoforms can overcome the barrier. Hence, missorting of Tau is likely isoform-specific and splicing-dependent (Zempel et al., 2017).

In summary, familial forms of tauopathy can occur due to mutations in the MAPT gene, which can cause Tau aggregation. Missense mutations are usually located near the microtubule binding domain (C-terminal), reducing the affinity of Tau binding and consequently leading to aggregation of Tau (Hong et al., 1998). Maintaining the equimolar ratio of 3R:4R Tau might be crucial to prevent Tau aggregation (Adams et al., 2010).

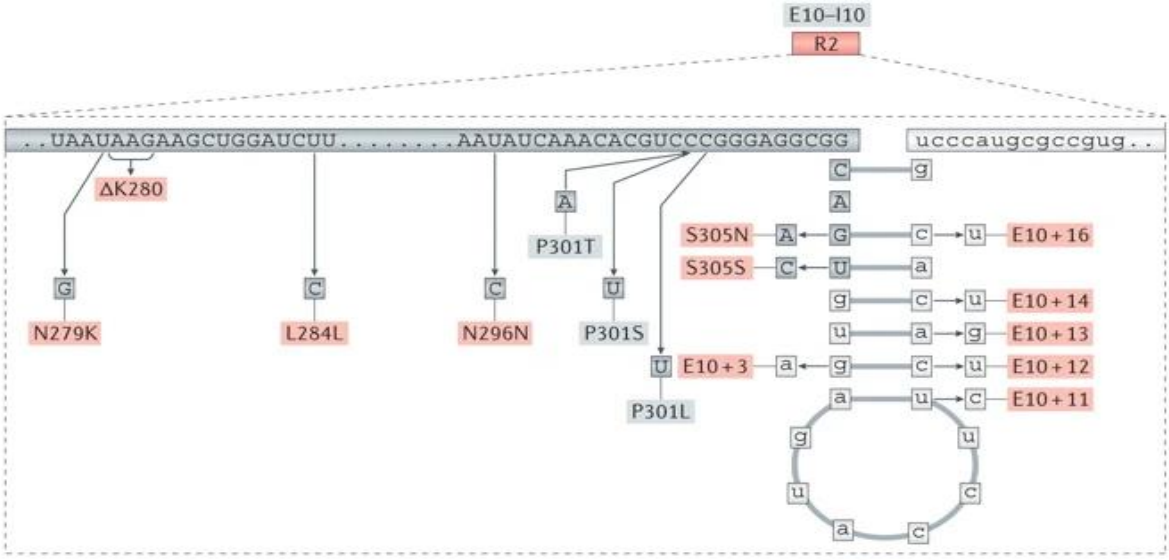

Figure 2: Mutations near Exon 10 and Intron 10 interface can influence splicing of the MAPT gene.
This figure illustrates disease-associated mutations near the exon 10 (E10)–intron 10 (I10) interface of the MAPT gene, which encodes the Tau protein. The sequence includes E10 (uppercase) and part of I10 (lowercase). Mutations affecting MAPT splicing, such as N279K, ΔK280, and various intronic mutations (E10+3 to E10+16), are highlighted in red boxes. These changes disrupt a stem-loop structure critical for regulating E10 inclusion, shifting the 3R/4R Tau isoform ratio. Missense mutations that alter Tau's amino acid sequence, such as P301S, are indicated with arrows. Such mutations are linked to tauopathies, including FTDP-17, by promoting pathological Tau isoform expression (Wang and Mandelkow, 2016).

1.4 Post-translational modifications of Tau and their pathological impact

Factors contributing to the Tau pathology, such as post-translational modifications (PTM), have been intensively studied. Endogenous Tau is natively unfolded (Mukrasch et al., 2009; Schweers et al., 1994) and shows little tendency for aggregation. However, the NFTs in AD mainly contain aggregated Tau that is hyperphosphorylated (Grundke-Iqbal et al., 1986; Köpke et al., 1993). Phosphorylation is the most investigated PTM of Tau due to its pathological impact.

Tau phosphorylation shows distinct temporal and spatial patterns critical for its physiological functions and its role in pathology. During development, Tau phosphorylation is naturally higher, with fetal Tau being more heavily phosphorylated compared to adult Tau, supporting neuronal growth and plasticity (Brion et al., 1994; Yu et al., 2009). Regionally, Tau phosphorylation varies across brain areas, with higher levels often observed in the hippocampus and neocortex, regions commonly affected in Alzheimer's disease (Muntané et al., 2008). Specific phosphorylation patterns also correlate with age, where diseased brains exhibit aberrant hyperphosphorylation in regions prone to neurodegeneration, such as the entorhinal cortex and hippocampus, which aligns with the early stages of tauopathy progression (Augustinack et al., 2002; Braak and Braak, 1991).

The phosphorylation at specific sites induces the pathologic effect of Tau, not only the phosphorylation as such (Morris et al., 2015; Wang and Mandelkow, 2016). A specific PTM signature for early disease-related alterations in AD was characterized. This pattern includes increased phosphorylation at sites pS198, pS199, and pS416, which correlate with soluble Tau multimerization (Ercan-Herbst et al., 2019). Tau phosphorylation at sites pS396/pS400/pT403 and pS404, located in the C-terminus of Tau, are highly abundant in AD patients, and are captured by the PHF1 antibody (Peter Davis) (Otvos et al., 1994; Wesseling et al., 2020). Tau pT212/pS214 epitopes are located in the proline-rich region of Tau and are in AD and are targeted by the AT100 antibody (Anderson et al., 2008; Wesseling et al., 2020) . In addition, Tau pS217 and pT181 are highly abundant Tau phospho-peptides, which currently serve as a cerebrospinal fluid biomarker for Tau pathology (Barthélemy et al., 2020; Janelidze et al., 2020). Recently, phospho-Tau pS262 and pS356 were identified as early indicators of Tau aggregation in AD, present at soluble Tau species, preceding NFT formation (Islam et al., 2025).

The phosphorylation state of Tau is a dynamic process influenced by a balance between kinase and phosphatase activities. The dephosphorylation of Tau is mediated by different protein phosphates (PP), of which PP2 is the most important one. PP2A is responsible for the majority of Tau dephosphorylation in the brain, ensuring proper microtubule binding and stability, which are essential for neuronal function (Liu et al., 2005). A reduction in PP2A activity has been linked to hyperphosphorylation of Tau, a hallmark observed in Alzheimer's disease, leading to its aggregation and neurofibrillary tangle formation (Gong et al., 2000). This pathological shift disrupts axonal transport and cellular communication, contributing to synaptic dysfunction and neurodegeneration (Goedert et al., 2006) . Tau can be phosphorylated by microtubule affinity-regulating kinases (MAPK), glycogen-synthase kinase 3 (GSK-3), cyclic AMP-dependent protein kinase (PKA) (Hanger et al., 2009) and others (www.tauptm.org). Hyperphosphorylation might reduce the affinity of Tau for binding to microtubules, either through affecting the binding domains (Morris et al., 2015) or by triggering conformational change of Tau (Lu et al., 1999). The phosphorylation might reduce the interaction with additional binding partners, which affects the axonal transport (Ittner et al., 2009). Hyperphosphorylation might also contribute to the AD pathology by inducing Tau missorting into dendritic spines, causing synaptic dysfunction (Hoover et al., 2010). Hyperphosphorylation at specific sites also inhibits ubiquitination, subsequently preventing proteosomal degradation of Tau (Dickey et al., 2007). Furthermore, hyperphosphorylation may inhibit the cleavage of Tau by caspases (Guillozet-Bongaarts et al., 2006).

1.5 Cell to Cell transmission

Tau can propagate from cell to cell regardless of its isoform or possible mutations and it seems that part of it is physiological (Dujardin et al., 2018). The mechanism of the cell to cell transmission of Tau in human brains remains not fully understood. Tau proteins disseminate between cells through secretion pathways. Initial evidence of intercellular transmission was found in transgenic mouse models, where Tau pathology spread along connected neuronal networks, mirroring human tauopathy (Clavaguera et al., 2009, 2013; Lasagna-Reeves et al., 2012).

Research conducted *in vivo* indicates that tau spreads among synaptically connected neurons, with oligomeric Tau deposits found at synaptic terminals in individuals with AD (Colom-Cadena et al., 2023; Liu et al., 2012). This transmission hypothesis is supported by Tau interacting with presynaptic vesicle proteins during activity-dependent secretion (Tracy et al., 2022). Calcium-dependent neuronal activity further promotes Tau release, possibly through synaptic transmission and exosomal pathways, exacerbating Tau pathology in recipient neurons (Pooler et al., 2013; Wang et al., 2017; Wu et al., 2016). In the extracellular release of Tau, various vesicles—including exosomes and ectosomes—are involved. Exosomes are small vesicles enclosed by a membrane that are released into the extracellular space when multivesicular bodies merge with the plasma membrane. Tau was found in exosomes derived from patients with tauopathies, as well as from experimental model systems (Ruan et al., 2020; Saman et al., 2012; Winston et al., 2019). Tau can also be released with ectosomes, larger vesicles shed directly from the plasma membrane upon neuronal stimulation (Dujardin et al., 2014). Additionally, Tau might spread via tunneling nanotubes, which are actin-based cellular protrusions that connect cells and may facilitate intercellular transfer (Rustom et al., 2004; Tardivel et al., 2016).

For internalization of Tau, neighboring neurons and glia use several pathways. Tau can bind to heparan sulfate proteoglycans (HSPGs) on cell surfaces, leading to aggregation (Goedert et al., 1996; Paudel and Li, 1999) and internalization (Holmes et al., 2013; Rauch et al., 2018). The lipoprotein receptor-related protein 1 (LPR1) was recently identified as a possible key regulator of Tau spread by controlling its endocytic uptake (Cooper et al., 2021; Rauch et al., 2020). Furthermore, muscarinic receptors (M1 and M3) might also facilitate Tau uptake *in vitro* (Morozova et al., 2019). Both neurons and glial cells, including astrocytes and microglia, play roles in spreading Tau pathology. Microglia can internalize and degrade extracellular Tau, providing a protective mechanism (Bolós et al., 2016; Brelstaff et al., 2018; Hopp et al., 2018). However, when degradation is ineffective, microglia might emit Tau seeds through exosomes, thereby contributing to the propagation of pathology (Asai et al., 2015; Zhu et al., 2022). Human astrocytes ingest and process dead neurons with Tau pathology, as well as synthetic fibrils and Tau aggregates from AD brain tissue, but they do not completely degrade them (Damisah et al., 2020; Lööv et al., 2015; Reid et al., 2020). Instead, the pathogenic Tau may be transmitted to nearby cells through secretion and transfer via tunneling nanotubes (Mothes et al., 2023).

1.6 Tau seeding and spreading in disease

In disease states, it was shown that pathological Tau, in forms of misfolded and aggregated Tau, can propagate from cell to cell (Clavaguera et al., 2009). AD brains show Tau pathology progression through different regions of the brain. In early stages of AD, NFTs appear in the transentorhinal cortex or the entorhinal cortex in the medial temporal lobe (Braak Stage I and

II). They progress into the hippocampal region (Braak Stage III and IV) and finally spread into the neocortex region (Braak Stage V and VI) (Braak and Braak, 1991; Serrano-Pozo et al., 2011). Spreading of pathology correlates with synaptic connectivity. The function of the progressively affected brain areas then correlates with the clinical symptoms, which include memory loss in early stages, followed by more severe cognitive dysfunction (Braak and Braak, 1991; Dickson, 2011).

One way to explain the spread of the disease, is to describe Tau propagation as a "prion-like" manner. It means that a "proteinaceous infectious particle" (Prusiner, 1982) is spreading through different regions of the organ, thereby transmitting the disease. In AD, these prion-like particles are Tau-seeds, containing aggregated Tau (Frost et al., 2009; Guo and Lee, 2011). The seeds are released into extracellular space (see chapter 1.5) and are able to enter connected, naive cells, where a seeded template-aggregation of endogenous Tau occurs (Brettschneider et al., 2015). Once Tau seeds are taken up by the naive cells, they can trigger Tau aggregation by inducing a chain-reaction of template-directed protein misfolding, followed by aggregation and subsequent seeded aggregation. This spread leads to the pathology propagation along synaptically connected brain regions.

There is evidence that seeding-competent Tau is oligomeric and hyperphosphorylated (Barini et al., 2022), however the exact biochemical and biophysical properties of the spreading Tau species remain not fully understood. It was also reported that seeding-competent Tau may not be restricted to insoluble fibrils but can also be soluble oligomeric Tau (Islam et al., 2025; Lasagna-Reeves et al., 2012). Tau transmission is not confined to AD but also plays roles on other tauopathies (Goedert and Spillantini, 2017). The brain region pattern of aggregated Tau and its propagation extent differs between tauopathies (Irwin et al., 2016; Williams et al., 2007), even showing distinct fibrillary structures in cryo-electron microscopy studies (Fitzpatrick et al., 2017; Shi et al., 2021).

1.7 Tau interacting proteins indicate involvement in multiple pathways in human brain

In AD, Tau undergoes hyperphosphorylation, misfolding, and aggregation, transitioning from its physiological role in stabilizing microtubules to a pathological state associated with neurotoxicity. Investigations into the interactome of Tau in the human brain have revealed its involvement in numerous molecular pathways and cellular processes that are disrupted in AD, providing critical insights into disease mechanisms.

Proteomic analyses have shown that Tau interacts with proteins that mediate aggregation and cytotoxicity, distinguishing the AD hippocampus from healthy controls (Ayyadevara et al., 2016). In its hyperphosphorylated state, Tau interacts with a specific subset of proteins that are involved in cytoskeletal organization, synaptic signaling, and mitochondrial function (Drummond et al., 2020). These interactions indicate that hyperphosphorylation drives Tau away from its physiological roles, impairing neuronal processes essential for synaptic and cellular integrity. Multiple studies identified RNA-binding proteins as interacting partners of Tau, implicating its role in regulating RNA metabolism and splicing (Drummond et al., 2020; Hondius et al., 2021; Kavanagh et al., 2022; Tracy et al., 2022). These findings highlight the connection between Tau pathology and widespread transcriptional dysregulation, suggesting that interactions with RNA-binding proteins are critical contributors to neuronal dysfunction in AD (Kavanagh et al., 2022). Proteomic analysis of NFTs isolated from human brain suggested proteins interacting with phosphorylated Tau are related to synaptic signalling, ribosome and

vesicle trafficking (Hondius et al., 2021). Additionally, Tau was identified to interact with proteolytic pathways and autophagy-related proteins in the disease context (Hondius et al., 2021). Interactions between Tau and endoplasmic reticulum (ER) proteins in AD brain suggest that Tau is involved in ER stress and dysfunction (Meier et al., 2015). These interactions likely impair protein folding and trafficking, exacerbating cellular stress and contributing to the loss of proteostasis in neurons. Furthermore, a Tau interactome generated from human iPS-derived neurons maps its influence on synaptic and mitochondrial processes (Tracy et al., 2022), both of which are crucial for neuronal function. Interactions with synaptic proteins suggest that Tau may regulate synaptic plasticity, while pathological Tau disrupts synaptic signaling, contributing to cognitive decline. Similarly, the associations with mitochondrial proteins indicate the role of Tau role in energy production and metabolic regulation.

Together, these studies reveal the diverse interactions in the human brain, which span cytoskeletal organization, synaptic signaling, RNA splicing, ER stress, and mitochondrial function. The transition of Tau from its physiological to pathological state underpins its role as a driver of neurodegeneration in AD. Investigating these interactions not only enhances the understanding of disease mechanisms but also highlights potential therapeutic targets to mitigate Tau-related toxicity and preserve neuronal function.

1.8 The role of Tau in synaptic dysfunction

Synapses play a critical role in brain function as they serve as the primary sites for neuronal communication. They facilitate the precise interconnections among neurons necessary for transmitting signals throughout the nervous system, thereby enabling various brain functions such as learning, memory, and cognition (Citri and Malenka, 2008).

Synapse loss and dysfunction are critical characteristics of numerous neurodegenerative diseases, including AD (Selkoe, 2002; Zhou et al., 2017). Synapse loss also strongly correlates with cognitive decline in patients (DeKosky and Scheff, 1990; Terry et al., 1991). Under normal conditions, Tau is predominantly an axonal protein that stabilizes microtubules. Emerging evidence suggests that physiological Tau also localizes to synapses (Fein et al., 2008; Tracy et al., 2022), where it may play roles in synaptic function and plasticity. At the synapse, Tau is thought to interact with cytoskeletal elements and signaling molecules, potentially influencing synaptic strength and neurotransmission (Robbins et al., 2021).

In case of Tau propagation, there is evidence suggesting that Tau seeds may spread via synaptic connections (de Calignon et al., 2012; Pickett et al., 2017), highlighting the importance of synapses in disease progression. Pathological forms of Tau disrupt both pre- and post-synaptic transmission, leading to impaired neuronal responses (Liu et al., 2012; Moreno et al., 2016; Wang et al., 2024). Soluble oligomeric forms of Tau and Aß were also found to be toxic to synapses (Kopeikina et al., 2012; Polydoro et al., 2014; Spires-Jones and Hyman, 2014). Furthermore, Tau disrupts synaptic function through mechanisms such as impairing vesicle transport (Zhou et al., 2017), or destabilizing the cytoskeleton (Alonso et al., 1997). Tau can impair AMPA and NMDA receptor trafficking, leading to reduced synaptic plasticity and disrupted long-term potentiation (Hoover et al., 2010). Additionally, pathological Tau may induce calcium homeostasis dysregulation (Gómez-Ramos et al., 2008), further exacerbating synaptic dysfunction. Apart from neurons, astrocytes and microglia play significant roles in synaptic dysfunction as microglia facilitate the spread of Tau seeds through synaptic connections (Španić et al., 2019), while reactive astrocytes contribute to synaptic

pruning (Eltom et al., 2024). Further research is needed to better understand how Tau disrupts synaptic function and its role in neurodegenerative diseases.

1.9 Autophagy in AD

The ubiquitin-proteasome system and the autophagy-lysosomal system are the 2 major proteolytic pathways regulating protein degradation in cells (Kirkin et al., 2009; Rubinsztein, 2006). Autophagy is a fundamental cellular process responsible for degrading and recycling cytoplasmic components, including damaged organelles and misfolded proteins (Levine and Kroemer, 2008; Xie and Klionsky, 2007). This mechanism is vital for maintaining cellular homeostasis and adapting to various stress conditions (Choi et al., 2013). The autophagic process involves the formation of double-membrane vesicles known as autophagosomes, which encapsulate cellular debris. These autophagosomes subsequently fuse with lysosomes, leading to the degradation of their contents by lysosomal enzymes. This degradation not only clears potentially harmful components but also recycles them to provide essential building blocks and energy (Ryter et al., 2013; Yamamoto et al., 2023).

Selective autophagy is a specialized form of autophagy that targets specific cellular components, such as damaged organelles, protein aggregates, or invading pathogens, for degradation. This process is crucial for maintaining cellular homeostasis and protecting against various diseases, including neurodegeneration (Fimia et al., 2012). The selectivity of autophagy is mediated by receptor proteins that recognize specific cargo and facilitate their sequestration into autophagosomes. These receptors typically contain LC3-interacting regions (LIRs) that bind to autophagosome-associated proteins like LC3/GABARAP, linking the cargo to the autophagic machinery (Johansen and Lamark, 2011). Selective autophagy receptors such as p62/SQSTM1, NBR1 and others (Bjørkøy et al., 2005; Gubas and Dikic, 2022; Kirkin et al., 2009; Pankiv et al., 2007) recognize ubiquitinated cargo proteins and recruit them to the autophagosome by directly interacting with Atg8 proteins such as LC3, leading to cargo degradation (Kirkin et al., 2009; Noda et al., 2010; Pankiv et al., 2007). Even though different receptors like p62 and NBR1 have structural similarities (Svenning et al., 2011), they can target different cargos for selective autophagy and act independently of each other (Kirkin et al., 2009; Kirkin and Rogov, 2019).

Dysregulation of autophagy has been implicated in various human diseases. For instance, impaired autophagy is associated with neurodegenerative disorders such as Alzheimer's and Parkinson's diseases, where the accumulation of protein aggregates occurs (Mizushima and Levine, 2020). Impaired autophagic process may contribute to neuronal damage and degeneration in AD (X. Liu et al., 2022; Roney et al., 2021; Zhang et al., 2022).

Autophagy is known to be involved in the degradation of Tau aggregates (Piras et al., 2016; Wang et al., 2009). Multiple selective autophagy receptors have been implicated in the context of Tau. For instance, NDP52/CALCOCO2 has been reported to mediate Tau turnover under oxidative stress conditions (Jo et al., 2014). Another study suggests that Optineurin serves as the autophagy receptor for soluble Tau species, while p62 acts as the receptor for aggregated Tau (Xu et al., 2019). Although p62 has been demonstrated to effectively recognize and bind Tau aggregates (Ferrari et al., 2024; Xu et al., 2019) this interaction does not always result in autophagic degradation within the brain. Recent findings in a reconstituted *in vitro* system revealed that Tau fibrils derived from AD brains can become excessively coated with p62. This excessive coating masks ubiquitin tags, thereby preventing the recruitment of other autophagy machinery components and hindering degradation (Ferrari et al., 2024). Neighbor

of BRCA1 gene 1 (NBR1) is also a selective autophagy receptor (Kirkin et al., 2009; Rasmussen et al., 2022). In comparison to p62, the role of NBR1 as an autophagy receptor is less well understood. Although p62 and NBR1 can form heteropolymers, they are also capable of acting independently during cargo degradation (Kirkin et al., 2009). For example, NBR1-mediated autophagy has been shown to occur even in the absence of p62 (Kirkin et al., 2009). Furthermore, a subset of NBR1 was observed in HAP1 cells that does not co-localize with p62 puncta, suggesting the existence of p62-independent functions for NBR1 (Savova et al., 2020).

1.10 Induced pluripotent stem cells as a model for Tau pathology

The lack of accurate disease models is one of the difficulties in finding a therapeutic cure for AD and other tauopathies. The use of patient brain cells for experimental studies, except for post-mortem tissue, is ethically unreasonable. So far, *in vivo* model systems to test therapeutic approaches mainly consist of mouse models, while *in vitro* models include murine neuronal cell culture systems. If not artificially induced, mouse models lack AD hallmarks such as plaques, tangles and neurodegeneration (Frigerio and Strooper, 2015; Götz and Ittner, 2008). Furthermore, murine cells show a different vulnerability to neurodegeneration compared to human neuronal cells (Espuny-Camacho et al., 2017).

Another *in vitro* method to investigate human pathologies is the induced Pluripotent Stem Cell (iPSC) system. In theory, any human cell type from healthy controls as well as patients can be derived through iPSC technology. A somatic cell can be reprogrammed back into the pluripotent state, by expression of stem cell relevant transcription factors. These induced pluripotent cells are subsequentially able to differentiate into somatic cells (Takahashi et al., 2007; Takahashi and Yamanaka, 2006; Yu et al., 2007). Human iPSCs have been reprogrammed into AD relevant neural cell types, such as neurons, astrocytes and microglia (Mungenast et al., 2016; Speicher et al., 2019; TCW et al., 2017). Human iPSCs are patient derived, hence they can include and reflect the human genetics.

In AD research, cortical neurons derived from human iPSCs are frequently used as cell models to investigate disease-relevant factors. iPSCs can be differentiated into cortical neurons through various methods that utilize transcription factors and growth factors (Shi et al., 2012). One advantage of using human iPSC-derived neurons is the ability to investigate specific disease-related genes without the confounding effects of previous overexpression. Additionally, many of the genes are neuron-specific and thus cannot be studied in other cell systems. However, challenges such as heterogeneity in cell composition, difficulties in upscaling the cells, and lengthy differentiation timelines remain significant obstacles. To address these issues, several protocols have been developed to facilitate more efficient and reproducible differentiation of iPSCs into neurons. One such approach is the direct, rapid, and robust differentiation of iPSCs into neurons by overexpressing the single transcription factor neurogenin-2 (Ngn2), which has been shown to effectively induce neuronal differentiation while mimicking the properties and maturation stages of cortical neurons (Zhang et al., 2013).

Another widely used and effective method is the dual SMAD inhibition protocol, which focuses on inhibiting the SMAD signaling pathways critical for maintaining pluripotency and preventing non-neuronal lineage specification, thereby promoting neural differentiation (Stuart M. Chambers et al., 2009). SMAD signaling is activated by Transforming Growth Factor-beta (TGF-β) and Bone Morphogenetic Proteins (BMPs). Dual inhibition with SB431542 (a TGF-β receptor inhibitor) and LDN-193189 (a BMP receptor inhibitor) suppresses these pathways, facilitating the rapid conversion of hiPSCs into neural progenitor cells (NPCs). Within 7–10

days, this protocol efficiently generates NPCs characterized by neural lineage markers such as PAX6 and Nestin, providing a foundation for generating functional neurons (Cao et al., 2017; Stuart M Chambers et al., 2009; Gaspard et al., 2008; Hansen et al., 2011; Manos et al., 2022; Verheyen et al., 2018a). This method is particularly useful for achieving high-efficiency differentiation and reproducibility in neuronal cultures.

It is possible to utilize the iPSC model to study Tau pathologies, since the cells can be modified to reflect the complex system of Tau expression and splicing up to a certain extent (TCW, 2019). In order to accelerate mature Tau splicing, MAPT mutations (E10+ 14 and E10 +16) can be incorporated into the endogenous Tau expressed by iPS-neurons. This enhances the alternative splicing of exon 10, leading to an increased expression of 4R Tau (Dawson et al., 2007; Iovino et al., 2015; Sposito et al., 2015). However, a model system originally exhibiting similar conditions compared to the adult human brain is so far not available. iPSC derived disease models often exhibit embryonic rather than adult cell phenotypes (Lapasset et al., 2011). In the fetal human brain, Tau is naturally hyperphosphorylated, a state that aids in neuronal development without leading to aggregation (Hefti et al., 2019). This suggests that unlike in tauopathies, physiological hyperphosphorylation in development does not inherently cause aggregation, indicating that additional pathological factors must be present for aggregation to occur (Hefti et al., 2019). The embryonic phenotype of iPS-derived neurons is a challenge in the case of AD research, since the sporadic form of the disease is characterized by late onset and by mature protein phenotypes, such as Tau aggregation. Artificial aging paradigms are proposed to accelerate the maturation progress of neurons, and to promote the expression of late-stage AD Tau isoforms (Klimmt et al., 2020). Furthermore, the utilization of 3-dimensional (3D) cell culture approaches might help to investigate late-stage hallmarks, such as tangles. Here, the cells are embedded into organoid models, which is supposed to simulate the *in vivo* cellular diversity (Lancaster et al., 2013; Paşca et al., 2015). However, it remains a challenge to study the adult pathologies of AD and other tauopathies in an embryonic iPS-derived phenotype or murine neurons. It is very important to gain further insights into developmental pathways or splicing mechanisms, and to adapt the iPS-derived neurons accordingly. This would lead to a novel iPS system that can reflect the adult human brain more precisely.

The addition of recombinant Tau aggregates or AD brain-derived sarkosyl-insoluble Tau to human iPS-derived cortical neurons can trigger the aggregation of endogenous Tau (Manos et al., 2022), mimicking Tau pathology *in vitro*. Human iPSCs are differentiated into cortical neurons, as previously described (Manos et al., 2022), by inhibiting dual SMAD signalling with a small molecule cocktail according to modified published protocols (Cao et al., 2017; Stuart M Chambers et al., 2009; Gaspard et al., 2008; Hansen et al., 2011; Manos et al., 2022; Verheyen et al., 2018a). After final plating, neurons are exposed to Tau seeds to introduce seeded Tau aggregation (Limorenko et al., 2023). In these experiments, the type of seed needs to be matched to the neuronal genotype for efficient templating (Manos et al., 2022): AD-brain derived sarkosyl-insoluble Tau seeds are used to induce Tau aggregation in human MAPT wild type (WT) neurons, endogenously expressing 0N3R Tau. For MAPT “triple mutant” (TM) (0N4R P301S/ E10+14/ E10+16) neurons expressing both 3R and 4R Tau with the FTD-associated P301S mutation, aggregation can be induced with recombinant Tau aggregates generated from 2N4R P301L Tau protein (Manos et al., 2022).

1.11 Tau-targeting therapeutic approaches in AD

Therapeutic strategies aim to alleviate symptoms, slow disease progression, or target the underlying pathology of AD. These approaches include already approved symptomatic treatments and disease-modifying therapies, or investigational strategies that address diverse mechanisms associated with AD.

Disease-modifying therapies aim to address the molecular mechanisms of AD, particularly Aß and Tau pathology. Among these, Aß-targeting therapies have garnered significant attention. Aß-targeting antibodies lecanemab and donanemab both received FDA approval and have shown promise in slowing cognitive decline in early AD while providing evidence of amyloid clearance (Dyck et al., 2022; Sims et al., 2023).

Emerging therapeutic approaches aim to target Tau pathology progesses and prevent the loss of its physiological roles in maintaining microtubule stability and axonal transport. One strategy is to target extracellular Tau by anti-Tau antibodies, that are designed to target specific Tau epitopes, reducing Tau aggregation and its propagation (Congdon and Sigurdsson, 2018). For instance, semorinemab has shown promise by decreasing Tau accumulation in mice (Ayalon et al., 2021), but then failed to slow cognitive decline, particularly in early stages of AD (Slomski, 2022). Similarly, gosuranemab and tilavonemab target N-terminal parts of Tau (Congdon and Sigurdsson, 2018; Kfoury et al., 2012; Yanamandra et al., 2013). Clinical trials for both antibodies showed negative results and were discontinued. Ongoing Tau antibody clinical trials target mid-region epitopes of Tau, eg. Bepranemab (Roche) targeting the microtubule-associated Tau epitope, as data indicated that these antibodies more potently interfere with propagation of pathogenic, aggregated Tau (Courade et al., 2018; Mullard, 2024).

Besides Tau-targeting antibodies, several amino-acid peptides repressing the aggregation of Tau were proposed as possible therapeutic approaches (Sievers et al., 2011). Small molecules that inhibit Tau-Tau binding or disrupt aggregates, such as TRx0237 (LMTX), have been investigated. Although early trials showed modest effects, further studies aim to refine these approaches (Gauthier et al., 2016; Wischik et al., 1996). Additionally, therapies targeting intracellular Tau and Tau phosphorylation are under exploration. Candidates such as glycogen synthase kinase-3 (GSK-3) inhibitors aim to reduce abnormal Tau hyperphosphorylation. Tideglusib, a GSK-3 inhibitor, showed potential in preclinical models by attenuating Tau pathology and improving cognitive outcomes, though clinical trials have faced challenges in demonstrating robust efficacy (Lovestone et al., 2015). Gene therapy and RNA-based approaches, such as antisense oligonucleotides targeting Tau mRNA, are also being developed to reduce pathological Tau expression and toxicity (DeVos et al., 2013). First in human clinical trials showed promising results such as dose-dependent reduction of CSF total Tau (Mummery et al., 2023). Other therapy approaches like Methylene blue and O-GlcNAcylation transferase inhibitors failed to show efficient impacting of Tau pathology in clinical trials (Burns et al., 2022; Guo et al., 2022).

Numerous challenges remain as current therapies often demonstrate limited efficacy and fail to address the complex, heterogeneous nature of AD pathology. Moreover, late-stage diagnosis hinders the potential for early intervention, when treatments might be most effective. While challenges remain, these therapies represent a critical step forward in addressing pathologic contributions to AD progression.

2 Project objective

Alzheimer's Disease, a devastating neurodegenerative disorder affecting millions of individuals worldwide, is characterized by progressive cognitive decline and memory loss, posing substantial challenges both to patients and healthcare systems. Despite its widespread impact and extensive research efforts, there is still no cure for AD, highlighting the urgent need for deeper exploration into its underlying mechanisms. This dissertation project focuses on the critical role of the Tau protein, which pathological forms and its propagation are implicated as one hallmark of the disease progression.

There is evidence that pathogenic seeding-competent Tau is oligomeric and hyperphosphorylated (Barini et al., 2022), however the exact biochemical and biophysical properties remain inadequately understood. In addition, the effect of Tau aggregation on the physiological functions of Tau as well as a potential impact on pathological dysfunction remains not fully understood.

To address these gaps, the first aim of this project was to explore Tau-interacting proteins directly in human brain, providing valuable insights into the differences between physiological and pathological Tau species. The project aims to uncover specific pathways that elucidate the functions of physiological Tau and subsequently, comparing it to the interactome analysis of pathological Tau species. This analysis will help to understand how the loss of physiological functions and the gain of pathological dysfunctions manifest in health and disease.

Previous studies gave great insights into the difference in interacting partners of Tau in AD and control brain tissue, using either one total Tau antibody (Tau-5) for pulldown of interacting proteins (Ayyadevara et al., 2016; Hsieh et al., 2019; Kavanagh et al., 2022; Meier et al., 2015), or the phospho-Tau antibody PHF1, to study interacting partners of Tau in AD brain tissue (Drummond et al., 2020). Currently, no study has comprehensively evaluated Tau interactomes by comparing the interacting partners of pathological Tau from AD brains to those of physiological Tau from control brains within a single proteomic analysis using both phospho- and total Tau specific antibodies. In this project, we employed three total Tau and three phospho-Tau antibodies for the co-immunoprecipitation of Tau interactors. This was conducted through parallel immunoprecipitations (IPs) from post-mortem brains of five individuals with AD and five age-matched controls. The subsequent identification of Tau species interactors was accomplished using label-free quantitation mass spectrometry and data-independent acquisition (DIA).

Human iPS-derived neurons provide a unique model system to study Tau pathology in a controlled and human-relevant context. Tau aggregation can be triggered by the uptake of seeding competent, misfolded and hyperphosphorylated Tau species into neurons, which leads to the misfolding and aggregation of endogenous Tau (Clavaguera et al., 2009; Iba et al., 2013) and encompasses the stepwise assembly of initially soluble Tau species, first forming small oligomers and subsequently larger, sarkosyl-insoluble Tau aggregates. This process can be modelled *in vitro* through the treatment of human iPS-derived neurons with purified recombinant or human AD brain-derived Tau seeds, leading to the aggregation of endogenous Tau in a concentration- and time-dependent process (Manos et al., 2022). This model system allows for the detailed study of intraneuronal changes associated with the Tau aggregation process.

Human iPS-derived neurons were employed as a secondary model system, to gain deeper insights into the Tau interactome. To achieve optimal experimental comparability, the same antibodies and mass spectrometry conditions were utilized. Seeded Tau aggregation was introduced to mimic pathological Tau species and to capture their corresponding interactors, whereas non-seeded iPS-derived neurons represent endogenous Tau and thus physiological Tau interactors. Pathway enrichment analysis of the overlapping proteins between the post-mortem and iPS-derived Tau interactomes allows for the identification and confirmation of key interacting pathways or proteins, enhancing our understanding of the molecular connections involved.

The seed-induced Tau aggregation models Tau pathology in iPS-derived neurons. This is a very widely used model system, however, the exact impact of the Tau aggregates to the neuronal environment remains unclear. The second aim of this project was to elucidate the neuronal response mechanisms to seed-induced Tau aggregation on the proteome and phospho-proteome level in human iPS-derived neurons. Mass spectrometry using Tandem-Mass-Tag (TMT)-labelling enabled the relative quantification of proteins and phospho-proteins in seeded and non-seeded conditions. The characterization of neuronal cell model systems plays a crucial role in drug discovery by providing a reliable platform for identifying novel therapeutic targets. These model systems allow us to study disease mechanisms, cellular responses, and molecular pathways in a controlled environment, thereby facilitating the identification of key regulators involved in neurodegenerative and neurological disorders. By refining and validating these models, the accuracy of target identification can be enhanced, ultimately contributing to the efficiency and success of drug discovery.

3 Material

3.1 Cell culture

table 1: chemicals/media and buffer compounds

Reagent/Chemical name	Supplier
Essential 8 Flex Medium	Gibco
Matrigel Basement Membrane Matrix Growth Factor reduced	Corning
Matrigel Basement Membrane Matrix	Corning
0.01% Poly-L-Ornithine	Sigma
Bovine Serum Albumin (BSA)	Serva
10% Bovine Serum Albumin (BSA) solution	Sigma-Aldrich
DMEM/F12 (+ L-Glut and Hepes)	Gibco
DMEM / high Glucose	Gibco
Optimem	Gibco
Neurobasal medium	Gibco
Penicillin/Streptomycin	Gibco
N2 Supplement 100x	Gibco
B27 Supplement without VitA 50x	Gibco/Life Technologies
GlutaMAX	Gibco
Doxyxycline Hydrochloride, ready made solution	Sigma-Aldrich
GDNF	R&D system
BDNF	R&D system
Roche compound RO	Roche
Rock Inhibitor Y-27632 (ROCI)	Calbiochem
Ascorbic Acid	Sigma-Aldrich
B27 Plus Neuronal Culture System	Gibco
dcAMP	Sigma-Aldrich
Laminin from Engelbreth-Holm-Swarm murine sarcoma basement membrane	Sigma-Aldrich
Accutase	Life Technologies
DPBS with Mg^{2+} Ca^{2+}	Life Technologies

DPBS without Mg^{2+} Ca^{2+}	Life Technologies
Versene (EDTA)	Gibco
PBS (20x)	Thermo Scientific
NaCl	Merck
Tris pH 7.5	Merck
EDTA	Sigma Life Science
EGTA	Merck
Triton-X 100	Roth
1x Protease inhibitor cOmplete™	Roche
1x phosphatase inhibitor PhosSTOP EASYpack	Roche
NaH_2PO_4	Merck
Tween 20 pH 7.4	Sigma-Aldrich
Glycerol	Sigma-Aldrich

table 2: Cell lines

Cell line name	Abbreviation	Cell type
BIOMEDi004-A (Coriell Fibroblast AG08125)	MAPT WT	iPS-derived neurons
MAPT P301S / E10+14+16 iNGN2 „triple mutant“ line	MAPT TM	iPS-derived neurons
BIOMEDi004-A (Coriell Fibroblast AG08125) with CRISPR Cas induced disruption of exon 1	MAPT KO	iPS-derived neurons
HEK cells with inserted Tau repeat domain (RD) part (aa 244-372; Exons 9-11) with P301S mutation	HEK293T-Tau-P301S-YFP	HEK biosensor cells

3.2 siRNA mediated knock down

table 3: siRNA and transfection reagents

Product name	Supplier

human SCRIB #M-010500-00-0005	Dharmacon siGenome smartpool
Human SQSTM1 (5 nmol) #M-010230-00-0005	Dharmacon siGenome smartpool
human NBR1 (5 nmol) #M-010522-01-0005	Dharmacon siGenome smartpool
human SV2a (5 nmol) #M-007631-01-0005	Dharmacon siGenome smartpool
human non-target NT 1 (5 nmol) #D-001210-01-05	Dharmacon siGenome smartpool
human MAPT (5 nmol) #M-012488-01-0005	Dharmacon siGenome smartpool
DharmaFECT 1 Transfection reagent	Dhamracon/Horizon Ltd
Lipofectamine 2000	Invitrogen

3.3 ELISA

table 4: antibodies used for ELISA

ELISA	Capture antibody	Detection Antibody
Assymmetric total Tau ELISA	Tau12 (2 µg/ml, Biolegend #806502)	HT7-Biotin (0.1 mg/ml, Thermo, # MN1000B)
Symmetric aggregated Tau ELISA	HT7 (2 µg/ml, Thermo #MN1000)	HT7-Biotin (0.1 mg/ml, Thermo, # MN1000B)
Protein standard 2N4R	Protein Standard	Abbvie GmbH &Co. KG

table 5: ELISA detection reagents

Antibody/reagent	Function	Supplier	Dilution
Streptavidin Poly-HRP	Conjugate	Thermo Scientific	1:10000 (0.5 mg/mL)
TMB substrate	Developing reagent	KEM EN TEC Diagnostics	

3.4 Western Blot

table 6: Antibodies for Western Blot

Primary Antibodies	Secondary Antibodies
NBR1 (mouse 5C3, abcam #ab55474) 1:1000	Goat anti-Mouse IgG (H+L) Poly-HRP Secondary Antibody, HRP (Invitrogen # 32230) 1:10000
LC3B (rabbit, Sigma # L7543-200 µl) 1:1000	Goat anti-Rabbit IgG (H+L) Poly-HRP Secondary Antibody, HRP (Invitrogen # 32260) 1:10000
77G7 Tau (mouse, Biolegend #816701) 1:1000	Goat anti-Mouse IgG (H+L) Poly-HRP Secondary Antibody, HRP (Invitrogen # 32230) 1:10000
GAPDH (mouse, Cell Signaling #97166S) 1:1000	Goat anti-Mouse IgG (H+L) Poly-HRP Secondary Antibody, HRP (Invitrogen # 32230) 1:10000
Actin (mouse, Merck # A5441) 1:4000	Goat anti-Mouse IgG (H+L) Poly-HRP Secondary Antibody, HRP (Invitrogen # 32230) 1:10000
Anti-HA antibody (mouse abcam #ab18181)	Goat anti-Mouse IgG (H+L) Poly-HRP Secondary Antibody, HRP (Invitrogen # 32230) 1:10000
Tau12 (mouse, Biolegend #806502) 1:5000	Goat anti-Mouse IgG (H+L) Poly-HRP Secondary Antibody, HRP (Invitrogen # 32230) 1:10000
	Pierce Streptavidin Poly HRP (mouse, Thermo #21140) 1:10000

3.5 qPCR

table 7: qPCR oligonucleotides and TaqMan primer

Name	Description	Supplier
GAPDH Hs99999905_m1	hGAPDH FAM-dye TaqMan Assay	Thermo Scientific
ActB Hs99999903_m1	hACTB FAM-dye TaqMan Assay	Thermo Scientific
MAPT Hs00902194_m1	hMAPT FAM-dye TaqMan Assay	Thermo Scientific

Hs00245918_m1 NBR1 human FAM-MGB	hNBR1 FAM-MGB Taqman assay	Thermo Scientific
Hs01059458_m1 SV2a human FAM-MGB	hSV2a FAM-MGB Taqman assay	Thermo Scientific
Hs01061917_g1 Sqstm1 human FAM-MGB	hSQSTM1 Taqman assay FAM-MGB	Thermo Scientific

3.6 Immunofluorescence staining

table 8: Antibodies for immunofluorescence staining

Primary antibody	Secondary antibody
MC1 aggregated Tau (mouse, Peter Davis) 1:2500	AlexaFluor 488 goat anti mouse (Invitrogen #A11001) 1:500
MAP2 (chicken, abcam #ab5392) 1:2500	AlexaFluor 647 goat anti-chicken (Invitrogen #A21449) 1:500
NBR1 (mouse 5C3, abcam #ab55474) 1:500	Cy™5 AffiniPure™ Donkey Anti-Mouse IgG (H+L) (Jackson, #715-175-151) 1:500
LC3B (rabbit, Sigma # L7543-200 µl) 1:500	Cy™3 AffiniPure™ Donkey Anti-Rabbit IgG (H+L) (Jackson, #711-165-152) 1:500

3.7 Cloning constructs

table 9: Primer to generate phospho-mutant NBR1 overexpression constructs

Construct	Mutagenesis primer	Primer sequence
Phospho-resistant	hNBR1 sense Mutagenesis Primer S486A	CTTTCCCCTCCGAAGAGGCCCCTGATAACA TTGAAAAG
Phospho-resistant	hNBR1 antisense Mutagenesis Primer S486A	CTTTTCAATGTTATCAGGGGCCTCTTCGGA GGGGAAAG
Phospho-mimetic	hNBR1 sense Mutagenesis Primer S486D	CTTTCCCCTCCGAAGAGGACCCTGATAACA TTGAAAAG
Phospho-mimetic	hNBR1 antisense Mutagenesis Primer S486D	CTTTTCAATGTTATCAGGGTCCTCTTCGGA GGGGAAAG

table 10: BioID overexpression constructs

Construct	Lentivirus containing cloned constructs	Cloned constructs contains
Tau-BioID	pCDH-CAG-hMAPT_tr.var.2_P301S-linker30-BioID2-HA-T2A-Bsd	Human MAPT P301S-linked to BioID2 via 30 aa linker, HA-tag, Blasticidin resistance
Tau-BioID	pCDH-CAG-hMAPT tr.var.2 P301S-linker10-BioID2-HA-T2A-Bsd	Human MAPT P301S-linked to BioID2 via 10 aa linker, HA-tag, Blasticidin resistance
BioID only	pCDH-CAG-BioID2-NES-HA-T2A-Bsd	BioID2, HA-tag, Blasticidin resistance, nuclear export sequence
Tau GFP	pCDH-CAG-TAU441 P301L-GFP-T2A-Puro	Human MAPT with P301L GFP expression tag

3.8 Immunoprecipitation (IP)

table 11: Human brain samples used for Tau interactome study obtained from Netherlands brain bank (NBB)

Sex	Age	Disease status	Braak Stage	Brain region
f	76	Ctrl	2	middle frontal gyrus
f	60	Ctrl	0	middle frontal gyrus
m	82	Ctrl	2	middle frontal gyrus
f	99	Ctrl	2	middle frontal gyrus
f	89	Ctrl	1	middle frontal gyrus
m	82	AD	5	middle frontal gyrus
f	71	AD	5	middle frontal gyrus
m	74	AD	5	middle frontal gyrus
f	64	AD	6	middle frontal gyrus
f	70	AD	5	middle frontal gyrus

table 12: Antibodies characterized via biochemical profiling and used for IP

Name	Supplier	Cat no	Used for IP study
AT100	Invitrogen	MN1060	Brain
Tau12	BioLegend	806502	Brain and iPS lysate

2B8	Jena Analytics	847-0102007603	Brain
IgG ctrl		raised against peptide Keyhole limpet hemocyanin (KLH)	Brain and iPS lysate
HT7	Invitrogen	MN1000	Brain and iPS lysate
PHF1	Peter Davis	n/a	Brain and iPS lysate
pS198	abcam	ab156622	Brain and iPS lysate
Tau5	Millipore	57781	
77G7	Biolegend	816701	
Tau46	Invitrogen	13-6400	
AT8	Invitrogen	MN1020	
MC1	Peter Davis	n/a	

table 13: Beads used for IP

Name	Supplier
Dynabeads™ M-280 Streptavidin magnetic beads	Invitrogen
Dynabeads™ M-280 Sheep Anti-Rabbit IgG magnetic beads	Invitrogen
Dynabeads™ M-280 Sheep Anti-Mouse IgG magnetic beads	Invitrogen

table 14: Antigens for biochemical profiling

Antigen	Description
sPHF	Recombinant soluble paired helical filament (sarkosyl-insoluble)
sPHF HFIP (1,1,1-3,3,3-hexafluor-2-isopropanol)	Denaturated, monomer, linearized rec seeds (sarkosyl-insoluble)
AD-SS1 (Braak V-VI)	Sarkosyl-soluble Tau - mix of momomers and small aggregates (sarkosyl-soluble)
Control SS1 (Braak 0-I)	Sarkosyl soluble Tau - No pathological Tau form (sakrosyl-soluble)
AD-P3	Native middle/ big sized Tau aggregates; no soluble Tau (sarkosyl-insoluble)

AD-P3 HFIP	Monomeric/ Linearized middle/big sized aggregates (sarkosyl-insoluble)
AD-PS1	small Tau aggregates (sarkosyl-insoluble)
AD S1 Pellet	No sarkosyl, big Tau aggregates (sarkosyl-insoluble)
AD and control lysate	All Tau species (sarkosyl soluble)
AD and control S1 IP input	Sarkosyl treatment, but no further centrifugation → soluble Tau forms, oligomers, smaller aggregates

3.9 Mass Spectrometry

table 15: Experimental overview of TMT-labelled samples

Sample number	TMT16-plex set	iPS-derived neuron genotype	Seed type	Time point
1	1	pool	-	-
2	1	MAPT KO	No seed	DIV49
3	1	MAPT KO	No seed	DIV49
4	1	MAPT KO	No seed	DIV49
5	1	MAPT KO	recombinant Tau seeds	DIV49
6	1	MAPT KO	recombinant Tau seeds	DIV49
7	1	MAPT KO	recombinant Tau seeds	DIV49
8	1	MAPT TM	No seed	DIV21
9	1	MAPT TM	No seed	DIV21
10	1	MAPT TM	No seed	DIV21
11	1	MAPT TM	No seed	DIV49
12	1	MAPT TM	No seed	DIV49
13	1	MAPT TM	No seed	DIV49
14	1	MAPT TM	recombinant Tau seeds	DIV49
15	1	MAPT TM	recombinant Tau seeds	DIV49
16	1	MAPT TM	recombinant Tau seeds	DIV49
1	2	pool	-	-
2	2	MAPT KO	No seed	DIV49
3	2	MAPT KO	No seed	DIV49

4	2	MAPT KO	No seed	DIV49
5	2	MAPT KO	AD-brain derived seeds	DIV49
6	2	MAPT KO	AD-brain derived seeds	DIV49
7	2	MAPT KO	AD-brain derived seeds	DIV49
8	2	MAPT WT	No seed	DIV21
9	2	MAPT WT	No seed	DIV21
10	2	MAPT WT	No seed	DIV21
11	2	MAPT WT	No seed	DIV49
12	2	MAPT WT	No seed	DIV49
13	2	MAPT WT	No seed	DIV49
14	2	MAPT WT	AD-brain derived seeds	DIV49
15	2	MAPT WT	AD-brain derived seeds	DIV49
16	2	MAPT WT	AD-brain derived seeds	DIV49

table 16: SP3 Mass Spec sample preparation

Name	Supplier	purpose
speedbead magnetic carboxylate	Cytiva	SP3 beads
sera-mag magnetic carboxylate	Cytiva	
Triethylammonuium hydrogen carbonate buffer (TEAB)	Merck Supleco	Lysis buffer
Tris(2-carboxyethyl)phosphin hydrochloride (TCEP)	Sigma	
2-Chloracetamid (CAA)	Sigma	
Acetonitril	Sigma	Clean up
Trifluoracetate (TFA)	Thermo Fisher	Acidify

3.10 Kits and consumables

table 17: Kits

Name	Supplier

TaqMan Fast Advanced Cells-to-CT Kit	Thermo Scientific
S-trap micro MS sample prep kit <100 µg	Protifi
Pierce™ BCA Protein Assay Kit	Thermo Fisher Scientific
Trans-Blot Turbo RTA Midi 0.45 µm LF PVDF Transfer Kit, for 40 blots	BioRad

table 18: Consumables

Product name	Supplier
Nunc 6-well plate	ThermoFisher
Corning 96 well biocoat plates, poly D Lysine, black/clear	Corning
DNA LoBind Tubes, 1.5 ml	Eppendorf
96 well Flat Clear Bottom Black Polystyrene TC-treated Microplates	Corning
Developing reagent TMB substrate, ready to use	KEM EN TEC Diagnostics
ELISA plate Maxi Sorp	Thermo Scientific
Deepwell Plate	Thermo Scientific
MicroAMP EduraPlate Optical 96-well Fast Yellow Reaction Plate	Applied Biosystems
4–20% Criterion™ TGX™ Precast Midi Protein Gel, 26 well, 15 µl	BioRad
SeeBlue Pre-stained protein standard	Invitrogen

3.11 Software

table 19: Software

Software	Supplier
Prism	GraphPad

RStudio	RStudio PBC
QuantStudio Real Time PCR Software	Thermo Fisher
MaxQuant and Perseus	Max Planck Institute
Spectronaut	Biognosys
Xcalibur	Thermo Fisher Scientific
BZ-X Analyzer	Keyence
Harmony Software	Revvity Inc

4 Methods

4.1 Human brain homogenization and sarkosyl treatment to generate IP input

5 cases of sporadic Alzheimer's disease (Braak stage V and VI) and 5 brains from non-affected control donors (Braak stage 0-II) were obtained from the Netherlands brain bank (table 8). 600 mg of frozen tissue samples dissected from middle frontal gyrus were homogenized using the FastPrep-24 5G System with the CoolTeenPrep adapter for 40 seconds, 6 m/sec in 5x volume TBS Lysate buffer (50 mM Tris, PH 7.4, 150 mM NaCl, 20 mM NaF, 1 mM Na2VO4, 0.5 mM MgSO4, 50x protease Inhibitor Roche #11697498001 and PhosStop Roche #04906845001).

Homogenates were sonicated using the Ultrasonic Processor UP 200s (Dr. Hielscher) with a 30% amplitude for 1.5 min on wet ice. Samples were centrifuged at 3000 xg for 5 min at 4°C. The supernatant was transferred into a fresh tube, remaining pellets were washed with PBS (including complete and PhosStop) on ice, and centrifuged at 3000xg, 4°C for 5 min. Supernatants were combined and adjusted with sarkosyl (N Lauroylsarcosine sodium salt, Sigma, #L9150) to obtain a final concentration of 1% sarkosyl. Next, samples were vortexed and incubated for 1.5 h at RT using an overhead rotator. All samples were desalted using ZebaSpin desalting columns (10 ml, 7K, Thermo Scientific #89893). The samples were frozen on dry ice and stored at -80°C until use.

4.2 Enzyme linked immunosorbent assay (ELISA)

To measure and quantify Tau level in biological samples, different ELISA methods were utilized. Symmetric ELISAs is a method to recognize an antigen of interest between two layers of antibodies – a capture and detection antibody. The capture antibody immobilizes the respective Tau species, eg. total Tau or phospho-Tau present in the sample. To measure total Tau levels symmetric ELISA were used with Tau12/HT7 as the capture/detection antibody pair (Barini et al., 2022) . To quantify aggregated Tau level, the same monoclonal antibody was used for both capturing and detecting Tau, which means that monomeric Tau species, where the epitope is not present twice, could not be detected (Ercan-Herbst et al., 2019). Here, the HT7/HT7 antibody pair was used for measuring aggregated Tau level.

In brief, MaxiSorp 384 well clear ELISA plates (Thermo Scientific, #464718) were incubated over night at 4°C with the capture antibody (final concentration 2 µg/ml in PBS-Glycerol (20%)). After blocking the plate for 1 hour with PBS-Tween + 2% BSA and 20% glycerol, the respective antigens, diluted in PBS-Tween + 0.1% BSA, were incubated for 2 hours at room temperature on the antibody coated plates to immobilize all total Tau present in the samples.

A Biotin-labelled detection antibody (concentration 0.2 µg/ml in PBS-Tween) recognized the epitopes of immobilized total Tau. A conjugated streptavidin-horseradish peroxidase (HRP, Thermo, #21140 1:10000), followed by a developing reagent containing 3,3',5,5'-tetramethylbenzidine (TMB, KEM EN TEC Diagnostics; #4800A) was added. TMB serves as a hydrogen donor in the oxidation reaction with HRP and yields a blue colour, when reacting with the HRP. The TMB substrate switches to a yellow colour, as soon as the stopping reagent 0.18 M H_2S0_4 is added. The optical density (OD 450 nm) was measured using the

Cytation 5 imaging reader (BioTek). For analysis, all samples are normalized to a recombinant total Tau or phospho-Tau standard, respectively (Barini et al., 2022; Frey et al., 2024).

4.3 Biochemical profiling

Specific antibodies recognizing different epitopes present on either N-, C- or central parts of human Tau (Ercan et al., 2017), as well as phospho- Tau antibodies, with epitopes associated with Tau pathology were carefully selected and validated for immunoprecipitation studies (table 12).

Sandwich ELISAs were performed to profile antibody binding affinities to different sarkosyl-soluble or insoluble Tau species (table 14). To represent a varied range of Tau species, antigens were sourced from AD and control brains, along with recombinant Tau (table 14). Antigens were obtained through sarkosyl extractions, allowing separation based on their size and diffusibility (Greenberg and Davies, 1990; Guo and Lee, 2011; Schlegel et al., 2019) (scheme 1).

In brief, human brain homogenate was centrifuged at 27,000 x g for 20 minutes at 4°C to separate the supernatant (S1) from the pellet (P1). The P1 pellet was then resuspended in a solution containing 10 mM Tris/HCl pH 7.4, 1 mM EGTA, 0.8 M NaCl, 10% sucrose, cOmplete protease inhibitor, and PhosSTOP phosphatase inhibitor at room temperature. This was followed by centrifugation at 27,000 x g for 20 minutes at 4°C, transferring the resulting supernatant (S2) into a new tube. The supernatants S1 and S2 were adjusted to a final concentration of 1% sarkosyl (Sigma #L-9150), incubated for 1.5 hours at room temperature with shaking at 750 rpm, and then ultracentrifuged at 150,000 x g for 1.5 h at 4°C. The supernatants, supernatant of supernatant 1 (SS1) and S3, containing soluble Tau, were separated. The corresponding pellets, PS1 and P3, which contained sarkosyl-insoluble Tau, were washed once in 200 µl TBS (25 mM Tris pH 7.4, 3 mM KCl, 140 mM NaCl) and resuspended in 120 µl TBS by vortexing and applying four sonication pulses (2 seconds each) using a probe sonicator Ultrasonic Processor UP 200s (Dr. Hielscher) at 35% amplitude. Tau was monomerized by boiling the samples for 5 min at 95°C in Leammli buffer. In the S1 fractions from AD brain samples, sarkosyl-soluble forms of Tau were identified, indicating the presence of smaller aggregates, whereas control S1 fractions did not contain pathological Tau species. The AD-P3 (pellet fraction number 3) fraction was abundant in sarkosyl-insoluble, large Tau aggregates linked to AD pathology.

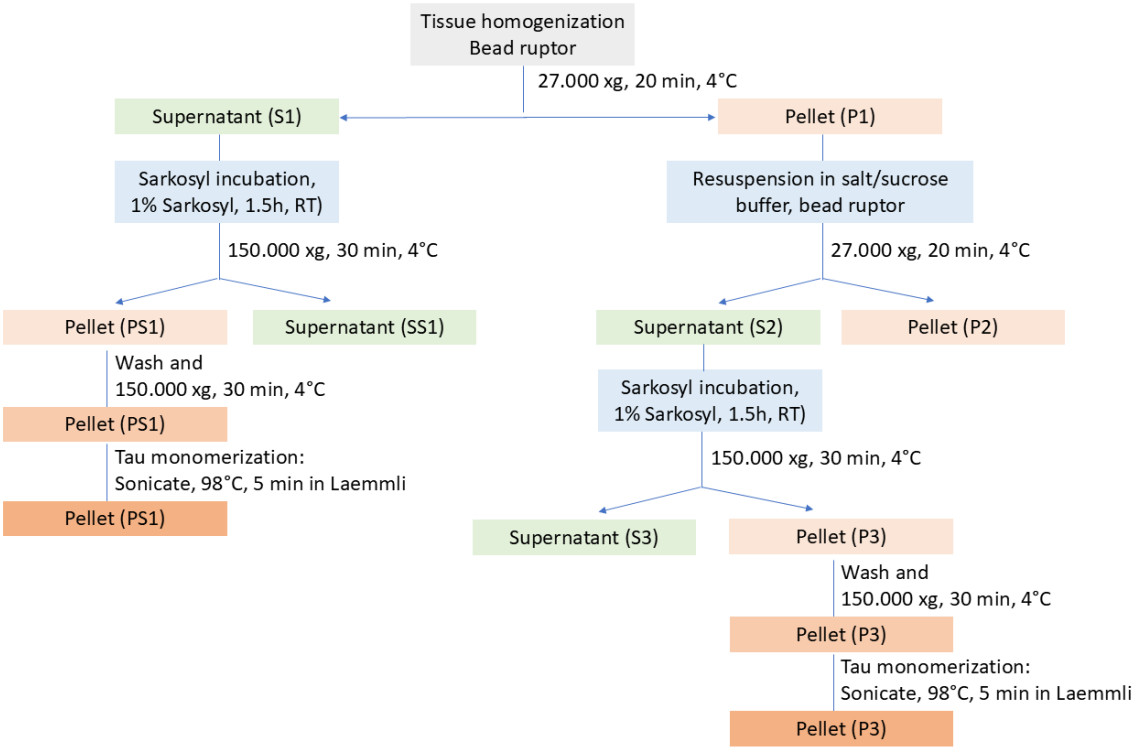

Figure 3: Sarkosyl-extraction scheme to generate AD and control brain derived Tau antigens for biochemical profiling

Schematic overview of the experimental workflow for the isolation of Sarkosyl-insoluble Tau from human brain tissue. Tissue was homogenized using a bead ruptor followed by centrifugation at 27,000 ×g for 20 minutes at 4 °C, generating Supernatant 1 (S1) and Pellet 1 (P1). Left branch: S1 underwent Sarkosyl incubation (1% Sarkosyl, 1.5 h, room temperature) followed by ultracentrifugation at 150,000 ×g for 30 minutes at 4 °C. This yielded Sarkosyl-insoluble Pellet PS1 and Sarkosyl-soluble Supernatant SS1. Pellet PS1 was washed and ultracentrifuged again, followed by Tau monomerization via sonication at 98 °C for 5 minutes in Laemmli buffer. P1 was resuspended in salt/sucrose buffer and homogenized again using the bead ruptor, followed by another 27,000 ×g centrifugation, generating Supernatant 2 (S2) and Pellet 2 (P2). S2 underwent the same Sarkosyl incubation and ultracentrifugation steps, resulting in Supernatant 3 (S3) and Pellet P3. Similar to the left branch, Pellet P3 was washed, ultracentrifuged again, and subjected to Tau monomerization via sonication at 98 °C for 5 minutes in Laemmli buffer. Abbreviations: PS1=pellet of supernatant 1, SS1= supernatant of supernatant 1, Extraction protocol adapted from (Schlegel et al., 2019).

The sandwich ELISA was performed as described above using 20 ng/ml of respective antigens. For the biochemical profiling, Tau antibodies (table 12) were used as capture antibodies, and either HT7 (#MN1000), or a mixture of two total Tau antibodies (Dako #A0024 and Thermo #PA5-27285) were used for detection. The measured Tau level were normalized to Tau standards, enabling the quantification of Tau abundance in ng/ml. The area under the curve (AUC) for each antibody detecting specific antigens was normalized to the capacity of a selected total Tau antibody pair (Tau12/HT7 or Tau12/Dako). The binding capacity was visualized as radar charts showing the AUC percentage of each antibodies binding capacity to respective antigens.

4.4 Co-immunoprecipitation Tau interactors from human brain or seeded iPS-derived neurons

Human brain homogenates (table 11) or iPS-derived cell lysates were applied during immunoprecipitation experiments using different total Tau or phospho-Tau antibodies (table 12). An isotype IgG control was included to exclude proteins non-specifically binding to beads. For immunoprecipitation from human brain, each input was normalized to 850 ng total Tau and added to 0.5 ml of antibody coated and DMP crosslinked beads. For the immunoprecipitation from seeded iPS-derived neurons, 50 µg of cell lysate was added to 100 µl of antibody coated and DMP crosslinked beads. To this end, the antibody-coated beads were immobilized on magnetic bead stand and washed once with ice cold PBS (20 mM Na-phosphate, 140 mM NaCl, pH 7.4). IP input material was incubated with the beads over night at 4°C while shaking. Next, the beads were washed three times with PBS containing 0.1% Triton X 100 for 10 min at RT. Tau and its binding partners were eluted by incubating the beads in 50 µl elution buffer (10 mM NaH2PO4, 5% sodium dodecyl sulfate (SDS, Sigma #L4509) at 95 °C for 10 min. Enrichment of Tau interactors was normalized to the IgG control.

4.5 IP-MS Proteomics Tau interactors from human brain or seeded iPS-derived neurons

Mass spectrometry proteomics was performed to analyse the interactors affinity purified with different Tau species. For sample preparation, the S-trap micro MS sample preparation kit (≤100 µg protein, protifi #97517) was utilized according to manufacturer's instructions. In brief, IP eluates were spiked with 2X lysis buffer (1:1 ratio, containing 10% SDS, 100 mM Triethylammonium hydrogen carbonate buffer (TEAB), pH 8.5), before being reduced with 120 mM Tris (2-carboxyethyl) phosphine hydrochloride (TCEP) for 15 minutes at 55°C and alkylated with 500 mM methyl methanethiosulfonate (MMTS) in isopropanol for 10 min at RT. Samples were acidified with 27.5% phosphoric acid and proteins were trapped into the S-trap micro columns by addition of binding buffer (100 mM TEAB in 90% methanol) and brief centrifugation at 10 000 xg for 30 sec. To clean the protein, the columns were washed three times with binding buffer, ensuring full removal of any remaining liquids after the last wash. Proteins trapped inside columns were digested with 2 µg Trypsin/LysC protease (Thermo, #1863467) in digestion buffer (50 mM TEAB) over night at 37°C in a water saturated atmosphere to avoid evaporation. Elution of peptides were performed by sequential addition of digestion buffer, followed by 0.2% formic acid and 50% acetonitrile elution buffer with in between centrifugation steps at 10000 xg for 1 min, respectively. Eluted peptides were dried using the Concentrator plus SpeedVac system (Eppendorf) at 45°C. Dried peptides were stored at -80°C until further usage.

Peptides were reconstituted in 0.1% formic acid and separated using an Ultimate 3000 RSLCnano HPLC over a nanoflow pre-column (µ-Precolumn, 300 µm x 5mm, C18 PepMap 100, 5µm 100 Å, Thermo Fisher #160454), followed by an analytical column (nanoEase M/Z peptide BEH, C18; 1.7 µmM 0.075 mm x 250 mm, Waters, #186008795). The mobile phase A consisted of 0.1% formic acid, and the mobile phase B consisted of acetonitrile + 0.1% formic acid. Peptides were separated by a gradient from 2% to 5% mobile phase B over 5 minutes, to 32% B over 55 minutes, to 40% B over 2 minutes, to 76% B over 2 minutes, while increasing the flow rate from 0.3 µl/ min to 0.5 µl/min at the last step, holding for 5 minutes. Eluted peptides were injected into an Orbitrap Exploris 240 mass spectrometer (ThermoScientific). Data independent MS1 spectra were acquired in positive mode at a 120 000 resolution at 380 – 980

m/z scan range, with an AGC target 300. For MS2 spectra acquisition, the range of 380-980 m/z was divided into 60 windows, with an isolation width of 10 m/z. at a resolution of 30000, with 1 microscan per spectrum and an AGC target of 3000.

4.6 Data analysis

For analysis of the Tau interactome DIA data, RAW files were searched in DIA-NN 1.8.1, allowing 2 missed trypsin cleavages and 3 variable modifications, enabling N-terminal M excision, cysteine carbamidomethylation and phosphorylation on peptides 7-30 residues in length. For the precursor ion generation, the library generation and deep learning spectra were enabled. The precursor's m/z range was restricted from 380 – 980. The fragment ion m/z range was set from 200 to 1800. Precursors and protein groups were filtered at 1% FDR. For analysis of interactome data derived from seeded iPS-derived neurons, DIA files were analyzed using the Spectronaut v.19 direct DIA experimental workflow with default settings and the following modifications: variable modifications included acetylation of N-terminal, oxidation of methionine, and deamidation of asparagine, with carbamidomethylation as a fixed modification. Trypsin specificity was allowed up to two missed cleavages, and both protein and PSM false discovery rates were set at 1%. Quantification was performed at the MS2 level, with the prototypic filter restricted to protein group-specific peptides. Data was filtered based on Q-value, and normalization was configured to automatic. The DIA spectra were searched against the UniProt human reference proteome database (3AUP00000564-2022.08.31-13.53.45.89), respectively, and a fasta file containing universal contaminants were included.

4.7 Seeded aggregation impact on iPS-derived neurons

4.7.1 Preparation of AD brain-derived sarkosyl insoluble seeds

Anonymized human post-mortem tissue was obtained from Discovery Life Sciences LLC, Huntsville, Alabama, USA. All material has been collected from donors from whom a written informed consent for a brain autopsy and the use of the material and clinical information for research purposes had been obtained by the respective brain bank.

All steps of generating AD-brain derived sarkosyl-isolube seeds were carried out on ice or at 4°C, unless stated otherwise. In brief, human AD brain tissue was homogenized in TBS lysate buffer (50 mM Tris/HCl, pH7.4, 150 mM NaCl, 20 mM NaF, 1 mM Na3Vo4, 0.5 mM MgSo4), containing complete protease inhibitor (Merck #11697498001) and PhosStop phosphatase inhibitor (Merck, # 04906845001), using the FastPrep-24 5G System with the CoolBigPrep adapter for 40 sec, 6 m/sec. Homogenates were centrifuged for 90 minutes at 27000xg (=15000 rpm) and 4°C to generate pellet P1. Next, P1 was resuspended in PBS (+ Complete + PhosStop) and sonicated using the Ultrasonic Processor UP 200s (Dr. Hielscher) with a 50% amplitude for 10 min, while stirring on ice. The sample was centrifuged for 20 minutes at 4000xg and again washed with PBS, before centrifugation for 20 min at 4000xg. The resulting supernatant was adjusted with N-Lauroylsarcosine sodium salt (Sigma #L-9150) in PBS buffer to obtain a final concentration of 1% sarkosyl and incubated for 1.5 h at room temperature (RT). The sample was ultracentrifuged at 150000xg and 4°C for 2h. Next, the resulting pellet was resuspended in PBS and sonicated using the Ultrasonic Processor UP 200s (Dr. Hielscher) with a 50% amplitude for 5 min. The sample was ultracentrifuged again at 150000xg and 4°C for 2h. The pellet was solubilized in PBS, degassed with helium, and sonicated for 5 min. After centrifuging for 10 min at 16200xg and 4°C, the final supernatant representing sarkosyl-

insoluble Tau seeds was collected. Total Tau levels were determined by ELISA (Frey et al., 2024) The seeds were stored in liquid nitrogen until usage.

4.7.2 Preparation of recombinant Tau seeds

Recombinant Tau "seeds" (Manos et al., 2022) were generated as previously described (Frey et al., 2024). Briefly, the full-length recombinant 2N4R Tau, with the P301L mutation, was isolated from E. coli, then dissolved in PBS (Gibco) with 1mM Dithiothreitol (DTT, Serva #20710.02) and incubated for 15 minutes at 55°C. After a 10-minute cooling period on ice, 40 µM Heparin (Sigma Aldrich #H3393) was introduced, leading to fibril formation over 7 days with agitation at 800 rpm at 37°C. Following centrifugation at 20000xg for 2.5 hours at 4°C, the Tau seeds were resuspended in PBS and sonicated using a ChIP sonic digital Sonicator (Branson, Germany) at 70% amplitude, with 10-second on/off cycles, for 30 minutes at 4°C.

4.7.3 HEK biosensor cell culture and Tau seeding

HEK 293T cells stably expressing YFP-tagged 4R Tau-repeat domain including the P301S mutation (Holmes et al., 2014) were used as a model for studying the degradation of Tau aggregates. These cells were maintained every 3 days in DMEM high glucose medium (Gibco, #31966-047), supplemented with 10% fetal bovine serum (FBS, Gibco, #26140-079) and 100 µg/ml Gentamicin (Gibco, #15750-045), at 37°C in an environment of 8% CO2. For seeded Tau aggregation, the cells were transfected with 100 nM recombinant Tau seeds. Transduction complexes were prepared by incubating recombinant seeds with Opti-MEM (Gibco, #31985-047) and Lipofectamine 2000 reagent (Invitrogen, #11668-019) at room temperature for 20 minutes before being added to the cells.

4.8 Human iPSC-derived neuronal culture and Tau seeding

The human inducible pluripotent stem cell lines used in this study are isogenic and derived from the line iPSC0028 (SIGi001-A), obtained from Sigma. The MAPT WT clone used in this study was an unedited subclone of the original iPSC0028 clone. In addition to the MAPT wild type (MAPT WT) neurons, expressing 0N3R Tau, genetic modifications were introduced to obtain MAPT knock out (MAPT KO) or MAPT "triple mutant" (MAPT TM) neurons (Manos et al., 2022). The MAPT TM line expresses MAPT P301S/ E10+14+16 Tau, whose pathogenic and splice site mutations lead to an increased expression of 4R Tau and includes the aggregation-promoting mutation P301S (Manos et al., 2022; Verheyen et al., 2018).

iPSCs were differentiated into cortical neurons, as previously described (Manos et al., 2022), by inhibiting dual SMAD signalling with a small molecule cocktail according to modified published protocols (Cao et al., 2017; Chambers et al., 2009; Gaspard et al., 2008; Hansen et al., 2011; Manos et al., 2022; Verheyen et al., 2018). At DIV14 (14 days in vitro) after final plating, neurons were exposed to Tau seeds to introduce seeded Tau aggregation (Limorenko et al., 2023). We compared the seed-induced changes of MAPT TM neurons with 100 nM recombinant Tau seeds (calculated according to the concentration of Tau monomer) to the changes obtained with seeding using 0.5 nM AD-brain derived seeds in MAPT WT neurons. The MAPT KO iPS-derived neurons seeded with both seed types, respectively, were used as a negative control for endogenous aggregation. The cells were cultured for additional 4 weeks to allow for seeded Tau aggregation to occur, with a 50% media change every 5 days. Cells were fixed 4 weeks post seeding in ice-cold methanol for 20 minutes on ice. Tau aggregation

was measured via immunofluorescence imaging, detecting the MC1-positive Tau aggregates as previously described (Limorenko et al., 2023; Manos et al., 2022).

4.9 Immunofluorescence staining (IF)

Paraformaldehyde (PFA) or Methanol Fixed cells were treated with a blocking buffer of 5% BSA in PBS for at least one hour at room temperature. Primary antibodies (table 8), diluted in the blocking buffer, were then applied to the cells and incubated overnight at 4°C. The following day, fluorophore-labeled secondary antibodies (table 8) were added at a 1:500 dilution in blocking buffer and incubated for one hour at room temperature in the dark. The cells underwent three 10-minute washes in PBS, with the final wash containing Hoechst (Dako) diluted 1:10000 in PBS for nuclei staining. Immunofluorescence staining was performed using the Operetta instrument (PerkinElmer) and images were analyzed with Harmony Software (Pevvity Inc). Imaging of Tau aggregation was captured at 40X magnification in confocal mode.

4.10 siRNA-mediated gene knock down

To achieve gene knockdown via small inhibitory RNA (siRNA), mature hiPS-derived neurons were transfected at DIV14. In preparation, the cell culture medium was replaced with a Pen-Strep-free complete medium one day before transfection. 5 µM siRNA (siGenome smartpool, Horizon Discovery, detailed in table 3) was thawed on ice and diluted in media at a 1:20 ratio, then mixed with Dharmafect 1 transfection reagent (Horizon Discovery #T-2001-03), which first was diluted in media at a 1:100 ratio, in a 1:1 proportion. After incubating for 20 minutes at room temperature, 20 µl of the transfection mixture was gradually added to the 80 µl of media already on the cells. Each experiment included a non-targeting siRNA control and a non-transfected control.

4.11 qPCR

Real-time quantitative polymerase chain reaction (qPCR) was conducted to assess knockdown efficiency following siRNA-mediated gene knockdown. The TaqMan Fast Advanced Cell-to-CT Kit (#A35374, Thermo Fisher) was used according to the manufacturer's instructions. Briefly, cells were lysed with the lysis solution containing DNase I, followed by a reverse transcription step to generate cDNA. Here, a master mix, consisting of the 2x Fast Advanced RT buffer and the 20x Fast Advanced RT enzyme mix, was added to the lysate. RNA was reverse transcribed into cDNA for 30 minutes at 37°C, followed by a RT inactivation step for 5 minutes at 95°C, using the MiniAmp Plus Thermal Cycler. Subsequently, various TaqMan assays (Thermo Fisher, table 7) combined with the TaqMan Advanced Master Mix were used to perform real-time qPCR measurements. The samples were analyzed with the QuantStudio 7 Flex PCR machine (Applied Biosystems) and the data were processed using the QuantStudio Real-Time PCR software.

4.12 Proteomics and Phosphoproteomics changes in iPS-derived neurons

4.12.1 Sample preparation

Prior to mass spectrometry, samples need to be prepared accordingly. In brief, 1.5 million iPS-derived neurons for each condition were lysed in 250 µl of mass spec sample prep lysis buffer, which contained 8M Urea, 100 mM Tris (pH 8), 100 mM TCEP (Sigma, #C0267-100G), 40 mM chloroacetamide (Sigma, #C4706-2G), a protease inhibitor cocktail (Sigma, #11836170001),

and a phosphatase inhibitor (Sigma, #4906837001), followed by reduction and alkylation. Protein concentrations for each sample were determined using a BCA protein assay (Thermo Fisher Scientific, #23225). An equal protein amount from each sample was aliquoted, diluted to 1.5 M urea with 100 mM Tris, and digested overnight with a trypsin/Lys-C enzyme mixture (Promega, V5071) at a 1:50 enzyme-to-substrate ratio. Each sample was then acidified to 0.1% TFA, desalted with 100 mg Strata-X polymeric reversed-phase desalting columns (Phenomenex, #8B-S100-ECH), and dried using vacuum centrifugation. Afterward, samples were desalted, lyophilized, and resuspended in 100 mM triethylammonium bicarbonate buffer in preparation for tandem mass tag (TMT) labeling.

4.12.2 TMT labeling

Two sets of TMTpro 16plex reagents were employed to chemically label the samples (n = 30) (table 15). Each reagent set labeled 15 samples using the respective TMT 16-plex isobaric chemical tag (Thermo Fisher Scientific, #A44520). The 16th channel included a mix of all 30 study samples to serve as a reference for normalization and cross-comparison of relative differences across the two TMT 16-plex sets. Each set of TMT 16-plex peptides was combined, quenched, and desalted a second time using Strata-X columns, then individually resuspended in 80% ACN with 0.1% TFA. Phosphopeptides were enriched using Qiagen Ni-NTA beads as described below, while the flowthrough from Fe-IMAC enrichment, containing non-phosphopeptides, was used for proteome quantification.

4.12.3 Phosphopeptide enrichment

Samples were concentrated through vacuum centrifugation and then resuspended in a solution containing 80% ACN and 0.15% TFA. Ni-NTA magnetic agarose beads (Qiagen #36113) were cleaned with 40 mM EDTA and rinsed with water, before chelating Fe3+ onto the beads for 30 minutes at room temperature and 1350 RPM in a ThermoMixer. The beads were washed with the same buffer used for the samples (80% ACN and 0.15% TFA) and distributed evenly across all samples at a rate of 500 µl of beads per mg of sample. FeIMAC beads were incubated with the samples in a ThermoMixer at room temperature and 1350 RPM for 30 minutes. Phosphopeptides were then eluted using a 50% ACN and 0.7% ammonium hydroxide solution, followed by immediate acidification with 4% FA. The eluate was concentrated and resuspended in 0.1% formic acid before injection for MS analysis. Each set of TMT phosphopeptide and proteome samples was fractionated using a Waters Acquity UPLC. Peptides were separated using a linear gradient starting with aqueous 20 mM ammonium formate, gradually increasing the organic phase content to 20 mM ammonium formate in 80% ACN, using a 2.1 x 100 mm UPLC column packed with 1.7 µm BEH C18 material (#186002352). Both phosphopeptide and proteome samples were divided into 12 fractions, concentrated through vacuum centrifugation, and resuspended in 0.1% formic acid.

4.12.4 Mass spectrometry

Thermo Fisher Scientific Ultimate 3000 RSLCnano HPLC, paired with a Thermo Fisher Scientific Fusion Orbitrap Lumos mass spectrometer was used for analysis of peptides and phospho-peptides. Peptides were eluted with a linear gradient from 6% to 35% ACN over 105 minutes, followed by a 16-minute column wash at 100% ACN. The Lumos was set to data-dependent acquisition (DDA) mode with an MS1 scan range of 300–800 m/z at a resolving power of 120,000. A normalized AGC target of 4E5 was used, with a maximum injection time of 50 milliseconds. Peptides with a charge state of 2–7 were considered for fragmentation, with a

dynamic exclusion set to 30 seconds. They were selected with a 0.8 m/z isolation window and an HCD normalized collision energy of 34%. Tandem mass spectra were analyzed in the Orbitrap at a resolving power of 50,000, with AGC targets of 50,000 for peptides and 100,000 for phosphopeptides, and a maximum injection time of 120 milliseconds. Each of the 12 phosphopeptide fractions was analyzed in duplicate, with two technical replicates injected for each fraction.

4.12.5 Proteomics and phosphoproteomics data analysis

MaxQuant version 1.6.17.0 with the experiment type set to TMTPro 16-plex chemical modifications was used to search the data. Tryptic enzyme digestion was specified with a maximum of two missed cleavages. Chemical modifications considered for data searching included a fixed modification of carbamidomethylation of cysteines and variable modifications of methionine oxidation, acetylation of protein N-termini, and phosphorylation of serine, threonine, and tyrosine residues (for phosphoproteome MS data searches). All data were searched against a target-decoy UniProt human protein database containing both canonical and reverse sequences of proteins and their isoforms, downloaded on September 05, 2021. Peptide spectral matches were filtered to an FDR of less than 1% using a target-decoy strategy. Protein identifications were also filtered to obtain a protein FDR of less than 1% using a target-decoy strategy to model false positives. Reporter ion MS2 spectra were used for TMTpro quantification with a precursor ion mass tolerance of 4.5 ppm and a fragment ion mass tolerance of 20 ppm for determining relative peptide and protein quantitation.

MaxQuant protein group and phosphosite quantitation tables were exported and analyzed using the R programming language. Reverse identifications, potential contaminants and proteins only identified by site were filtered. Protein group and phosphosite intensities were normalized using variance stabilization normalization using the vsn package. Differential expression was tested using limma and empirical Bayes variance estimation while adjusting for a batch effect coming from multiple neuronal progenitor cell differentiation rounds from which the biological replicates were derived. The Benjamini-Hochberg procedure was used to adjust for multiple testing. Pathway enrichment analysis was performed using the clusterprofiler package.

4.13 Western Blot

Samples were heated at 95°C for 10 minutes in 2X Laemmli buffer (Bio-Rad #1610737) with Dithiothreitol (DTT, Serva #20710.02), then separated on a 4-20% Criterion TGX precast gel (Bio-Rad #5671095) and transferred onto methanol-activated polyvinylidene fluoride (PVDF) membranes using the Trans-Blot Turbo RTA transfer kit (Bio-Rad, #1704275) and Trans-Blot Turbo Transfer System (Bio-Rad). The membranes were blocked overnight at 4°C with 2% BSA (Serva) in Tris-buffered saline (TBS, 25 mM Tris, 150 mM NaCl, pH 7.4) containing 0.05% Tween. Subsequently, membranes were incubated with primary antibodies (table 6) for 2 hours at RT. After several washes, they were incubated for 1 hour at room temperature with the respective secondary biotinylated antibody (also listed in table 6) diluted in TBST (TBS + 0.05% Tween20) with 0.1% BSA. Signal detection was performed using SuperSignal West Femto (Thermo Scientific #34095) or Clarity (Bio-Rad #170561) substrate and visualized with the Chemidoc reader (Bio-Rad).

4.14 Bead preparation and Co-immunoprecipitation

Magnetic Dynabeads M-280 (table 13) were washed three times with phosphate buffered saline (PBS, 20 mM NaH2PO4; 140 mM NaCl; pH 7,4) +0.1% bovine serum albumin (BSA, Serva #11926) and immobilized on an MPC-L magnet (Invitrogen). The beads were incubated with the respective antibody (table 12, 40 µg antibody/ml beads) over night at 4°C. The antibody-coated beads were washed 4 times for 30 min with PBS + 0.1% BSA and then cross-linked using Dimethyl Pimelimidate (DMP, Thermo Scientific #21667, 20 mM in Triethanolamine). The beads were washed 4 times for 5 min using Triethanolamine (in Millipore #1.08379.0250; 0.2M, pH 8.2), before incubation with DMP for 30 min while shaking at RT. After immobilization and removal of the supernatant, 50 mM Tris/HCL was added to the beads and incubated for 15 min while shaking at RT. Next, the cross-linked beads were washed four times with PBS+0.1%BSA. The beads were stored in PBS+ 0.1% BSA+ 0.02% Na-Azide at 4°C until further usage.

For immunoprecipitation, the antibody coated Dynabeads were immobilized on a magnetic stand and washed once with ice cold PBS. Cell or brain lysates corresponding to 50 µg total protein were added to 0.1 ml beads and incubated over night at 4°C while shaking. Next, the beads were washed three times with PBS containing 0.1% Triton X 100 for 10 minutes at RT. Co-precipitating interacting proteins were eluted by incubating the beads in 25 µl Laemmli buffer at 95°C for 10 minutes.

4.15 Cloning of NBR1 fragments with or without mutations in expression vector pCMV6 Entry

The human NBR1 cDNA was PCR amplified from a commercially available plasmid (Origene, NM_005899, RC215397) using specific primers (table 9) and cloned into the pCMV6 Entry mammalian expression vector (Origene PSD100001) using Acc65I (FD0904) and NotI (FD0593) (FastDigest, ThermoFisher Scientific) restriction enzymes. Phospho-mimetic (S to D) and phospho-resistant (S to A) mutations at S486 of NBR1 were introduced using a site-directed mutagenesis kit (Agilent, #200521) with appropriate primers (table 9). The accuracy of the mutagenesis in the purified DNA plasmid was confirmed by sequencing.

4.16 HEK biosensor cells overexpression of phospho-NBR1

For transfection with NBR1 overexpression plasmids, HEK biosensor cells were plated at a density of 10000 cells per well into a 96 well or 300000 cells per well into a 6 well plate, respectively, precoated with Poly-L-ornithin (PLO, Sigma #P4957). 24 h post plating, cells were transfected with overexpression constructs. Lipofectamine 2000 reagent (Invitrogen, #11668-019) and DNA plasmids were diluted in Opti-MEM (Gibco, # 31985-047) and incubated for 20 min at RT, before addition to the cells for a final concentration of 2500 ng DNA and 5 µl Lipofectamine (6 well) or 100 ng DNA and 0.1 µl Lipofectamine per well (96 well). 24h post transfection, cells were transduced with 100 nM recombinant Tau seeds, to introduce seeded Tau aggregation. Transduction complexes were generated by incubation of recombinant seeds with Opti-MEM and Lipofectamine 2000 reagent for 20 minutes at room temperature, before addition to the cells. Simultaneously, cells were treated with Bafilomycin (100 nM) to inhibit autophagy flux for 24 hours before lysis or fixation. 24h post seeding, cells were either fixed for 20 minutes at RT with 4% paraformaldehyde (PFA) for IF staining, or lysed in lysis buffer (150 mM NaCl, 20 mM Tris pH 7.5, 1 mM EDTA, 1 mM EGTA, 1% Triton x100 + Complete

Protease inhibitor (Roche) and PhosStop phosphatase inhibitor (Roche) to perform Western Blot analysis.

4.17 BioID in iPS-derived neurons

Human inducible pluripotent stem cells were infected with four different lentiviruses carrying Tau-BioID constructs or BioID-only constructs (table 10) at iPSC stage. After infection with the letiviral particles carrying the Tau-BioID constructs, the cells were differentiated into neurons within a time span of 14 days, using a Doxycycline inducible (Bioneer) NGN2 overexpression system (Zhang et al., 2013). The parental cell line was BIOMEDi004-A (Coriell Fibroblast AG08125) with CRISPR Cas induced disruption of exon 1 MAPT knockout (KO). Construct cloning and lentivirus generation was conducted by Origene.

In brief, cells were washed once with PBS and 1 ml Accutase was added to detach cells from wells, 5x amount of N2B27-1 medium was added to dilute the accutase and cell suspension was centrifuged for 5 min at 300xg. The supernatant was removed, and cells were carefully resuspended in Neuronal maintenance medium + 10 µM Rock inhibitor (Y-27632, Millipore #688000) + 500 nM RO compound (Sellekchem #S1676) + 500 nM Cyclopamine (Millipore # 239806). Meanwhile, the virus was thawed on ice. Cells were plated with a density of 600.000 cells per condition and simultaneously infected with one of the constructs using either MOI2 or MOI3. Cells were kept in half of the total medium, while virus was diluted in another half of total medium. Both suspensions were carefully combined and directly transferred to plates, that were previously matrigel coated. First, a complete medium exchange was conducted 24h post infection using StemFlex medium. The second complete medium change was conducted 48h post infection using Stemflex medium supplemented with Blasticidin and Puromycin to start the selection process. A third medium exchange was conducted on day 3 after replate, again using StemFlex medium containing selection antibiotics. Cells were incubated overnight, before medium was replaced with E8 Flex medium (Gibco), without antibiotics, and cells were maintained for another 3 days, until split in E8 Flex medium.

DIV0, the media was replaced with 4-5 mL of N2B27M complete medium per well, containing 2 µg/ml Doxycycline (Dox, Sigma). This step was required to dilute the ROCI and start the differentiation of iPSCs into neurons. The cells were maintained for two days at 37°C.

DIV2, the differentiated iPSCs were replated into PLO and Matrigel pre-coated 96 well plates (Corning). Cells were washed with DPBS without Mg2+ and Ca2+. 1 mL of Accutase, containing 10 µM ROCI per well was added and the plates were incubated for 5-10 minutes at 37°C, until the cells were completely detached. Next, the cells were collected in 7 mL B27 base media or in split medium (DMEM/F12, containing 0.1 % BSA) and centrifuged at 300 g for 5 minutes. The pellet was resuspended in B27M media, containing 2 µg/ml Dox, 500 nM Roche compound (RO, Roche) and 10 µM ROCI.

DIV3, 50% of the media was replaced with fresh B27M complete media per well, containing Dox and RO, in order to dilute the ROCl. DIV6, 50% of the media was again replaced with fresh B27M complete. DIV6, 50% of the media was replaced with B27M complete. The cells were maintained at 37°C, until they were utilized for experimental assays on DIV14 or DIV49.

Twenty-four hours before cell lysis, cells were treated with 250 µM biotin (Sigma #B4501) diluted in media. Subsequently, co-immunoprecipitation was performed to capture all biotin-labeled proximity proteins. Briefly, magnetic Dynabeads M280 Streptavidin (Invitrogen #11205D) were washed with PBS and blocked with PBS containing 0.1% BSA for 1 hour at room

temperature. A total of 150 µg of protein lysate was added to the binding buffer (PBS with 20 mM Na-phosphate, 140 mM NaCl, pH 7.4, and 0.1% Triton X-100, using a 1:4 ratio of lysate to binding buffer) and incubated overnight at 4°C. Beads were then washed four times with washing buffer.

For elution, beads were boiled for 10 minutes at 95°C in an elution buffer containing 0.1% SDS, 100 mM TEAB, 10 mM TCEP, and 50 mM CAA (eluate 1). Subsequently, on-bead digestion of peptides was performed overnight at 37°C by adding 0.5 µg/µl Trypsin/Lys-C to eluate 1, which still contained the beads. Peptides were purified using SP3 (Hughes et al., 2019) cleanup for mass spectrometry by adding 10 µl of SP3 beads per sample (a 1:1 mixture of SpeedBead Magnetic Carboxylate [Cytiva #45152105050250] and Sera-Mag Magnetix Carboxylate [Cytiva #24152105050250]). Acetonitrile was added to a final concentration of 95%, and samples were incubated for 20 minutes at room temperature. The supernatant was discarded, and beads were washed twice with acetonitrile. After complete drying to remove residual acetonitrile, beads were reconstituted in 20 µl of 0.1% TFA and sonicated for 5 minutes. The eluates were then transferred, and DIA mass spectrometry and data analysis was performed as described in section 4.5. and 4.6.

5 Results

5.1 Proteomics-based distinction of physiological from pathological Tau interactome in human brain

5.1.1 Phospho-Tau antibodies differentiate between sarkosyl-soluble and sarkosyl-insoluble Tau

The Tau interactome is expected to provide valuable insights into pathways and proteins affected by Tau, which may change as disease progresses, helping to understand the underlying biology, and potentially uncovering novel targets for therapeutic intervention. Despite this potential, no prior studies have systematically compared the interactomes of physiological and pathological Tau in AD.

To address this, the Tau interactome was thoroughly investigated in human brain tissue from AD and control patients. To directly compare physiological to pathological Tau interactomes, both phosphorylated and total Tau antibodies were utilized within the same experiment. Phospho-Tau antibodies selectively bind to phosphorylated Tau epitopes, whereas total Tau antibodies detect all forms of Tau, regardless of phosphorylation status. The physiological Tau interactome was examined using total Tau antibodies in control brain tissue, while the pathological Tau interactome was specifically targeted with phospho-Tau antibodies in AD brain tissue. Pathological Tau encompasses phosphorylated and aggregated Tau capable of inducing seeded Tau aggregation. Interactomes of Tau species that were precipitated with different antibodies from the same sample were then compared.

In this study, three total Tau and three phospho-Tau antibodies were utilized for co-immunoprecipitation of interactors from five human AD and five age-matched control postmortem brains, respectively. The parallel IPs were followed by label free quantitation mass spectrometry and data independent acquisition (DIA) to identify interactors of the respective Tau species (figure 4).

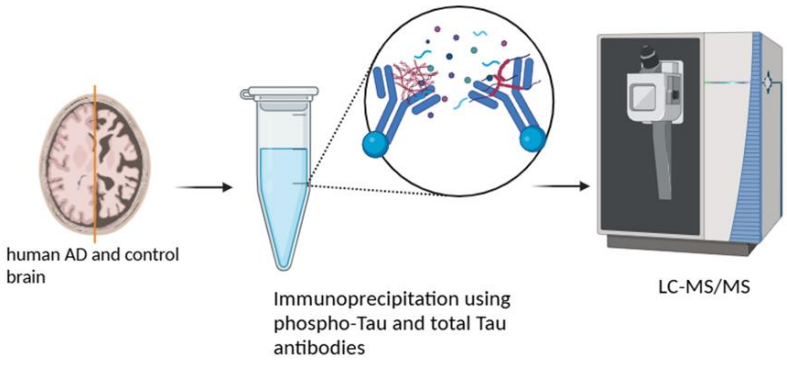

Figure 4: Proteomic analysis of Tau interacting proteins in human AD and control brain using different total Tau and phospho-Tau antibodies

***a** Human AD and control brain tissue are lysed and subjected to immunoprecipitation using three total Tau and phospho-Tau antibodies. The parallel IPs are followed by label free quantitation mass spectrometry and data independent acquisition to identify interactors of the respective Tau species. n=5 human AD and 5 human control brain samples. Figure created with Biorender.*

First, immunoprecipitation antibodies were selected. Here, the aim was to select phospho-Tau antibodies that specifically target phosphorylated Tau species and Tau aggregates, while also confirming that total Tau antibodies could capture all forms of Tau. Various antibodies, each recognizing different Tau epitopes, were characterized through biochemical profiling (figure 5). This profiling employed a sandwich ELISA method to assess the binding capacity and specificity of different total Tau or phospho-Tau antibodies (figure 5a, table 12) against various Tau antigens (table 14). The characterized antibodies served as capture antibodies, while a total Tau antibody was used as a detection antibody.

The antigens, representing diverse Tau species, were sourced from AD and control brains, along with recombinant Tau (table 14). Antigen fractions were obtained via sarkosyl extractions from human AD or control brain tissue, which allowed for separation based on size and diffusibility (figure 3) (Greenberg and Davies, 1990; Guo and Lee, 2011; Schlegel et al., 2019). The fractions included brain lysates, or sarkosyl-treated pellet (P3) fractions, which contain sarkosyl-insoluble aggregated forms of Tau, and supernatant (S) or the supernatant of supernatant (SS) fractions, which contain sarkosyl-soluble forms of Tau (figure 3). Hexafluoroisopropanol (HFIP) treatment denatured the antigens, exposing hidden phospho-sites and linearizing Tau aggregates. Additionally, recombinant Tau seeds (sPHFs) were included to evaluate binding efficacy. The area under the curve (AUC) for each antibody detecting specific antigens was normalized to the capacity of a chosen sandwich total Tau antibody pair. Since the capture antibodies originated from different species, comparisons were confined to the same species. Mouse capture antibodies were normalized to the Tau12_Dako capture-detection pair, and rabbit capture antibodies were normalized to the Tau12_HT7 capture-detection pair. To The AUC results were depicted in a radar chart. As far as the species allowed, all total Tau antibodies and all phospho-Tau antibodies were compared with each other in a radar chart. (figure 5b+c).

Biochemical profiling of the antibodies demonstrated that the total Tau antibodies HT7, 2B8, and Tau12 effectively bind to both sarkosyl-soluble and sarkosyl-insoluble Tau species, without distinguishing between AD, control, or recombinant sPHFs, as expected (figure 5b). In contrast, Tau5 and Tau46 exhibited lower binding efficiency across different antigens, particularly failing to detect SS1 species in both AD and control samples (figure 5b). The conformation-specific MC1 antibody, known to recognize aggregated forms of Tau, detected recombinant sPHFs, as well as sarkosyl-insoluble Tau species in the AD P3 fraction. However, MC1 did not recognize any aggregates in the AD SS1 fraction (figure 5b). While Tau 77G7 captured most Tau species, its binding capacity for recombinant seeds was reduced compared to other total Tau antibodies (figure 5b).

Almost all phospho-Tau antibodies specifically capture antigens derived from AD brains but not from control brains, as anticipated (figure 5c). Since recombinant Tau seeds lack phosphorylation, they are generally not recognized by most phospho-Tau antibodies. However, the pT231 and pS416 antibodies did exhibit binding, indicating potential nonspecific interactions (figure 5c). Like MC1, the pS416 Tau antibody demonstrated a conformational effect differentiating between HFIP-treated and non-treated antigens (figure 5c). The majority of phospho-Tau antibodies followed a similar biochemical profiling pattern, whereas PHF1, AT100, pS198 and AT8 showed a particular strong binding capacity for AD pellet fractions and Tau species present in AD lysate (figure 5c).

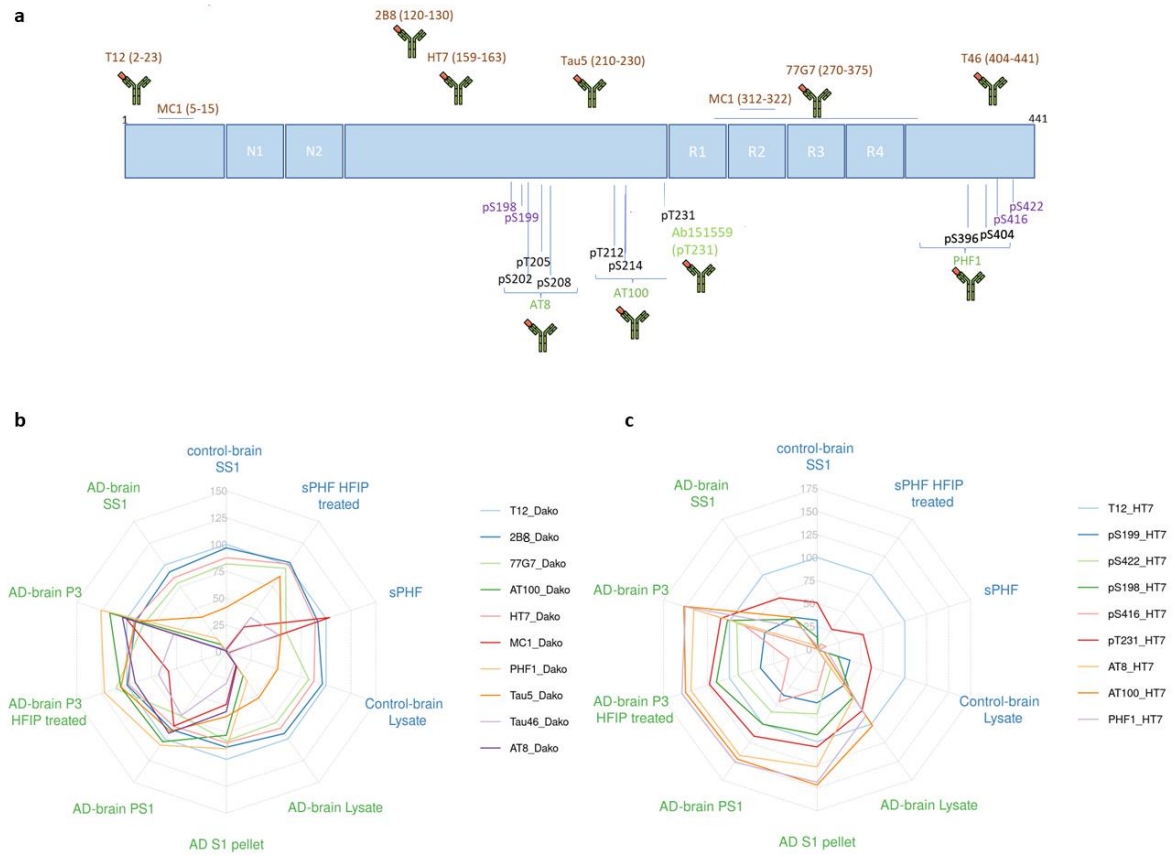

Figure 5: Biochemical profiling shows different binding capacities of total Tau vs phospho-Tau antibodies to Tau antigens

***a** Epitope map of Tau antibodies (brown), and phospho-Tau antibodies (green and purple) for characterization via biochemical profiling. **b+c** Sandwich ELISAs were performed to characterize binding efficiency of different Tau antibodies to selected AD and control relevant Tau antigens, area under the curve (AUC) was normalized to the AUC obtained for T12_Dako (b) or T12_HT7 (c) depending on antibody species. As far as the species allowed, all total Tau antibodies and all phospho-Tau antibodies were compared with each other in a radar chart. Total Tau antibodies 2B8, HT7, and Tau12 recognize all forms of Tau. In contrast, Tau5, Tau46, and 77G7 show weaker binding across Tau species, particularly in AD and control SS1 fractions and recombinant sPHFs. HFIP treatment of antigens highlights conformational sensitivity of the MC1 and pS416 antibodies. Phospho-Tau antibodies can distinguish between phosphorylated Tau in AD and control tissues. AT100, PHF1, and pS198 robustly detect Tau in AD brain-derived fractions and AD SS1. As expected, phospho-Tau antibodies do not detect recombinant sPHFs, except for pT231, which also binds Tau in control brain fractions and recombinant sPHFs—suggesting potential nonspecific binding. Antigens were derived from sarkosyl-extraction protocol (figure 3). Abbreviations: P=pellet, S=supernatant, SS1 = supernatant of supernatant 1, sPHF= soluble paired helical filaments (recombinant Tau seeds), HFIP= Hexafluorisopropanol, P3= pellet 3, PS1= pellet of supernatant S1*

Next, brain material anticipated as IP input was selected. Therefore, human brain tissue from AD patients (Braak stages IV-VI) and age-matched control brains (Braak stages 0-II) were obtained from biobanks (table 11). To verify the presence of Tau aggregates in AD brains as opposed to control brains, an aggregated Tau ELISA method was employed to measure aggregated Tau levels in the respective brain homogenates. In this method, the same monoclonal antibody was used for both capturing and detecting Tau, which means that monomeric Tau species, where the epitope is not present twice, could not be detected (Ercan-Herbst et al., 2019). A range of AD brain lysates were assessed for aggregated Tau levels (table 20).

table 20: ELISA results allowed selection of brain homogenates via aggregated/total Tau ratio

Homogenate	Total Tau [ng/ml]	Aggregated Tau [ng/ml]	Ratio [aggregated Tau/total Tau]
AD1	8458	4594	0.54
AD2	9342	3679	0.39
AD3	8342	3810	0.46
AD4	5571	4665	0.84
AD5	10244	4661	0.46
AD6	12170	2235	0.18
AD7	9773	3676	0.38
AD8	12154	1660	0.14
Ctrl1	10328	762	0.07
Ctrl2	13608	1507	0.11
Ctrl3	13785	920	0.07
Ctrl4	10995	955	0.09
Ctrl5	8559	479	0.06

AD1-AD5 samples were chosen for further analysis because they exhibited the highest ratio of aggregated Tau to total Tau (table 20). Before proceeding with immunoprecipitation, the brain homogenates underwent sarkosyl treatment (AD S1 and control S1 IP input), containing sarkosyl-soluble and sarkosyl-insoluble Tau species. ELISA assays for total Tau and aggregated Tau validated that total Tau levels were consistent in AD and control S1 samples, whereas aggregated Tau was only detectable in AD brain-derived samples, as anticipated (figure 6a).

A second round of biochemical profiling was conducted to verify the antibodies' binding affinity to AD and control S1 IP input (figure 6b+c), normalized to the binding capacity of Tau12_HT7 or Tau12_Dako. PHF1 effectively differentiated between S1 inputs from AD and control brains, whereas pS198, pS199, and pT231 also identified Tau in control S1 inputs, albeit to a lesser extent. Similar to PHF1, AT100 and AT8 exhibited a consistent biochemical profile, showing strong binding affinity to AD S1 inputs, with no binding to standards or control S1 inputs. In contrast, pS416 showed weaker binding affinity to AD S1 input compared to other phospho-Tau antibodies. While 2B8 and HT7 detected all antigens with similar specificity, Tau5 and 77G7 displayed reduced binding capacity to the pTau standard (figure 6c). MC1 and Tau46 did not detect Tau present in control S1 inputs (figure 6c).

Based on the biochemical profiling, total Tau antibodies HT7, 2B8, and Tau12, along with phospho-Tau antibodies AT100, pS198, and PHF1, were selected for further immunoprecipitation experiments (figure 6d). These antibodies met the profiling criteria, with phospho-Tau antibodies targeting phospho-Tau and sarkosyl-insoluble Tau aggregates, present in AD derived antigens, while total Tau antibodies effectively detected all forms of Tau.

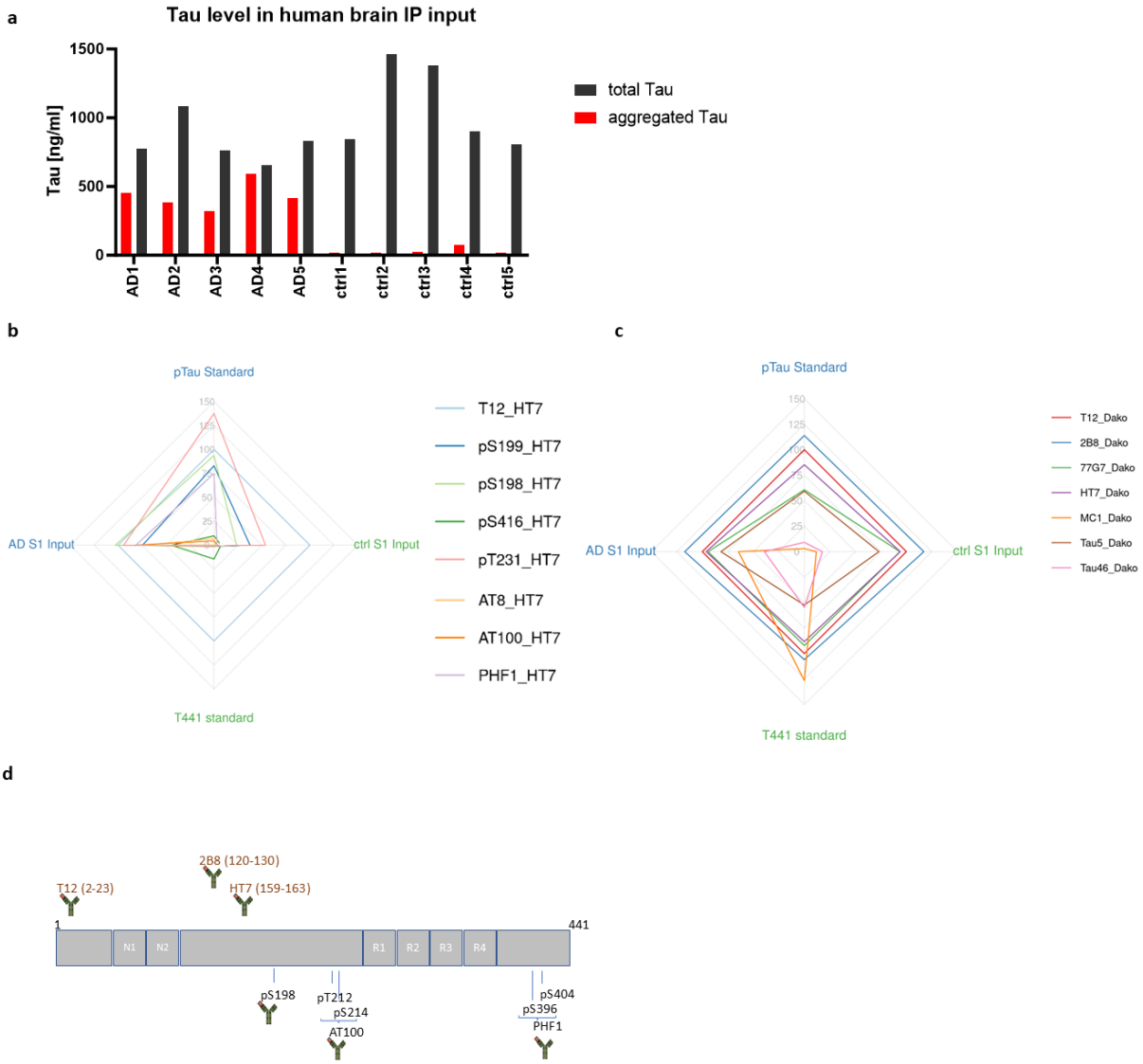

Figure 6: Selection of AD and control brain tissue and antibodies for immunoprecipitation

***A** Brain tissue for IP input was selected from five sarkosyl-treated human AD and control brains (S1 IP input) based on total Tau and aggregated Tau levels measured by ELISA. Both AD and control S1 inputs showed high total Tau levels, whereas aggregated Tau (red) was found exclusively in AD brain S1 input. **b+c** Biochemical profiling was performed via a sandwich ELISA with AD S1 and control S1 input, additionally utilizing phospho-Tau and total Tau standard (T441) as antigens. Phospho-Tau antibodies primarily recognize phosphorylated forms of Tau in the AD S1 input and the phospho-Tau standard. AT100 and AT8 phospho- Tau antibodies exclusively detect Tau in the AD S1 input. Total Tau antibodies identified Tau species in both the AD and control brain S1 input, as well as in the total Tau or phospho-Tau standards. Tau46 antibody do not detect Tau species in the control S1 input. The area under the curve for each antibody's binding capacity is normalized to the AUC obtained for T12_HT7 (b) or T12_Dako (c), according to the capture antibody species. n=pool of 5 AD or control S1 inputs used. **d** Epitope map of Tau antibodies selected for immunoprecipitation experiments. Total Tau: HT7, 2B8, Tau12; phospho-Tau: pS198, AT100, PHF1.*

Test IPs from human brains were performed, followed by a sequential elution process, with the secondary elution including a boiling step to fully release bound proteins from the beads. The total Tau levels in each IP fraction were quantified via ELISA (figure 7). The secondary elution turned out to be necessary to elute the full amount of Tau captured by Tau12 (figure 7), hence the IP eluate 2 was used as input for subsequent MS. The total Tau levels in each fraction were normalized to the Tau levels present in the corresponding S1 input before

immunoprecipitation (figure 7). The eluates from IPs with total Tau antibodies HT7, Tau12, and 2B8 contained the majority of total Tau, indicating efficient capture. In contrast, immunoprecipitation with phospho-Tau antibodies resulted in only a small portion of Tau detected in the eluates, with a higher proportion remaining in the supernatant. This suggests that phospho-Tau antibodies exhibit greater specificity for less abundant, phosphorylated Tau species. Using IgG control as the IP antibody did not result in Tau co-immunoprecipitation, indicating no unspecific binding.

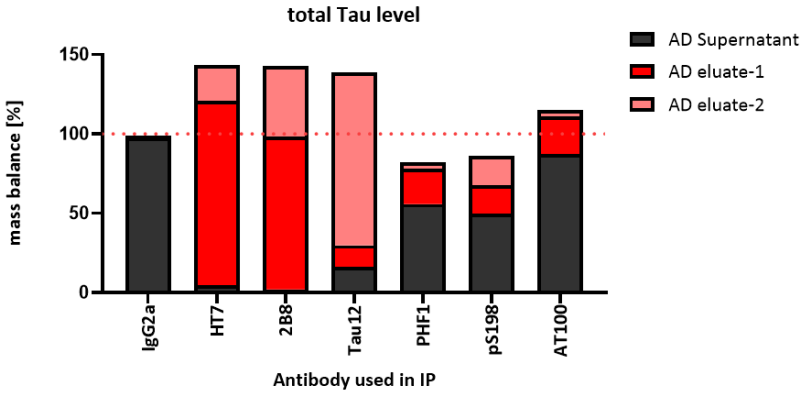

Figure 7: Tau abundance in IP eluates from human AD brain differs according to bait antibody

Total Tau levels in different immunoprecipitation (IP) fractions were quantified using a total Tau ELISA. Following IP from human AD brain S1 input with phospho-Tau antibodies (pS198, AT100, PHF1), a portion of total Tau remained in the supernatant (black), while a smaller fraction was detected in the eluate (red). In contrast, total Tau antibodies (HT7, 2B8, Tau12) efficiently captured nearly all Tau, which was recovered in the eluates. "Eluate 2" represents the fraction obtained after an additional boiling step to ensure complete dissociation from the IP beads. Minimal Tau was pulled down with IgG, confirming specificity. The graph shows the percentage distribution of total Tau across supernatant and eluates relative to the input (mass balance). Test IP; input n = pool of 5 AD S1 input.

To assess the seeding capability of any remaining Tau species post immunoprecipitation, a HEK Biosensor seeding assay was utilized (Holmes et al., 2014). This assay allowed the quantification of seeding potency of remaining Tau species, after immunodepleting with different Tau antibodies (figure 8a). Thus, it can confirm that the respective bait antibodies for immunoprecipitation capture the seeding-competent Tau species.

The HEK Biosensor seeding assay utilizes human embryonic kidney (HEK) cells that express the fluorescently tagged repeat-domain of Tau, including the P301S mutation. Seeded Tau aggregation can be introduced by the addition of external Tau seeds, leading to the formation of intracellular aggregates, which can be visualized and quantified due to the fluorescent reporter attached to Tau.

Notably, only the AD brain IP input contained seeding-competent Tau, while IP input from the control brain did not induce seeded Tau aggregation (figure 8b). The seeding capacity of AD brain samples was significantly decreased after immunodepleting with all Tau antibodies, but specifically with phospho-Tau antibodies PHF1 and pS198 (figure 8b). Even though the amount of Tau captured by the phospho-Tau antibodies is lower, compared to the total Tau antibodies (figure 7), this biosensor seeding assay confirmed that the phospho-Tau antibodies specifically captured the seeding-competent, pathology-relevant Tau species.

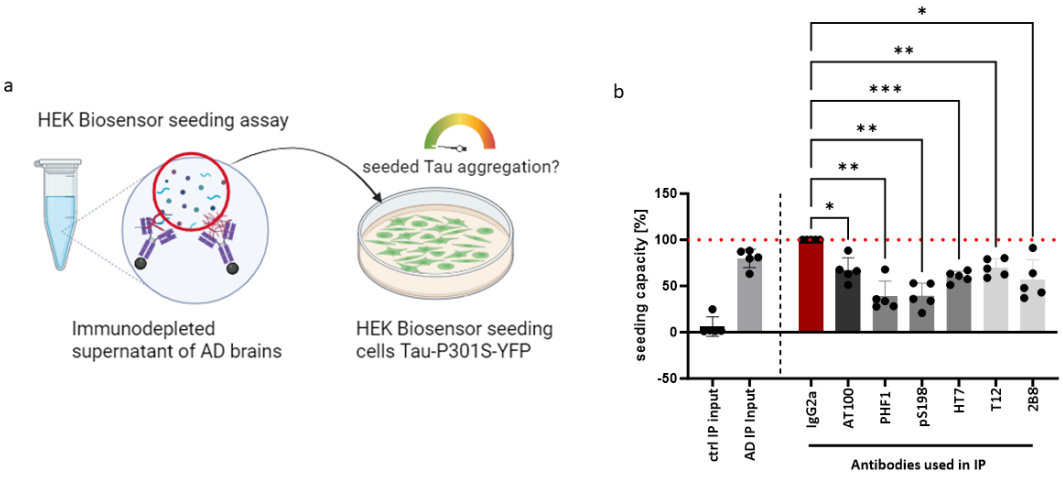

Figure 8: Tau species captured by IP antibodies were seeding-competent

***a** HEK biosensor cells expressing Tau-P301S-YFP develop fluorescent puncta detectable by microscopy upon exposure to AD brain-derived material containing pathogenic, seeding-competent Tau (Holmes et al., 2014). This assay was used to evaluate control and AD brain IP input, as well as Tau-immunodepleted AD brain samples, for residual seeding activity. Figure created with BioRender. **b** Seeding activity was assessed using the HEK biosensor assay, revealing that AD brain IP input contains seeding-competent Tau, whereas control brain input does not. Immunodepletion with Tau antibodies reduced this seeding activity, with phospho-Tau antibodies PHF1 and pS198 having the most pronounced effect. Seeding capacity is expressed relative to the mean of the IgG2a IP samples (red line). Statistical analysis: ONE WAY ANOVA ($p<0.0001$) with Dunnett's multiple comparison test *p=0.02, **p=0.005, ***p=0.0005. Immunodepletion of n= 5 human AD S1 brain samples, respectively.*

5.2 Data independent acquisition mass spectrometry to identify Tau interacting proteins

The careful selection of brain tissue and antibodies ensured that total Tau antibodies capture all Tau species, while the phospho-Tau antibodies accurately differentiated between physiological and pathological Tau, which is phosphorylated and seeding-competent.

The selected antibodies and brain samples were used to investigate Tau-interacting proteins directly in the human brain. Brain tissue from individuals with AD control subjects was lysed and subjected to immunoprecipitation using the selected total Tau antibodies (HT7, Tau12, and 2B8) and phospho-Tau antibodies (PHF1, pS198, and AT100). The eluates resulting from the parallel immunoprecipitations were analyzed by label-free quantitation mass spectrometry and data-independent acquisition to identify interactors specific for each Tau species. Only proteins with significantly higher enrichment compared to the IgG control were classified as interactors.

Quality control of the mass spectrometry run confirmed 81% of data acquisition completeness and the identification of 2686 proteins across all samples (figure 9a). Proteomic analysis showed the clustering of samples according to disease state and IP bait antibody (figure 9b), ensuring the similarity of biological replicates and indicates a significant difference in interactomes of Tau in AD and control (figure 9b).

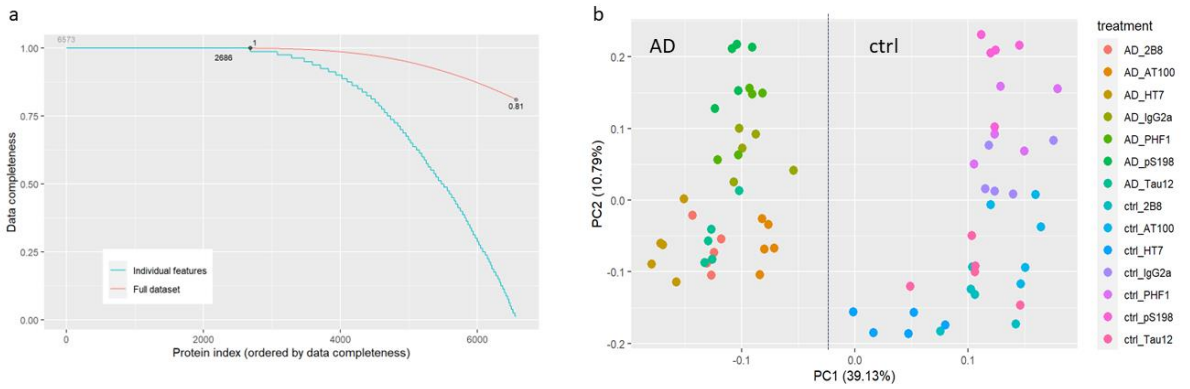

Figure 9: DIA analysis confirmed data completeness and clustering of samples according to disease state and bait antibody

***a** Data completeness of 81% was confirmed by MS quality control. A total number of 2686 proteins were identified across all samples. **b** Principal component analysis (PCA) of the proteomic data shows a clear separation of AD (left) from control brain (right) samples. Furthermore, the IP samples cluster according to the bait antibody. n=5 human brain samples, respectively; n=3 total Tau or total Tau IP antibodies, respectively. IgG was included as a negative control.*

5.3 Difference in Tau abundance according to IP bait antibody

To assess the efficiency of the Tau immunoprecipitation experiment, the levels of Tau in IP eluates measured by mass spectrometry were analyzed and compared to the IgG control (figure 10). Total Tau antibodies (HT7, 2B8, Tau12) extracted more Tau from AD brains than phospho-Tau antibodies (AT100, PHF1, pS198) (figure 10). In control brains, antibodies 2B8, Tau12, and HT7 efficiently immunoprecipitated Tau, whereas phospho-Tau antibodies captured only minimal Tau levels (figure 10). These results align with the ELISA-based analyses (figure 7). Among the phospho-Tau antibodies, AT100 captured the least amount of Tau from human AD brain samples (figure 10).

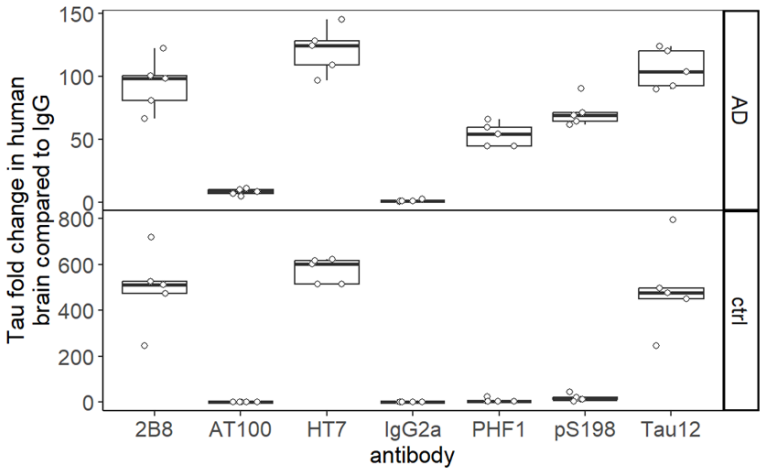

Figure 10: Different Tau abundance according to IP bait antibody

Tau abundance in IP eluates was quantified by DIA-MS and compared to IgG controls. Total Tau antibodies (HT7, 2B8, Tau12) pulled down significantly more Tau from AD brain samples than phospho-Tau antibodies (AT100, PHF1, pS198), with AT100 yielding the lowest Tau levels. In control brain samples, 2B8, Tau12, and HT7 also effectively immunoprecipitated Tau, whereas phospho-Tau antibodies captured only minimal amounts. Tau levels are shown as fold change relative to background levels from IgG2a IPs. Statistical analysis: Differential expression analysis using linear regression with limma and empirical Bayes moderation and subsequent multiple testing

correction using the Benjamini-Hochberg procedure; in AD brain: 2B8 vs IgG adjusted p-value=5.73e-19; AT100 vs IgG adjusted p-value=7.53e-10; HT7 vs IgG adjusted p-value=2.27e-20; PHF1 vs IgG=4.4e-18; pS198 vs IgG adjusted p-value=4.89e-19; Tau12 vs IgG adjusted p-value=2.53e-19; in control brain: 2B8 vs IgG adjusted p-value=1.21e-13; AT100 vs IgG adjusted p-value=0.752; HT7 vs IgG adjusted p-value=3.19e-15; PHF1 vs IgG adjusted p-value=0.00423; pS198 vs IgG adjusted p-value=0.00000251; Tau12 vs IgG adjusted p-value=1.32e-13; n= 5 human brain samples, respectively.

5.4 Phospho-Tau is immunoprecipitated from human AD and control brain

The significant enrichment of Tau combined with the highly sensitive DIA method enabled the analysis of phosphorylated Tau species without the need for prior phospho-peptide enrichment. Specifically, using phospho-Tau antibodies for immunoprecipitation allowed us to explore the phosphorylation pattern on the Tau species precipitated with each antibody.

The patient frequency plots display the number of AD and control human brains in which Tau phospho-sites were detected (figure 11a+b). The phosphorylation patterns in AD and control brains were quite similar, with sites distributed across the N- and C-terminals as well as the proline-rich region of Tau. The enriched phospho-peptides included many known AD epitopes such as pS212, pT217, pT231, pS396, and pS404 (Wesseling et al., 2020) (figure 11a+b).

Notably, Tau phospho-sites were also found in control brains, with some sites appearing in all five brain samples analyzed, such as pT231, pS199 or pS396/404 (figure 11b). Biochemical profiling also confirmed the presence of the pS198 Tau epitope, but not the AT100 or PHF1 epitopes, in control brain lysate (figure 5c). Notably, Tau phospho-sites pS289 and pT263 were detected in all five AD brains following immunoprecipitation with all three antibodies, but appeared in at most one of the control brain samples.

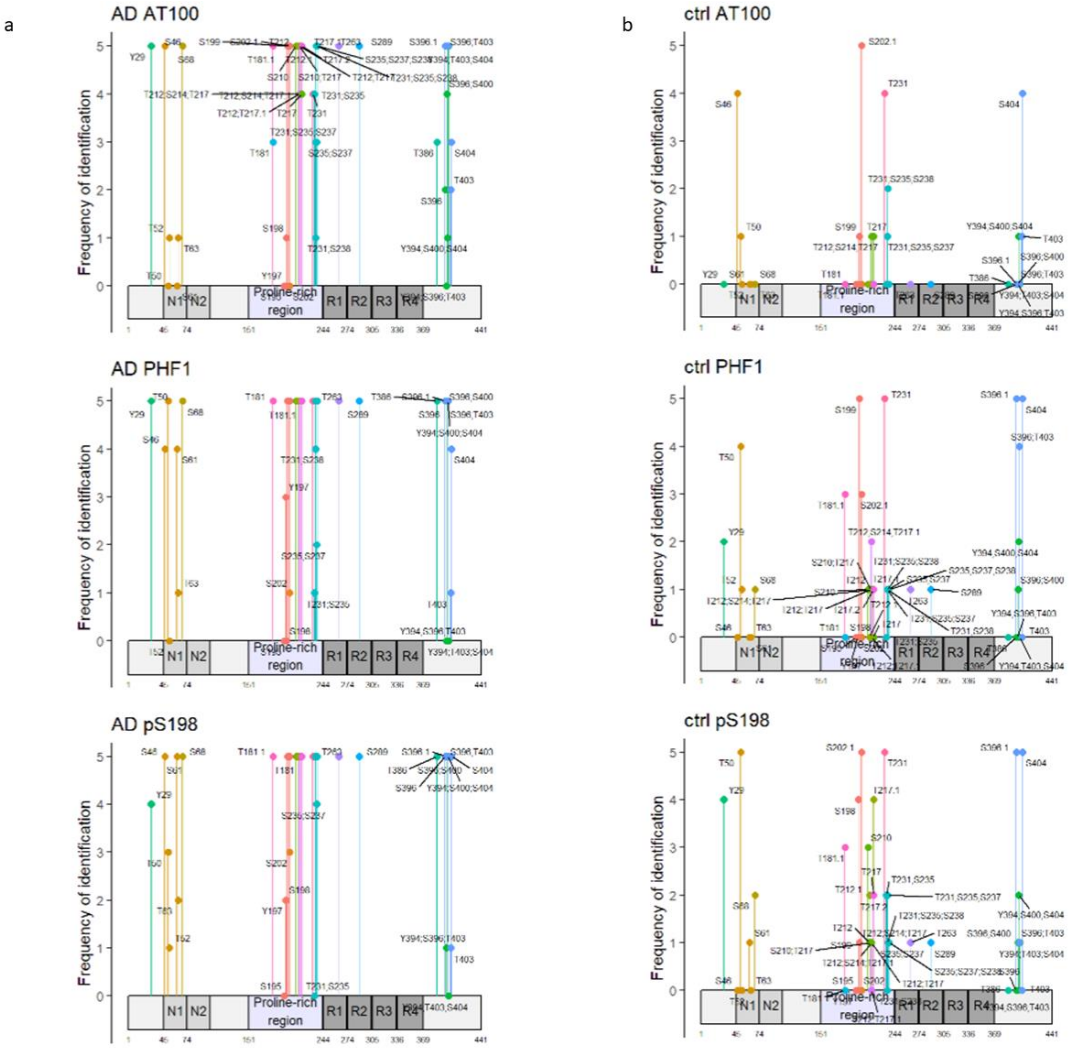

Figure 11: Phospho-Tau peptides are present in human AD and control brain

The frequency of identifications reflects the number of brains in which the phospho-sites were detected via MS after IP with phospho-Tau antibodies. ***a*** *Phospho-peptide analysis following immunoprecipitation with AT100, PHF1, and pS198 antibodies from AD brain samples revealed frequent phosphorylation in the N- and C-terminal regions of Tau, as well as the proline-rich domain. Similar phospho-sites were identified across all three phospho-Tau antibodies, with most sites consistently enriched in all five AD brain samples.* ***b*** *In control brains, a comparable distribution of Tau phospho-peptides was observed, though not uniformly across all samples. Only specific sites, such as pT231 and pS396/404, were consistently detected in all five control brain sample. n=5 human brain tissues, respectively.*

Next, the relative signal intensity of each detected phospho-peptide was analyzed and normalized to the total tau abundance. After IP with phospho-Tau antibodies it was evident that triple-phosphorylated epitopes, such as pS212/pS214/pT217; pT231/pS235/pS238, were consistently detected across the majority of 5 AD samples (figure 12a). Relative abundance of double-phospho-peptide pS396/pS400 was high after IP with PHF1 antibody. Notably, although the AT100 antibody pulled down less total Tau compared to other phospho-Tau antibodies (figure 10), it strongly enriched phospho-peptides (figure 12). The pT231, pS396, pS404, and pT403 epitopes were strongly enriched in all human AD samples after immunoprecipitation with both PHF1 and pS198. Interestingly, pT181—a well-established biomarker of AD pathology—was robustly detected after IP with the AT100 antibody (figure 12a). Overall, phospho-peptide abundance was higher in AD brains than in controls (figure

12), consistent with the concept that Tau becomes hyperphosphorylated as AD progresses, potentially disrupting its normal function (Alonso et al., 2001, 1997, 1994). While phospho-Tau peptides such as pT181, pT217, and pS396/403 were abundant after immunoprecipitation with PHF1 and pS198 from control brains (figure 12b), their relative abundance was substantially lower compared to that observed in AD brains.

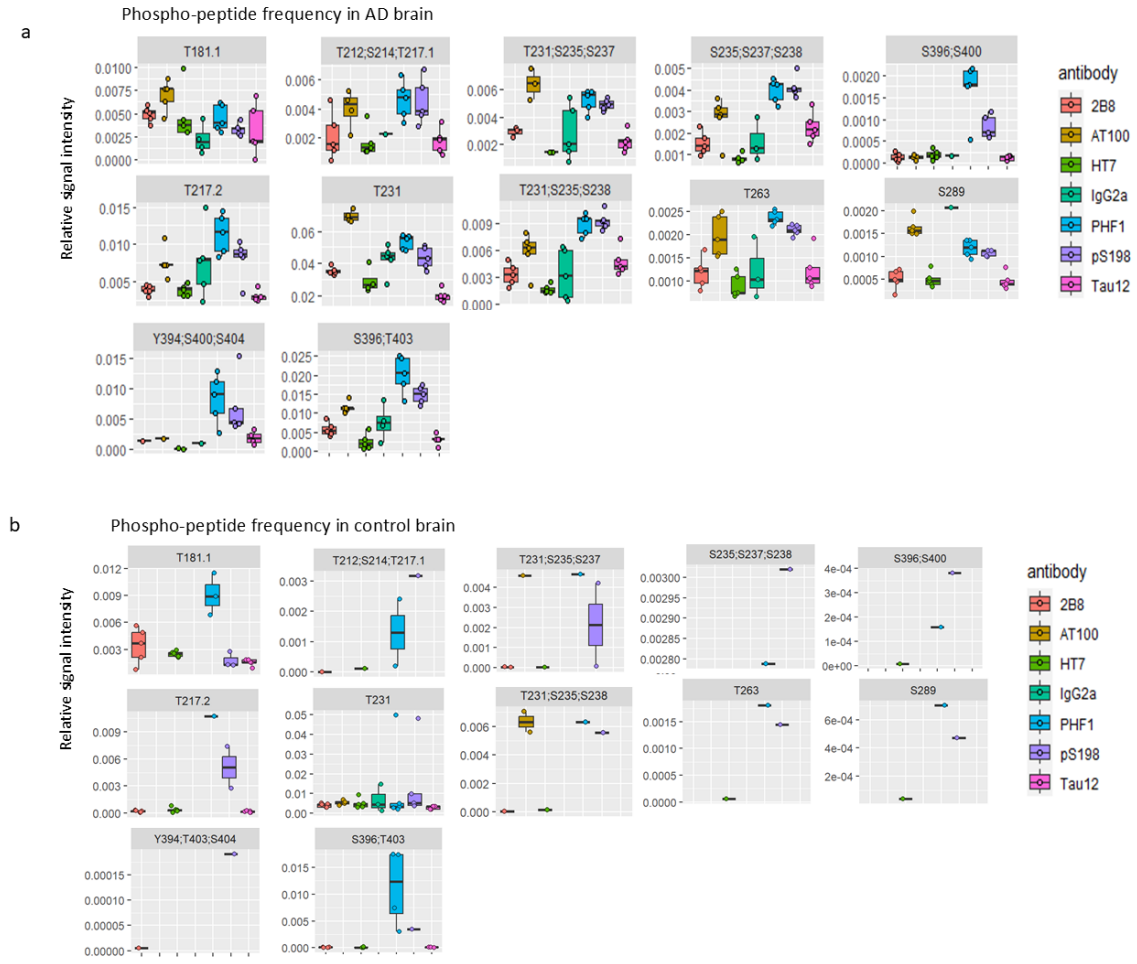

Figure 12: Phospho-peptide frequency in AD and control brain normalized to total Tau

***a** In AD brains, the signal intensity of phospho-peptide abundances relative to total Tau abundance indicates a higher signal intensity after pulldown with phospho-Tau antibodies (AT100, PHF1, pS198) compared to total Tau antibodies (2B8, Tau12, HT7) or the IgG control. Relative signal intensity of phospho- peptides such as pT212/S214/S217 or pT231/S235/S237 or pS235/S237/S238 were high after pulldown with PHF1 and pS198 phospho-Tau antibodies. pT263 and pS289 Tau phospho-peptides were highly abundant after IP with phospho antibodies. **b** In control brains, the frequency of phospho-peptide pT181, particularly after pulldown with PHF1, shows a high relative signal intensity. However, this occurs in fewer brain samples and with lower signal intensity compared to the AD brain samples. n= 5 human brain tissue, respectively.*

5.5 Tau interactors in human AD and control brain

Interactors of physiological and pathological Tau, that were co-immunoprecipitated with total Tau or phospho-Tau antibodies from human AD and control brains, were analyzed by DIA MS. All proteins with significantly enrichment compared to the IgG control were classified as

interaction candidates (figure 13). All antibodies depicted a significant enrichment of interactors from both AD and control brain, compared to IgG (figure 13).

A comparable number of interactors was detected for each antibody in both AD and control brain samples (figure 13, highlighted in red in the top corner of each comparison). Among the tested total Tau antibodies, HT7 captured the highest number of potential interactors, while Tau12 co-immunoprecipitated the fewest. As anticipated, phospho-Tau antibodies PHF1 and pS198 co-immunoprecipitated more proteins from AD brains than from control brains. Among the phospho-Tau antibodies, the fewest number of interactors were detected after IP with AT100.

In AD brains, Tau enrichment was observed across all antibodies. In control brains, Tau was primarily enriched by total Tau antibodies, with reduced enrichment noted when using phospho-Tau antibodies. Notably, Tau enrichment from control brains with the AT100 antibody was evident (figure 13).

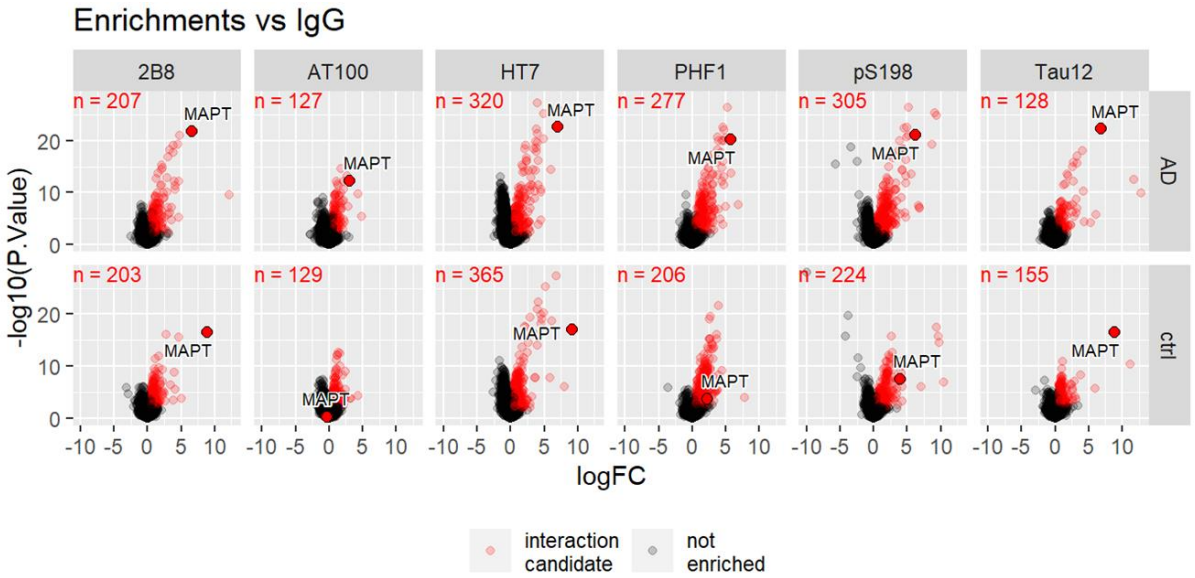

Figure 13: Enrichment of Tau interactors in human AD and control brain

DIA MS identification of Tau interactors immunoprecipitated using total Tau (HT7, Tau12, 2B8) or phospho-Tau (AT100, PHF1, pS198) antibodies from human AD and control brain tissue, with enrichment over IgG. Tau was notably enriched with all antibodies, with phospho-Tau antibodies showing a strong enrichment from AD brains and total Tau antibodies enriched in both AD and control brains. Phospho-Tau antibodies did not immunoprecipitate Tau from control brains. n upper corner (red)= number of interaction candidates. Statistical analysis: differential expression analysis using linear regression with limma and empirical Bayes moderation and subsequent multiple testing correction using the Benjamini-Hochberg procedure. Proteins with adjusted p-value<0.05 and logFC >1.5 were considered as interaction candidates. n= 5 human brain samples, respectively.

5.5.1 Metal ion and transmembrane transporter proteins are significantly enriched among Tau interactors in control brain

First, the Tau interacting proteins captured with total Tau antibodies from human AD and control brain were analyzed in more detail by performing Gene ontology (GO) term analysis.

In control brain, 62 proteins were consistently identified with all three total Tau antibodies (figure 14a). GO term analysis of the overlapping total Tau interactors identified significant enrichment of pathways related to metal ion transport, cation transmembrane transport and ion homeostasis (figure 14a+b). In-depth analysis showed that among the enriched proteins

associated with metal ion transport, several proteins with the solute carrier (SLC) function co-immunoprecipitated with total Tau (figure 14c). In AD brain, 60 proteins were consistently identified as Tau interactors with all total Tau antibodies (figure 14d). GO term analysis showed that these proteins are related to chemical synaptic transmission, trans-synaptic signalling or microtubule-based processes, however, this enrichment was not statistically significant (figure 14e).

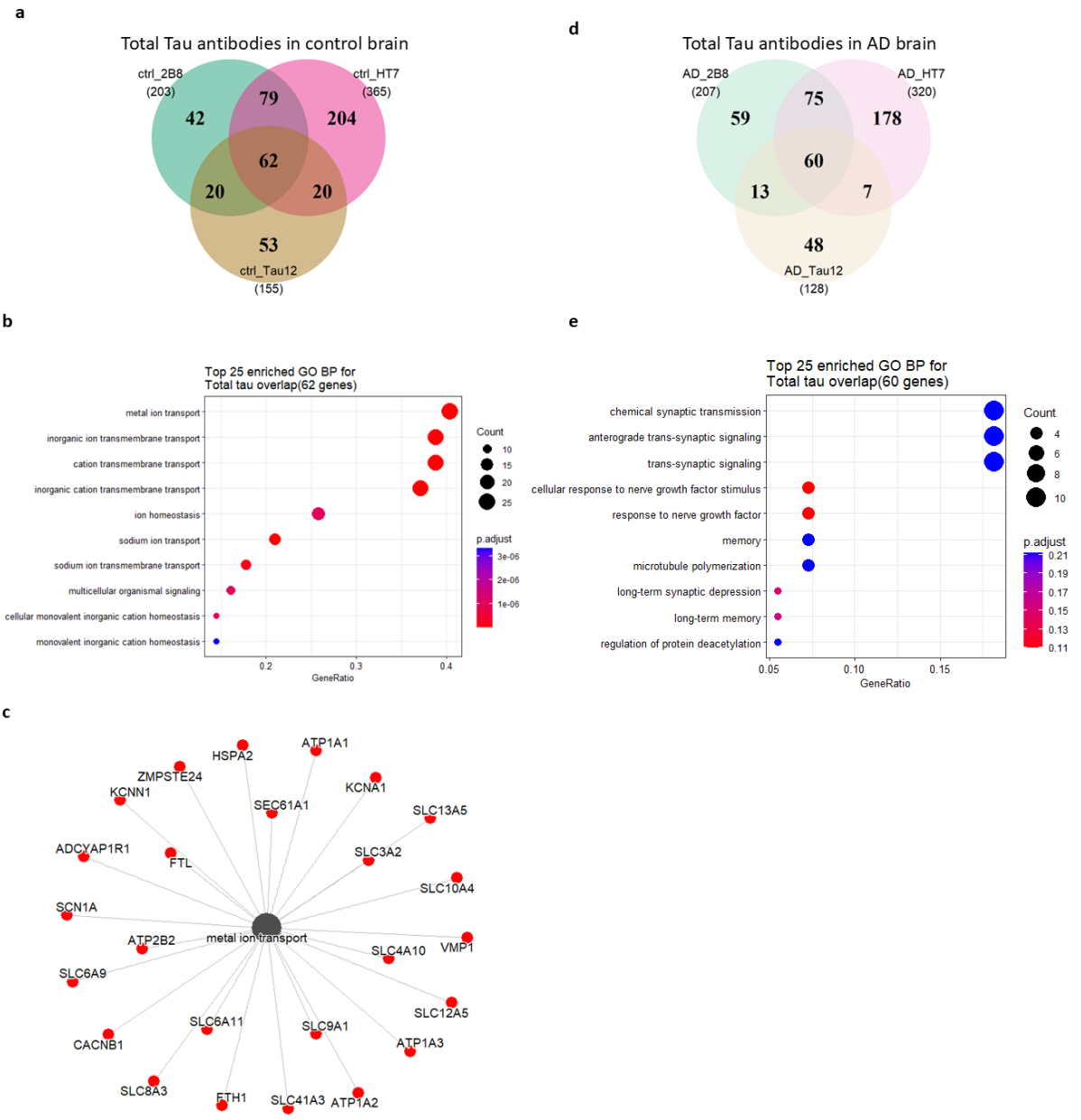

Figure 14: Ion and transmembrane transport processes are significantly enriched among total Tau interactors in human control brain

***a** 62 Tau interactors were identified with all three total Tau antibodies in control brains after immunoprecipitation with total Tau antibodies. **b** GO term analysis of Tau interactors identified with all total Tau antibodies (2B8, Tau12, HT7) from control brain (62) shows significant enrichment of proteins related to ion transport and transmembrane transport pathways. Statistical analysis: Hypergeometric tests using Benjamini-Hochberg*

procedure for multiple testing adjustment. Proteins with an unadjusted p-value < 0.01 were included in this enrichment analysis. ***c*** *Detailed analysis of total Tau interactors in control brain belong to the "metal ion transport" GO term.* ***d*** *60 Tau interactors were consistently identified in AD brain after immunoprecipitation with total Tau antibodies.* ***e*** *GO term analysis of consistent Tau interactors from AD brains (60) shows no significant pathway enrichment, although some interactors belong to the categories of "synaptic transmission" and "synaptic signalling" pathways. Statistical analysis: Hypergeometric tests using Benjamini-Hochberg procedure for multiple testing adjustment. n=5 human brain samples, respectively.*

5.5.2 Total Tau interactors are enriched in synaptic vesicle membrane proteins

Synapse loss is one of the hallmarks of AD (Selkoe, 2002; Zhou et al., 2017), closely follows Tau aggregation and correlates with cognitive decline (DeKosky and Scheff, 1990; Terry et al., 1991). In AD, the role of Tau in synaptic dysfunction (Moreno et al., 2016) remains incompletely understood. It remains unclear whether the disruption of the interaction between Tau and synaptic proteins contributes to synaptic dysfunction in AD or if this disruption is a result of synapse loss.

To investigate the relationship between Tau and synaptic proteins, a SynGo analysis (https://www.syngoportal.org/) was conducted on the Tau interactome dataset. This analysis provides insights into synapse-related genes and their functions through ontology annotations and functional enrichment analysis.

The SynGo analysis revealed that significantly enriched total Tau interactors, consistently immunoprecipitated using all total Tau antibodies from control brain tissue, were integral components of synaptic vesicle membranes (figure 15a).

Strikingly, synaptic vesicle proteins SV2A, SV2B, SV2C from the same family were consistently enriched as components of synaptic vesicle membranes (figure 15a). SV2s are transmembrane glycoproteins expressed in neurons and endocrine cells, primarily localized to synaptic vesicles (Buckley and Kelly, 1985). SV2A was identified as a total Tau interactor Tau, significantly enriched in human control brains (figure 15b).

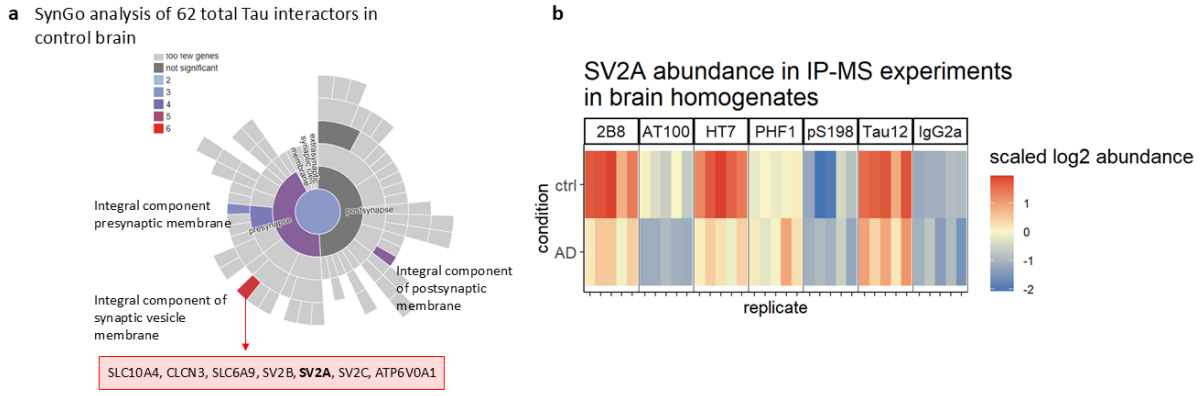

Figure 15: Synaptic vesicle protein SV2a is enriched as a total Tau interactor in human control brain

a *SynGO analysis for 62 Tau interactors that were consistently identified after immunoprecipitation with total Tau antibodies from control brains shows a significant enrichment of these proteins as integral components of the synaptic vesicle membrane, including SV2A, SV2B and SV2C. SynGo statistical analysis: Hypergeometric test with Benjamini-Hochberg procedure to adjust for multiple testing.* ***b*** *IP-MS showed that the synaptic interactor SV2A was significantly enriched as a Tau interactor in control brains after immunoprecipitation with total Tau antibodies 2B8, HT7 and Tau12, but not with phospho-Tau antibodies. Statistical analysis: differential expression analysis using linear regression with limma and empirical Bayes moderation and subsequent multiple testing correction using the Benjamini-Hochberg procedure. n= 5 human brain samples, respectively.*

5.5.3 Levels of the synaptic vesicle protein SV2A do not impact Tau pathology *in vitro*

To further investigate the potential role of SV2A in Tau pathology, iPS-derived cortical neurons were used as a model system. The addition of recombinant Tau aggregates or AD brain-derived sarkosyl-insoluble Tau to human iPS-derived neurons can trigger the aggregation of endogenous Tau (Manos et al., 2022), thereby mimicking *in vitro* the Tau pathology present in human brain. This seed-induced aggregation was evaluated using immunofluorescence staining with the Tau conformation-specific antibody MC1 (Manos et al., 2022) (figure 16a+b).

To test the impact of SV2a on Tau pathology, siRNA-mediated knock down of SV2a was conducted in iPS-derived neurons, followed by seed-induced Tau aggregation. Neurons treated with siRNA targeting MAPT served as a negative control, as no Tau aggregation is observed. The knockdown of SV2A resulted in no significant change in Tau aggregation (figure 16a+b).

Tau aggregation correlates with the presence of a phospho-Tau epitope recognized by the AT100 antibody (pS212/214), measurable by ELISA (Barini et al., 2022; Frey et al., 2024) (figure 16c). The addition of seeds to iPS-derived neurons significantly increases the AT100 signal in neurons, while the treatment with MAPT siRNA reduces this effect (figure 16c). siRNA-mediated knock down of SV2a had no effect on the levels of hyperphosphorylated Tau (figure 16c). Quantitative PCR analysis confirmed a 70% reduction in SV2A expression four weeks post-siRNA treatment, which was the final timepoint of the aggregation study (figure 16d).

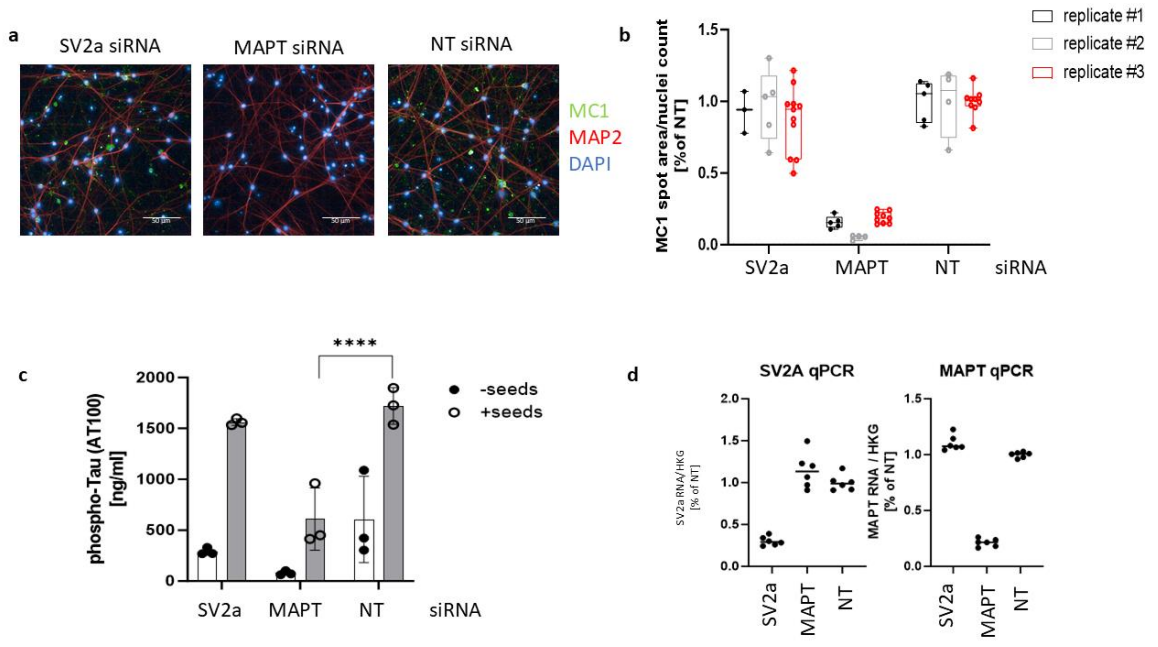

Figure 16: Synaptic vesicle protein SV2a knock down does not impact Tau pathology in iPS-derived neurons

a+b *Representative IF images and quantification of MC1-positive Tau aggregates (green) showed no significant change of Tau aggregation after siRNA-mediated knock down of SV2a in iPS-derived neurons (magnification: 40x; scale bar: 50 µm). n=3 biological replicates.* ***c*** *AT100-Tau level measured by phospho-Tau ELISA showed no significant change after SV2a knockdown, compared to NT control. Statistical analysis: TWO WAY ANOVA (p<0.0001) with Dunnett's multiple comparison test, adjusted p-value ****p<0.0001. The graph shows a representative biological replicate with three technical replicates.* ***d*** *qPCR analysis shows reduction of SV2A or MAPT gene expression is reduced by ~70% after knock down, respectively, normalized to HKG and NT control. n= 3 biological replicates, graphs show a representative biological replicate with six technical replicates.*

In addition to the role of SV2a in synaptic dysfunction, it is of considerable interest in neuropharmacology as the target of the antiepileptic drug Levetiracetam (LVA) (Lynch et al., 2004), which helps to reduce seizures by inhibiting synaptic vesicle exocytosis and neurotransmitter release (Labate et al., 2006). Studies in animal models and early clinical trials have suggested that levetiracetam may help reduce Tau-related neurotoxicity by stabilizing synaptic activity and improving neuronal function (Das et al., 2018; Thompson et al., 2024), however whether LVA might affect Tau aggregation remains unknown.

Therefore, iPS-derived neurons were treated with LVA prior and during seed-induced Tau aggregation for 1 day, 1 week, 2 weeks or 4 weeks to study the potential effects on Tau pathology. Levetiracetam treatment did not result in any significant changes in AT100 phospho-Tau (figure 17a), or Tau aggregation (figure 17b), compared to the DMSO control. This suggests that the impact of Levetiracetam on Tau phosphorylation and aggregation is limited under the conditions tested.

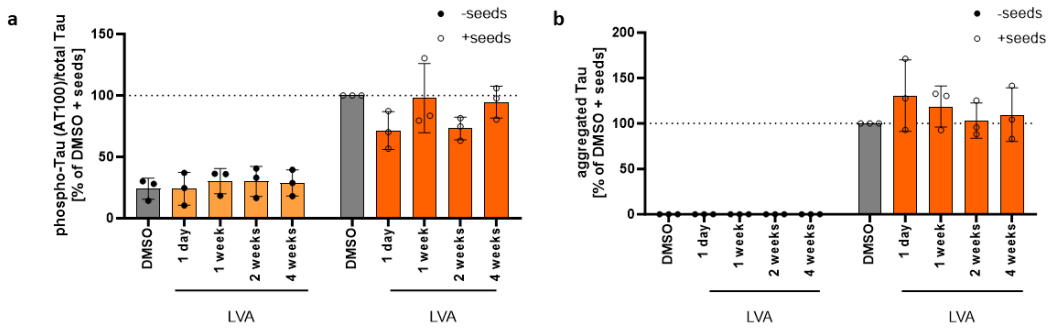

Figure 17: SV2a antagonist Levetiracetam (LVA) does not impact Tau pathology in vitro

iPS-derived MAPT TM neurons were seeded with recombinant Tau seeds and additionally treated with SV2a-targeting compound Levetiracetam (LVA) for 1 day, 1 week, 2 weeks or 4 weeks. ***a*** *AT100-Tau level measured by ELISA showed increased phospho-Tau levels after seeding, but no time-course dependent change after LVA treatment, compared to DMSO control.* ***b*** *Aggregated Tau level measured by ELISA were increased after seeding, but showed no change after LVA treatment, compared to DMSO control. Graph shows n= 3 technical replicates of a single biological replicate.*

5.5.4 RNA-binding proteins are significant interactors of phospho-Tau in AD and control brain

In addition to total Tau antibodies, phospho-Tau antibodies (AT100, PHF1 and pS198) were used for co-immunoprecipitation to selectively capture phosphorylated and seeding competent, thus pathological Tau species and their interacting partners from human brain. The AT100 phospho-Tau antibody captured less Tau than PHF1 and pS198 (figure 10, figure 13), and this corresponds to a smaller number of co-immunoprecipitated interacting proteins in AD and control brains compared to the other phospho-Tau antibodies (figure 13, figure 18a and c). Thus, only the overlapping proteins identified with both PHF1 and pS198 were selected for further analysis. In AD brains, 135 proteins were identified, which were consistently captured by the phospho-Tau antibodies PHF1 and pS198 (figure 18a). GO term analysis revealed a significant enrichment of pathways related to RNA binding and splicing as the most enriched for these interactors of phospho-Tau in AD (figure 18b). Interestingly, phospho-Tau antibodies also captured interacting proteins in control brains (figure 18c), with the same significant pathway enrichment for RNA binding and splicing as in AD brain (figure 18d), indicating the interaction of RNA proteins with both physiological and pathological Tau.

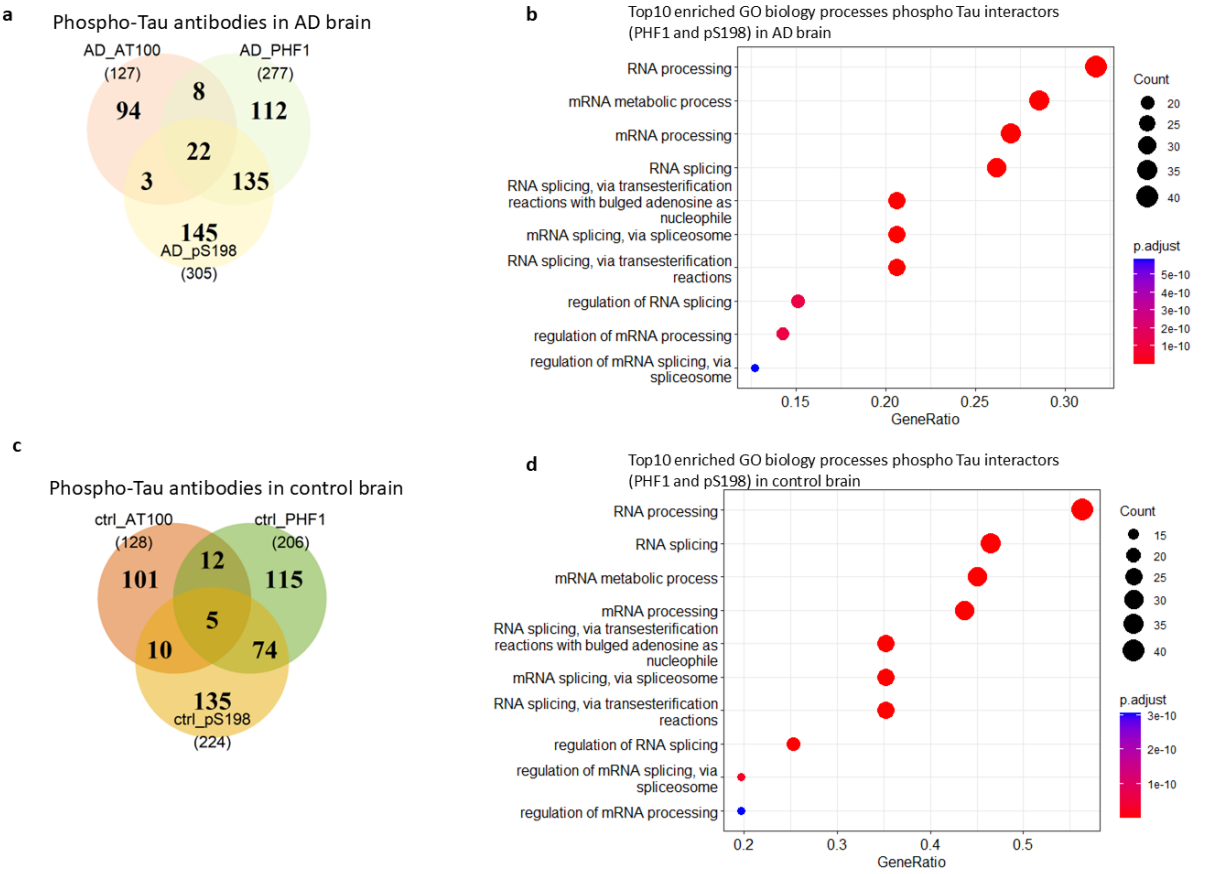

Figure 18: RNA-binding proteins are significantly enriched as interactors of phospho-Tau from human AD and control brain

***a** 135 Tau interactors were consistently identified in AD brains after immunoprecipitation using PHF1 or pS198 phospho-Tau antibodies. **b** GO term enrichment analysis of phospho-Tau interactors immunoprecipitated by PHF1 and pS198 in AD brains shows a significant enrichment of RNA-binding and splicing related proteins**. **c** 74 Tau interactors were consistently identified in AD brains after PHF1 or pS198 antibody pulldown. **d** GO term enrichment analysis of phospho-Tau interactors immunoprecipitated by PHF1 and pS198 in AD brains shows a significant enrichment of RNA-processing and splicing related proteins**. Statistical analysis: Hypergeometric tests using Benjamini-Hochberg procedure for multiple testing adjustment. Proteins with an unadjusted p-value < 0.01 were included in this analysis. n=5 human brain samples, respectively.*

5.6 Human iPS-derived neurons as a secondary model to study Tau interacting partners

Human iPS-derived neurons were used as a secondary model for identifying Tau interaction partners, as the *in vitro* model can mimic Tau pathology by inducing seeded Tau aggregation. Seeded Tau aggregation was used to replicate pathological Tau species and identify their associated interactors, while non-seeded iPS-derived neurons are anticipated to capture physiological Tau interactors. (figure 19). In these experiments, the type of seed needs to be matched to the neuronal genotype for efficient templating (Manos et al., 2022): AD- brain derived sarkosyl-insoluble Tau seeds were used to induce Tau aggregation in human MAPT wild type (WT) neurons, endogenously expressing the 0N3R Tau isoform. For iPS-derived MAPT “triple mutant” (TM) (0N4R P301S/ E10+14/ E10+16) neurons expressing both 3R and 4R Tau with the FTD-associated P301S mutation, aggregation was induced with recombinant Tau aggregates generated from 2N4R P301S Tau protein (Manos et al., 2022) (figure 19). All iPS-derived cell lines used in this study were isogenic to ensure maximal comparability.

To closely match the co-immunoprecipitation experimental conditions of the previous human brain interactome experiment, a combination of T12 and HT7 antibodies was used for total Tau immunoprecipitation (HT7/T12), while phospho-Tau immunoprecipitation was performed using a mix of PHF1 and pS198 antibodies (pS198/PHF1). The parallel co-IPs were followed by label free mass spectrometry and DIA processing to find Tau interacting proteins and pathways (figure 19).

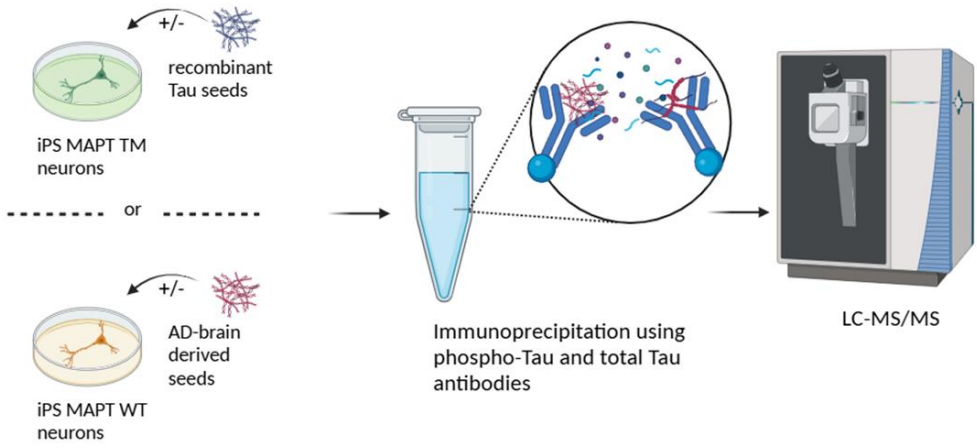

Figure 19: Tau interactome study in human iPS-derived neurons

Tau interactome workflow for seeded iPS-derived neurons. iPS-derived MAPT "triple mutant" TM (E10+14, E10+16, P301S) were seeded with recombinant Tau seeds, while MAPT WT neurons were seeded with AD-brain derived seeds. Lysates were subjected to immunoprecipitation using a combination of total Tau (HT7/T12) or phospho-Tau (PHF1/pS198) antibodies, respectively. Label free quantitation mass spectrometry and data independent acquisition was used to identify co-immunoprecipitated Tau interacting proteins. Control immunoprecipitations were performed using IgG. n=3 biological replicates. Figure created with Biorender.

Next, Pathway enrichment analysis of the overlapping proteins between post-mortem and iPS-derived Tau interactomes allowed for the identification and validation of key pathways and interactors, deepening our understanding of the molecular networks associated with Tau. This complementary approach goes beyond literature-based comparisons, aiming to determine which Tau interactors are also present *in vitro*. Such validation enables more detailed mechanistic studies. By confirming interactions in a controlled iPS-derived system, this strategy strengthens confidence in their relevance to disease-related processes. Identifying pathways common to both iPS-derived neurons and human brain tissue suggests that specific interactors may play a meaningful role in modulating Tau function or dysfunction.

5.6.1 Tau interactors in iPS-derived neurons

First, the enriched Tau interactors in seeded and non-seeded iPS-derived MAPT TM and MAPT WT neurons were analyzed (figure 20). Interactors were considered as significant for Tau after enrichment over IgG control (figure 20). This consistency in IP antibodies used for immunoprecipitation ensures that findings from iPS-derived neurons can be reliably compared to those from human brain samples, aiming to validate and recapitulate interactors *in vitro*. Notably, the number of interaction candidates for total Tau and phosphor Tau was higher in seeded samples, compared to the non-seded samples.

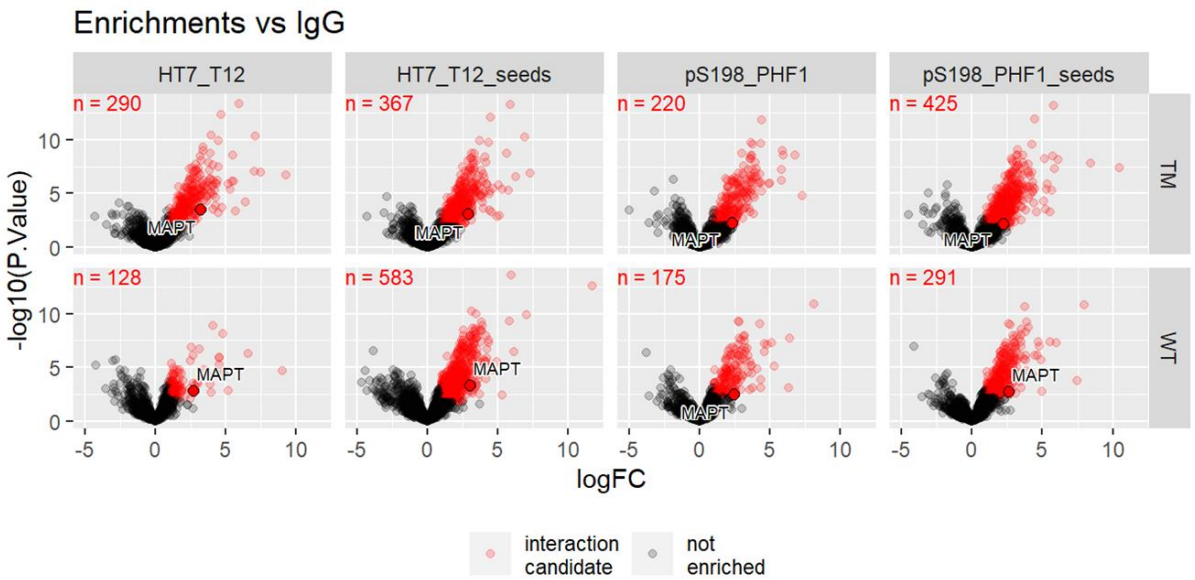

Figure 20: Enrichment of Tau interactors in seeded and non-seeded iPS-derived neurons

DIA MS identification of Tau interactors immunoprecipitated with total Tau (HT7_T12) or phospho-Tau (pS198_PHF1) from seeded or non-seeded iPS-derived MAPT TM or MAPT WT neurons, enriched over IgG. Tau was significantly enriched with all antibodies, especially after immunoprecipitation with total Tau antibody mixture. red n upper corner= number of interaction candidates. Statistical analysis: differential expression analysis using linear regression with limma and empirical Bayes moderation and subsequent multiple testing correction using the Benjamini-Hochberg procedure. Proteins with adjusted p-value<0.05 and logFC >2 were considered as interaction candidates. n= 3 biological replicates.

Considering the multiple experimental conditions, the initial focus was on interactors consistently co-immunoprecipitated with either the phospho-Tau mix (pS198/PHF1) or the total Tau mix (HT7/T12), in comparison to the IgG control (figure 21a+c). At this stage, variations in neuronal genotype and the presence of seed-induced Tau aggregation were not factored in, as all conditions were included in the analysis.

Pathway enrichment analysis of overlapping genes enriched across all conditions with phospho-Tau (pS198/PHF1) revealed a significant enrichment of proteins associated with developmental growth and neuron projection extension (figure 21b). Similarly, interactors co-immunoprecipitated with the total Tau mix (HT7/T12) in iPS-derived neurons were compared across different genotypes and seeded versus non-seeded conditions, showing enrichment in pathways related to cell junction organization and the regulation of protein localization (figure 21c+d). However, these GO term enrichments were not statistically significant.

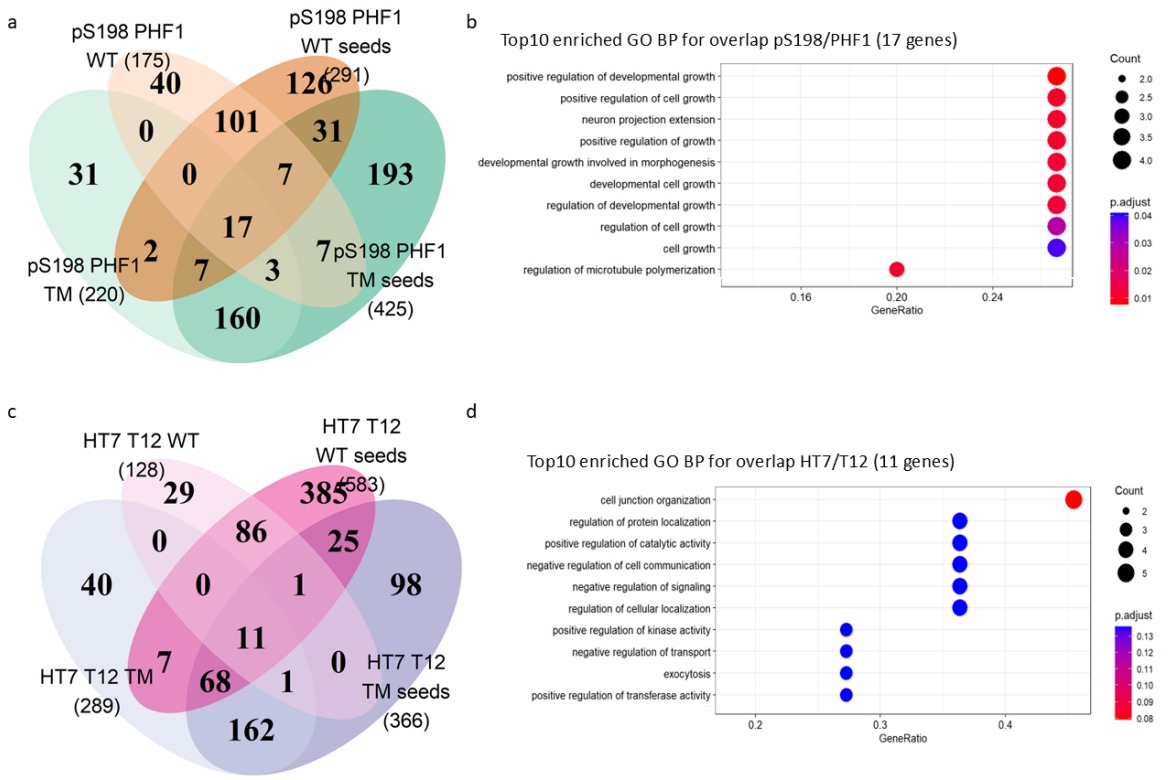

Figure 21: Total Tau and phospho-Tau interactors differ in iPS-derived neurons

***a** 17 Tau interactors were consistently identified in iPS-derived MAPT TM or MAPT WT neurons after phosphor-Tau (pS198/PHF1) antibody pulldown. **b** GO term enrichment analysis of phospho-Tau interactors immunoprecipitated by pS198/PHF1 show a significant enrichment of proteins related to developmental growth and neuron projection extension. **c** 11 Tau interactors were consistently identified in iPS-derived MAPT TM or MAPT WT neurons after total Tau (HT7/T12) antibody pulldown. **d** GO term enrichment analysis of phospho-Tau interactors immunoprecipitated by HT7/T12 show a non-significant enrichment of proteins related to cell junction organization and regulation of protein localization. Statistical analysis: Hypergeometric tests using Benjamini-Hochberg procedure for multiple testing adjustment. Proteins with an unadjusted p-value < 0.01 were included in this analysis. n=3 biological replicates.*

Additionally, interactors of seeded versus non-seeded Tau in iPS-derived neurons were analyzed (figure 22). To gain a broader understanding of proteins interacting with Tau aggregates, seeded conditions were compared without considering the specific seed type used or the iPS genotype. Due to the low number of overlapping interactors, especially in non-seeded comparisons, three out of four conditions were included in the pathway analysis. This approach increased the number of genes considered and made the overlap criteria less stringent (figure 22a+c, red square). Interactors commonly identified with aggregated Tau in seeded iPS-derived neurons were associated with the regulation of developmental and mRNA metabolic processes (figure 22b), though GO term pathway analysis did not reveal significant enrichment.

Conversely, GO term analysis revealed that interactors identified with both total Tau and phospho-Tau antibodies in non-seeded iPS-derived neurons were significantly enriched in pathways related to cell export processes, signal release, and exocytosis (figure 22d).

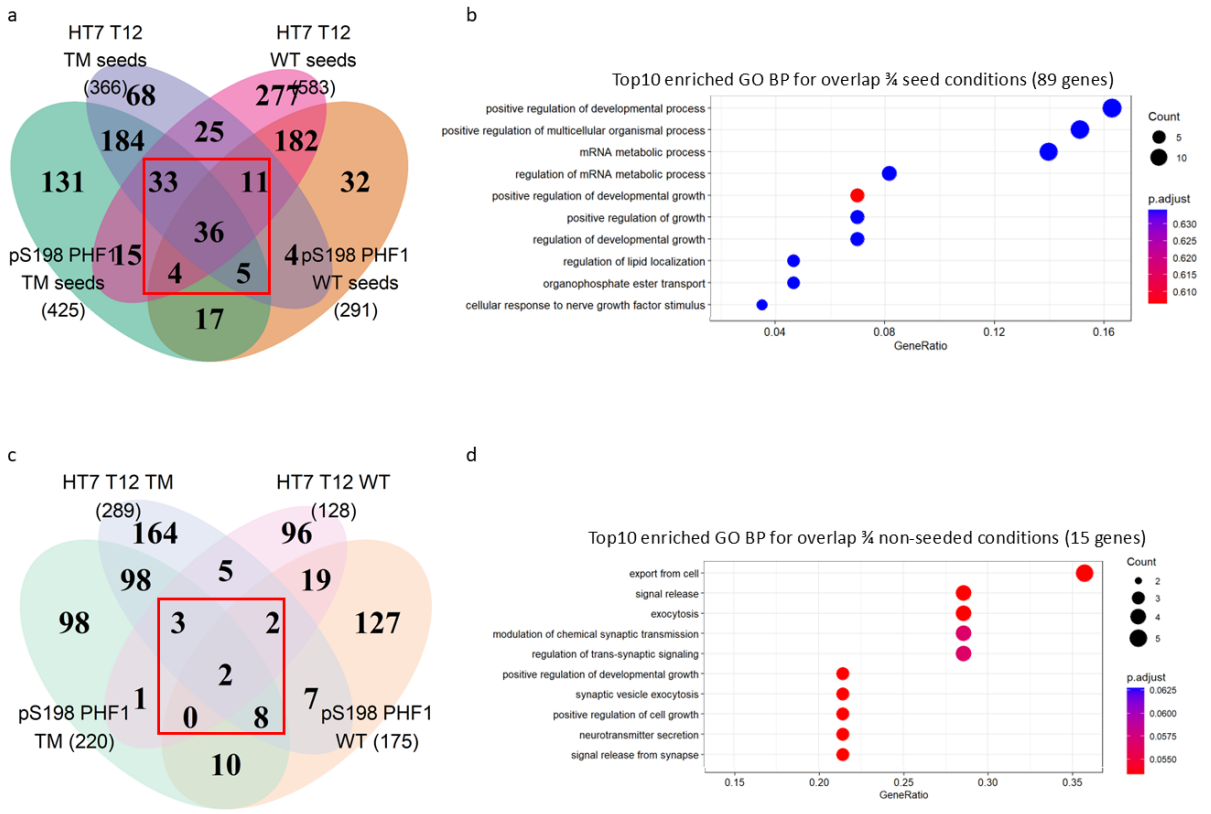

Figure 22: Cell export end exocytosis proteins are significant enriched Tau interactors in non-seeded iPS-derived neurons

***a** 89 Tau interactors were consistently identified in iPS-derived MAPT TM or MAPT WT neurons after seed-induced Tau aggregation with either phospho-Tau (pS198/PHF1) or total Tau (HT7/T12) antibody immunoprecipitation. **b** GO term enrichment analysis of three out of four conditions (red square figure a) show a non-significant enrichment of proteins related to developmental processes. **c** Few Tau interactors were consistently identified in non-seeded iPS-derived MAPT TM or MAPT WT neurons with either phospho-Tau (pS198/PHF1) or total Tau (HT7/T12) antibody pulldown. **b** GO term enrichment analysis of three out of four conditions (red square figure c) show a non-significant enrichment of proteins related to developmental processed GO term enrichment analysis of phospho-Tau interactors immunoprecipitated by HT7/T12 show a significant enrichment of proteins related to cell export and exocytosis. Statistical analysis: Hypergeometric tests using Benjamini-Hochberg procedure for multiple testing adjustment. Proteins with an unadjusted p-value < 0.01 were included in this analysis. n= 3 biological replicates.*

5.7 Microtubule-associated and RNA binding/splicing proteins are consistently identified as Tau interactors in human brain and iPS-derived neurons

In order to focus more precisely on proteins and related pathways that were identified as Tau interactors in both iPS-derived neurons and human brain, the overlap between the respective datasets were analyzed. GO term enrichment analysis of various comparisons were conducted (table 21).

The comparisons evaluated the interactors of pathological Tau species in seeded iPS-derived MAPT TM or MAPT WT neurons and those in the human AD brain. Tau interactors in non-seeded MAPT TM or MAPT WT neurons were compared to those identified in human control brains. To assess the overlap between the respective antibodies used, interactors captured with the pS198/PHF1 phospho-Tau mixture i*n vitro* were compared to those of pS198 and

PHF1 in the post-mortem human brain. Similarly, proteins co-immunoprecipitated with the HT7/T12 total Tau mix *in vitro* were compared to interactors of HT7 and T12 in the human brain.

The top significantly enriched pathways found to overlap between Tau interactors identified both *in vitro* and in the human brain were related to microtubule-associated processes and RNA binding and splicing (table 21). Notably, enrichment of RNA binding and splicing pathways was significant only among overlapping proteins co-immunoprecipitated with phospho-Tau (pS198/PHF1) or total Tau (HT7/T12) antibodies in vitro, compared to the respective interactors identified with pS198 and HT7 in human brain samples. This significance was observed exclusively when comparing overlapping proteins from iPS-derived MAPT TM neurons and appeared in both AD and control samples (table 21).

In addition, proteins interacting with Tau in both the human brain and iPS-derived neurons were related to microtubule-based processes and microtubule polymerization (table 21). Interestingly, these findings were consistent for both phospho-Tau and total Tau interactors detected in comparisons between AD and seeded iPS-derived neurons, as well as between control and unseeded iPS-derived neurons (table 21).

table 21: Overlapping GO term pathways in human brain and iPS-derived neurons

overlap	IP antibody	iPS genotype	Tau seeds	IP antibody	Human brain	Overlap top enriched GO term	p.adjust; gene count & GeneRatio
1	pS198/PHF1	MAPT WT	seeds	PHF1	AD	Microtubule-based process and polymerization	<0.0002; 7 & 0.5
2	pS198/PHF1	MAPT WT	seeds	pS198	AD	Microtubule-based	<0.008; 6 & 0.4
3	pS198/PHF1	MAPT TM	seeds	PHF1	AD	Microtubule organization	<0.01; 7 & 0.3
4	pS198/PHF1	MAPT TM	seeds	pS198	AD	RNA binding/splicing	<0.05; 6& 0.3
5	HT7/T12	MAPT TM	seeds	Tau12	AD	Microtubule-polymerization	<0.07; 2 & 0.3
6	HT7/T12	MAPT WT	seeds	Tau12	AD	Microtubule-polymerization	<0.02; 5 & 0.3
7	HT7/T12	MAPT TM	seeds	HT7	AD	RNA binding/splicing	<0.005; 10 & 0.04
8	HT7/T12	MAPT WT	seeds	HT7	AD	Cell organelle localization, synaptic vesicle	<0.03; 7 & 0.25
9	pS198/PHF1	MAPT WT	-	PHF1	ctrl	Microtubule-based process	<0.0002; 7 & 0.5
10	pS198/PHF1	MAPT WT	-	pS198	ctrl	Microtubule-based process and polymerization	<0.002; 6; 0.45
11	pS198/PHF1	MAPT TM	-	PHF1	ctrl	Microtubule-based process and polymerization	<0.01; 5 & 0.3
12	pS198/PHF1	MAPT TM	-	pS198	ctrl	RNA binding/splicing	<0.04; 6 & 0.3
13	HT7/T12	MAPT TM	-	Tau12	ctrl	Microtubule-polymerization	<0.07; 2; 0.3
14	HT7/T12	MAPT TM	-	HT7	ctrl	RNA binding/splicing	<0.005; 10 & 0.04
15	HT7/T12	MAPT WT	-	Tau12	ctrl	Protein polymerization	<0.02; 5; 0.3
16	HT7/T12	MAPT WT	-	HT7	ctrl	Organelle organization, axonal transport	<0.035; 7 & 0.25

Overall, 16 comparisons of enriched GO term pathways overlapping in human brain and iPS-derived neurons were examined (table 21). Subsequently, the proteins involved in these overlapping pathways were scrutinized to determine which individual proteins were most frequently identified as Tau interactors (table 22). Proteins related to microtubule processes were identified as frequent interactors of Tau, including DYRK1A, AP3B2, AP3B1, CLIP1 and MAP1B (table 22). Interestingly, these proteins were identified as Tau interactors in both iPS-derived genotypes and human brain types, as well as with both total and phospho-Tau antibodies. This suggests that Tau interacts with microtubule-related proteins regardless of its physiological or pathological condition.

table 22: Most often identified Tau interactors in human brain and iPS-derived neurons

protein	GO term	iPS genotype	Tau IP antibody	Human brain	Number of overlaps
DYRK1A	Microtubule-associated/RNA processing	MAPT WT and TM	Total and phospho Tau	AD and ctrl	13x
AP3B1	Microtubule-associated	MAPT WT	Total and phospho Tau	AD and ctrl	5x
AP3B2	Microtubule-associated	MAPT WT	Total and phospho Tau	AD and ctrl	5x
CLIP1	Microtubule polymerization	MAPT WT	Phospho Tau	AD and ctrl	4x
MAP1B	Microtubule-associated	MAPT WT and TM	Phospho Tau	AD and ctrl	3x

DYRK1A emerged as the most frequently identified Tau interactor in both human brains and iPS-derived neurons, appearing in 13 out of 16 comparisons (table 22). It showed interactions with both phospho-Tau and total Tau, regardless of the presence of Tau aggregates in iPS-derived neurons or the type of human brain tissue.

The adaptin family proteins AP3B1 and AP3B2 were also notable Tau interactors, as both subunits co-immunoprecipitated with total Tau and phospho-Tau, but only when there was protein overlap between MAPT WT neurons and AD or control brains (table 22). Proteomic analysis revealed an interaction between CLIP1 and phospho-Tau in MAPT WT neurons, aligning with phospho-Tau interactions observed in both AD and control human brain samples. Microtubule-associated protein MAP1B was found to interact with Tau in iPS-derived neurons, regardless of genotype or seed-induced Tau aggregation, as well as in both AD and control human brain samples. Notably, MAP1B interacted exclusively with phospho-Tau, not with total Tau, indicating its upregulation in response to pathological Tau.

As RNA binding and splicing proteins were significantly enriched Tau interactors (table 21), a more detailed analysis of the enriched proteins were conducted (figure 23). Figure 23a shows the overlapping proteins related to RNA binding and splicing, consistently captured with the phospho-Tau antibody pS198 from human AD or control brain and pS198/PHF1 from iPS-derived MAPT TM neurons (table 21, comparison 4 and 12). Similarly, RNA binding and splicing proteins captured with HT7/T12 from iPS-derived MAPT TM neurons, which overlap with HT7 co-immunoprecipitated interactors from AD or control are shown (figure 23b, table 21, comparison 7 and 4).

Interestingly, even though the same pathways were enriched for interaction with both total Tau and phospho-Tau, the specific proteins involved did not always overlap. Splicing factors SRSF2 and SRSF4 predominantly interacted with phospho-Tau pS198 *in vitro* (figure 23a), while the total Tau HT7 antibody captured interactors such as SNRPF and SNRPB (figure 23b), which are core components of the small ribonucleoprotein particles of the spliceosome (Wahl et al., 2009). DYRK1A and CPEB3 were found to interact with both phospho-Tau and total Tau, overlapping in iPS-derived neurons and the human brain. (figure 23a+b).

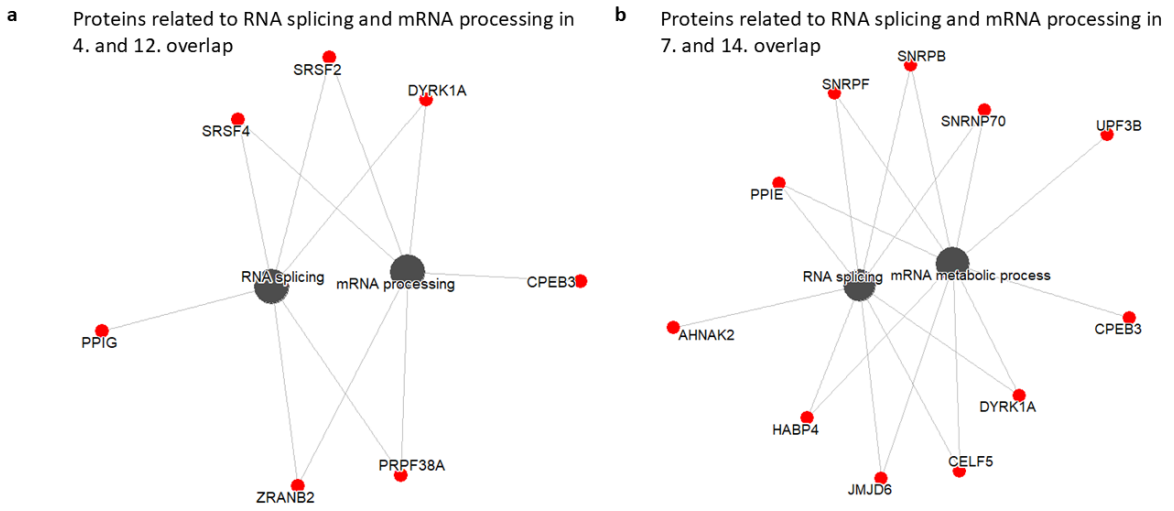

Figure 23: RNA-binding proteins are significantly enriched as interacting proteins of Tau overlapping in human AD and control brain and in iPS-derived MAPT TM neurons

Detailed analysis of overlapping Tau interactors in human brain and iPS-derived MAPT TM neurons, which were enriched in GO terms related to RNA binding/splicing processes. ***a*** *Specific analysis of proteins involved in RNA splicing and mRNA processing were enriched with phospho-Tau pS198 in both human AD and control brain samples, overlapping with interactors co-immunoprecipitated with pS198/PHF1 in iPS-derived MAPT TM neurons (comparison 4 and 12 in table 21).* ***d*** *Detailed analysis of proteins related to RNA splicing and mRNA metabolic processes enriched with total Tau HT7 in human AD and control brain, overlapping with interactors found with HT7/T12 in iPS-derived MAPT TM neurons (comparison 7 and 14 in table 21). n=3 biological replicates.*

5.8 Establishing BioID in iPS-derived neurons as complementary method to study Tau interacting proteins *in vitro*

Technical artefacts, such as homogenization of human brain samples or lysing iPS-derived neurons can induce artificial protein interactions, while transient or weak interactions may be lost. A promising solution is the development of techniques for labeling interacting proteins in living cells, allowing for real-time study of Tau interactions. The proximity-dependent biotin identification (Bio-ID) method is particularly effective for capturing transient or weak interactions, mapping protein interaction networks within their native cellular context (Roux et al., 2013). This method involves fusing the target protein to BirA (Choi-Rhee et al., 2004; Cronan, 2005; Roux et al., 2012), a modified enzyme that attaches biotin to nearby proteins. Biotinylated proteins are isolated using streptavidin beads and identified via mass spectrometry. As mammalian cells do not express other biotin ligases, this method specifically introduces the bacterial BirA enzyme.

To investigate Tau-interacting proteins in live cells, a human iPS-derived cell line was created to stably express Tau linked to BioID (BirA). iPSCs were infected before neuronal differentiation, while the cells were still dividing, enabling the generation of lines that stably express the desired constructs. A MAPT Knock out (KO) background was used as the parental line.

iPSCs were infected with lentiviral particles containing MAPT 2N4R P301S as a bait protein, with BioID positioned at the N-terminus of Tau to facilitate proximity labeling of proteins that interact with Tau (Tau-BioID) (figure 24a). Multiple expression constructs with linker lengths of either 10 or 30 amino acids between Tau and the BioID construct were tested to optimize

labeling efficiency. As a control for unspecific biotin labelling of the biotin ligase, a construct containing only the Bio-ID with a nuclear export signal (NES) was used to subtract biotin-background noise (BioID-only) (figure 24b). For both Tau-BioID and BioID only constructs, a blasticidin (BSD) resistance gene was included, which was separated from BioID via a T2A peptide (figure 24).

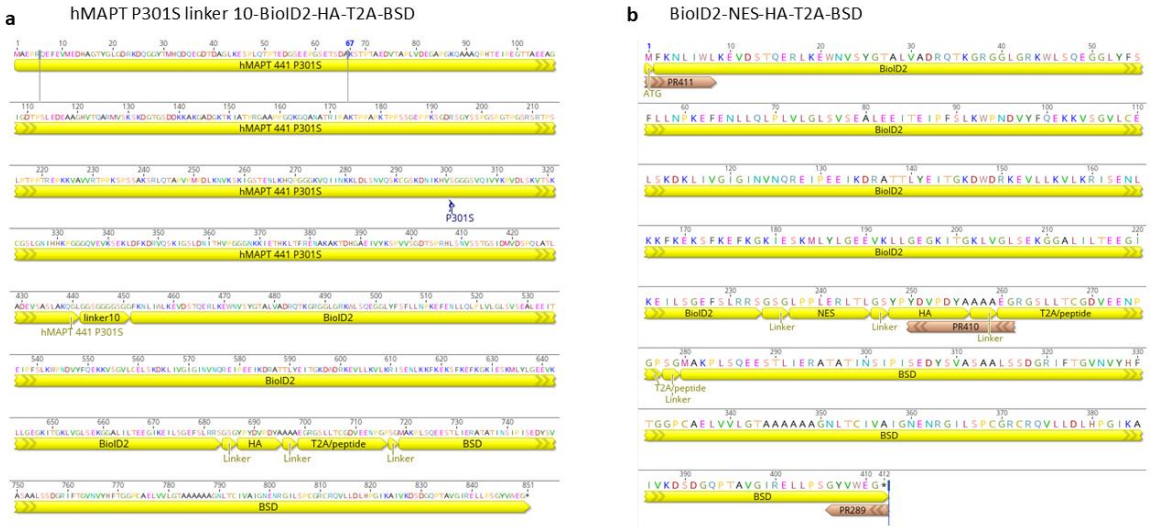

Figure 24: Cloning constructs of Tau-Bio ID and BioID only

*Overview of cloning constructs of **a** Tau-Bio ID construct contained human MAPT P301S linked to BioID2, exemplary linker length between Tau and BioID of 10 amino acids is shown. The construct is labeled with a HA-tag and contains a blasticidin (BSD) resistance gene, connected via a T2A peptide sequence. **b** BioID only cloning construct, including BioID2 with a nuclear export sequence (NES). A BSD resistance gene is linked via a T2A peptide.*

To generate stably expressing cell lines, the cloned constructs were introduced into lentiviral particles, which were used for infection at iPSC state. After infection, the cells were differentiated into neurons using a doxycycline inducible NGN2 overexpression system (Zhang et al., 2013). Differentiation of neurons was carried out during 49 days in vitro (DIV49) (figure 25). Over a period of 6 weeks, both iPS-derived neuronal cell lines, expressing either Tau-BioID or BioID-only, developed a visible neuronal network (figure 25).

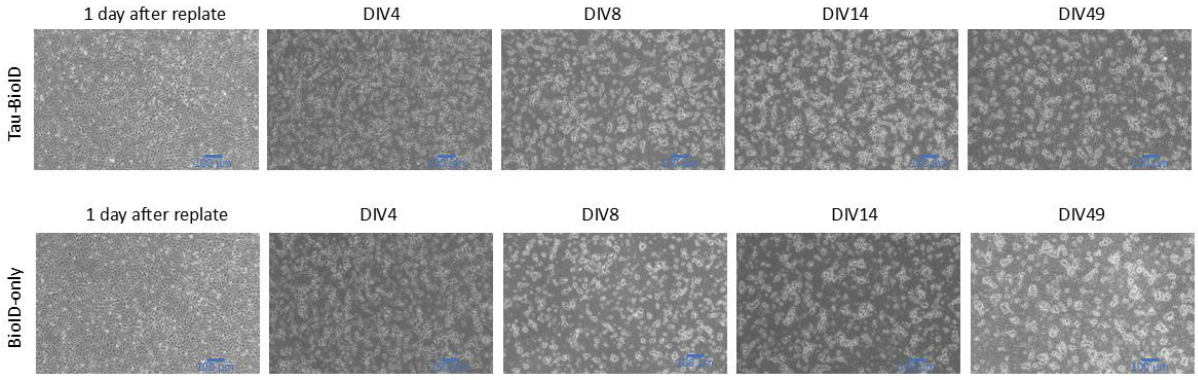

Figure 25: Differentiation of iPS-derived neurons stably expressing Tau-BioID or BioID-only constructs

Representative brightfield images of the different differentiation stages of the iPS- derived neurons 1 day after replate, DIV4, 8, 14 and 49. Differentiation from single cells into neuronal network is visible. Images were taken with a 10x magnification. (scale bar: 100 µm). n= 3 biological replicates, shown are representative images.

To confirm the successful expression of the Tau-BioID constructs, Western Blot and IF staining were performed (figure 26). iPSC lines generated with different multiplicity of infection (MOI) levels, either 2 or 3, were compared to identify lines with optimal Tau-BioID expression. A cell line infected with Tau linked to GFP was used as a positive control for Tau expression. Tau was stably expressed in all iPS-derived neurons infected with Tau-BioID constructs, regardless of MOI or whether a 10 or 30 amino acid linker length was used (figure 26a). The presence of a double band in neurons expressing the Tau-BioID constructs, as detected with the Tau12 antibody (figure 26a), might result from incomplete cleavage of the T2A peptide (figure 26b). As expected, no Tau was detected in cells expressing the BioID-only constructs or in the MAPT KO parental line (figure 26a). The biotin ligase was stably expressed in all cell lines, with enhanced expression observed in cells that also expressed BioID linked to Tau (figure 26a). IF imaging visualized that both Tau-BioID and the BioID molecule were mainly expressed in the neurite network, with occasional cell body staining (figure 26b).

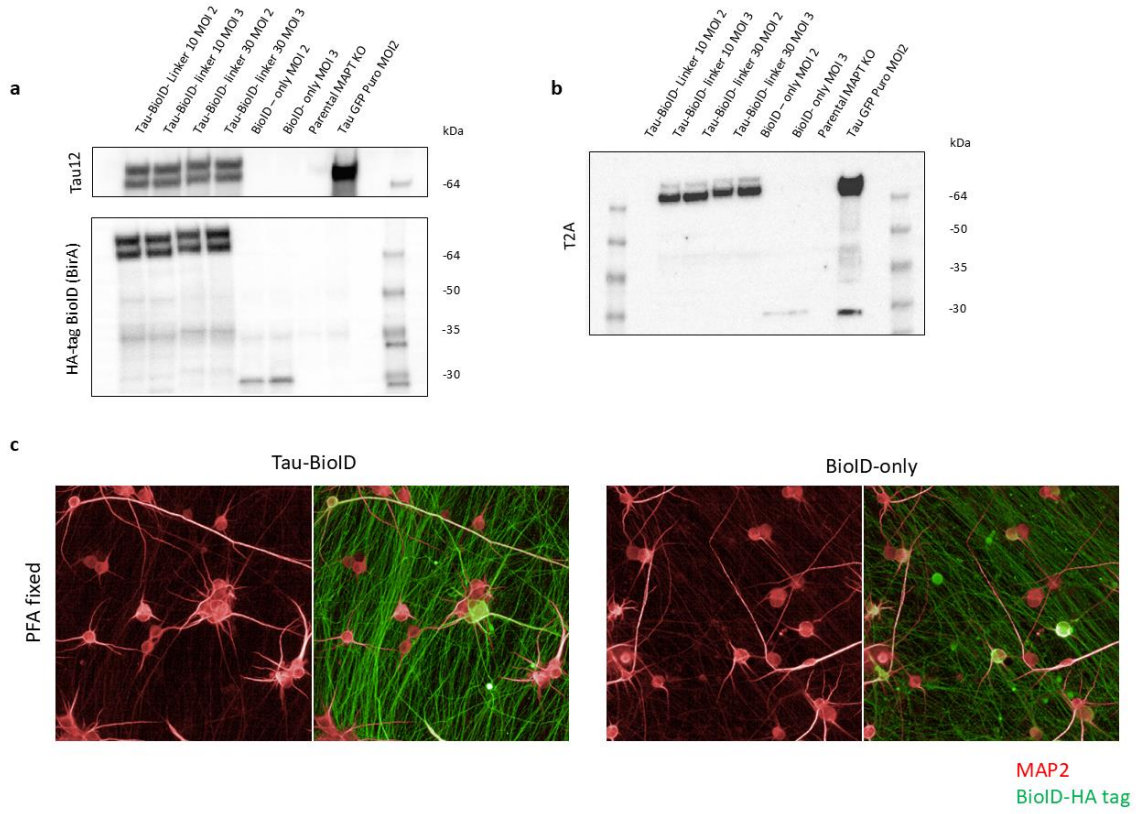

Figure 26: Human iPS-derived neurons stably overexpress Tau-BioID or BioID-only

***a** Western blot analysis of iPS-derived neurons expressing Tau-BioID infected with different MOI 2 or 3 and linker lengths 10 or 30 amino-acids or BioID-only at DIV14 showed stable Tau12 expression in cells infected with Tau constructs. Tau linked to GFP was included as a positive control for Tau expression. Cells infected with Tau-BioID constructs and BioID-only constructs demonstrated strong expression of the BioID-HA tag, unlike neurons expressing Tau-GFP or the parental MAPT KO line. No difference was observed regarding Tau or HA-tag expression comparing the different Tau-BioID and BioID-only constructs. **b** The T2A peptide signal remained detectable, indicating incomplete cleavage, as it was observed at levels similar to those of Tau or BioID. **c** Representative immunofluorescence staining of PFA-fixed neurons at DIV49 demonstrated stable expression of the dendritic marker MAP2 (red) and BioID (green). BioID was primarily located in the neurite network (magnification: 40x; scale bar: 400 µm). The data includes n=3 biological replicates, with representative images and western blots presented.*

To confirm the functionality of the expressed BioID ligase, external biotin was added to the cells. Biotin labeling was detected via a streptavidin-poly-HRP Western Blot (figure 27). BioID labeling was successful, as indicated by multiple biotinylated protein bands on the western blot, observed only in neurons expressing the BioID constructs (figure 27). This confirms the functionality of the ligase. As expected, no biotin labeling was detected in the parental MAPT KO or Tau-GFP cell line (figure 27). Neurons not exposed to external biotin show almost no Poly-HRP signal (figure 27), confirming the specificity of the signal. Since cells expressing BioID-only that were infected with an MOI3 displayed stronger biotin labeling compared to the cell line generated with MOI2 (figure 27), constructs with MOI3 were selected for subsequent experiments. No differences were observed between constructs with linker lengths of 10 and 30 amino acids. To ensure a potentially wider labeling radius, Tau-BioID with a 30-amino-acid linker was selected for subsequent experiments.

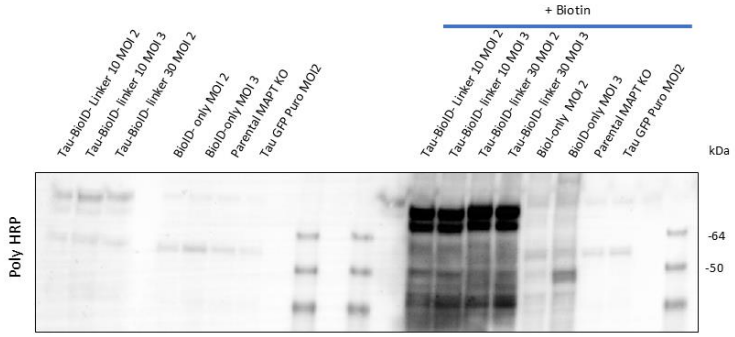

Figure 27: Biotin addition confirmed BioID functionality in iPS-derived neurons

iPS-derived neurons expressing Tau-BioID with different MOIs of 2 or 3 and linker lengths of 10 or 30 amino acids, or BioID-only, were treated with external biotin (right side blot). Neurons expressing Tau-BioID and BioID-only constructs displayed streptavidin-poly-HRP positive labeling of multiple protein bands. No differences were observed among constructs containing Tau-BioID. BioID-only neurons with MOI3 exhibited a stronger streptavidin-poly-HRP signal compared to the MOI2 condition. Labeling occurred only in cells expressing Tau-BioID or BioID-only, and not in the parental MAPT KO or Tau-GFP control lines. No streptavidin-poly-HRP signal was detected in cells not treated with biotin (left side blot). n=3 biological replicates; a representative western blot is shown.

To examine the interacting partners of both soluble Tau and Tau aggregates, Tau-BioID neurons were exposed to recombinant Tau seeds to trigger Tau aggregation. Neurons expressing BioID-only constructs were also seeded as a negative control. At DIV49, seed-induced aggregation of Tau was analyzed by immunofluorescence staining using the Tau conformation-specific antibody MC1 (Manos et al., 2022) (figure 28a). Neurons expressing Tau-BioID show successful seed-induced Tau aggregation, while cells expressing BioID-only did not exhibit Tau aggregates (figure 28a+b).

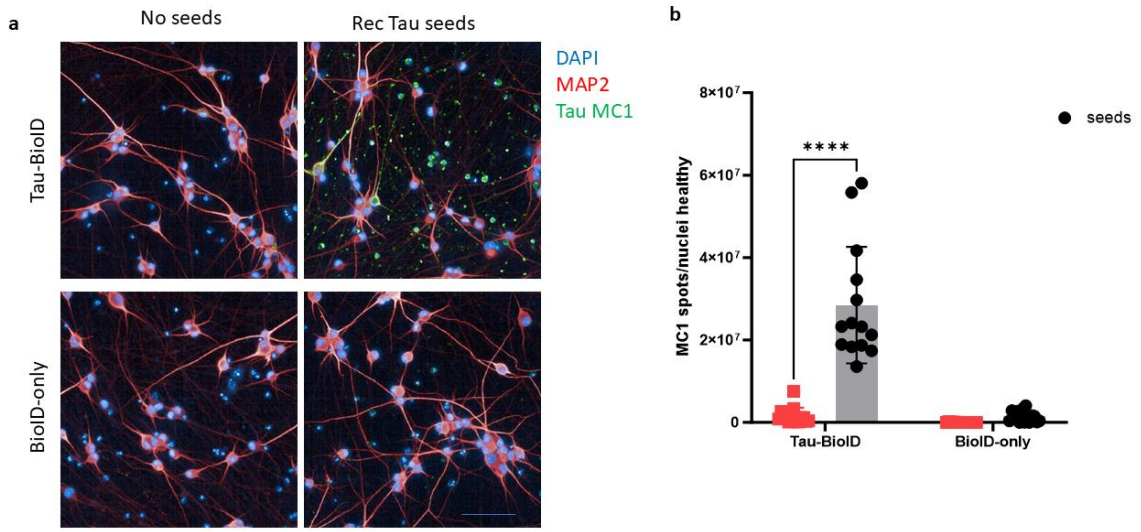

Figure 28: Seeded-Tau aggregation can be induced in Tau-BioID neurons

***a** Representative IF images and quantification of MC1-positive Tau aggregates (green) in iPS-derived neurons expressing Tau-BioID or BioID-only (magnification: 40x; scale bar: 400 µm). **b** MC1 staining, normalized to the number of healthy nuclei, revealed significantly increased Tau aggregation after seeding of Tau-BioID neurons, but not in unseeded Tau-BioID neurons or BioID-only neurons. Statistical analysis: TWO WAY ANOVA (p<0.0001 Tau BioID seeds vs no seeds and p=ns for BioID-only seeds vs no seeds) with Tukey's multiple comparison test ****p<0.0001. n=3 biological replicates. The graph shows a representative biological replicate with n=13 technical replicates*

After successfully establishing Tau-BioID expression in iPS-derived neurons and introducing seeded Tau aggregation, biotin was added to label all proteins in close proximity to Tau. Subsequently, immunoprecipitation was carried out using streptavidin beads to capture the biotin-labeled proteins. An on-bead digestion was performed, and the IP eluates were analyzed via mass spectrometry in DIA mode, enabling comprehensive and unbiased identification of Tau-associated proteins. BioID-only conditions served as a negative control for biotin-labelled protein background.

When comparing Tau-BioID to BioID-only, the primary protein significantly enriched in Tau-BioID neurons was Tau (MAPT) itself (figure 29a), confirming the accuracy of the overexpression constructs. Overall, there was a substantial overlap in the proximity-labeled proteins between Tau-BioID and BioID-only (figure 29a), with only two additional proteins significantly enriched in Tau-BioID lysates. Furthermore, when comparing non-seeded Tau-BioID with the seeded condition, no significant changes were observed (figure 29b), indicating that the formation of Tau aggregates did not lead to significant changes in the proximity-labelled proteins.

Comparison between seeded Tau-BioID and seeded BioID-only expressing neurons revealed a significant change in 6 proximity-labelled proteins (figure 29c), including the two proteins already observed in the non-seeded comparison (figure 29a). GO term enrichment analysis identified these proteins as related to microtubule-based processes and cytoskeleton organization (figure 29d).

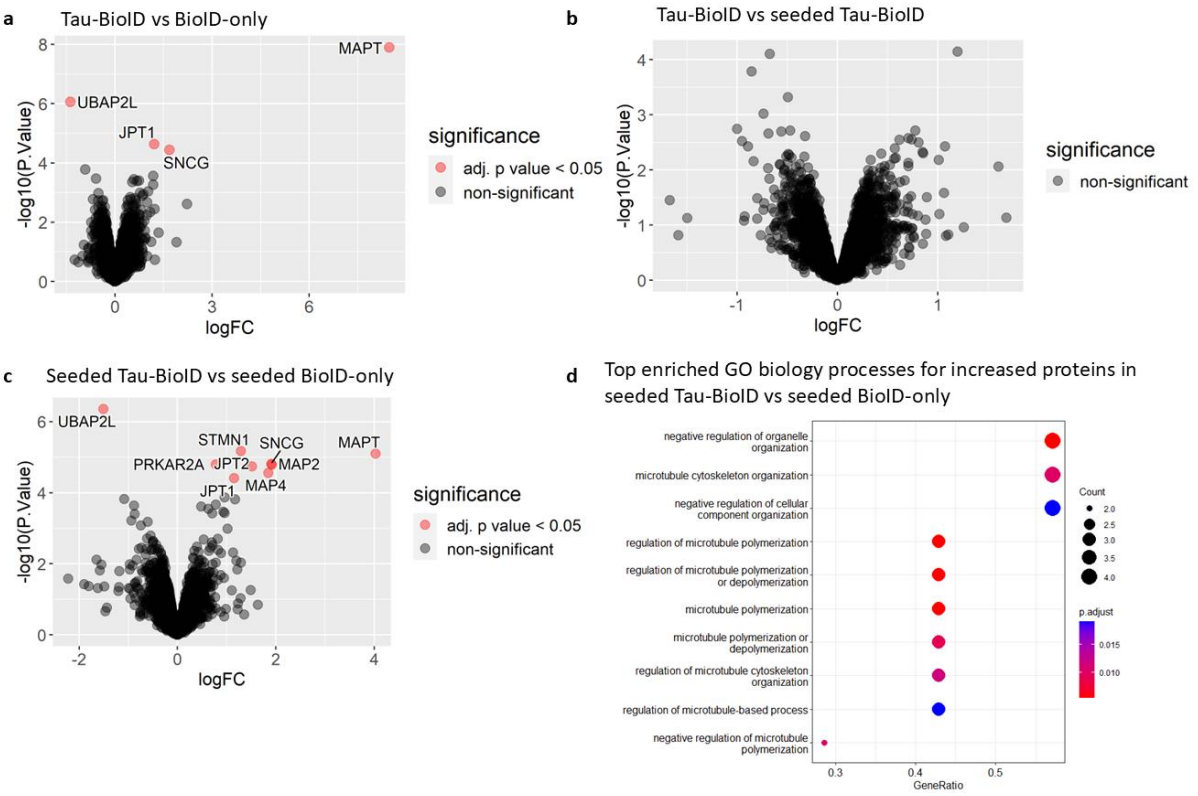

Figure 29: Microtubule-associated proteins were significantly enriched as Tau interactors Tau-BioID iPS-derived neurons

***a** Proteomics analysis shows large overlap between BioID-only and Tau-BioID proximity-labelled proteins. Significant enrichment of Tau in Tau-BioID neurons confirms difference of expression constructs. **b** Seed-induced Tau aggregation does not impact proximity-labelled proteins, compared to non-seeded Tau-BioID neurons. **c** Differential expression analysis between seeded iPS-derived neurons expressing Tau-BioID vs BioID-only demonstrated significant enrichment of six proximity-labelled proteins, along with Tau itself, in Tau-BioID cells. Statistical analysis: Differential expression analysis using linear regression with limma and empirical Bayes moderation and subsequent multiple testing correction using the Benjamini-Hochberg procedure. **d** GO term enrichment analysis indicated that these enriched proximity-labelled proteins are associated with microtubule-binding and cytoskeleton organization processes. Statistical analysis: Hypergeometric tests using Benjamini-Hochberg procedure for multiple testing adjustment. Proteins with an unadjusted p-value < 0.01 were included in this analysis. n=3 biological replicates.*

Proteins related to microtubule-associated processes were also significantly enriched as Tau interactors in seeded iPS-derived MAPT neurons and human AD and control brain (table 21). Although these findings are meaningful in connection with Tau, as it is a microtubule-associated protein (Binder et al., 1985), other Tau interactors observed in seeded iPS-derived neurons or the human brain, such as RNA-binding proteins or synapse-related proteins, were not replicated in the Tau-BioID study.

5.9 Proteomics and phospho-proteomics analysis of seeded iPS-derived neurons

Following results are included in a publication: Neu et al., 2025 under review.

5.9.1 Proteome changes upon maturation of iPS-derived neurons

By introducing exogenous Tau seeds into iPS-derived neurons, Tau misfolding, hyperphosphorylation, and aggregation, can be effectively induced, thereby mimicking pathological processes in a controlled environment.

Even though extensively used, the detailed proteomic response to Tau aggregation in cortical iPS-derived neurons neurons has not been thoroughly examined. To investigate this, quantitative tandem mass tag (TMT) labeling along with mass spectrometry-based proteomics and phospho-proteomics on both seeded and unseeded human iPS-derived cortical MAPT TM and MAPT WT neurons were conducted (figure 30). Again, the seed type was matched to the neuronal genotype, thus MAPT TM neurons were seeded with recombinant Tau seeds, while Tau aggregation in MAPT WT neurons was induced by addition of AD-brain derived seeds. As negative controls, MAPT KO iPS-derived neurons were treated with the corresponding seed material to confirm that any observed effects were due to the aggregation of endogenous Tau and not artifacts from the introduction of proteinaceous material (figure 30). All iPS-derived cell lines used in this investigation were isogenic to ensure maximum comparability.

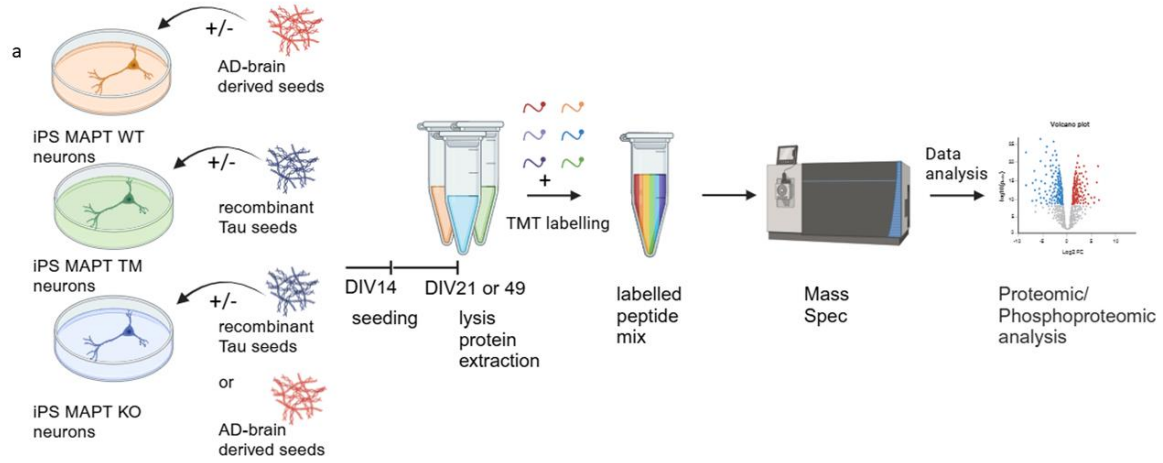

Figure 30: Proteomics and phospho-proteomics changes upon maturation or after seed-induced Tau aggregation in iPS-derived neurons

Overview of the multiplexed proteomics experiment: Human iPS-derived MAPT TM, MAPT WT, and MAPT KO neurons were seeded with either recombinant Tau seeds or AD-brain-derived sarkosyl-insoluble seeds, respective to the neuronal genotype (Manos et al., 2022). To investigate changes caused by Tau aggregation, proteomic and phospho-proteomic analyses were conducted. These studies utilized TMT-labeling followed by semiquantitative Mass Spectrometry. Maturation effects were assessed by comparing non-seeded MAPT TM and MAPT WT neurons lysed at two time points: DIV21 (1 week) and DIV49 (4 weeks). n=3 biological replicates. Figure created with BioRender.

First, the proteomic changes occurring during the maturation of iPS-derived neurons independent of Tau aggregation were investigated by comparing iPS-derived MAPT TM and MAPT WT neurons after maturation for 21 or 49 days in vitro (DIV21 vs. DIV49).

GO enrichment analysis of proteomic changes indicated a substantial overlap in the biological processes that were upregulated over time in both iPS-derived MAPT TM and MAPT WT iPS-derived neurons, with enrichments in metabolic and mitochondrial GO terms (figure 31a). A detailed examination of individual proteins within the "chemical synaptic transmission" GO term showed a trend towards an increase over time in MAPT TM neurons (figure 31b), however the observed proteins were also abundant in MAPT WT neurons. Thus, neurons of both genotypes mature over time, potentially at different rates. This finding aligns with the phospho-proteomics data, where synaptic GO terms were significantly upregulated at DIV49 in neurons of both genotypes, although a larger gene ratio was observed for MAPT TM neurons for most GO terms (figure 31c).

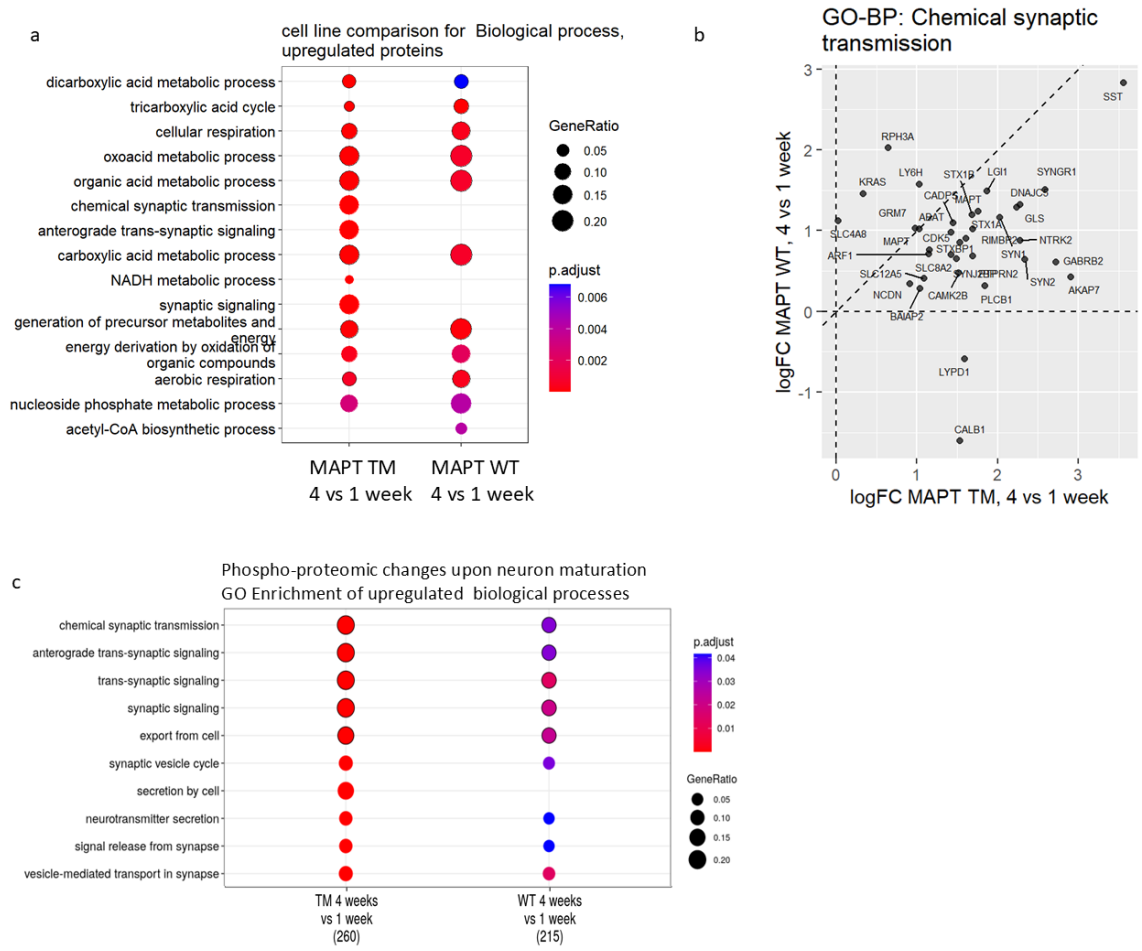

Figure 31: Synaptic signaling and synaptic transmission proteins are enriched over time in MAPT TM iPS-derived neurons

***a** GO term enrichment analysis of proteomic changes over time, comparing 4 weeks (DIV49) vs 1 week (DIV21), indicated a significant overlap in upregulated biological processes between unseeded MAPT WT and MAPT TM iPS-derived neurons. However, synaptic-related terms were significantly enriched only in MAPT TM neurons. Proteins with an unadjusted p-value < 0.01 were included in this analysis. **b** A detailed examination of proteins associated with the "chemical synaptic transmission" GO term revealed a trend of increased expression over time in MAPT TM iPS-derived neurons, compared to MAPT WT neurons. **c** GO term enrichment analysis of biological processes in the phospho-proteome indicates that synaptic terms are enriched in MAPT TM neurons when comparing mature (4 weeks) cultures to young (1 week) cultures. Statistical analysis: Hypergeometric tests using*

Benjamini-Hochberg procedure for multiple testing adjustment. GeneRatio=number of genes in input list associated with GO term/total number of genes in input list. n= 3 biological replicates

5.9.2 Seeded Tau aggregation induces phospho-proteomic changes in human iPS-derived neurons

Next, the impact of seed-induced Tau aggregation in iPS-derived neurons on the proteome and phospho-proteome was assessed. Tau seeds were introduced on DIV14, and samples for mass spectrometry analyses were collected on DIV49, a timepoint when robust seed-induced aggregation of endogenous Tau can be observed in both MAPT TM and MAPT WT neurons (Manos et al., 2022). Interestingly, seeded Tau aggregation did not lead to any significant changes at the proteomic level in any of the three neuronal lines (figure 32), suggesting that the formation of endogenous Tau aggregates does not result in major, persistent proteome changes at the timepoint analyzed.

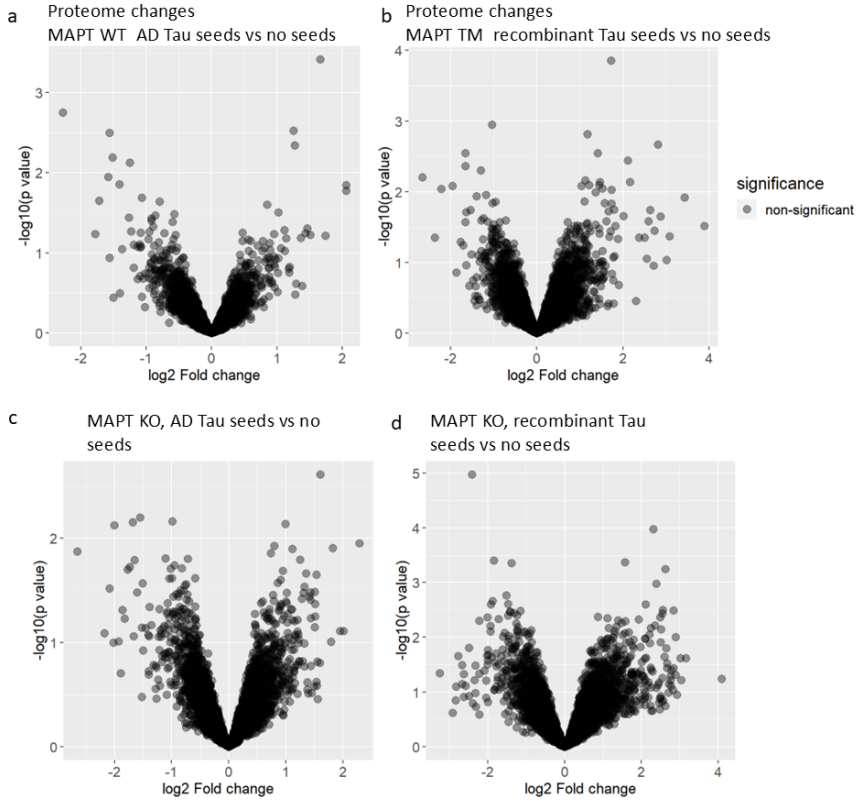

Figure 32: Seeded Tau aggregation does not impact the proteome of human iPS-derived neurons

***a + b** Proteomic analysis of iPS-derived neurons indicated no significant changes following seeding in either MAPT WT or TM iPS-derived neurons, compared to non-seeded controls. **c+d** No significant changes on the proteomic level upon seeding with either recombinant Tau seeds or AD brain-derived seeds in MAPT KO neurons. Statistical analysis: Differential expression analysis using linear regression with limma and empirical Bayes moderation and subsequent multiple testing correction using the Benjamini-Hochberg procedure. n=3 biological replicates.*

Additionally, phospho-proteomic analysis after seed-induced Tau aggregation was conducted. AD-brain derived seed induced Tau aggregation did not lead to significant changes on the phospho-proteome of iPS-derived MAPT WT neurons (figure 33a). Phospho-proteomic analysis revealed a significant impact of endogenous Tau aggregation on iPS-derived MAPT TM neurons (figure 33b) which were seeded with recombinant Tau seeds. Neither recombinant Tau seeds, nor AD-brain derived seeds caused changes in the phospho-proteome

of iPS-derived MAPT KO neurons (figure 33c+d), confirming that the changes detected in MAPT TM cells are due to the aggregation of endogenously expressed Tau.

In iPS-derived MAPT TM neurons, the most prominent increase in phosphorylation after seeding was found on MAPT (figure 33b), indicating the hyperphosphoylation of Tau. This is in agreement with previous studies (Manos et al., 2022) and demonstrates that seeded aggregation in this *in vitro* model recapitulates a main feature of pathological Tau in AD (Grundke-Iqbal et al., 1986; Köpke et al., 1993). In particular, phosphorylation at T231, T235, T237, S356 and T361 was significantly increased post seeding (numbering corresponds to amino acid positions in Tau isoform 2N4R), with additional sites showing a trend towards an increased phosphorylation (figure 33b). These phosphosites are among the Tau phosphorylation events identified as pathologically relevant in AD patient brain (Wegmann et al., 2021; Wesseling et al., 2020), confirming the relevance of the in vitro seeding model system. In iPS-derived MAPT WT neurons seeded with AD-brain-derived seeds, no statistically significant changes in the phospho-proteome were detected (figure 33a). However, a trend toward increased phosphorylation was observed at MAPT sites T231, T235, and T237, which is consistent with the changes reported in MAPT TM neurons.

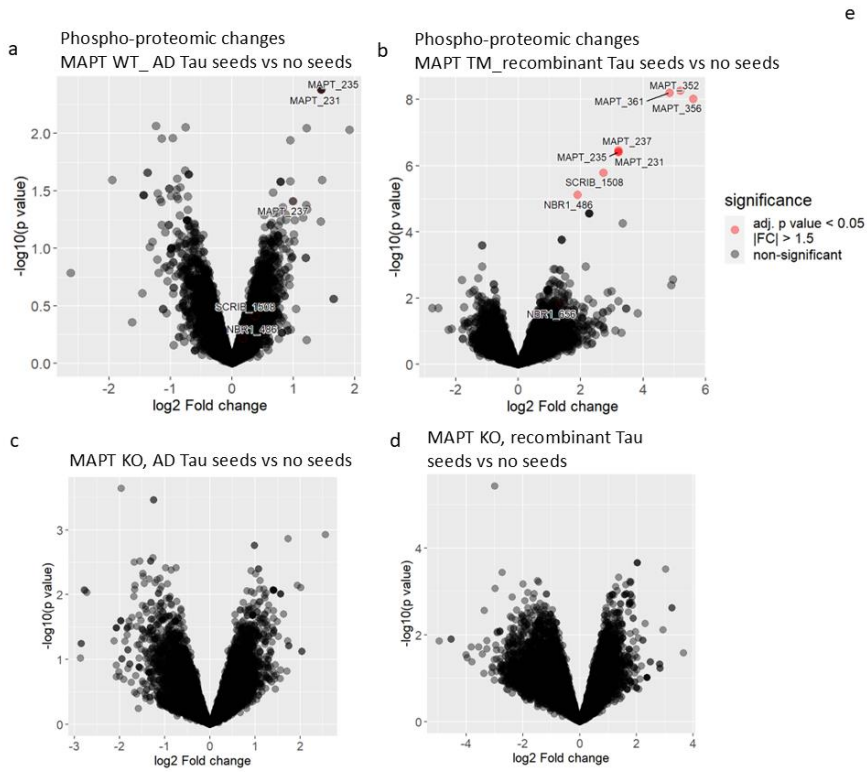

Figure 33: Seed-induced Tau aggregation significantly impacts phospho-proteome in iPS-derived MAPT TM neurons

***a** Phospho-proteomic analysis showed no significant changes after seeding with AD-brain derived seeds in iPS-derived MAPT WT neurons. **b** Phospho-proteomic changes revealed a significant increase in multiple phospho-peptides after seeding with recombinant Tau seeds in MAPT TM iPS-derived neurons. Phosphorylation was significantly increased at Tau peptides aa356, aa231, aa235, aa361, and aa237 (highlighted in red) as well as SCRIB aa1508 and NBR1 aa486, compared to non-seeded controls. **c+d** No significant changes on the phospho-proteomic level upon seeding with either recombinant Tau seeds or AD brain-derived seeds in MAPT KO neurons. Statistical analysis: Differential expression analysis was conducted using linear regression with limma and empirical Bayes moderation and subsequent multiple testing correction using the Benjamini-Hochberg procedure. n=3 biological replicates.*

In addition to Tau, two other phospho-sites were significantly increased after seeding in iPS-derived MAPT TM neurons: SCRIB_1508 and NBR1_486 (figure 33b; figure 34). A second phosphorylation site on NBR1 at aa656 also exhibited a trend toward increased phosphorylation (figure 34b). SCRIB (Scribble) is a presynaptic scaffold protein primarily active in synapse (Moreau et al., 2010), and has been implicated in Tau-induced toxicity in Drosophila (Feuillette et al., 2020). NBR1 is a selective autophagy receptor (Rasmussen et al., 2022) that facilitates the recruitment of ubiquitinated proteins to the autophagosome, resulting in their subsequent degradation (Kirkin et al., 2009; Matsumoto et al., 2011; Rasmussen et al., 2022).

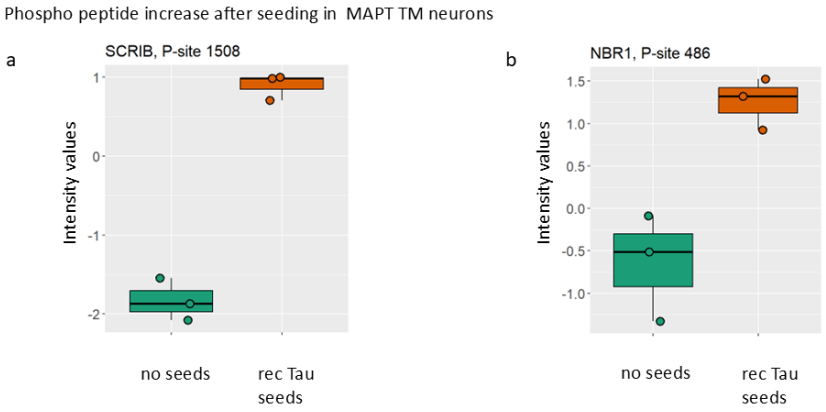

Figure 34: Phospho-peptide SCRIB_1508 and NBR1_486 increase after seeding in iPS-derived MAPT TM neurons

*Apart from Tau, only **a** SCRIB and **b** NBR1 proteins showed significantly elevated phosphorylation in seeded MAPT TM iPS-derived neurons. Specifically, phosphorylation increased at SCRIB's aa1508 site, while NBR1 demonstrated a significant phosphorylation increase at aa486 and a tendency towards increase at aa656. Statistical analysis: Differential expression analysis using linear regression with limma and empirical Bayes moderation and subsequent multiple testing correction using the Benjamini-Hochberg procedure. SCIRB_1508 adjusted p-value= 0.00673; NBR1_486 adjusted p-value= 0.0277; NBR1_656 adjusted p-value=1; n= 3 biological replicates.*

5.10 NBR1 interacts with pathological Tau in human AD brain and iPS-derived neurons

NBR1 as a selective autophagy receptor is an interesting target to follow up on, as its potential impact on Tau aggregation and its degradation has not been described yet.

First, previously generated Tau interactome datasets from human brain (section 5.1) and iPS-derived neurons (section 5.6) were leveraged to identify whether NBR1 is consistently present as a Tau-interacting protein, particularly in the context of Tau aggregation.

Co-immunoprecipitation experiments using total Tau and phospho-Tau antibodies in human postmortem brains (figure 4), revealed that NBR1 was a significantly enriched and highly abundant interaction partner of phospho-Tau, since it co-precipitated with both PHF1 and pS198 antibodies in human brain (figure 35a). No significant co-immunoprecipitation of NBR1 was found using control brain lysates or total Tau antibodies on AD brain lysates (figure 35a), even though Tau itself was efficiently pulled down under these conditions (figure 10). The AT100 antibody yielded very low amounts of Tau protein in the immunoprecipitation from AD brain samples (figure 10), which likely explains the lack of NBR1 signal in these reactions (figure 35a).

DIA mass spectrometry analysis of the Tau interactome in seeded iPS-derived neurons revealed that NBR1 interacts with Tau in seeded iPS-derived MAPT TM neurons (figure 35b).

NBR1 was not detected as a Tau interactor in non-seeded iPS-derived MAPT TM neurons, suggesting that the interaction occurs after Tau aggregates are formed. NBR1 was not identified as a Tau interactor in iPS-derived MAPT WT neurons, which is in line with the fact that increased NBR1 phosphorylation was only observed in the MAPT TM line after seeding.

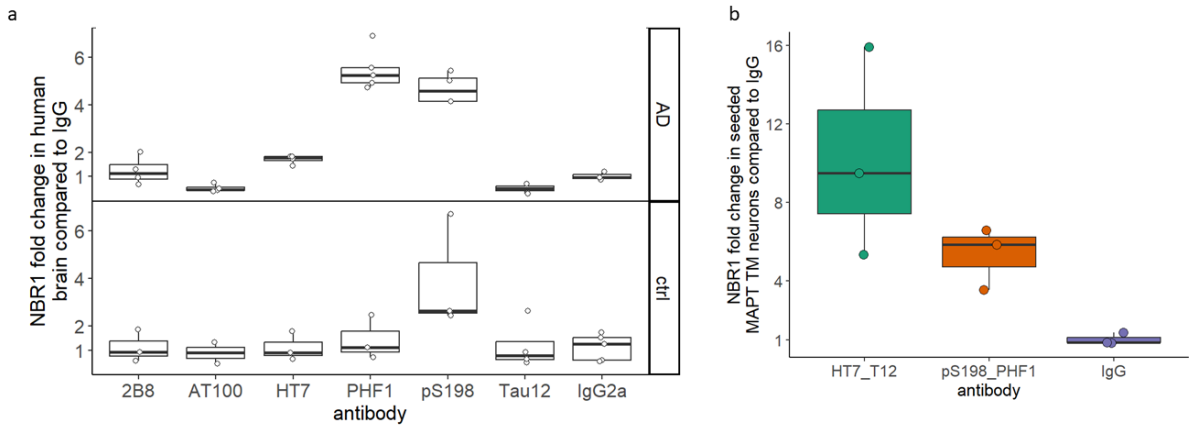

Figure 35: NBR1 interacts with pathological Tau in human AD and seeded iPS-derived neurons

***a** NBR1 interacts with phospho-Tau in human AD patient brain samples. For IP experiments from control brains or with total Tau antibodies from AD brain, no significant difference to background levels observed in the respective IgG control IPs was found. Statistical analysis: NBR1 in PHF1_AD vs IgG_AD adjusted p-value= 0.000014; pS198_AD vs IgG_AD adjusted p-value= 0.000042. All other comparisons were not statistically significant. n= 5 biological replicates for AD and control brain. **b** NBR1 interacts with total Tau and phospho-Tau in seeded iPS-derived MAPT TM neurons, compared to IgG control. Statistical analysis: HT7_T12 vs IgG adjusted p-value =0.0058; PHF1_pS198 vs IgG adjusted p-value= 0.021; Differential expression analysis using linear regression with limma and empirical Bayes moderation and subsequent multiple testing correction using the Benjamini-Hochberg; n=3 biological replicates.*

Taken together, these data confirm the specific interaction between NBR1 and the hyperphosphorylated, pathological forms of Tau in human AD brain, consistent with findings from the *in vitro* model. This interaction may suggest a potential involvement of NBR1 as a receptor for Tau aggregates in the context of autophagy-mediated degradation.

5.10.1 Loss of NBR1 increases Tau aggregate levels in iPS-derived neurons

Since NBR1 interacts with endogenous Tau in iPSC-derived neurons following seed-induced aggregation (Figure 35b), its potential effect on Tau aggregation in this model system was evaluated. To explore this, NBR1 was knocked down using siRNA, followed by an analysis of seed-induced aggregation of endogenous Tau. To determine if effects were specific to NBR1, the functionally related autophagy receptor protein p62 was also examined. Quantitative PCR analysis confirmed ~50% knockdown efficiency for all NBR1, ~40% knock down efficiency for p62 and ~75% knock down efficiency for MAPT 4 weeks after siRNA treatment, marking the final timepoint of the aggregation experiment (figure 36).

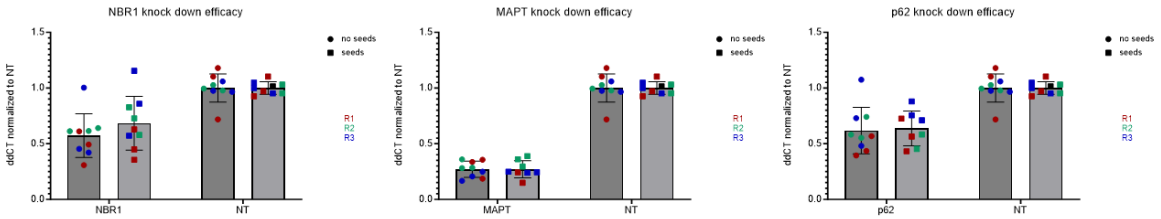

Figure 36: siRNA mediated knock down of NBR1, MAPT and p62 in iPS-derived neurons showed efficient knock down

Quantitative PCR analysis showed efficient knock down genes in iPS-derived neurons 4 weeks post seeding: NBR1 is reduced by ~50%, expression of p62 is reduced by ~40% and expression of MAPT is reduced by ~75%. Knockdown efficiencies were independent of seed treatment and normalized to housekeeping genes and non-targeting control siRNA. n=3 biological replicates and three technical replicates.

The seed-induced aggregation of endogenous Tau was assessed using immunofluorescence staining with the Tau conformation-specific antibody MC1 (Manos et al., 2022) (figure 37a+b). Neurons treated with siRNA against MAPT served as a negative control, exhibiting no Tau aggregation. Knockdown of p62 had a marginal, non-significant effect on increasing Tau aggregation (figure 37b). In contrast, NBR1 knockdown significantly increased Tau aggregation compared to cells treated with non-targeting control siRNA (NT) (figure 37b).

Tau aggregation is also linked to the appearance of the epitope recognized by the antibody AT100 (pS212/214), which can be measured and quantified by ELISA (Barini et al., 2022; Frey et al., 2024) (figure 37c). In this assay, siRNA-mediated knockdown of NBR1 significantly increased the amount of hyperphosphorylated Tau (figure 37c), while knockdown of the autophagy receptor p62 had no significant effect, confirming the specific influence of NBR1 on seeded Tau aggregation.

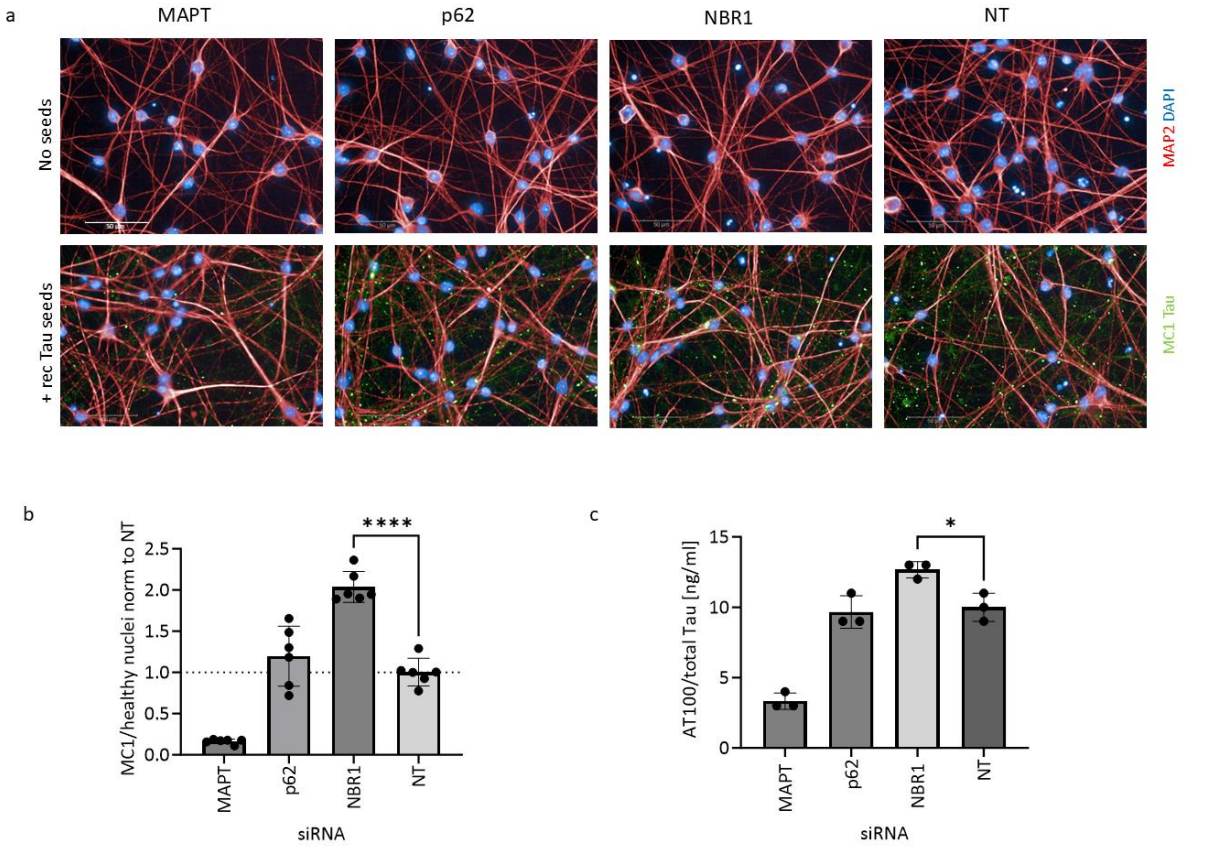

Figure 37: NBR1 knockdown increased Tau aggregation and phosphorylation in iPS-derived neurons

a + b *Representative IF images and quantification of MC1-positive Tau aggregates (green) show a significant increase of Tau aggregation after siRNA-mediated knock down of NBR1. NT: non-targeting siRNA. Statistical analysis: ONE WAY ANOVA (p<0.0001) with Dunnett's multiple comparison test, ****p<0.0001. n=3 biological replicates. The graph shows a representative biological replicate with six technical replicates.* **c** *ELISA quantification shows significant increase of AT100-phospho-Tau in seeded neurons after NBR1 knock down, compared to NT control. Statistical analysis: ONE WAY ANOVA (p<0.0001) with Dunnett's multiple comparison test, *p=0.013. n=3 biological replicates. The graph shows a representative biological replicate with three technical replicates.*

The direct impact of reduced NBR1 expression on Tau aggregate levels in iPS-derived neurons was thus demonstrated. Together with the finding that NBR1 specifically interacts with phosphorylated Tau after the induction of seeding the data strongly suggests that NBR1 may be an autophagy receptor for Tau aggregates.

5.10.2 NBR1 is recruited to Tau aggregates in seeded HEK biosensor cells

To study the effect of NBR1 and NBR1 phosphorylation on Tau aggregation in more detail, next a simpler cell system was utilized, compared to iPS-derived neurons: HEK 293T cells stably expressing the YFP-tagged repeat domain of Tau including the P301S mutation (Holmes and Diamond, 2014). As described above, this model is widely used as a biosensor to analyse the effects of genetic and pharmacological interventions on Tau aggregation, and due to the fast aggregation kinetics in this system, treatments that acutely block autophagy can be used to study aggregate degradation.

The co-localization of endogenous NBR1 with Tau aggregates and the turnover of these complexes was investigated. Seeded Tau aggregation was induced in HEK biosensor cells through the addition of recombinant Tau seeds (Holmes et al., 2014) (figure 38a+c). To

determine if NBR1 and Tau undergo lysosomal degradation, treatment with bafilomycin C was implemented to halt autophagic flux. The signals for NBR1 and Tau were quantified using IF staining (figure 38a-d). After bafilomycin treatment, an increased Tau aggregation was observed (figure 38c). As expected, bafilomycin treatment of HEK biosensor cells led to an increased NBR1 signal, reflecting inhibited clearance of NBR1 (figure 38a+b). Interestingly, even the addition of Tau seeds alone was sufficient to prompt NBR1 clustering into bright spots co-localized with Tau aggregates (figure 38b). The combined treatment with Tau seeds and bafilomycin resulted in more Tau aggregates, although the number of NBR1 spots did not rise beyond levels seen with bafilomycin alone (figure 38b). Further analysis revealed that approximately 80% of Tau aggregates were also positive for NBR1, indicating efficient recruitment of endogenous NBR1 to Tau aggregates in the seeded HEK biosensor cells (figure 38d). This co-localization percentage was unaffected by the simultaneous addition of bafilomycin and Tau seeds.

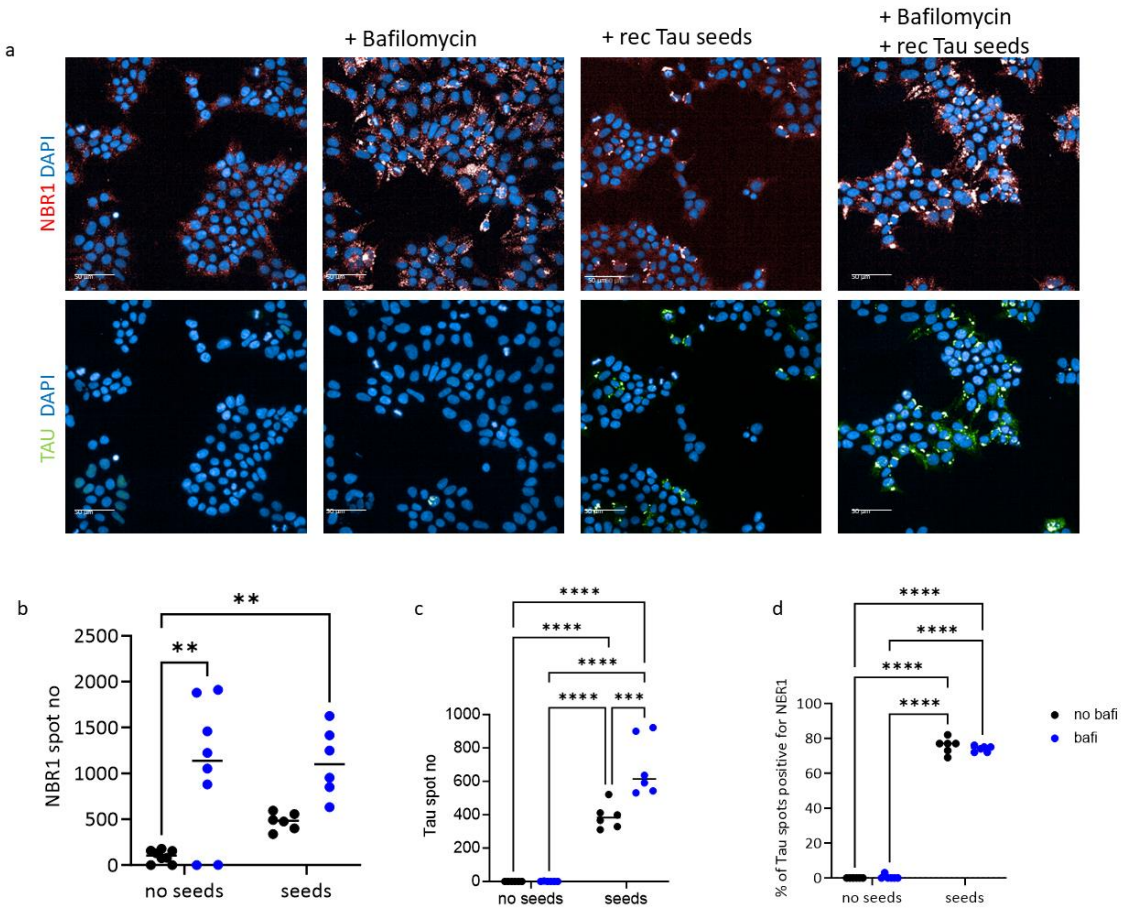

Figure 38: NBR1 co-localizes with Tau aggregates in HEK Biosensor cells

***a** Representative IF images of HEK biosensor cells (DAPI in blue, NBR1 in red) after seeding (Tau in green). **b** Quantification shows an increase in punctate staining of endogenous NBR1 following Tau aggregation induction, with a further increase observed after concurrent bafilomycin treatment. **c** Tau aggregates become noticeable post-seeding and their numbers increase following bafilomycin treatment. **d** 80% of Tau spots also display a positive NBR1 signal, with no change in co-localization observed after the addition of bafilomycin. Statistical analysis: TWO WAY ANOVA (p<0.0001 bafi and p=ns seeds) with Tukey's multiple comparison test **p<0.001, ***p=0.002, ****p<0.0001. n=3 biological replicates. The graph shows a representative biological replicate with six technical replicates.*

To establish that NBR1 spot formation relies on Tau aggregation, siRNA was used to decrease Tau expression in HEK biosensor cells. IF imaging allowed the quantification of NBR1 or Tau spots, after respective siRNA knock down (figure 39). Following seed addition, a significant reduction in Tau aggregates was observed compared to cells transfected with NT siRNA (figure 39b). This reduction was accompanied by a decrease in NBR1 spots (figure 39b), suggesting that these structures depend on Tau aggregation within HEK biosensor cells.

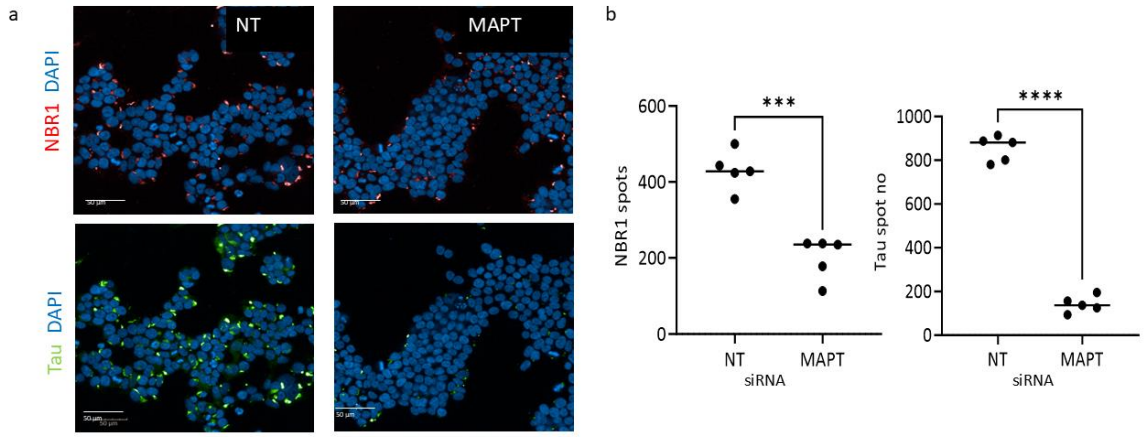

Figure 39: siRNA-mediated knock down of Tau reduced NBR1 in HEK biosensor seeding cells

***a** Representative IF images of HEK biosensor cells treated with siRNA against MAPT or non-targeting control siRNA (NT). **b** Quantification of IF spots show reduction of both NBR1 and MAPT after siRNA- mediated knock down of MAPT, compared to NT control. ***p<0.001, ****p<0.0001 (unpaired Student's t-test). n=3 biological replicates. The graph shows a representative biological replicate with five technical replicates.*

To ascertain the direct interaction between NBR1 and Tau in HEK biosensor cells, co-immunoprecipitation experiments were performed. As anticipated, bafilomycin treatment resulted in enhanced levels of the autophagy marker LC3 (Redmann et al., 2017) due to the blocked degradation of LC3-II bound to autophagosomes (figure 40a). Remarkably, Tau co-immunoprecipitated with NBR1 only after seed addition (figure 40b), implying that NBR1 interacts with aggregated Tau in this cellular context. Co-immunoprecipitation of Tau significantly increased with both seed and bafilomycin treatments, suggesting that NBR1/Tau complexes undergo autophagic degradation. Additionally, LC3-II co-immunoprecipitated with NBR1 after bafilomycin treatment, confirming the association of NBR1 with functional autophagosomes (figure 40b).

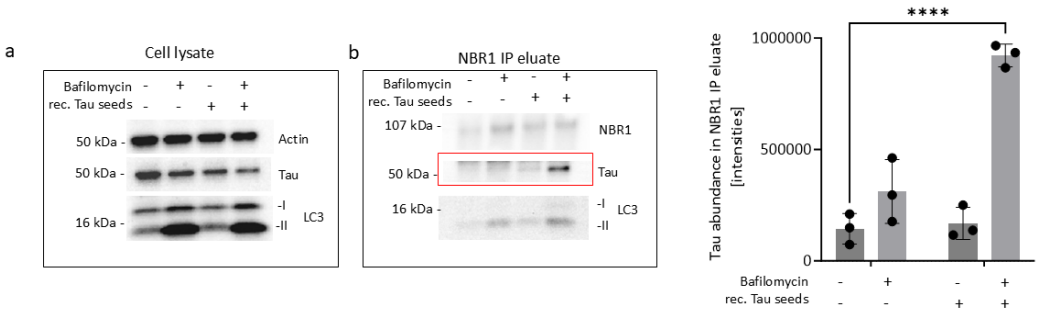

Figure 40: NBR1 interacts with Tau in seeded HEK Biosensor cells

***a** LC3-II expression increases in HEK Biosensor seeding cells after treatment with bafilomycin. Slight reduction of Tau can be observed after Bafilomycin treatment. **b** Co-immunoprecipitation confirms the interaction of*

*endogenous NBR1 with Tau in seeded HEK biosensor cells, which increases upon treatment with Bafilomycin. LC3-II increases and preferentially interacts with NBR1 upon Bafilomycin treatment. NBR1 is only detectable by Western blotting after enrichment by immunoprecipitation. Statistical analysis: TWO WAY ANOVA ($p<0.0001$ with Bafilomycin and seeds) with Dunnett's multiple comparison test ****$p<0.0001$. n=3 biological replicates.*

5.10.3 NBR1 phosphorylation may not impact Tau aggregation in HEK biosensor cells

Subsequently, the effect of phospho-NBR1 on autophagy in HEK biosensor cells was explored. Constructs for NBR1 overexpression were developed with either phospho-mimetic (S/D) or phospho-resistant (S/A) mutations at the S486 site, which had shown increased phosphorylation following seeding in human iPS-derived neurons (figure 30). Transfection of HEK biosensor cells with S486D (phospho-mimetic), S486A (phospho-resistant), or WT NBR1 produced comparable NBR1 levels (Figure 41a). Following transfection, the cells were treated with bafilomycin, and Tau aggregation was induced by adding recombinant Tau seeds. Analysis of lysates revealed no differences in LC3-II accumulation after bafilomycin treatment across the different NBR1 constructs, regardless of Tau seed presence. Additionally, Tau levels remained unchanged (Figure 41a).

To test whether phosphorylation of NBR1 interferes with the NBR1/Tau interaction observed in this model (figure 39b), co-immunoprecipitation was performed using cell lysates overexpressing phospho-mimetic, phospho-resistant or WT NBR1 (figure 41b). The analysis of the NBR1 immunoprecipitation eluate demonstrated a clear enrichment of NBR1. Furthermore, co-immunoprecipitation with LC3-II was again evident. Despite the enhanced detection of Tau in the eluates from samples subjected to seeded Tau aggregation and bafilomycin treatment (Figure 41b), the co-immunoprecipitated Tau signal was notably weaker compared to samples without prior NBR1 overexpression (Figure 41c). Additionally, biological replicates displayed considerable variability (Figure 41b) when compared to native HEK cells subjected to Co-IP (Figure 41c). No differences were observed between the mutant and wild-type NBR1 overexpression in terms of their effects on Tau/NBR1 interactions.

Overall, these findings indicate that modifications at S486 may not influence autophagy in the HEK system. Additionally, the phosphorylation of NBR1 did not seem to impact Tau/NBR1 interaction. However, phospho-mimic and phospho-resistant mutations at this site may not accurately represent the biochemical changes associated with actual phosphorylation in this HEK cell model, and different tools may need to be developed.

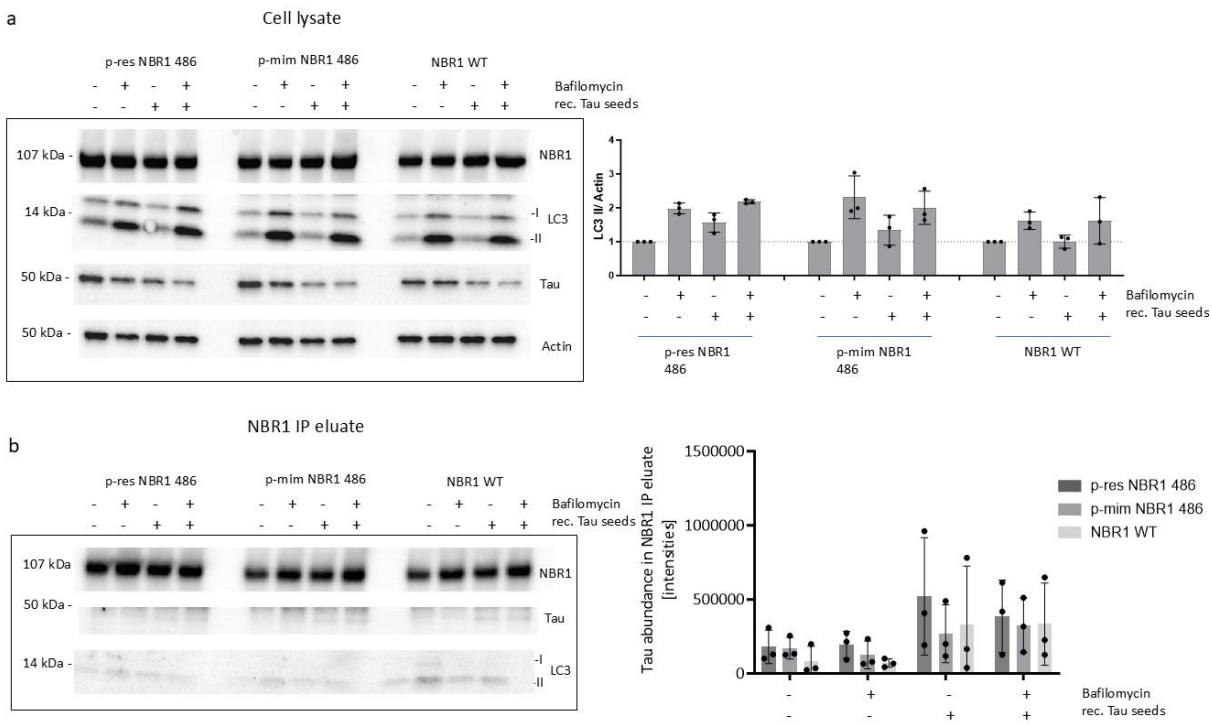

Figure 41: Overexpression of phospho-mutant NBR1 does not alter autophagy expression or interferes with Tau interaction in HEK biosensor model

a *HEK Biosensor seeding cells were transfected with NBR1 phospho-mimetic (S486D), -resistant (S486A) and WT NBR1 overexpression constructs. Next, cells were treated with bafilomycin and Tau aggregation was induced through seeding. Levels of LC3- II are not altered by overexpression of any NBR1 construct. No difference in Tau levels between cells expressing phospho-mutant or wild type NBR1 was observed.* ***b*** *Following NBR1 overexpression (phospho-mimic, phospho-resistant and WT) and subsequent co-immunoprecipitation, it was observed that Tau no longer co-eluted with NBR1, while LC3-II remained detectable. No differences between the phospho-mutants and the WT NBR1 were observed. NBR1 was strongly detected after enrichment by immunoprecipitation. n= 3 biological replicates, representative blots are shown.*

6 Discussion

6.1 Tau interactome in human brain differs in health and disease

As pathological Tau is one of the hallmarks of AD (Kosik et al., 1986), several antibodies targeting pathological Tau and its propagation have entered clinical trials, aiming to prevent Tau aggregation and spreading in neurodegenerative diseases like AD. These antibodies, including gosuranemab (Biogen) (Kim et al., 2021), tilavonemab (Abbvie) (Florian et al., 2023), semorinemab (Gentech) (Teng et al., 2022) , and zagotenemab (Eli-Lilly) (Fleisher et al., 2024), were designed to target extracellular Tau, especially the N-terminal Tau epitopes. When patients receive a diagnosis, pathological Tau is often already present throughout the brain (Arnsten et al., 2021). This underscores the necessity for further strategies aimed at targeting intracellular pathological Tau aggregates, as well as understanding and repairing the pathway dysfunctions caused by these intracellular pathological Tau formations.

Previous mass spectrometry proteomics studies gave great insights into the difference in interacting partners of Tau in AD and control brain tissue, using either one total Tau antibody (Tau-5) for pulldown of interacting proteins (Ayyadevara et al., 2016; Hsieh et al., 2019; Meier et al., 2015), or the phospho-Tau antibody PHF1, to study interacting partners of Tau in AD brain tissue only (Drummond et al., 2020). Recently, a proximity-based Tau interactome was conducted in human brain tissue using phospho-Tau AT8 as a probe for profiling of proteomes across different tauopathy brains including AD, CBD, PiD and PSP (Morderer et al., 2025). Mass spectrometry experiments are inherently variable between runs due to factors like instrument calibration, sample preparation, and environmental conditions, making it essential to conduct comparisons within a single batch to ensure valid and reliable results (Aebersold and Mann, 2003; Mann et al., 2013).

To date, no study has directly compared the interacting partners of pathological Tau from AD brains with physiological Tau from control brains within a single proteomic analysis using multiple total and phospho-Tau antibodies. This doctoral thesis addressed that gap by analyzing the Tau interactome from human AD and control brain tissue, employing three total Tau and three phospho-Tau antibodies. To ensure clear differentiation between physiological and pathological Tau species, a biochemical profiling process was employed to carefully select IP antibodies (figure 5). In addition to choosing appropriate antibodies, five brains each from AD and control samples were pre-selected to include only AD brain samples with high levels of aggregated Tau, while ensuring that the total Tau levels remained similar between AD and control brain samples (table 20). All samples underwent mass spectrometry analysis within a single experiment using the data-independent acquisition mode. Interacting partners enriched by Tau antibodies were normalized against the IgG control and considered for analysis.

Biochemical profiling indicated a similar profile for the phospho-Tau antibody, detecting respective phospho-Tau epitopes mainly in human AD brain. However, total Tau abundance captured by AT100 was much lower, compared to PHF1 or pS198 (figure 10). This was also the reason for focusing on the overlapping proteins immunoprecipitated with PHF1 and pS198 for the pathway enrichment analysis, excluding AT100. Epitope accessibility might be a key explanation for this reduced abundance of Tau after AT100 IP. The AT100 antibody recognizes a specific phosphorylation-dependent epitope (pT212/pS214) (Anderson et al., 2008) that may be buried within the folded structure of sarkosyl-insoluble Tau aggregates, potentially limiting its ability to capture Tau compared to antibodies like PHF1 and pS198, which target

regions of Tau filaments that might be more exposed. Additionally, epitope competition could play a role: if the binding site of AT100 overlaps with regions involved in Tau-Tau interactions or interactions with other proteins within the aggregates, steric hindrance could prevent efficient antibody binding. This could further contribute to the lower total Tau abundance captured by AT100 compared to other phosphorylation-specific antibodies. AT100 does not capture as much seeding competent Tau, compared to other phospho-Tau antibodies (figure 8), which makes it not as suitable as an IP bait antibody.

Here, it was observed that phospho-Tau epitopes are not exclusive to AD brains but also appear in control brains (figure 11), indicating that Tau phosphorylation has a physiological role under normal conditions. In AD, however, there is a significant increase in phospho-Tau abundance. This supports the known dual role of Tau phosphorylation. Under physiological conditions, phosphorylation regulates the binding of Tau to microtubule, allowing for the dynamic remodeling of the cytoskeletons (AVILA et al., 2004). However, in AD, excessive phosphorylation leads to Tau misfolding, aggregation, and functional loss (Iqbal et al., 2005). Strikingly, Tau phospho-sites T50, pT202, pT231 and pS396/pS404 were found in at least 4 of the control patient samples (figure 11b), similar to what was reported elsewhere (Wesseling et al., 2020). The control brain used for the IP experiments originated from elderly age-matched control brain donors, so it is possible that the phospho-sites detected here represent an early stage of the disease (Duquette et al., 2021; Wesseling et al., 2020). The phospho-sites identified in control brains could suggest that these specific sites are important for microtubule stability and Tau's binding to microtubule proteins, thereby influencing axonal transport under normal physiological conditions (Morris et al., 2011; Wesseling et al., 2020). Interestingly, Tau phospho-sites pT263 and pS289 were highly abundant in AD brains, but not in control brains (figure 11). While pS289 is known to enhance the oligomerization of Tau (Man et al., 2023), there is no evidence about pathological relevance of pT263. Given its proximity to S262, which was reported to affect microtubule stability (Meyer et al., 1995) and was recently proposed as novel biomarker for soluble Tau assemblies in AD (Islam et al., 2025), pT263 might be involved in similar processes. However, the pT263 and pS289 sites have not been extensively studied and could represent potential novel biomarkers for Tau pathology in AD.

6.2 Distinct human Tau interacting proteins are present in health and disease

Pathway enrichment analyses of proteins interacting with total Tau in healthy controls revealed that these interactors are predominantly associated with pathways related to metal ion transport (figure 14a-c). There is evidence of an imbalance of metal ions sodium (Na^+) and potassium (K^+) in AD, as elevated levels were reported in AD patient brain (Vitvitsky et al., 2012). Additionally, calcium (Ca^{2+}) signaling and homeostasis is crucial for neuronal functions such as synaptic transmission and plasticity (Wojda et al., 2008). AD brains showed increased levels of Ca^{2+}, which was reported to affect phosphorylation of Tau (Pierrot et al., 2006; Wojda et al., 2008).

Many of the enriched proteins in these pathways belonged to the solute carrier (SLC) family, a superfamily of membrane transporters present in the brain (Hu et al., 2020). The SLC family includes transporters for various metal ions like Na^+ and Ca^{2+} and is also involved in amino acid transport (Hu et al., 2020). SLC1A2, primarily located in astrocytes, is a significant Na^+-dependent glutamate transporter, the main excitatory neurotransmitter in the human brain (Takahashi et al., 2015). Although some evidence suggests that SLC1A2 interacts exclusively

with phospho-Tau (Sasaki et al., 2009), this study reports an interaction with total Tau in healthy human brains. The here reported observation that proteins related to metal ion homeostasis significantly interact with physiological Tau underscores its potential role in maintaining neuronal ion balance, crucial for neuroprotection, neuronal signaling, action potential and neurotransmitter release. Notably, many of these metal ion transporters were identified as synaptic proteins (figure 15a).

Total Tau interactors in AD patient brain contain proteins related to chemical synaptic transmission and synaptic signalling, however this enrichment was not significant (figure 14d+e). A potential explanation for this non-significant enrichment might be a technical artifact causing a reduced abundance of total Tau after immunoprecipitation from AD brain compared to control brain (figure 10). The probable reason for the decreased total Tau amount is normalization to the high total Tau levels captured by the IgG antibody, as Tau aggregates might also bind to these control beads. This normalization can result in lower Tau abundance values in AD brains, leading to only non-significant enrichment of Tau interactors compared to IgG. The non-significant enrichment of synaptic proteins may also result from synapse loss, a characteristic feature of AD (Selkoe, 2002), leading to fewer synaptic proteins being available from the outset. Conversely, the diminished interaction between phospho-Tau and synaptic proteins could be a contributing factor to the synaptic dysfunction seen in AD, given that these interactions seem vital for preserving normal synaptic function and integrity, which are crucial for cognitive processes. The absence of metal ion transport proteins among the physiological Tau interactors in the AD brain may suggest that disease progression disrupts Tau's normal interactions with these proteins. This disruption could indicate that metal ion transporters lose their functional capacity in AD, thereby contributing to neuronal dysfunction and accelerating neurodegeneration. Alternatively, the aggregation and hyperphosphorylation of Tau may impair its physiological role in supporting ion homeostasis, which in turn could further destabilize neuronal environments. Importantly, many of the metal ion transporters identified in healthy Tau interactomes are synaptic proteins, and since synapse loss is a well-established feature of AD, the absence of these interactions may simply reflect the degeneration of synaptic compartments. Thus, the missing Tau-metal ion transporter interactions may result from a combination of Tau dysfunction, transporter failure, and synaptic loss within the AD brain.

Interestingly, phospho-Tau interactors in both human AD and control brain show enrichment in pathways related to RNA binding and splicing, indicating that phosphorylated Tau may associate with proteins involved in RNA processing (figure 16). Multiple studies identified RNA-binding proteins as interacting partners of Tau in human AD and control brain (Drummond et al., 2020; Hondius et al., 2021; Kavanagh et al., 2022) as well as iPS-derived neurons (Tracy et al., 2022), implicating its role in regulating RNA metabolism and splicing in both physiology and disease states. These findings highlight the connection between Tau pathology and widespread transcriptional dysregulation, suggesting that interactions with RNA-binding proteins are critical contributors to neuronal dysfunction in AD (Kavanagh et al., 2022).

6.3 Comparison of Tau interactors in seeded or non-seeded iPS-derived neurons and human brain

Human iPS-derived neurons can be utilized as *in vitro* model for tauopathy, as seed-induced Tau aggregation can be introduced (Manos et al., 2022). To date, this model has not been

utilized for a Tau interactome study that differentiates between non-seeded, endogenous soluble tau and seed-induced aggregated Tau (figure 19). To closely align with the experimental approach of the Tau interactome study from human brain, the same antibodies were employed for phospho-Tau and total Tau to co-immunoprecipitate the interacting proteins. Crucially, to gain a comprehensive understanding of which proteins significantly interact with Tau in both the human brain and the *in vitro* model, overlaps between the respective conditions were analyzed. This overlap is noteworthy because consistently identified hits can validate interactions already observed in humans, thereby emphasizing a strong interaction between Tau and the respective proteins. Although the interactome study in iPS-derived neurons does not aim to encompass all activities occurring in the human brain, the events that are replicated can be further investigated *in vitro*.

Proteins that were enriched Tau interactors in both iPS-derived neurons and AD and control brain were related to microtubule-associated processed and RNA-binding and splicing (table 21). Proteins related to RNA splicing/binding pathways were enriched in AD and control brain, whereas they only interacted with Tau in the iPS-derived MAPT TM neurons, and not in the MAPT WT neurons. One possible explanation lies in the differences in Tau isoform expression between the iPSC-derived neuronal models. In MAPT WT neurons, Tau is predominantly expressed as the fetal 0N3R isoform, whereas MAPT TM neurons show an increased proportion of 4R Tau due to splice site mutations E10+14 and E10+16, in addition to the FTD-associated P301S mutation (Hutton et al., 1998; Manos et al., 2022). In the adult human brain, both 3R and 4R Tau isoforms are expressed at roughly equal levels (Andreadis, 2005; Spillantini and Goedert, 1998). Given that the control and AD brain tissues were derived from older individuals, it is more likely that RNA-binding proteins consistently interact with pathological, adult-like Tau in MAPT TM neurons.

Proteins of the serine/arginine (SR)-rich splicing factor family (SRSF) were commonly identified interacting with phospho-Tau in human AD brain and in seeded iPS-derived neurons, among others (figure 23). SRSF proteins are known to regulate the alternative splicing of MAPT exon 10, either promote (eg SRSF1, SRSF2, SRSF10) or suppress (SRSF3, SRSF4) its inclusion, leading to elevated or reduced expression of 4R Tau isoforms, respectively (Buchholz and Zempel, 2024; Corsi et al., 2022; Li et al., 2023). Interestingly, mis-regulation of a splicing complex, involving SRSF4, and the hence altered alternative splicing of exon 10, was shown to cause frontotemporal dementia (Wang et al., 2011). Additional RNA binding proteins were found to co-aggregate with Tau in human brain samples derived from different neurodegenerative diseases (Guo et al., 2021), suggesting a role in Tau aggregation. SNRPB and SNRPF are core components of the small ribonucleoprotein particles of the spliceosome (Wahl et al., 2009), which disruption was implicated to result in neurodegeneration (Hsieh et al., 2019). Reduction of TIA1, a RNA binding protein, led to decreased Tau aggregation (Ash et al., 2021), and even delayed neurodegeneration in mice (Apicco et al., 2018). The concept of liquid-liquid phase separation includes the formation of phase-separated RNA granules in response to cellular stress signals (Shin and Brangwynne, 2017), which contain Tau (Zhang et al., 2017). However, in AD, this process is believed to become irreversible, potentially acting as a seed for Tau aggregation (Wegmann et al., 2018). These granules contain RNA binding proteins (Ash et al., 2021), which may provide an explanation for the recurring interaction with Tau in a pathological context. It remains to be elucidated whether the interaction of Tau with RNA-binding proteins modulates Tau aggregation.

In the analysis, microtubule-associated proteins, alongside RNA binding proteins, emerged as the most prominent Tau interactors in both human brains and iPS-derived neurons (table 21).

Dual-specificity tyrosine phosphorylation-regulated kinase 1A (DYRK1A) consistently appeared as a Tau interactor in AD and control brains as well as in iPS-derived neurons (table 22). This consistent presence suggests that DYRK1A plays a role in Tau-associated processes under both physiological and pathological conditions. GO term enrichment analysis assigned DYRK1A to RNA binding and splicing pathways as well as microtubule-associated processes (table 22). It is a dual specific Serin/Threonine kinase (Kentrup et al., 1996) involved in critical signaling pathways that influence neurogenesis, developmental processes, and differentiation (Arron et al., 2006; Mercer et al., 2005; Tejedor et al., 1995). Acting as a signaling hub, DYRK1A coordinates diverse cellular activities through its broad substrate phosphorylation capability, thereby bridging RNA metabolism and cytoskeletal dynamics. First, DYRK1A contributes to microtubule stability by phosphorylating key microtubule-associated proteins, including Tau (Bessone et al., 2022; Ori-McKenney et al., 2016). It has been directly linked to Tau hyperphosphorylation at key phospho-sites such as pS202, pT212, and pS404 (Ryoo et al., 2007; WOODS et al., 2001), a process implicated in the pathogenesis of both AD and Down Syndrome (Liu et al., 2008; Wegiel et al., 2011). Secondly, DYRK1A is also implicated in RNA-related functions. It phosphorylates splicing factors (Graaf et al., 2006), interacts with transcription factors (Galceran et al., 2003) and may regulate alternative splicing of MAPT exon 10 (Ding et al., 2012). These functions align with its enrichment in gene ontology terms related to both microtubule-processes and RNA-binding proteins.

DYRK1A also plays a crucial role in neuronal development through pathways such as NOTCH signaling (Fernandez-Martinez et al., 2009; Tejedor and Hämmerle, 2011). Its multifaceted involvement in both cytoskeletal organization and RNA processing reflects its importance in neurodevelopment and cell cycle regulation. Given its central role in Tau phosphorylation and neuronal signaling, DYRK1A has emerged as a promising therapeutic target. Inhibitors such as SM07883 (Melchior et al., 2019) and DYR219 (Branca et al., 2017) have shown efficacy in preclinical models by reducing Tau hyperphosphorylation, thereby enhancing synaptic plasticity and potentially delaying AD onset (T. Liu et al., 2022). However, therapeutic targeting of DYRK1A remains challenging. Its structural similarity to other kinases and broad regulatory functions—including RNA splicing, synaptic activity, and transcriptional control—pose a significant risk of off-target effects (Park et al., 2009).

Our findings broaden the current understanding of DYRK1A's role in Tau regulation. While its interaction with Tau has been previously linked to pathological hyperphosphorylation in AD (Ryoo et al., 2007; WOODS et al., 2001), here, it is demonstrated that DYRK1A also interacts with Tau in age-matched control brains and iPSC-derived neurons. This consistent interaction across both diseased and non-diseased contexts, including fetal-like Tau forms expressed in iPSC neurons, suggests a physiological role for DYRK1A in Tau regulation beyond pathology. These results indicate that DYRK1A may be involved in Tau-related processes throughout development and aging, potentially influencing splicing, phosphorylation, and microtubule dynamics under normal conditions. It is currently unknown whether the interaction with DYRK1A contributes to Tau aggregation.

Tau is known for binding to microtubules (Binder et al., 1985; Weingarten et al., 1975), and thus naturally interacts with other microtubule-associated proteins like MAP1B, which help organize and stabilize microtubules (Goodson and Jonasson, 2018). MAP1B, besides Tau, is one of the principal neuronal microtubule-associated proteins (Bloom et al., 1985; Cleveland

et al., 1977; Noble et al., 1989). AP3B1 and B2 were found to interact with phospho and total Tau in MAPT WT iPS-derived neurons and AD and control patients. AP3B1 and 2 are part of the clathrin adapter protein or adaptin protein family, which play a crucial role in intracellular trafficking (Shin et al., 2021). AP3s especially are involved in trafficking between endosomes, lysosomes and synaptic vesicles (Faúndez et al., 1998) and are known to be involved in neuronal development through NOTCH signalling (Wilkin et al., 2008). These interactions serve as evidence that Tau retains certain normal functions even in the context of Alzheimer's disease.

In summary, the overlapping interactomes of Tau derived from human brains and iPS-derived neurons indicate that Tau interacts with RNA-binding and splicing proteins, as well as microtubule-associated proteins. Further studies are necessary to explore the direct involvement of these proteins in Tau pathology.

6.4 SV2A repression does not impact Tau pathology in iPS-derived neurons

Tau is increasingly recognized as a synaptic protein, with studies showing its presence at both pre- and postsynaptic sites (Colom-Cadena et al., 2023). Its interactions are dynamic and modulated by synaptic activity, suggesting a role in synaptic function and plasticity (Tracy et al., 2022). Activity-dependent changes in Tau localization and binding partners point to a regulatory function in processes such as neurotransmitter release, vesicle trafficking, and signal transduction (Robbins et al., 2021). Here, Tau was found to interact with a distinct set of proteins related to synaptic pathways in the human brain, particularly in control samples, with a notable enrichment for components of the synaptic vesicle membrane. Notably, multiple members of the synaptic vesicle protein 2 family, including SV2A were significantly enriched among Tau interactors in human control brain (figure 15).

While the exact role of SV2A is not fully understood, it is implicated in calcium-dependent exocytosis and neurotransmitter loading in synaptic vesicles (Mendoza-Torreblanca et al., 2013), synaptic vesicle regulation (Buckley and Kelly, 1985) and potentially the transport of vesicle constituents (Rossi et al., 2022). Mutations in SV2A link the loss of function of SV2A to epilepsy (Calame et al., 2021; Serajee and Huq, 2015; Wang et al., 2019). SV2A positron emission tomography (PET) tracers are used to measure synaptic density in living patients. Using this method, a longitudinal decrease in SV2a was shown to correlate with Tau accumulation across various regions in human AD brain (Vanderlinden et al., 2024, 2022). This association suggests that elevated baseline Tau levels are predictive of longitudinal SV2A loss, which might reflect synaptic dysfunction due to Tau pathology (Vanderlinden et al., 2024; Vanhaute et al., 2020). It was hypothesized that the loss of interaction between Tau and SV2A might contribute to increased Tau aggregation. However, siRNA-mediated knockdown of SV2A in seeded iPS-derived neurons did not alter Tau pathology (figure 16). While SV2A plays a key role in synaptic vesicle cycling and neurotransmitter release, it may not directly regulate the molecular pathways driving Tau aggregation or hyperphosphorylation. Tau pathology is multifactorial and likely influenced by alternative mechanisms independent of SV2A. Moreover, compensatory processes within neurons may buffer the effects of SV2A loss, preserving Tau pathology despite reduced expression. A potential follow-up experiment would be to overexpress SV2A in iPS-derived neurons to assess whether increased SV2A levels modulate Tau aggregation in the opposite direction.

Levetiracetam (LVA) is an antiepileptic drug that modulates SV2A and reduces neuronal hyperexcitability (Lynch et al., 2004). There is an ongoing clinical trial for treating

hyperexcitability in AD with LVA (Beath Israel Lahey Health, ID NCT03875638, 2019P000091), investigating the connection between cortical hyperexcitability, irregularities in brain network function, and cognitive impairment. In mouse studies it was shown that while LVA treatment resulted in slight decrease of Tau pathology, it did not result in any cognitive improvements (Thompson et al., 2024).

Due to this emerging evidence suggesting that LVA influences Tau pathology, this thesis investigated whether treating iPS-derived neurons with Levetiracetam affected Tau aggregation, and in parallel evaluating the potential effect of SV2A on Tau aggregation. No impact of LVA on Tau pathology was observed (figure 17). This lack of impact may be attributed to several factors: firstly, LVA might not directly affect the interaction of Tau and SV2A, as its primary mechanism is modulating SV2A activity, thus reducing neuronal hyperexcitability (Sanchez et al., 2012; Yang et al., 2021). There is evidence for increased hyperexcitability in iPS-derived neurons bearing FAD or APOE4 mutations (Anastacio et al., 2022; Burley et al., 2022; Ghatak et al., 2019), and it was shown that Tau pathology is increased in mice with chronic hyperexcitability (Nishida et al., 2024; Shimojo et al., 2020). However, it is unclear if hyperexcitability plays a significant role in driving Tau pathology in the iPS-derived neuronal model employed in this study. Thus, the iPS-derived neurons may not exhibit the hyperexcitability or seizure-like activity that LVA typically mitigates. Potentially, neurons may need to be stimulated in order to see a significant effect. Additionally, the neuronal model does not include key elements of an *in vivo* microenvironment, particularly glial cells and neuroinflammatory processes. Such factors can strongly influence synaptic function and potential effects of LVA on Tau pathology may not be evident in their absence.

6.5 BioID is a valid complementary method to identify Tau interactors *in vitro*

While IP-MS interactome studies provide valuable insights into Tau biology, they are limited by technical challenges. Homogenization of human brain tissue and iPS-derived neurons can induce artificial interactions, while weak or transient associations may be lost during lysis. To address these issues, proximity-labeling approaches such as BioID offer a promising alternative. BioID enables the labeling of interacting proteins in living cells, preserving the native context and capturing dynamic or low-affinity interactions (Roux et al., 2012). This method uses a fusion of the protein of interest with a modified biotin ligase (BirA), which biotinylates nearby proteins. These labeled interactors can then be enriched and identified via mass spectrometry, providing a more physiologically relevant view of Tau's interaction network.

In this study, the Tau interactome was characterized using Tau-BioID proximity labeling in iPS-derived neurons. The presence of microtubule-associated proteins as interactors of seeded Tau-BioID (figure 29) indicates that the observed cellular interactions might reflect the physiological function of Tau rather than the pathological Tau, as the physiological Tau acts as a microtubule-associated protein in neural stability and maintenance of microtubule (Feinstein and Wilson, 2005; Weingarten et al., 1975). In the Tau-BioID vs BioID-only comparisons, no other pathways were significantly enriched and the main enriched differentially expressed protein was Tau itself. These results suggest a high background of biotin-labeled proteins, which potentially only allowed for the highly abundant proteins, rather than transient interactions, to be detected. The addition of biotin for 24 hours until lysis may also restrict the detection of highly dynamic real-time protein interactions. Unwanted biotin, which is likely already contained in the culture media (Lyra-Leite et al., 2023) may

furthermore be problematic for BioID experiments because it can lead to excessive, non-specific biotinylation of proteins. Since BioID relies on a biotin ligase to label nearby interactors, uncontrolled biotin levels may increase background noise by biotinylating proteins indiscriminately.

The BioID experiment utilized the iNGN2 differentiation protocol (Zhang et al., 2013), a rapid and efficient method for generating neurons. While these neurons displayed all essential characteristics and Tau aggregation was observed (figure 26, 27, 28), this approach may overlook certain factors contributing to the reported vulnerability of cortical excitatory neurons in AD (Fu et al., 2018; Verheyen et al., 2018b). Furthermore, the accelerated NGN2 differentiation process could result in more immature synaptic development and a lack of regional identity. These aspects may be better recapitulated using the dual SMAD inhibition protocol (Cao et al., 2017; Stuart M. Chambers et al., 2009; Gaspard et al., 2008; Manos et al., 2022). Therefore, for future studies, repeating the BioID experiment with this alternative neuronal model could enhance seed-induced Tau aggregation, potentially leading to a more distinct enrichment of pathological Tau interactors.

Another area for improvement could be the design of the Tau-BioID construct used in this study. Tau expression was observed as a double band with constructs linking Tau to the biotin ligase (figure 26a). This double band may be a result of inefficient cleavage of the T2A sequence potentially resulting in the expression of protein products partially fused to the blasticidin resistance gene (figure 26b). T2A is a self-cleaving peptide sequence used to enable the expression of two proteins from a single transcript (Liu et al., 2017). Incomplete T2A cleavage in a BioID experiment can be problematic because it may result in the blasticidin-resistance gene not being fully separated from the biotin ligase. If cleavage is incomplete, the biotin ligase could remain attached, affecting its proper localization or function, which might lead to non-specific biotinylation. Taken together, Tau interactors were related to microtubule-associated pathways, aligning with already identified pathway enrichments for Tau in human brain and iPS-derived neurons. Although the generated iPS-derived neurons showed successful and stable expression of Tau-BioID and BioID- only proteins and seeded Tau aggregation could be successfully introduced, several options for improvements remain. Optimizing the differentiation protocol with dual SMAD inhibition and refining cloning constructs for cleaner cleavage could enhance the sensitivity and specificity of the BioID experiment. Despite the challenges and areas for improvement, it is still worth the effort to refine the BioID approach, as it remains a valuable complementary method for identifying Tau interactors in a live-cell system. Unlike traditional biochemical approaches that require cell lysis and homogenization, potentially introducing artificial proximity effects, BioID enables the capture of interactors in their native cellular environment (Roux et al., 2013).

6.6 A potential role for the autophagy receptor NBR1 in the degradation of Tau aggregates

The second part of this doctoral project aimed to clarify how seeded Tau aggregation affects the neuronal proteome and phospho-proteome in human iPS-derived neurons (figure 30). It was observed that seeded Tau aggregation significantly modified the phospho-proteome of iPS-derived MAPT TM neurons, notably increasing phospho-peptides on endogenous Tau at sites known to be relevant to AD such as pT231, pT235, and pS356 (Stefanoska et al., 2022; Wegmann et al., 2021; Wesseling et al., 2020). These phosphorylation sites, particularly Tau pT231 and pT235, are known to appear in Tau tangles during the early stages of AD

(Augustinack et al., 2002; Luna-Muñoz et al., 2005). Additional phospho-sites like pT181, a common biomarker, and pS396/404 (PHF1 epitope) were identified, which are common in the brains of AD patients and linked to the seeding capability of Tau (Wesseling et al., 2020). No significant changes post-seeding were noted in iPS-derived MAPT WT neurons, although there was a trend towards increased phosphorylation at sites MAPT pT231, pT235, and pT237. These results align with previous findings which documented slower aggregation kinetics and less prominent somato-dendritic aggregate formation in WT neurons, compared to those derived from MAPT TM iPS (Manos et al., 2022) .

Unexpectedly, there were no significant long-term alterations in the neuronal proteome following the induction of endogenous Tau aggregation through seed addition, in systems using either WT Tau or neurons expressing 3R and 4R Tau with the P301S mutation (MAPT TM) (figure 32). This is also in alignment with no detected proteomic alterations after seeding in iNGN2 Tau-BioID neurons (figure 29b). Several factors could explain this outcome: firstly, neither we nor others have detected cell death post-seeding in iPS-derived neuronal models (Bravo et al., 2024a; Manos et al., 2022), indicating that the aggregates formed are not acutely toxic in vitro. The neurons exhibit rapid aggregation kinetics within the four-week experimental period, possibly allowing the accumulation of larger, less harmful aggregates, bypassing the more toxic intermediate structures. Furthermore, the model system lacks additional AD-related pathologies, such as amyloid-beta plaques or neuroinflammatory triggers, which might be required to fully replicate Tau pathology and enhance Tau seeding effects. Lastly, Tau aggregates might cause changes in protein localization and/or solubility rather than protein abundance, potentially leading to functional consequences such as loss or gain of function for the affected proteins. These changes are not detectable in the current experimental setup and warrant further investigation in future studies.

Interestingly, iPS-derived MAPT TM neurons showed higher levels of synaptic protein expression compared to MAPT WT neurons, possibly indicating accelerated neuronal maturation. MAPT mutations associated with FTD can affect the expression of synaptic, endolysosomal, and developmental genes in iPS-derived neurons (Minaya et al., 2023), suggesting that mutant Tau expression could influence synaptic function and neuronal development. Additionally, the MAPT E10+14/E10+16 mutation results in an increased expression of the 4R Tau isoform (Manos et al., 2022), leading iPS-derived MAPT TM neurons to resemble a more mature Tau isoform expression pattern, potentially further impacting neuronal maturation. Collectively, the differences in Tau isoform expression, the P301S mutation, and the observed accelerated maturation in MAPT TM neurons may explain the variations in Tau aggregation kinetics and the pronounced effects of seeding on the phospho-proteome in this model compared to MAPT WT neurons.

Beyond the changes observed in Tau protein itself, the phospho-proteomic analysis identified a significant increase in NBR1 phosphorylation at S486 in seeded MAPT TM neurons. Phosphorylation of autophagy receptors is known to occur frequently at sites N-terminal to the LC3-binding LIR repeat domains and within these domains (Schreiber and Peter, 2014). These phosphorylation events can influence the interaction between autophagy receptors and Atg8-like proteins such as LC3 (Schreiber and Peter, 2014). Notably, the new NBR1 phosphosites discovered in this study are located 77 and 76 amino acids upstream of the two LIR domains in NBR1: pS486, significantly upregulated post-seeding in our neuronal system, is near the LIR2 domain (aa563-566), while pS656, which shows a tendency towards increased phosphorylation post-seeding, is near the LIR1 domain (aa732-735). The consistent distance

of each site to an LIR domain implies potential regulatory functions yet to be identified. Using HEK biosensor cells expressing an aggregation-prone Tau fragment, the recruitment of NBR1 into seed-induced Tau aggregates was demonstrated. The addition of Bafilomycin increased the number of both NBR1 and Tau spots. Additionally, enhanced co-immunoprecipitation of Tau with NBR1 when seeds and Bafilomycin were present was observed, indicating that the NBR1/Tau complexes are likely subject to autophagic degradation in this system. However, the overexpression of phospho-mimic and phospho-resistant NBR1 mutants did not influence autophagy or Tau aggregation in the HEK cell system. This may be due to a neuron-specific role of NBR1 phosphorylation not replicated in immortalized cell lines. To overcome this experimental limitation, iPS-derived neurons could be used instead of HEK cells, so that the phospho-NBR1 mutants would be introduced into the cell by means of a virus and expressed stably. Potentially, these cells would capture the impact of (phospho-) NBR1 to Tau more comprehensively. Alternatively, phospho-mimic and phospho-resistant mutations might not fully capture the biochemical changes of actual phosphorylation, suggesting a need for alternative investigative tools.

Additionally, the interaction between phosphorylated Tau and NBR1 was verified using IP-MS experiments on both iPS-derived neurons and human brain tissue. Co-immunoprecipitation and thus interaction was observed solely in seeded MAPT TM iPS-derived neurons in vitro and in human AD patient brains. In contrast, this interaction was absent in non-demented control donor brains, non-seeded MAPT TM neurons, and MAPT WT iPS-derived neurons, aligning with the absence of NBR1 phosphorylation after seeding in this model. Previous studies have suggested that p62 acts as an autophagy receptor for aggregated Tau (Xu et al., 2019). However, even though p62 binds to Tau aggregates, this does not always lead to their autophagic degradation. In particular, excessive p62 accumulation on Tau fibrils can inhibit the recruitment of additional autophagy proteins, a phenomenon observed in Alzheimer's disease (Ferrari et al., 2024). While the role of NBR1 as an autophagy receptor is not as well understood as for p62, it is known that these two proteins can independently facilitate the degradation of cargo (Kirkin et al., 2009; Savova et al., 2020). The findings reported here suggest that in MAPT TM iPS-derived neurons NBR1 has a significant impact on the clearance of Tau aggregates: the knockdown of NBR1 led to a strong increase in Tau aggregates, while the knockdown of p62 had no significant effect. Taken together, the data thus suggest that NBR1 plays an important role in the degradation machinery for Tau aggregates in neurons. To accurately clarify the role of NBR1 in the degradation of pathological aggregates, future studies are needed to clarify the mechanistic mode of action.

7 Outlook

The exploration of Tau interactomes offers promising avenues for identifying therapeutic targets that could combat Tau pathology and its implications in neurodegenerative diseases like AD.

This doctoral thesis identified RNA-binding proteins and microtubule-associated proteins as key Tau interactors in both human brain tissue and iPS-derived neurons. Their consistent detection across models points to a significant role in modulating Tau aggregation and pathology. Future studies could focus on specific candidates—such as DYRK1A or splicing regulators from the SRSF family—by manipulating their expression in iPS-derived neurons. Such *in vitro* approaches could help clarify their direct contribution to Tau pathology and reveal potential targets for therapeutic intervention. RNA-binding proteins interact with Tau and may play a role in regulating its alternative splicing, thereby influencing the expression of distinct Tau isoforms. This regulation likely differs between healthy and AD conditions. Future research could explore how Tau isoform expression changes in iPS-derived neurons following the knockdown of specific RNA-binding proteins identified as Tau interactors. Gaining insight into how these proteins affect Tau splicing may reveal targets to correct aberrant isoform expression and reduce pathological aggregation.

Beyond these broad classes of interactors, specific proteins such as SV2A offer intriguing potential as therapeutic targets. SV2A showed no impact on Tau aggregation after knock down in iPS-derived neurons, however, future experiments could involve the overexpression of the protein to study the reverse effect on Tau aggregation. Additionally, since SV2a has a role in vesicular transport, future studies might explore how its interaction with Tau influence Tau trafficking and accumulation within synapses.

The fidelity of current methodologies like BioID experiments, which map protein interactions, could be improved to enhance their accuracy and applicability. One area of improvement is the refinement of cloning constructs to ensure efficient T2A cleavage, essential for reliable data. Additionally, exploring alternative cell differentiation systems may provide robust environments for these experiments, leading to more precise mapping of the Tau interactome.

Similarly, the potential function of NBR1 as an autophagy receptor in Tau pathology requires further investigation. Future studies might involve understanding the mechanism of action. Using a more disease-relevant cell model system, such as iPS-derived neurons, NBR1 overexpression constructs could be introduced, including the identified phosphorylation site, and the impact on Tau pathology could be evaluated. Furthermore, ubiquitination assays may be performed, to investigate whether NBR1 facilitates ubiquitination of Tau aggregates, which would mark them for selective autophagy. Understanding its mechanism could lead to therapies aimed at enhancing autophagic processes to clear Tau aggregates and reduce their neurotoxic effects.

8 Acknowledgements

I would like to express my deepest gratitude to all those who have supported me throughout this PhD journey, and to AbbVie GmbH for funding this project and my position.

First and foremost, I am sincerely thankful to my PhD supervisor, Prof. Dr. Stefan Lichtenthaler, for his guidance, encouragement, and scientific mentorship. His openness to questions and timely feedback have been invaluable. I also deeply appreciated the warm welcome during my visits to Munich and the constructive input that significantly enriched my thesis. I would also like to thank the members of my PhD committee, Priv.-Doz. Dr. Johannes Glöckner and Prof. Dr. Mikael Simons, for their insightful contributions.

A special thank you goes to Dr. Dagmar Ehrnhöfer, my AbbVie PhD supervisor. I am immensely grateful for the opportunity she created for me—this position has been central to my professional and personal growth. Her unwavering support enabled many meaningful experiences, such as visiting the US site and participating in international conferences. I deeply appreciate her trust in me to work on such an exciting PhD project. Her creative insights, endless ideas, and exceptional feedback on papers and my thesis have been truly invaluable. I am forever grateful for all she has done for me.

I also want to thank my bioinformatics buddy, Dr. Iwan Parfentev, whose expertise and patience were essential throughout this journey. I'm especially thankful for his willingness to tackle my countless questions and figure requests with dedication and clarity.

My heartfelt thanks go to Andreas Striebinger, the biochemistry guru, who taught me everything about best lab practices and biochemistry methods. Being part of our dream team in lab 353—with David—made lab work a joy. Our daily coffee and science talks, paired with our shared sense of humor, turned every workday into something to look forward to. PhD life with the two of you was an incredible experience I will always cherish.

I'd also like to thank the entire Tau team and the Neuroscience Discovery colleagues in LU for being the most supportive and kind team one could hope for. I'm deeply grateful to many of you—for teaching me how not to kill iPS-derived neurons, letting me jump the sample queue at the mass spectrometer, and always offering your support and expertise when needed.

Finally, I want to thank my family—my parents, my brother (and Eddie)—for their constant encouragement. Time spent with you always helps me recharge and regain strength.

The most important thank you goes to Janni, my best friend and love. Thank you for standing by my side through all stages of life and for being my sunshine.

9 References

Adams, S.J., DeTure, M.A., McBride, M., Dickson, D.W., Petrucelli, L., 2010. Three Repeat Isoforms of Tau Inhibit Assembly of Four Repeat Tau Filaments. PLoS ONE 5, e10810. https://doi.org/10.1371/journal.pone.0010810

Aebersold, R., Mann, M., 2003. Mass spectrometry-based proteomics. Nature 422, 198–207. https://doi.org/10.1038/nature01511

Alonso, A. del C., Grundke-Iqbal, I., Barra, H.S., Iqbal, K., 1997. Abnormal phosphorylation of tau and the mechanism of Alzheimer neurofibrillary degeneration: Sequestration of microtubule-associated proteins 1 and 2 and the disassembly of microtubules by the abnormal tau. Proc. Natl. Acad. Sci. 94, 298–303. https://doi.org/10.1073/pnas.94.1.298

Anastacio, H.T.D., Matosin, N., Ooi, L., 2022. Neuronal hyperexcitability in Alzheimer's disease: what are the drivers behind this aberrant phenotype? Transl. Psychiatry 12, 257. https://doi.org/10.1038/s41398-022-02024-7

Anderson, J.M., Hampton, D.W., Patani, R., Pryce, G., Crowther, R.A., Reynolds, R., Franklin, R.J.M., Giovannoni, G., Compston, D.A.S., Baker, D., Spillantini, M.G., Chandran, S., 2008. Abnormally phosphorylated tau is associated with neuronal and axonal loss in experimental autoimmune encephalomyelitis and multiple sclerosis. Brain 131, 1736–1748. https://doi.org/10.1093/brain/awn119

Andreadis, A., 2005. Tau gene alternative splicing: expression patterns, regulation and modulation of function in normal brain and neurodegenerative diseases. Biochim. Biophys. Acta (BBA) - Mol. Basis Dis. 1739, 91–103. https://doi.org/10.1016/j.bbadis.2004.08.010

Andreadis, A., Broderick, J.A., Kosik, K.S., 1995. Relative exon affinities and suboptimal splice site signals lead to non-equivalence of two cassette exons. Nucleic Acids Res. 23, 3585–3593. https://doi.org/10.1093/nar/23.17.3585

Andreadis, A., Brown, W.M., Kosik, K.S., 1992. Structure and novel exons of the human tau gene. Biochemistry 31, 10626–33. https://doi.org/10.1021/bi00158a027

Apicco, D.J., Ash, P.E.A., Maziuk, B., LeBlang, C., Medalla, M., Abdullatif, A.A., Ferragud, A., Botelho, E., Ballance, H.I., Dhawan, U., Boudeau, S., Cruz, A.L., Kashy, D., Wong, A., Goldberg, L.R., Yazdani, N., Zhang, C., Ung, C.Y., Tripodis, Y., Kanaan, N.M., Ikezu, T., Cottone, P., Leszyk, J., Li, H., Luebke, J., Bryant, C.D., Wolozin, B., 2018. Reducing the RNA binding protein TIA1 protects against tau-mediated neurodegeneration in vivo. Nat. Neurosci. 21, 72–80. https://doi.org/10.1038/s41593-017-0022-z

Aranda, M.P., Kremer, I.N., Hinton, L., Zissimopoulos, J., Whitmer, R.A., Hummel, C.H., Trejo, L., Fabius, C., 2021. Impact of dementia: Health disparities, population trends, care interventions, and economic costs. J. Am. Geriatr. Soc. 69, 1774–1783. https://doi.org/10.1111/jgs.17345

Arboleda-Velasquez, J.F., Lopera, F., O'Hare, M., Delgado-Tirado, S., Marino, C., Chmielewska, N., Saez-Torres, K.L., Amarnani, D., Schultz, A.P., Sperling, R.A., Leyton-Cifuentes, D., Chen, K., Baena, A., Aguillon, D., Rios-Romenets, S., Giraldo, M., Guzmán-Vélez, E., Norton, D.J., Pardilla-Delgado, E., Artola, A., Sanchez, J.S., Acosta-Uribe, J., Lalli, M., Kosik, K.S., Huentelman, M.J., Zetterberg, H., Blennow, K., Reiman, R.A., Luo, J., Chen, Y., Thiyyagura, P., Su, Y., Jun, G.R., Naymik, M., Gai, X., Bootwalla, M., Ji, J., Shen, L., Miller, J.B., Kim, L.A., Tariot, P.N., Johnson, K.A., Reiman, E.M., Quiroz, Y.T., 2019. Resistance to autosomal dominant Alzheimer's disease in an APOE3 Christchurch homozygote: a case report. Nat. Med. 25, 1680–1683. https://doi.org/10.1038/s41591-019-0611-3

Arnsten, A.F.T., Datta, D., Tredici, K.D., Braak, H., 2021. Hypothesis: Tau pathology is an initiating factor in sporadic Alzheimer's disease. Alzheimer's Dement. 17, 115–124. https://doi.org/10.1002/alz.12192

Arron, J.R., Winslow, M.M., Polleri, A., Chang, C.-P., Wu, H., Gao, X., Neilson, J.R., Chen, L., Heit, J.J., Kim, S.K., Yamasaki, N., Miyakawa, T., Francke, U., Graef, I.A., Crabtree, G.R., 2006. NFAT dysregulation by increased dosage of DSCR1 and DYRK1A on chromosome 21. Nature 441, 595–600. https://doi.org/10.1038/nature04678

Asai, H., Ikezu, S., Tsunoda, S., Medalla, M., Luebke, J., Haydar, T., Wolozin, B., Butovsky, O., Kügler, S., Ikezu, T., 2015. Depletion of microglia and inhibition of exosome synthesis halt tau propagation. Nat. Neurosci. 18, 1584–1593. https://doi.org/10.1038/nn.4132

Ash, P.E.A., Lei, S., Shattuck, J., Boudeau, S., Carlomagno, Y., Medalla, M., Mashimo, B.L., Socorro, G., Al-Mohanna, L.F.A., Jiang, L., Öztürk, M.M., Knobel, M., Ivanov, P., Petrucelli, L., Wegmann, S., Kanaan, N.M., Wolozin, B., 2021a. TIA1 potentiates tau phase separation and promotes generation of toxic oligomeric tau. Proc. Natl. Acad. Sci. United States Am. 118, e2014188118. https://doi.org/10.1073/pnas.2014188118

Augustinack, J.C., Schneider, A., Mandelkow, E.-M., Hyman, B.T., 2002a. Specific tau phosphorylation sites correlate with severity of neuronal cytopathology in Alzheimer's disease. Acta Neuropathol. 103, 26–35. https://doi.org/10.1007/s004010100423

AVILA, J., LUCAS, J.J., PÉREZ, M., HERNÁNDEZ, F., 2004. Role of Tau Protein in Both Physiological and Pathological Conditions. Physiol. Rev. 84, 361–384. https://doi.org/10.1152/physrev.00024.2003

Ayalon, G., Lee, S.-H., Adolfsson, O., Foo-Atkins, C., Atwal, J.K., Blendstrup, M., Booler, H., Bravo, J., Brendza, R., Brunstein, F., Chan, R., Chandra, P., Couch, J.A., Datwani, A., Demeule, B., DiCara, D., Erickson, R., Ernst, J.A., Foreman, O., He, D., Hötzel, I., Keeley, M., Kwok, M.C.M., Lafrance-Vanasse, J., Lin, H., Lu, Y., Luk, W., Manser, P., Muhs, A., Ngu, H., Pfeifer, A., Pihlgren, M., Rao, G.K., Scearce-Levie, K., Schauer, S.P., Smith, W.B., Solanoy, H., Teng, E., Wildsmith, K.R., Yadav, D.B., Ying, Y., Fuji, R.N., Kerchner, G.A., 2021. Antibody semorinemab reduces tau pathology in a transgenic mouse model and engages tau in patients with Alzheimer's disease. Sci. Transl. Med. 13. https://doi.org/10.1126/scitranslmed.abb2639

Ayyadevara, S., Balasubramaniam, M., Parcon, P.A., Barger, S.W., Griffin, W.S.T., Alla, R., Tackett, A.J., Mackintosh, S.G., Petricoin, E., Zhou, W., Reis, R.J.S., 2016a. Proteins that mediate protein aggregation and cytotoxicity distinguish Alzheimer's hippocampus from normal controls. Aging Cell 15, 924–939. https://doi.org/10.1111/acel.12501

Barini, E., Plotzky, G., Mordashova, Y., Hoppe, J., Rodriguez-Correa, E., Julier, S., LePrieult, F., Mairhofer, I., Mezler, M., Biesinger, S., Cik, M., Meinhardt, M.W., Ercan-Herbst, E., Ehrnhoefer, D.E., Striebinger, A., Bodie, K., Klein, C., Gasparini, L., Schlegel, K., 2022a. Tau in the brain interstitial fluid is fragmented and seeding–competent. Neurobiol. Aging 109, 64–77. https://doi.org/10.1016/j.neurobiolaging.2021.09.013

Barthélemy, N.R., Bateman, R.J., Hirtz, C., Marin, P., Becher, F., Sato, C., Gabelle, A., Lehmann, S., 2020. Cerebrospinal fluid phospho-tau T217 outperforms T181 as a biomarker for the differential diagnosis of Alzheimer's disease and PET amyloid-positive patient identification. Alzheimer's Res. Ther. 12, 26. https://doi.org/10.1186/s13195-020-00596-4

Bejanin, A., Schonhaut, D.R., Joie, R.L., Kramer, J.H., Baker, S.L., Sosa, N., Ayakta, N., Cantwell, A., Janabi, M., Lauriola, M., O'Neil, J.P., Gorno-Tempini, M.L., Miller, Z.A., Rosen, H.J., Miller, B.L., Jagust, W.J., Rabinovici, G.D., 2017. Tau pathology and neurodegeneration contribute to cognitive impairment in Alzheimer's disease. Brain 140, 3286–3300. https://doi.org/10.1093/brain/awx243

Bellenguez, C., Küçükali, F., Jansen, I. E., Kleineidam, L., Moreno-Grau, S., Amin, N., Naj, A. C., Campos-Martin, R., Grenier-Boley, B., Andrade, V., Holmans, P. A., Boland, A., Damotte, V., Lee, S. J. van der, Costa, M. R., Kuulasmaa, T., Yang, Q., Rojas, I. de, Bis, J. C., … Lambert, J.-C. (2022). New insights into the genetic etiology of Alzheimer's disease and related dementias. *Nature Genetics*, *54*(4), 412–436. https://doi.org/10.1038/s41588-022-01024-z

Bessone, I.F., Navarro, J., Martinez, E., Karmirian, K., Holubiec, M., Alloatti, M., Goto-Silva, L., Yepez, C.A., Martins-de-Souza, D., Nascimento, J.M., Bruno, L., Saez, T.M., Rehen, S.K., Falzone, T.L., 2022. DYRK1A Regulates the Bidirectional Axonal Transport of APP in Human-Derived Neurons. J. Neurosci. 42, 6344–6358. https://doi.org/10.1523/jneurosci.2551-21.2022

Binder, L.I., Frankfurter, A., Rebhun, L.I., 1985. The distribution of tau in the mammalian central nervous system. J. cell Biol. 101, 1371–1378. https://doi.org/10.1083/jcb.101.4.1371

Biundo, F., Prete, D.D., Zhang, H., Arancio, O., D'Adamio, L., 2018. A role for tau in learning, memory and synaptic plasticity. Sci. Rep. 8, 3184. https://doi.org/10.1038/s41598-018-21596-3

Bjørkøy, G., Lamark, T., Brech, A., Outzen, H., Perander, M., Øvervatn, A., Stenmark, H., Johansen, T., 2005. p62/SQSTM1 forms protein aggregates degraded by autophagy and has a protective effect on huntingtin-induced cell death. J. Cell Biol. 171, 603–614. https://doi.org/10.1083/jcb.200507002

Bloom, G.S., Luca, F.C., Vallee, R.B., 1985. Microtubule-associated protein 1B: identification of a major component of the neuronal cytoskeleton. Proc. Natl. Acad. Sci. 82, 5404–5408. https://doi.org/10.1073/pnas.82.16.5404

Bolós, M., Llorens-Martín, M., Jurado-Arjona, J., Hernández, F., Rábano, A., Avila, J., 2016. Direct Evidence of Internalization of Tau by Microglia In Vitro and In Vivo. J. Alzheimer's Dis. 50, 77–87. https://doi.org/10.3233/jad-150704

Braak, H., Braak, E., 1991. Neuropathological stageing of Alzheimer-related changes. Acta Neuropathol. 82, 239–259. https://doi.org/10.1007/bf00308809

Branca, C., Shaw, D.M., Belfiore, R., Gokhale, V., Shaw, A.Y., Foley, C., Smith, B., Hulme, C., Dunckley, T., Meechoovet, B., Caccamo, A., Oddo, S., 2017. Dyrk1 inhibition improves Alzheimer's disease-like pathology. Aging Cell 16, 1146–1154. https://doi.org/10.1111/acel.12648

Bravo, C.P., Giani, A.M., Madero-Perez, J., Zhao, Z., Wan, Y., Samelson, A.J., Wong, M.Y., Evangelisti, A., Cordes, E., Fan, L., Ye, P., Zhu, D., Pozner, T., Mercedes, M., Patel, T., Yarahmady, A., Carling, G.K., Sterky, F.H., Lee, V.M.Y., Lee, E.B., DeTure, M., Dickson, D.W., Sharma, M., Mok, S.-A., Luo, W., Zhao, M., Kampmann, M., Gong, S., Gan, L., 2024a. Human iPSC 4R tauopathy model uncovers modifiers of tau propagation. Cell 187, 2446-2464.e22. https://doi.org/10.1016/j.cell.2024.03.015

Bravo, C.P., Naguib, S.A., Gan, L., 2024b. Cellular and pathological functions of tau. Nat. Rev. Mol. Cell Biol. 25, 845–864. https://doi.org/10.1038/s41580-024-00753-9

Brelstaff, J., Tolkovsky, A.M., Ghetti, B., Goedert, M., Spillantini, M.G., 2018. Living Neurons with Tau Filaments Aberrantly Expose Phosphatidylserine and Are Phagocytosed by Microglia. Cell Rep. 24, 1939-1948.e4. https://doi.org/10.1016/j.celrep.2018.07.072

Brettschneider, J., Tredici, K.D., Lee, V.M.-Y., Trojanowski, J.Q., 2015. Spreading of pathology in neurodegenerative diseases: a focus on human studies. Nat. Rev. Neurosci. 16, 109–120. https://doi.org/10.1038/nrn3887

Brion, J.-P., Octave, J.N., Couck, A.M., 1994. Distribution of the phosphorylated microtubule-associated protein tau in developing cortical neurons. Neuroscience 63, 895–909. https://doi.org/10.1016/0306-4522(94)90533-9

Buchholz, S., Zempel, H., 2024a. The six brain-specific TAU isoforms and their role in Alzheimer's disease and related neurodegenerative dementia syndromes. Alzheimer's Dement. 20, 3606–3628. https://doi.org/10.1002/alz.13784

Buckley, K., Kelly, R.B., 1985. Identification of a transmembrane glycoprotein specific for secretory vesicles of neural and endocrine cells. J. cell Biol. 100, 1284–1294. https://doi.org/10.1083/jcb.100.4.1284

Burley, S., Beccano-Kelly, D.A., Talbot, K., Llana, O.C., Wade-Martins, R., 2022. Hyperexcitability in young iPSC-derived C9ORF72 mutant motor neurons is associated with increased intracellular calcium release. Sci. Rep. 12, 7378. https://doi.org/10.1038/s41598-022-09751-3

Burns, S., Selman, A., Sehar, U., Rawat, P., Reddy, A.P., Reddy, P.H., 2022. Therapeutics of Alzheimer's Disease: Recent Developments. Antioxidants 11, 2402. https://doi.org/10.3390/antiox11122402

Caceres, A., Kosik, K.S., 1990. Inhibition of neurite polarity by tau antisense oligonucleotides in primary cerebellar neurons. Nature 343, 461–463. https://doi.org/10.1038/343461a0

Calame, D.G., Herman, I., Riviello, J.J., 2021. A de novo heterozygous rare variant in SV2A causes epilepsy and levetiracetam-induced drug-resistant status epilepticus. Epilepsy Behav. Rep. 15, 100425. https://doi.org/10.1016/j.ebr.2020.100425

Candia, R.F., Cohen, L.S., Morozova, V., Corbo, C., Alonso, A.D., 2022. Importin-Mediated Pathological Tau Nuclear Translocation Causes Disruption of the Nuclear Lamina, TDP-43 Mislocalization and Cell Death. Front. Mol. Neurosci. 15, 888420. https://doi.org/10.3389/fnmol.2022.888420

Cao, S.-Y., Hu, Y., Chen, C., Yuan, F., Xu, M., Li, Q., Fang, K.-H., Chen, Y., Liu, Y., 2017a. Enhanced derivation of human pluripotent stem cell-derived cortical glutamatergic neurons by a small molecule. Sci. Rep. 7, 3282. https://doi.org/10.1038/s41598-017-03519-w

Chambers, Stuart M., Fasano, C.A., Papapetrou, E.P., Tomishima, M., Sadelain, M., Studer, L., 2009. Highly efficient neural conversion of human ES and iPS cells by dual inhibition of SMAD signaling. Nat. Biotechnol. 27, 275–280. https://doi.org/10.1038/nbt.1529

Chen, J., Kanai, Y., Cowan, N.J., Hirokawa, N., 1992. Projection domains of MAP2 and tau determine spacings between microtubules in dendrites and axons. Nature 360, 674–677. https://doi.org/10.1038/360674a0

Choi, A.M.K., Ryter, S.W., Levine, B., 2013. Autophagy in Human Health and Disease. N. Engl. J. Med. 368, 1845–1846. https://doi.org/10.1056/nejmc1303158

Choi-Rhee, E., Schulman, H., Cronan, J.E., 2004. Promiscuous protein biotinylation by Escherichia coli biotin protein ligase. Protein Sci. 13, 3043–3050. https://doi.org/10.1110/ps.04911804

Citri, A., Malenka, R.C., 2008. Synaptic Plasticity: Multiple Forms, Functions, and Mechanisms. Neuropsychopharmacology 33, 18–41. https://doi.org/10.1038/sj.npp.1301559

Clavaguera, F., Akatsu, H., Fraser, G., Crowther, R.A., Frank, S., Hench, J., Probst, A., Winkler, D.T., Reichwald, J., Staufenbiel, M., Ghetti, B., Goedert, M., Tolnay, M., 2013. Brain homogenates from human tauopathies induce tau inclusions in mouse brain. Proc. Natl. Acad. Sci. 110, 9535–9540. https://doi.org/10.1073/pnas.1301175110

Clavaguera, F., Bolmont, T., Crowther, R.A., Abramowski, D., Frank, S., Probst, A., Fraser, G., Stalder, A.K., Beibel, M., Staufenbiel, M., Jucker, M., Goedert, M., Tolnay, M., 2009a. Transmission and spreading of tauopathy in transgenic mouse brain. Nat. Cell Biol. 11, 909–913. https://doi.org/10.1038/ncb1901

Cleveland, D.W., Hwo, S.-Y., Kirschner, M.W., 1977. Purification of tau, a microtubule-associated protein that induces assembly of microtubules from purified tubulin. J. Mol. Biol. 116, 207–225. https://doi.org/10.1016/0022-2836(77)90213-3

Colom-Cadena, M., Davies, C., Sirisi, S., Lee, J.-E., Simzer, E.M., Tzioras, M., Querol-Vilaseca, M., Sánchez-Aced, É., Chang, Y.Y., Holt, K., McGeachan, R.I., Rose, J., Tulloch, J., Wilkins, L., Smith, C., Andrian, T., Belbin, O., Pujals, S., Horrocks, M.H., Lleó, A., Spires-Jones, T.L., 2023. Synaptic oligomeric tau in Alzheimer's disease — A potential culprit in the spread of tau pathology through the brain. Neuron 111, 2170-2183.e6. https://doi.org/10.1016/j.neuron.2023.04.020

Congdon, E.E., Sigurdsson, E.M., 2018. Tau-targeting therapies for Alzheimer disease. Nat. Rev. Neurol. 14, 399–415. https://doi.org/10.1038/s41582-018-0013-z

Cooper, J.M., Lathuiliere, A., Migliorini, M., Arai, A.L., Wani, M.M., Dujardin, S., Muratoglu, S.C., Hyman, B.T., Strickland, D.K., 2021. Regulation of tau internalization, degradation, and seeding by LRP1 reveals multiple pathways for tau catabolism. J. Biol. Chem. 296, 100715. https://doi.org/10.1016/j.jbc.2021.100715

Corsi, A., Bombieri, C., Valenti, M.T., Romanelli, M.G., 2022. Tau Isoforms: Gaining Insight into MAPT Alternative Splicing. Int. J. Mol. Sci. 23, 15383. https://doi.org/10.3390/ijms232315383

Courade, J.-P., Angers, R., Mairet-Coello, G., Pacico, N., Tyson, K., Lightwood, D., Munro, R., McMillan, D., Griffin, R., Baker, T., Starkie, D., Nan, R., Westwood, M., Mushikiwabo, M.-L., Jung, S., Odede, G., Sweeney, B., Popplewell, A., Burgess, G., Downey, P., Citron, M., 2018. Epitope determines efficacy of therapeutic anti-Tau antibodies in a functional assay with human Alzheimer Tau. Acta Neuropathol. 136, 729–745. https://doi.org/10.1007/s00401-018-1911-2

Cronan, J.E., 2005. Targeted and proximity-dependent promiscuous protein biotinylation by a mutant Escherichia coli biotin protein ligase. J. Nutr. Biochem. 16, 416–418. https://doi.org/10.1016/j.jnutbio.2005.03.017

Cummings, D.M., Liu, W., Portelius, E., Bayram, S., Yasvoina, M., Ho, S.-H., Smits, H., Ali, S.S., Steinberg, R., Pegasiou, C.-M., James, O.T., Matarin, M., Richardson, J.C., Zetterberg, H., Blennow, K., Hardy, J.A., Salih, D.A., Edwards, F.A., 2015. First effects of rising amyloid-β in transgenic mouse brain: synaptic transmission and gene expression. Brain 138, 1992–2004. https://doi.org/10.1093/brain/awv127

Damisah, E.C., Hill, R.A., Rai, A., Chen, F., Rothlin, C.V., Ghosh, S., Grutzendler, J., 2020. Astrocytes and microglia play orchestrated roles and respect phagocytic territories during neuronal corpse removal in vivo. Sci. Adv. 6, eaba3239. https://doi.org/10.1126/sciadv.aba3239

Das, M., Maeda, S., Hu, B., Yu, G.-Q., Guo, W., Lopez, I., Yu, X., Tai, C., Wang, X., Mucke, L., 2018. Neuronal levels and sequence of tau modulate the power of brain rhythms. Neurobiol. Dis. 117, 181–188. https://doi.org/10.1016/j.nbd.2018.05.020

Dawson, H.N., Cantillana, V., Chen, L., Vitek, M.P., 2007. The Tau N279K Exon 10 Splicing Mutation Recapitulates Frontotemporal Dementia and Parkinsonism Linked to Chromosome 17 Tauopathy in a Mouse Model. J. Neurosci. 27, 9155–9168. https://doi.org/10.1523/jneurosci.5492-06.2007

de Calignon, A., Polydoro, M., Suárez-Calvet, M., William, C., Adamowicz, D.H., Kopeikina, K.J., Pitstick, R., Sahara, N., Ashe, K.H., Carlson, G.A., Spires-Jones, T.L., Hyman, B.T., 2012. Propagation of Tau Pathology in a Model of Early Alzheimer's Disease. Neuron 73, 685–697. https://doi.org/10.1016/j.neuron.2011.11.033

DeKosky, S.T., Scheff, S.W., 1990. Synapse loss in frontal cortex biopsies in Alzheimer's disease: Correlation with cognitive severity. Ann. Neurol. 27, 457–464. https://doi.org/10.1002/ana.410270502

Delisle, M.-B., Murrell, J.R., Richardson, R., Trofatter, J.A., Rascol, O., Soulages, X., Mohr, M., Calvas, P., Ghetti, B., 1999. A mutation at codon 279 (N279K) in exon 10 of the Tau gene causes a tauopathy with dementia and supranuclear palsy. Acta Neuropathol. 98, 62–77. https://doi.org/10.1007/s004010051052

DeVos, S.L., Goncharoff, D.K., Chen, G., Kebodeaux, C.S., Yamada, K., Stewart, F.R., Schuler, D.R., Maloney, S.E., Wozniak, D.F., Rigo, F., Bennett, C.F., Cirrito, J.R., Holtzman, D.M., Miller, T.M., 2013. Antisense Reduction of Tau in Adult Mice Protects against Seizures. J. Neurosci. 33, 12887–12897. https://doi.org/10.1523/jneurosci.2107-13.2013

Dickey, C.A., Kamal, A., Lundgren, K., Klosak, N., Bailey, R.M., Dunmore, J., Ash, P., Shoraka, S., Zlatkovic, J., Eckman, C.B., Patterson, C., Dickson, D.W., Nahman, N.S., Hutton, M., Burrows, F., Petrucelli, L., 2007. The high-affinity HSP90-CHIP complex recognizes and selectively degrades phosphorylated tau client proteins. J. Clin. Investig. 117, 648–658. https://doi.org/10.1172/jci29715

Dickson, D.W., 2011. Neurodegeneration: The Molecular Pathology of Dementia and Movement Disorders 1–5. https://doi.org/10.1002/9781444341256.ch1

Digma, L.A., Madsen, J.R., Reas, E.T., Dale, A.M., Brewer, J.B., Banks, S.J., Initiative, for the A.D.N., 2019. Tau and atrophy: domain-specific relationships with cognition. Alzheimer's Res. Ther. 11, 65. https://doi.org/10.1186/s13195-019-0518-8

Ding, S., Shi, J., Qian, W., Iqbal, K., Grundke-Iqbal, I., Gong, C.-X., Liu, F., 2012. Regulation of alternative splicing of tau exon 10 by 9G8 and Dyrk1A. Neurobiol. Aging 33, 1389–1399. https://doi.org/10.1016/j.neurobiolaging.2010.11.021

Dixit, R., Ross, J.L., Goldman, Y.E., Holzbaur, E.L.F., 2008. Differential Regulation of Dynein and Kinesin Motor Proteins by Tau. Science 319, 1086–1089. https://doi.org/10.1126/science.1152993

Dorsey, E.R., George, B.P., Leff, B., Willis, A.W., 2013. The coming crisis: obtaining care for the growing burden of neurodegenerative conditions. Neurology 80, 1989–96. https://doi.org/10.1212/wnl.0b013e318293e2ce

Dreyfuss, G., Kim, V.N., Kataoka, N., 2002. Messenger-RNA-binding proteins and the messages they carry. Nat. Rev. Mol. Cell Biol. 3, 195–205. https://doi.org/10.1038/nrm760

Drubin, D.G., Caput, D., Kirschner, M.W., 1984. Studies on the expression of the microtubule-associated protein, tau, during mouse brain development, with newly isolated complementary DNA probes. J. Cell Biol. 98, 1090–1097. https://doi.org/10.1083/jcb.98.3.1090

Drummond, E., Pires, G., MacMurray, C., Askenazi, M., Nayak, S., Bourdon, M., Safar, J., Ueberheide, B., Wisniewski, T., 2020b. Phosphorylated tau interactome in the human Alzheimer's disease brain. Brain 143, 2803–2817. https://doi.org/10.1093/brain/awaa223

D'Souza, I., Schellenberg, G.D., 2005. Arginine/serine-rich protein interaction domain-dependent modulation of a tau exon 10 splicing enhancer: altered interactions and mechanisms for functionally antagonistic FTDP-17 mutations Delta280K AND N279K. J. Biol. Chem. 281, 2460–9. https://doi.org/10.1074/jbc.m505809200

Dujardin, S., Bégard, S., Caillierez, R., Lachaud, C., Carrier, S., Lieger, S., Gonzalez, J.A., Deramecourt, V., Déglon, N., Maurage, C.-A., Frosch, M.P., Hyman, B.T., Colin, M., Buée, L., 2018. Different tau species lead to heterogeneous tau pathology propagation and misfolding. Acta Neuropathol. Commun. 6, 132. https://doi.org/10.1186/s40478-018-0637-7

Dujardin, S., Bégard, S., Caillierez, R., Lachaud, C., Delattre, L., Carrier, S., Loyens, A., Galas, M.-C., Bousset, L., Melki, R., Aurégan, G., Hantraye, P., Brouillet, E., Buée, L., Colin, M., 2014. Ectosomes: A New Mechanism for Non-Exosomal Secretion of Tau Protein. PLoS ONE 9, e100760. https://doi.org/10.1371/journal.pone.0100760

Duquette, A., Pernègre, C., Carpentier, A.V., Leclerc, N., 2021. Similarities and Differences in the Pattern of Tau Hyperphosphorylation in Physiological and Pathological Conditions: Impacts on the Elaboration of Therapies to Prevent Tau Pathology. Front. Neurol. 11, 607680. https://doi.org/10.3389/fneur.2020.607680

Dyck, C.H. van, Swanson, C.J., Aisen, P., Bateman, R.J., Chen, C., Gee, M., Kanekiyo, M., Li, D., Reyderman, L., Cohen, S., Froelich, L., Katayama, S., Sabbagh, M., Vellas, B., Watson, D., Dhadda, S., Irizarry, M., Kramer, L.D., Iwatsubo, T., 2022. Lecanemab in Early Alzheimer's Disease. N. Engl. J. Med. 388, 9–21. https://doi.org/10.1056/nejmoa2212948

Efthymiou, A.G., Goate, A.M., 2017. Late onset Alzheimer's disease genetics implicates microglial pathways in disease risk. Mol. Neurodegener. 12, 43. https://doi.org/10.1186/s13024-017-0184-x

Eltom, K., Mothes, T., Libard, S., Ingelsson, M., Erlandsson, A., 2024. Astrocytic accumulation of tau fibrils isolated from Alzheimer's disease brains induces inflammation, cell-to-cell propagation and neuronal impairment. Acta Neuropathol. Commun. 12, 34. https://doi.org/10.1186/s40478-024-01745-8

Ercan, E., Eid, S., Weber, C., Kowalski, A., Bichmann, M., Behrendt, A., Matthes, F., Krauss, S., Reinhardt, P., Fulle, S., Ehrnhoefer, D.E., 2017. A validated antibody panel for the characterization of tau post-translational modifications. Mol. Neurodegener. 12, 87. https://doi.org/10.1186/s13024-017-0229-1

Ercan-Herbst, E., Ehrig, J., Schöndorf, D.C., Behrendt, A., Klaus, B., Ramos, B.G., Oriol, N.P., Weber, C., Ehrnhoefer, D.E., 2019. A post-translational modification signature defines changes in soluble tau correlating with oligomerization in early stage Alzheimer's disease brain. Acta Neuropathol. Commun. 7, 192. https://doi.org/10.1186/s40478-019-0823-2

Espuny-Camacho, I., Arranz, A.M., Fiers, M., Snellinx, A., Ando, K., Munck, S., Bonnefont, J., Lambot, L., Corthout, N., Omodho, L., Eynden, E.V., Radaelli, E., Tesseur, I., Wray, S., Ebneth, A., Hardy, J., Leroy, K., Brion, J.-P., Vanderhaeghen, P., Strooper, B.D., 2017. Hallmarks of Alzheimer's Disease in Stem-Cell-Derived Human Neurons Transplanted into Mouse Brain. Neuron 93, 1066-1081.e8. https://doi.org/10.1016/j.neuron.2017.02.001

Faúndez, V., Horng, J.-T., Kelly, R.B., 1998. A Function for the AP3 Coat Complex in Synaptic Vesicle Formation from Endosomes. Cell 93, 423–432. https://doi.org/10.1016/s0092-8674(00)81170-8

Fein, J.A., Sokolow, S., Miller, C.A., Vinters, H.V., Yang, F., Cole, G.M., Gylys, K.H., 2008. Co-Localization of Amyloid Beta and Tau Pathology in Alzheimer's Disease Synaptosomes. Am. J. Pathol. 172, 1683–1692. https://doi.org/10.2353/ajpath.2008.070829

Feinstein, S.C., Wilson, L., 2005. Inability of tau to properly regulate neuronal microtubule dynamics: a loss-of-function mechanism by which tau might mediate neuronal cell death. Biochim. Biophys. Acta (BBA) - Mol. Basis Dis. 1739, 268–279. https://doi.org/10.1016/j.bbadis.2004.07.002

Fernandez-Martinez, J., Vela, E.M., Tora-Ponsioen, M., Ocaña, O.H., Nieto, M.A., Galceran, J., 2009. Attenuation of Notch signalling by the Down-syndrome-associated kinase DYRK1A. J. Cell Sci. 122, 1574–1583. https://doi.org/10.1242/jcs.044354

Ferrari, L., Bauer, B., Qiu, Y., Schuschnig, M., Klotz, S., Anrather, D., Juretschke, T., Beli, P., Gelpi, E., Martens, S., 2024a. Tau fibrils evade autophagy by excessive p62 coating and TAX1BP1 exclusion. Sci. Adv. 10, eadm8449. https://doi.org/10.1126/sciadv.adm8449

Ferreira, S.T., Klein, W.L., 2011. The Aβ oligomer hypothesis for synapse failure and memory loss in Alzheimer's disease. Neurobiol. Learn. Mem. 96, 529–543. https://doi.org/10.1016/j.nlm.2011.08.003

Feuillette, S., Charbonnier, C., Frebourg, T., Campion, D., Lecourtois, M., 2020. A Connected Network of Interacting Proteins Is Involved in Human-Tau Toxicity in Drosophila. Front. Neurosci. 14, 68. https://doi.org/10.3389/fnins.2020.00068

Fimia, G.M., Kroemer, G., Piacentini, M., 2012. Molecular mechanisms of selective autophagy. Cell Death Differ. 20, 1–2. https://doi.org/10.1038/cdd.2012.97

Fitzpatrick, A.W.P., Falcon, B., He, S., Murzin, A.G., Murshudov, G., Garringer, H.J., Crowther, R.A., Ghetti, B., Goedert, M., Scheres, S.H.W., 2017. Cryo-EM structures of tau filaments from Alzheimer's disease. Nature 547, 185–190. https://doi.org/10.1038/nature23002

Fleisher, A.S., Munsie, L.M., Perahia, D.G.S., Andersen, S.W., Higgins, I.A., Hauck, P.M., Lo, A.C., Sims, J.R., Brys, M., Mintun, M., Investigators, P.-A.S., 2024. Assessment of Efficacy and Safety of Zagotenemab: Results From PERISCOPE-ALZ, a Phase 2 Study in Early Symptomatic Alzheimer Disease. Neurology 102, e208061. https://doi.org/10.1212/wnl.0000000000208061

Florian, H., Wang, D., Arnold, S.E., Boada, M., Guo, Q., Jin, Z., Zheng, H., Fisseha, N., Kalluri, H.V., Rendenbach-Mueller, B., Budur, K., Gold, M., 2023. Tilavonemab in early Alzheimer's disease: results from a phase 2, randomized, double-blind study. Brain 146, 2275–2284. https://doi.org/10.1093/brain/awad024

Frandemiche, M.L., Seranno, S.D., Rush, T., Borel, E., Elie, A., Arnal, I., Lanté, F., Buisson, A., 2014. Activity-Dependent Tau Protein Translocation to Excitatory Synapse Is Disrupted by Exposure to Amyloid-Beta Oligomers. J. Neurosci. 34, 6084–6097. https://doi.org/10.1523/jneurosci.4261-13.2014

Frey, B., Holzinger, D., Taylor, K., Ehrnhoefer, D.E., Striebinger, A., Biesinger, S., Gasparini, L., O'Neill, M.J., Wegner, F., Barghorn, S., Höglinger, G.U., Heym, R.G., 2024. Correction: Tau seed amplification assay reveals relationship between seeding and pathological forms of tau in Alzheimer's disease brain. Acta Neuropathol. Commun. 12, 115. https://doi.org/10.1186/s40478-024-01825-9

Frigerio, C.S., Strooper, B.D., 2015. Alzheimer's Disease Mechanisms and Emerging Roads to Novel Therapeutics. Annu. Rev. Neurosci. 39, 1–23. https://doi.org/10.1146/annurev-neuro-070815-014015

Frost, B., Jacks, R.L., Diamond, M.I., 2009. Propagation of Tau Misfolding from the Outside to the Inside of a Cell*. J. Biol. Chem. 284, 12845–12852. https://doi.org/10.1074/jbc.m808759200

Fu, H., Hardy, J., Duff, K.E., 2018. Selective vulnerability in neurodegenerative diseases. Nat. Neurosci. 21, 1350–1358. https://doi.org/10.1038/s41593-018-0221-2

Galceran, J., Graaf, K. de, Tejedor, F.J., Becker, W., 2003. The MNB/DYRK1A protein kinase: genetic and biochemical properties. J. neural Transm. Suppl. 139–48. https://doi.org/10.1007/978-3-7091-6721-2_12

Gao, L., Wang, J., Wang, Y., Andreadis, A., 2007. SR protein 9G8 modulates splicing of tau exon 10 via its proximal downstream intron, a clustering region for frontotemporal dementia mutations. Mol. Cell. Neurosci. 34, 48–58. https://doi.org/10.1016/j.mcn.2006.10.004

Gaspard, N., Bouschet, T., Hourez, R., Dimidschstein, J., Naeije, G., Ameele, J. van den, Espuny-Camacho, I., Herpoel, A., Passante, L., Schiffmann, S.N., Gaillard, A., Vanderhaeghen, P., 2008a. An intrinsic mechanism of corticogenesis from embryonic stem cells. Nature 455, 351–357. https://doi.org/10.1038/nature07287

Gauthier, S., Feldman, H.H., Schneider, L.S., Wilcock, G.K., Frisoni, G.B., Hardlund, J.H., Moebius, H.J., Bentham, P., Kook, K.A., Wischik, D.J., Schelter, B.O., Davis, C.S., Staff, R.T., Bracoud, L., Shamsi, K., Storey, J.M.D., Harrington, C.R., Wischik, C.M., 2016. Efficacy and safety of tau-aggregation inhibitor therapy in patients with mild or moderate Alzheimer's disease: a randomised, controlled, double-blind, parallel-arm, phase 3 trial. Lancet 388, 2873–2884. https://doi.org/10.1016/s0140-6736(16)31275-2

Ghatak, S., Dolatabadi, N., Trudler, D., Zhang, X., Wu, Y., Mohata, M., Ambasudhan, R., Talantova, M., Lipton, S.A., 2019. Mechanisms of hyperexcitability in Alzheimer's disease hiPSC-derived neurons and cerebral organoids vs isogenic controls. eLife 8, e50333. https://doi.org/10.7554/elife.50333

Ghetti, B., Oblak, A.L., Boeve, B.F., Johnson, K.A., Dickerson, B.C., Goedert, M., 2015. Invited review: Frontotemporal dementia caused by microtubule-associated protein tau gene (MAPT) mutations: a chameleon for neuropathology and neuroimaging. Neuropathol. Appl. Neurobiol. 41, 24–46. https://doi.org/10.1111/nan.12213

Ghigna, C., Valacca, C., Biamonti, G., 2008. Alternative Splicing and Tumor Progression. Curr. Genom. 9, 556–570. https://doi.org/10.2174/138920208786847971

Giannakopoulos, P., Herrmann, F.R., Bussière, T., Bouras, C., Kövari, E., Perl, D.P., Morrison, J.H., Gold, G., Hof, P.R., 2003. Tangle and neuron numbers, but not amyloid load, predict cognitive status in Alzheimer's disease. Neurology 60, 1495–1500. https://doi.org/10.1212/01.wnl.0000063311.58879.01

Goedert, M., 2004. Tau protein and neurodegeneration. Semin. Cell Dev. Biol. 15, 45–49. https://doi.org/10.1016/j.semcdb.2003.12.015

Goedert, M., Crowther, R.A., Spillantini, M.G., 1998. Tau Mutations Cause Frontotemporal Dementias. Neuron 21, 955–958. https://doi.org/10.1016/s0896-6273(00)80615-7

Goedert, M., Jakes, R., 1990. Expression of separate isoforms of human tau protein: correlation with the tau pattern in brain and effects on tubulin polymerization. EMBO J. 9, 4225–4230. https://doi.org/10.1002/j.1460-2075.1990.tb07870.x

Goedert, M., Jakes, R., Spillantini, M.G., Hasegawa, M., Smith, M.J., Crowther, R.A., 1996. Assembly of microtubule-associated protein tau into Alzheimer-like filaments induced by sulphated glycosaminoglycans. Nature 383, 550–553. https://doi.org/10.1038/383550a0

Goedert, M., Klug, A., Crowther, R.A., 2006. Tau protein, the paired helical filament and Alzheimer's disease. J. Alzheimer's Dis. 9, 195–207. https://doi.org/10.3233/jad-2006-9s323

Goedert, M., Spillantini, M.G., 2017. Propagation of Tau aggregates. Mol. brain 10, 18. https://doi.org/10.1186/s13041-017-0298-7

Goedert, M., Spillantini, M.G., Jakes, R., Rutherford, D., Crowther, R.A., 1989a. Multiple isoforms of human microtubule-associated protein tau: sequences and localization in neurofibrillary tangles of Alzheimer's disease. Neuron 3, 519–526. https://doi.org/10.1016/0896-6273(89)90210-9

Goedert, M., Spillantini, M.G., Potier, M.C., Ulrich, J., Crowther, R.A., 1989b. Cloning and sequencing of the cDNA encoding an isoform of microtubule-associated protein tau containing four tandem repeats: differential expression of tau protein mRNAs in human brain. EMBO J. 8, 393–399. https://doi.org/10.1002/j.1460-2075.1989.tb03390.x

Gómez-Ramos, A., Díaz-Hernández, M., Rubio, A., Miras-Portugal, M.T., Avila, J., 2008. Extracellular tau promotes intracellular calcium increase through M1 and M3 muscarinic receptors in neuronal cells. Mol. Cell. Neurosci. 37, 673–681. https://doi.org/10.1016/j.mcn.2007.12.010

Gong, C.-X., Lidsky, T., Wegiel, J., Zuck, L., Grundke-Iqbal, I., Iqbal, K., 2000. Phosphorylation of Microtubule-associated Protein Tau Is Regulated by Protein Phosphatase 2A in Mammalian Brain IMPLICATIONS FOR NEUROFIBRILLARY DEGENERATION IN ALZHEIMER'S DISEASE*. J. Biol. Chem. 275, 5535–5544. https://doi.org/10.1074/jbc.275.8.5535

Goodson, H.V., Jonasson, E.M., 2018. Microtubules and Microtubule-Associated Proteins. Cold Spring Harb. Perspect. Biol. 10, a022608. https://doi.org/10.1101/cshperspect.a022608

Götz, J., Halliday, G., Nisbet, R.M., 2018. Molecular Pathogenesis of the Tauopathies. Annu. Rev. Pathol.: Mech. Dis. 14, 1–23. https://doi.org/10.1146/annurev-pathmechdis-012418-012936

Götz, J., Ittner, L.M., 2008. Animal models of Alzheimer's disease and frontotemporal dementia. Nat. Rev. Neurosci. 9, 532–544. https://doi.org/10.1038/nrn2420

Graaf, K. de, Czajkowska, H., Rottmann, S., Packman, L.C., Lilischkis, R., Lüscher, B., Becker, W., 2006. The protein kinase DYRK1A phosphorylates the splicing factor SF3b1/SAP155 at Thr434, a novel in vivo phosphorylation site. BMC Biochem. 7, 7–7. https://doi.org/10.1186/1471-2091-7-7

GRAVELEY, B.R., 2000. Sorting out the complexity of SR protein functions. RNA 6, 1197–1211. https://doi.org/10.1017/s1355838200000960

Greenberg, S.G., Davies, P., 1990. A preparation of Alzheimer paired helical filaments that displays distinct tau proteins by polyacrylamide gel electrophoresis. Proc. Natl. Acad. Sci. 87, 5827–5831. https://doi.org/10.1073/pnas.87.15.5827

Grundke-Iqbal, I., Iqbal, K., Quinlan, M., Tung, Y.C., Zaidi, M.S., Wisniewski, H.M., 1986a. Microtubule-associated protein tau. A component of Alzheimer paired helical filaments. J. Biol. Chem. 261, 6084–6089. https://doi.org/10.1016/s0021-9258(17)38495-8

Gubas, A., Dikic, I., 2022. A guide to the regulation of selective autophagy receptors. FEBS J. 289, 75–89. https://doi.org/10.1111/febs.15824

Guillozet-Bongaarts, A.L., Cahill, M.E., Cryns, V.L., Reynolds, M.R., Berry, R.W., Binder, L.I., 2006. Pseudophosphorylation of tau at serine 422 inhibits caspase cleavage: in vitro evidence and implications for tangle formation in vivo. J. Neurochem. 97, 1005–1014. https://doi.org/10.1111/j.1471-4159.2006.03784.x

Guo, J.L., Lee, V.M.-Y., 2011. Seeding of Normal Tau by Pathological Tau Conformers Drives Pathogenesis of Alzheimer-like Tangles*. J. Biol. Chem. 286, 15317–15331. https://doi.org/10.1074/jbc.m110.209296

Guo, Q., Dammer, E.B., Zhou, M., Kundinger, S.R., Gearing, M., Lah, J.J., Levey, A.I., Shulman, J.M., Seyfried, N.T., 2021. Targeted Quantification of Detergent-Insoluble RNA-Binding Proteins in Human Brain Reveals Stage and Disease Specific Co-aggregation in Alzheimer's Disease. Front. Mol. Neurosci. 14, 623659. https://doi.org/10.3389/fnmol.2021.623659

Guo, Y., Li, S., Zeng, L.-H., Tan, J., 2022. Tau-targeting therapy in Alzheimer's disease: critical advances and future opportunities. Ageing Neurodegener. Dis. 2, null-null. https://doi.org/10.20517/and.2022.16

Haass, C., Selkoe, D.J., 1993. Cellular processing of β-amyloid precursor protein and the genesis of amyloid β-peptide. Cell 75, 1039–1042. https://doi.org/10.1016/0092-8674(93)90312-e

Hanger, D.P., Anderton, B.H., Noble, W., 2009. Tau phosphorylation: the therapeutic challenge for neurodegenerative disease. Trends Mol. Med. 15, 112–119. https://doi.org/10.1016/j.molmed.2009.01.003

Hansen, D.V., Rubenstein, J.L.R., Kriegstein, A.R., 2011. Deriving Excitatory Neurons of the Neocortex from Pluripotent Stem Cells. Neuron 70, 645–660. https://doi.org/10.1016/j.neuron.2011.05.006

Hardy, J., Selkoe, D.J., 2002. The Amyloid Hypothesis of Alzheimer's Disease: Progress and Problems on the Road to Therapeutics. Science 297, 353–356. https://doi.org/10.1126/science.1072994

Hardy, J.A., Higgins, G.A., 1992. Alzheimer's Disease: The Amyloid Cascade Hypothesis. Science 256, 184–185. https://doi.org/10.1126/science.1566067

Heemels, M.-T., 2016. Neurodegenerative diseases. Nature 539, 179–179. https://doi.org/10.1038/539179a

Hefti, M.M., Kim, S., Bell, A.J., Betters, R.K., Fiock, K.L., Iida, M.A., Smalley, M.E., Farrell, K., Fowkes, M.E., Crary, J.F., 2019. Tau Phosphorylation and Aggregation in the Developing Human Brain. J. Neuropathol. Exp. Neurol. 78, 930–938. https://doi.org/10.1093/jnen/nlz073

Heneka, M.T., Carson, M.J., Khoury, J.E., Landreth, G.E., Brosseron, F., Feinstein, D.L., Jacobs, A.H., Wyss-Coray, T., Vitorica, J., Ransohoff, R.M., Herrup, K., Frautschy, S.A., Finsen, B., Brown, G.C., Verkhratsky, A., Yamanaka, K., Koistinaho, J., Latz, E., Halle, A., Petzold, G.C., Town, T., Morgan, D., Shinohara, M.L., Perry, V.H., Holmes, C., Bazan, N.G., Brooks, D.J., Hunot, S., Joseph, B., Deigendesch, N., Garaschuk, O., Boddeke, E., Dinarello, C.A., Breitner, J.C., Cole, G.M., Golenbock, D.T., Kummer, M.P., 2015. Neuroinflammation in Alzheimer's disease. Lancet Neurol. 14, 388–405. https://doi.org/10.1016/s1474-4422(15)70016-5

Heneka, M.T., Kummer, M.P., Latz, E., 2014. Innate immune activation in neurodegenerative disease. Nat. Rev. Immunol. 14, 463–477. https://doi.org/10.1038/nri3705

Hirokawa, N., Shiomura, Y., Okabe, S., 1988. Tau proteins: the molecular structure and mode of binding on microtubules. J. Cell Biol. 107, 1449–1459. https://doi.org/10.1083/jcb.107.4.1449

Holmes, B.B., DeVos, S.L., Kfoury, N., Li, M., Jacks, R., Yanamandra, K., Ouidja, M.O., Brodsky, F.M., Marasa, J., Bagchi, D.P., Kotzbauer, P.T., Miller, T.M., Papy-Garcia, D., Diamond, M.I., 2013. Heparan sulfate proteoglycans mediate internalization and propagation of specific proteopathic seeds. Proc. Natl. Acad. Sci. 110, E3138–E3147. https://doi.org/10.1073/pnas.1301440110

Holmes, B.B., Diamond, M.I., 2014. Prion-like Properties of Tau Protein: The Importance of Extracellular Tau as a Therapeutic Target*. J. Biol. Chem. 289, 19855–19861. https://doi.org/10.1074/jbc.r114.549295

Holmes, B.B., Furman, J.L., Mahan, T.E., Yamasaki, T.R., Mirbaha, H., Eades, W.C., Belaygorod, L., Cairns, N.J., Holtzman, D.M., Diamond, M.I., 2014a. Proteopathic tau seeding predicts tauopathy in vivo. Proc. Natl. Acad. Sci. 111, E4376–E4385. https://doi.org/10.1073/pnas.1411649111

Hondius, D.C., Koopmans, F., Leistner, C., Pita-Illobre, D., Peferoen-Baert, R.M., Marbus, F., Paliukhovich, I., Li, K.W., Rozemuller, A.J.M., Hoozemans, J.J.M., Smit, A.B., 2021. The proteome of granulovacuolar degeneration and neurofibrillary tangles in Alzheimer's disease. Acta Neuropathol. 141, 341–358. https://doi.org/10.1007/s00401-020-02261-4

Hong, M., Zhukareva, V., Vogelsberg-Ragaglia, V., Wszolek, Z., Reed, L., Miller, B.I., Geschwind, D.H., Bird, T.D., McKeel, D., Goate, A., Morris, J.C., Wilhelmsen, K.C., Schellenberg, G.D., Trojanowski, J.Q., Lee, V.M.-Y., 1998. Mutation-Specific Functional Impairments in Distinct Tau Isoforms of Hereditary FTDP-17. Science 282, 1914–1917. https://doi.org/10.1126/science.282.5395.1914

Hong, X., Peng, C., Wei, W., Tian, Q., Liu, Y., Yao, X., Zhang, Y., Cao, F., Wang, Q., Wang, J., 2010. Essential role of tau phosphorylation in adult hippocampal neurogenesis. Hippocampus 20, 1339–1349. https://doi.org/10.1002/hipo.20712

Hoover, B.R., Reed, M.N., Su, J., Penrod, R.D., Kotilinek, L.A., Grant, M.K., Pitstick, R., Carlson, G.A., Lanier, L.M., Yuan, L.-L., Ashe, K.H., Liao, D., 2010. Tau Mislocalization to Dendritic Spines Mediates Synaptic Dysfunction Independently of Neurodegeneration. Neuron 68, 1067–1081. https://doi.org/10.1016/j.neuron.2010.11.030

Hopp, S.C., Lin, Y., Oakley, D., Roe, A.D., DeVos, S.L., Hanlon, D., Hyman, B.T., 2018. The role of microglia in processing and spreading of bioactive tau seeds in Alzheimer's disease. J. Neuroinflammation 15, 269. https://doi.org/10.1186/s12974-018-1309-z

Hsieh, Y.-C., Guo, C., Yalamanchili, H.K., Abreha, M., Al-Ouran, R., Li, Y., Dammer, E.B., Lah, J.J., Levey, A.I., Bennett, D.A., Jager, P.L.D., Seyfried, N.T., Liu, Z., Shulman, J.M., 2019a. Tau-Mediated Disruption of the Spliceosome Triggers Cryptic RNA Splicing and Neurodegeneration in Alzheimer's Disease. Cell Rep. 29, 301-316.e10. https://doi.org/10.1016/j.celrep.2019.08.104

Hu, C., Tao, L., Cao, X., Chen, L., 2020. The solute carrier transporters and the brain: Physiological and pharmacological implications. Asian J. Pharm. Sci. 15, 131–144. https://doi.org/10.1016/j.ajps.2019.09.002

Hughes, C.S., Moggridge, S., Müller, T., Sorensen, P.H., Morin, G.B., Krijgsveld, J., 2019. Single-pot, solid-phase-enhanced sample preparation for proteomics experiments. Nat. Protoc. 14, 68–85. https://doi.org/10.1038/s41596-018-0082-x

Hutton, M., Lendon, C.L., Rizzu, P., Baker, M., Froelich, S., Houlden, H., Pickering-Brown, S., Chakraverty, S., Isaacs, A., Grover, A., Hackett, J., Adamson, J., Lincoln, S., Dickson, D., Davies, P., Petersen, R.C., Stevens, M., Graaff, E. de, Wauters, E., Baren, J. van, Hillebrand, M., Joosse, M., Kwon, J.M., Nowotny, P., Che, L.K., Norton, J., Morris, J.C., Reed, L.A., Trojanowski, J., Basun, H., Lannfelt, L., Neystat, M., Fahn, S., Dark, F., Tannenberg, T., Dodd, P.R., Hayward, N., Kwok, J.B.J., Schofield, P.R., Andreadis, A., Snowden, J., Craufurd, D., Neary, D., Owen, F., Oostra, B.A., Hardy, J., Goate, A., Swieten, J. van, Mann, D., Lynch, T., Heutink, P., 1998. Association of missense and 5′-splice-site mutations in tau with the inherited dementia FTDP-17. Nature 393, 702–705. https://doi.org/10.1038/31508

Iba, M., Guo, J.L., McBride, J.D., Zhang, B., Trojanowski, J.Q., Lee, V.M.-Y., 2013. Synthetic Tau Fibrils Mediate Transmission of Neurofibrillary Tangles in a Transgenic Mouse Model of Alzheimer's-Like Tauopathy. J. Neurosci. 33, 1024–1037. https://doi.org/10.1523/jneurosci.2642-12.2013

Iovino, M., Agathou, S., González-Rueda, A., Velasco-Herrera, M.D.C., Borroni, B., Alberici, A., Lynch, T., O'Dowd, S., Geti, I., Gaffney, D., Vallier, L., Paulsen, O., Káradóttir, R.T., Spillantini, M.G., 2015. Early maturation and distinct tau pathology in induced pluripotent stem cell-derived neurons from patients with MAPT mutations. Brain 138, 3345–3359. https://doi.org/10.1093/brain/awv222

Iqbal, K., Alonso, A. del C., Chen, S., Chohan, M.O., El-Akkad, E., Gong, C.-X., Khatoon, S., Li, B., Liu, F., Rahman, A., Tanimukai, H., Grundke-Iqbal, I., 2005. Tau pathology in Alzheimer disease and other tauopathies. Biochim. Biophys. Acta (BBA) - Mol. Basis Dis. 1739, 198–210. https://doi.org/10.1016/j.bbadis.2004.09.008

Irwin, D.J., Brettschneider, J., McMillan, C.T., Cooper, F., Olm, C., Arnold, S.E., Deerlin, V.M.V., Seeley, W.W., Miller, B.L., Lee, E.B., Lee, V.M. -Y., Grossman, M., Trojanowski, J.Q., 2016. Deep clinical and neuropathological phenotyping of Pick disease. Ann. Neurol. 79, 272–287. https://doi.org/10.1002/ana.24559

Islam, T., Hill, E., Abrahamson, E.E., Servaes, S., Smirnov, D.S., Zeng, X., Sehrawat, A., Chen, Y., Kac, P.R., Kvartsberg, H., Olsson, M., Sjons, E., Gonzalez-Ortiz, F., Therriault, J., Tissot, C., Popolo, I.D., Rahmouni, N., Richardson, A., Mitchell, V., Zetterberg, H., Pascoal, T.A., Lashley, T., Wall, M.J., Galasko, D., Rosa-Neto, P., Ikonomovic, M.D., Blennow, K., Karikari, T.K., 2025. Phospho-tau serine-262 and serine-356 as biomarkers of pre-tangle soluble tau assemblies in Alzheimer's disease. Nat. Med. 31, 574–588. https://doi.org/10.1038/s41591-024-03400-0

Ittner, L.M., Götz, J., 2011. Amyloid-β and tau — a toxic pas de deux in Alzheimer's disease. Nat. Rev. Neurosci. 12, 67–72. https://doi.org/10.1038/nrn2967

Ittner, L.M., Ke, Y.D., Götz, J., 2009. Phosphorylated Tau Interacts with c-Jun N-terminal Kinase-interacting Protein 1 (JIP1) in Alzheimer Disease*. J. Biol. Chem. 284, 20909–20916. https://doi.org/10.1074/jbc.m109.014472

Iwatsubo, T., 2004. The γ-secretase complex: machinery for intramembrane proteolysis. Curr. Opin. Neurobiol. 14, 379–383. https://doi.org/10.1016/j.conb.2004.05.010

Iwatsubo, T., Odaka, A., Suzuki, N., Mizusawa, H., Nukina, N., Ihara, Y., 1994. Visualization of Aβ42(43) and Aβ40 in senile plaques with end-specific Aβ monoclonals: Evidence that an initially deposited species is Aβ42(43). Neuron 13, 45–53. https://doi.org/10.1016/0896-6273(94)90458-8

Jahn, H., 2013. Memory loss in Alzheimer's disease. Dialogues Clin. Neurosci. 15, 445–454. https://doi.org/10.31887/dcns.2013.15.4/hjahn

Janelidze, S., Mattsson, N., Palmqvist, S., Smith, R., Beach, T.G., Serrano, G.E., Chai, X., Proctor, N.K., Eichenlaub, U., Zetterberg, H., Blennow, K., Reiman, E.M., Stomrud, E., Dage, J.L., Hansson, O., 2020. Plasma P-tau181 in Alzheimer's disease: relationship to other biomarkers, differential diagnosis, neuropathology and longitudinal progression to Alzheimer's dementia. Nat. Med. 26, 379–386. https://doi.org/10.1038/s41591-020-0755-1

Jo, C., Gundemir, S., Pritchard, S., Jin, Y.N., Rahman, I., Johnson, G.V.W., 2014. Nrf2 reduces levels of phosphorylated tau protein by inducing autophagy adaptor protein NDP52. Nat. Commun. 5, 3496. https://doi.org/10.1038/ncomms4496

Johansen, T., Lamark, T., 2011. Selective autophagy mediated by autophagic adapter proteins. Autophagy 7, 279–296. https://doi.org/10.4161/auto.7.3.14487

Kavanagh, T., Halder, A., Drummond, E., 2022a. Tau interactome and RNA binding proteins in neurodegenerative diseases. Mol. Neurodegener. 17, 66. https://doi.org/10.1186/s13024-022-00572-6

Kentrup, H., Becker, W., Heukelbach, J., Wilmes, A., Schürmann, A., Huppertz, C., Kainulainen, H., Joost, H.-G., 1996. Dyrk, a Dual Specificity Protein Kinase with Unique Structural Features Whose Activity Is Dependent on Tyrosine Residues between Subdomains VII and VIII (∗). J. Biol. Chem. 271, 3488–3495. https://doi.org/10.1074/jbc.271.7.3488

Kettenmann, H., Hanisch, U.-K., Noda, M., Verkhratsky, A., 2011. Physiology of Microglia. Physiol. Rev. 91, 461–553. https://doi.org/10.1152/physrev.00011.2010

Kfoury, N., Holmes, B.B., Jiang, H., Holtzman, D.M., Diamond, M.I., 2012. Trans-cellular Propagation of Tau Aggregation by Fibrillar Species*. J. Biol. Chem. 287, 19440–19451. https://doi.org/10.1074/jbc.m112.346072

Kim, B., Mikytuck, B., Suh, E., Gibbons, G.S., Deerlin, V.M.V., Vaishnavi, S.N., Spindler, M.A., Massimo, L., Grossman, M., Trojanowski, J.Q., Irwin, D.J., Lee, E.B., 2021. Tau immunotherapy is associated with glial responses in FTLD-tau. Acta Neuropathol. 142, 243–257. https://doi.org/10.1007/s00401-021-02318-y

Kimura, T., Whitcomb, D.J., Jo, J., Regan, P., Piers, T., Heo, S., Brown, C., Hashikawa, T., Murayama, M., Seok, H., Sotiropoulos, I., Kim, E., Collingridge, G.L., Takashima, A., Cho, K., 2014. Microtubule-associated protein tau is essential for long-term depression in the hippocampus. Philos. Trans. R. Soc. B: Biol. Sci. 369, 20130144. https://doi.org/10.1098/rstb.2013.0144

Kirkin, V., Lamark, T., Sou, Y.-S., Bjørkøy, G., Nunn, J.L., Bruun, J.-A., Shvets, E., McEwan, D.G., Clausen, T.H., Wild, P., Bilusic, I., Theurillat, J.-P., Øvervatn, A., Ishii, T., Elazar, Z., Komatsu, M., Dikic, I., Johansen, T., 2009a. A Role for NBR1 in Autophagosomal Degradation of Ubiquitinated Substrates. Mol. Cell 33, 505–516. https://doi.org/10.1016/j.molcel.2009.01.020

Kirkin, V., McEwan, D.G., Novak, I., Dikic, I., 2009c. A Role for Ubiquitin in Selective Autophagy. Mol. Cell 34, 259–269. https://doi.org/10.1016/j.molcel.2009.04.026

Kirkin, V., Rogov, V.V., 2019. A Diversity of Selective Autophagy Receptors Determines the Specificity of the Autophagy Pathway. Mol. Cell 76, 268–285. https://doi.org/10.1016/j.molcel.2019.09.005

Klimmt, J., Dannert, A., Paquet, D., 2020. Neurodegeneration in a dish: advancing human stem-cell-based models of Alzheimer's disease. Curr. Opin. Neurobiol. 61, 96–104. https://doi.org/10.1016/j.conb.2020.01.008

Kondo, S., Yamamoto, N., Murakami, T., Okumura, M., Mayeda, A., Imaizumi, K., 2004. Tra2 beta, SF2/ASF and SRp30c modulate the function of an exonic splicing enhancer in exon 10 of tau pre-mRNA. Genes cells : devoted Mol. Cell. Mech. 9, 121–30. https://doi.org/10.1111/j.1356-9597.2004.00709.x

Kopeikina, K., Hyman, B., Spires-Jones, T., 2012. Soluble forms of tau are toxic in Alzheimer's disease. Transl. Neurosci. 3, 223–233. https://doi.org/10.2478/s13380-012-0032-y

Köpke, E., Tung, Y.C., Shaikh, S., Alonso, A.C., Iqbal, K., Grundke-Iqbal, I., 1993a. Microtubule-associated protein tau. Abnormal phosphorylation of a non-paired helical filament pool in Alzheimer disease. J. Biol. Chem. 268, 24374–24384. https://doi.org/10.1016/s0021-9258(20)80536-5

Kosik, K.S., Joachim, C.L., Selkoe, D.J., 1986. Microtubule-associated protein tau (tau) is a major antigenic component of paired helical filaments in Alzheimer disease. Proc. Natl. Acad. Sci. 83, 4044–4048. https://doi.org/10.1073/pnas.83.11.4044

Labate, A., Colosimo, E., Gambardella, A., Leggio, U., Ambrosio, R., Quattrone, A., 2006. Levetiracetam in patients with generalised epilepsy and myoclonic seizures: An open label study. Seizure 15, 214–218. https://doi.org/10.1016/j.seizure.2005.12.004

Lacovich, V., Espindola, S.L., Alloatti, M., Devoto, V.P., Cromberg, L.E., Čarná, M.E., Forte, G., Gallo, J.-M., Bruno, L., Stokin, G.B., Avale, M.E., Falzone, T.L., 2017. Tau Isoforms Imbalance Impairs the Axonal Transport of the Amyloid Precursor Protein in Human Neurons. J. Neurosci. 37, 58–69. https://doi.org/10.1523/jneurosci.2305-16.2016

Lahiri, D.K., Maloney, B., Basha, M.R., Ge, Y.W., Zawia, N.H., 2007. How and when environmental agents and dietary factors affect the course of Alzheimer's disease: the "LEARn" model (latent early-life associated regulation) may explain the triggering of AD. Curr. Alzheimer Res. 4, 219–28. https://doi.org/10.2174/156720507780362164

Lancaster, M.A., Renner, M., Martin, C.-A., Wenzel, D., Bicknell, L.S., Hurles, M.E., Homfray, T., Penninger, J.M., Jackson, A.P., Knoblich, J.A., 2013. Cerebral organoids model human brain development and microcephaly. Nature 501, 373–379. https://doi.org/10.1038/nature12517

Lapasset, L., Milhavet, O., Prieur, A., Besnard, E., Babled, A., Aït-Hamou, N., Leschik, J., Pellestor, F., Ramirez, J.-M., Vos, J.D., Lehmann, S., Lemaitre, J.-M., 2011. Rejuvenating senescent and centenarian human cells by reprogramming through the pluripotent state. Genes Dev. 25, 2248–2253. https://doi.org/10.1101/gad.173922.111

Lasagna-Reeves, C.A., Castillo-Carranza, D.L., Sengupta, U., Guerrero-Munoz, M.J., Kiritoshi, T., Neugebauer, V., Jackson, G.R., Kayed, R., 2012. Alzheimer brain-derived tau oligomers propagate pathology from endogenous tau. Sci. Rep. 2, 700. https://doi.org/10.1038/srep00700

Lei, P., Ayton, S., Finkelstein, D.I., Spoerri, L., Ciccotosto, G.D., Wright, D.K., Wong, B.X.W., Adlard, P.A., Cherny, R.A., Lam, L.Q., Roberts, B.R., Volitakis, I., Egan, G.F., McLean, C.A., Cappai, R., Duce, J.A., Bush, A.I., 2012. Tau deficiency induces parkinsonism with dementia by impairing APP-mediated iron export. Nat. Med. 18, 291–295. https://doi.org/10.1038/nm.2613

Levine, B., Kroemer, G., 2008. Autophagy in the Pathogenesis of Disease. Cell 132, 27–42. https://doi.org/10.1016/j.cell.2007.12.018

Lewcock, J.W., Schlepckow, K., Paolo, G.D., Tahirovic, S., Monroe, K.M., Haass, C., 2020. Emerging Microglia Biology Defines Novel Therapeutic Approaches for Alzheimer's Disease. Neuron 108, 801–821. https://doi.org/10.1016/j.neuron.2020.09.029

Li, D., Yu, W., Lai, M., 2023. Towards understandings of serine/arginine-rich splicing factors. Acta Pharm. Sin. B 13, 3181–3207. https://doi.org/10.1016/j.apsb.2023.05.022

Lichtenthaler, S.F., 2010. Alpha-secretase in Alzheimer's disease: molecular identity, regulation and therapeutic potential: Alpha-secretase in Alzheimer's disease. J. Neurochem. 116, 10–21. https://doi.org/10.1111/j.1471-4159.2010.07081.x

Lichtenthaler, S.F., Tschirner, S.K., Steiner, H., 2022. Secretases in Alzheimer's disease: Novel insights into proteolysis of APP and TREM2. Curr. Opin. Neurobiol. 72, 101–110. https://doi.org/10.1016/j.conb.2021.09.003

Limorenko, G., Tatli, M., Kolla, R., Nazarov, S., Weil, M.-T., Schöndorf, D.C., Geist, D., Reinhardt, P., Ehrnhoefer, D.E., Stahlberg, H., Gasparini, L., Lashuel, H.A., 2023. Fully co-factor-free ClearTau platform produces seeding-competent Tau fibrils for reconstructing pathological Tau aggregates. Nat. Commun. 14, 3939. https://doi.org/10.1038/s41467-023-39314-7

Liu, C., Götz, J., 2013. Profiling Murine Tau with 0N, 1N and 2N Isoform-Specific Antibodies in Brain and Peripheral Organs Reveals Distinct Subcellular Localization, with the 1N Isoform Being Enriched in the Nucleus. PLoS ONE 8, e84849. https://doi.org/10.1371/journal.pone.0084849

Liu, F., Gong, C.-X., 2008. Tau exon 10 alternative splicing and tauopathies. Mol. Neurodegener. 3, 8. https://doi.org/10.1186/1750-1326-3-8

Liu, F., Grundke-Iqbal, I., Iqbal, K., Gong, C., 2005. Contributions of protein phosphatases PP1, PP2A, PP2B and PP5 to the regulation of tau phosphorylation. Eur. J. Neurosci. 22, 1942–1950. https://doi.org/10.1111/j.1460-9568.2005.04391.x

Liu, F., Liang, Z., Wegiel, J., Hwang, Y., Iqbal, K., Grundke-Iqbal, I., Ramakrishna, N., Gong, C., 2008. Overexpression of Dyrk1A contributes to neurofibrillary degeneration in Down syndrome. FASEB J. 22, 3224–3233. https://doi.org/10.1096/fj.07-104539

Liu, L., Drouet, V., Wu, J.W., Witter, M.P., Small, S.A., Clelland, C., Duff, K., 2012. Trans-Synaptic Spread of Tau Pathology In Vivo. PLoS ONE 7, e31302. https://doi.org/10.1371/journal.pone.0031302

Liu, T., Wang, Y., Wang, J., Ren, C., Chen, H., Zhang, J., 2022. DYRK1A inhibitors for disease therapy: Current status and perspectives. Eur. J. Med. Chem. 229, 114062. https://doi.org/10.1016/j.ejmech.2021.114062

Liu, X., Ye, M., Ma, L., 2022. The emerging role of autophagy and mitophagy in tauopathies: From pathogenesis to translational implications in Alzheimer's disease. Front. Aging Neurosci. 14, 1022821. https://doi.org/10.3389/fnagi.2022.1022821

Liu, Z., Chen, O., Wall, J.B.J., Zheng, M., Zhou, Y., Wang, L., Vaseghi, H.R., Qian, L., Liu, J., 2017. Systematic comparison of 2A peptides for cloning multi-genes in a polycistronic vector. Sci. Rep. 7, 2193. https://doi.org/10.1038/s41598-017-02460-2

Llibre-Guerra, J.J., Fernandez, M.V., Joseph-Mathurin, N., Bian, S., Carter, K., Li, Y., Aschenbrenner, A.J., Pottier, C., Sigurdson, W., McDade, E., Gordon, B.A., Renton, A.E., Benzinger, T.L.S., Ibañez, L., Barthelemy, N., Johnson, M., Hassenstab, J., Wang, G., Goate, A.M., Western, D., Wang, C., Hobbs, D., Daniels, A., Karch, C., Morris, J.C., Cruchaga, C., Johnson, E.C.B., Bateman, R.J., Aguillon, D., Allegri, R.F., Baena, A., Baker, B., Banks, J., Barthélemy, N.R., Bartzel, J., Bateman, R., Bechara, J.A., Berman, S.B., Bocanegra, Y., Brooks, W.S., Cash, D.M., Chen, A., Chen, C., Chhatwal, J.P., Mendez, P.C., Courtney, L., Daniels, A.J., Day, G.S., Devenney, E., Fagan, A.M., Farlow, M., Flores, S., Fox, N.C., Franklin, E., Fulton-Howard, B., Goyal, M., Graber-Sultan, S., Graff-Radford, N.R., Gremminger, E., Hellm, C., Holtzman, D.M., Hornbeck, R., Huey, E.D., Ibanez, L., Ikeuchi, T., Ikonomovic, S., Ishiguro, T., Ishii, K., Jackson, K., Jerome, G., Jucker, M., Karch, C.M., Kasuga, K., Keefe, S., Koudelis, D., Kuder-Buletta, E., Fougère, C. la, Laske, C., Lee, J.-H., Levey, A.I., Levin, J., Leon, Y.M., Lopera, F., Lu, R., Maa, C., Marsh, J., Martin, M., Martins, R., Massoumzadeh, P., Masters, C., McCullough, A., McKay, N., Minton, M., Mori, H., Nicklaus, J., Nie, Y., Niimi, Y., Noble, J.M., Obermueller, U., Perrin, R.J., Picarello, D.M., Pulizos, C., Ramirez, L., Reischl, G., Ringman, J., Rizzo, J., Rödenbeck, Y., Roh, J.H., Rosa-Neto, P., Ryan, N.S., Sabaredzovic, E., Salloway, S., Sanchez-Valle, R., Schofield, P.R., Scott, J., Senda, M., Serna, L., Seyfried, N.T., Simmons, A., Skrbec, K., Smith, J., Stauber, J., Stout, S., Supnet-Bell, C., Surace, E., Timofejavaite, R., Vazquez, S., Vlassenko, A., Vöglein, J., Wang, Q., Wang, Y., Xiong, C., Xu, X., Xu, J., Ziegemeier, A., Ziegemeier, E., 2025. Longitudinal analysis of a dominantly inherited Alzheimer disease mutation carrier protected from dementia. Nat. Med. 1–9. https://doi.org/10.1038/s41591-025-03494-0

Long, J.M., Holtzman, D.M., 2019. Alzheimer Disease: An Update on Pathobiology and Treatment Strategies. Cell 179, 312–339. https://doi.org/10.1016/j.cell.2019.09.001

Lööv, C., Mitchell, C.H., Simonsson, M., Erlandsson, A., 2015. Slow degradation in phagocytic astrocytes can be enhanced by lysosomal acidification. Glia 63, 1997–2009. https://doi.org/10.1002/glia.22873

Love, J.E., Hayden, E.J., Rohn, T.T., 2015. Alternative Splicing in Alzheimer's Disease. J. Park.'s Dis. Alzheimer's Dis. 2, 6. https://doi.org/10.13188/2376-922x.1000010

Lovestone, S., Boada, M., Dubois, B., Hüll, M., Rinne, J.O., Huppertz, H.-J., Calero, M., Andrés, M.V., Gómez-Carrillo, B., León, T., Ser, T. del, investigators, for the A., 2015. A Phase II Trial of Tideglusib in Alzheimer's Disease. J. Alzheimer's Dis. 45, 75–88. https://doi.org/10.3233/jad-141959

Lu, P.-J., Wulf, G., Zhou, X.Z., Davies, P., Lu, K.P., 1999. The prolyl isomerase Pin1 restores the function of Alzheimer-associated phosphorylated tau protein. Nature 399, 784–788. https://doi.org/10.1038/21650

Luna-Muñoz, J., García-Sierra, F., Falcón, V., Menéndez, I., Chávez-Macías, L., Mena, R., 2005. Regional conformational change involving phosphorylation of tau protein at the Thr231, precedes the structural change detected by Alz-50 antibody in Alzheimer's disease. J. Alzheimer's Dis. 8, 29–41. https://doi.org/10.3233/jad-2005-8104

Lynch, B.A., Lambeng, N., Nocka, K., Kensel-Hammes, P., Bajjalieh, S.M., Matagne, A., Fuks, B., 2004. The synaptic vesicle protein SV2A is the binding site for the antiepileptic drug levetiracetam. Proc. Natl. Acad. Sci. 101, 9861–9866. https://doi.org/10.1073/pnas.0308208101

Lyra-Leite, D.M., Copley, R.R., Freeman, P.P., Pongpamorn, P., Shah, D., McKenna, D.E., Lenny, B., Pinheiro, E.A., Weddle, C.J., Gharib, M., Javed, H., Fonoudi, H., Sapkota, Y., Burridge, P.W., 2023. Nutritional

requirements of human induced pluripotent stem cells. Stem Cell Rep. 18, 1371–1387. https://doi.org/10.1016/j.stemcr.2023.05.004

Majounie, E., Cross, W., Newsway, V., Dillman, A., Vandrovcova, J., Morris, C.M., Nalls, M.A., Ferrucci, L., Owen, M.J., O'Donovan, M.C., Cookson, M.R., Singleton, A.B., Silva, R. de, Morris, H.R., 2013. Variation in tau isoform expression in different brain regions and disease states. Neurobiol. Aging 34, 1922.e7-1922.e12. https://doi.org/10.1016/j.neurobiolaging.2013.01.017

Man, V.H., He, X., Han, F., Cai, L., Wang, L., Niu, T., Zhai, J., Ji, B., Gao, J., Wang, J., 2023. Phosphorylation at Ser289 Enhances the Oligomerization of Tau Repeat R2. J. Chem. Inf. Model. 63, 1351–1361. https://doi.org/10.1021/acs.jcim.2c01597

Mann, M., Kulak, N.A., Nagaraj, N., Cox, J., 2013. The Coming Age of Complete, Accurate, and Ubiquitous Proteomes. Mol. Cell 49, 583–590. https://doi.org/10.1016/j.molcel.2013.01.029

Manos, J.D., Preiss, C.N., Venkat, N., Tamm, J., Reinhardt, P., Kwon, T., Wu, J., Winter, A.D., Jahn, T.R., Yanamandra, K., Titterton, K., Karran, E., Langlois, X., 2022a. Uncovering specificity of endogenous TAU aggregation in a human iPSC-neuron TAU seeding model. iScience 25, 103658. https://doi.org/10.1016/j.isci.2021.103658

Matsumoto, G., Wada, K., Okuno, M., Kurosawa, M., Nukina, N., 2011. Serine 403 Phosphorylation of p62/SQSTM1 Regulates Selective Autophagic Clearance of Ubiquitinated Proteins. Mol. Cell 44, 279–289. https://doi.org/10.1016/j.molcel.2011.07.039

Mattson, M.P., 2004. Pathways towards and away from Alzheimer's disease. Nature 430, 631–639. https://doi.org/10.1038/nature02621

McKee, A.C., Cantu, R.C., Nowinski, C.J., Hedley-Whyte, E.T., Gavett, B.E., Budson, A.E., Santini, V.E., Lee, H.-S., Kubilus, C.A., Stern, R.A., 2009. Chronic Traumatic Encephalopathy in Athletes: Progressive Tauopathy After Repetitive Head Injury. J. Neuropathol. Exp. Neurol. 68, 709–735. https://doi.org/10.1097/nen.0b013e3181a9d503

Meier, S., Bell, M., Lyons, D.N., Ingram, A., Chen, J., Gensel, J.C., Zhu, H., Nelson, P.T., Abisambra, J.F., 2015a. Identification of Novel Tau Interactions with Endoplasmic Reticulum Proteins in Alzheimer's Disease Brain. J. Alzheimer's Dis. 48, 687–702. https://doi.org/10.3233/jad-150298

Melchior, B., Mittapalli, G.K., Lai, C., Duong-Polk, K., Stewart, J., Güner, B., Hofilena, B., Tjitro, A., Anderson, S.D., Herman, D.S., Dellamary, L., Swearingen, C.J., Sunil, K.C., Yazici, Y., 2019. Tau pathology reduction with SM07883, a novel, potent, and selective oral DYRK1A inhibitor: A potential therapeutic for Alzheimer's disease. Aging Cell 18, e13000. https://doi.org/10.1111/acel.13000

Mendoza-Torreblanca, J.G., Vanoye-Carlo, A., Phillips-Farfán, B.V., Carmona-Aparicio, L., Gómez-Lira, G., 2013. Synaptic vesicle protein 2A: basic facts and role in synaptic function. Eur. J. Neurosci. 38, 3529–3539. https://doi.org/10.1111/ejn.12360

Mercer, S.E., Ewton, D.Z., Deng, X., Lim, S., Mazur, T.R., Friedman, E., 2005. Mirk/Dyrk1B mediates survival during the differentiation of C2C12 myoblasts. J. Biol. Chem. 280, 25788–801. https://doi.org/10.1074/jbc.m413594200

Meyer, H.E., Mandelkow, E.-M., Drewes, G., Trinczek, B., Illenberger, S., Biernat, J., Schmitt-Ulms, G., Mandelkow, E., 1995. Microtubule-associated Protein/Microtubule Affinity-regulating Kinase (p110mark) A NOVEL PROTEIN KINASE THAT REGULATES TAU-MICROTUBULE INTERACTIONS AND DYNAMIC INSTABILITY BY PHOSPHORYLATION AT THE ALZHEIMER-SPECIFIC SITE SERINE 262 (∗). J. Biol. Chem. 270, 7679–7688. https://doi.org/10.1074/jbc.270.13.7679

Minaya, M.A., Mahali, S., Iyer, A.K., Eteleeb, A.M., Martinez, R., Huang, G., Budde, J., Temple, S., Nana, A.L., Seeley, W.W., Spina, S., Grinberg, L.T., Harari, O., Karch, C.M., 2023. Conserved gene signatures

shared among MAPT mutations reveal defects in calcium signaling. Front. Mol. Biosci. 10, 1051494. https://doi.org/10.3389/fmolb.2023.1051494

Mizushima, N., Levine, B., 2020. Autophagy in Human Diseases. N. Engl. J. Med. 383, 1564–1576. https://doi.org/10.1056/nejmra2022774

Morderer, D., Wren, M.C., Liu, F., Kouri, N., Maistrenko, A., Khalil, B., Pobitzer, N., Salemi, M.R., Phinney, B.S., Bu, G., Zhao, N., Dickson, D.W., Murray, M.E., Rossoll, W., 2025. Probe-dependent Proximity Profiling (ProPPr) Uncovers Similarities and Differences in Phospho-Tau-Associated Proteomes Between Tauopathies. Mol. Neurodegener. 20, 32. https://doi.org/10.1186/s13024-025-00817-0

Moreau, M.M., Piguel, N., Papouin, T., Koehl, M., Durand, C.M., Rubio, M.E., Loll, F., Richard, E.M., Mazzocco, C., Racca, C., Oliet, S.H.R., Abrous, D.N., Montcouquiol, M., Sans, N., 2010. The Planar Polarity Protein Scribble1 Is Essential for Neuronal Plasticity and Brain Function. J. Neurosci. 30, 9738–9752. https://doi.org/10.1523/jneurosci.6007-09.2010

Moreno, H., Morfini, G., Buitrago, L., Ujlaki, G., Choi, S., Yu, E., Moreira, J.E., Avila, J., Brady, S.T., Pant, H., Sugimori, M., Llinás, R.R., 2016. Tau pathology-mediated presynaptic dysfunction. Neuroscience 325, 30–38. https://doi.org/10.1016/j.neuroscience.2016.03.044

Mori, H., Nishimura, M., Namba, Y., Oda, M., 1994. Corticobasal degeneration: a disease with widespread appearance of abnormal tau and neurofibrillary tangles, and its relation to progressive supranuclear palsy. Acta Neuropathol. 88, 113–121. https://doi.org/10.1007/bf00294503

Morishima-Kawashima, M., 2014. Molecular mechanism of the intramembrane cleavage of the β-carboxyl terminal fragment of amyloid precursor protein by γ-secretase. Front. Physiol. 5, 463. https://doi.org/10.3389/fphys.2014.00463

Morozova, V., Cohen, L.S., Makki, A.E.-H., Shur, A., Pilar, G., Idrissi, A.E., Alonso, A.D., 2019. Normal and Pathological Tau Uptake Mediated by M1/M3 Muscarinic Receptors Promotes Opposite Neuronal Changes. Front. Cell. Neurosci. 13, 403. https://doi.org/10.3389/fncel.2019.00403

Morris, H.R., Osaki, Y., Holton, J., Lees, A.J., Wood, N.W., Revesz, T., Quinn, N., 2003. Tau exon 10 +16 mutation FTDP-17 presenting clinically as sporadic young onset PSP. Neurology 61, 102–4. https://doi.org/10.1212/01.wnl.0000072325.27824.a5

Morris, J.C., Storandt, M., Miller, J.P., McKeel, D.W., Price, J.L., Rubin, E.H., Berg, L., 2001. Mild Cognitive Impairment Represents Early-Stage Alzheimer Disease. Arch. Neurol. 58, 397–405. https://doi.org/10.1001/archneur.58.3.397

Morris, M., Knudsen, G.M., Maeda, S., Trinidad, J.C., Ioanoviciu, A., Burlingame, A.L., Mucke, L., 2015. Tau post-translational modifications in wild-type and human amyloid precursor protein transgenic mice. Nat. Neurosci. 18, 1183–1189. https://doi.org/10.1038/nn.4067

Morris, M., Maeda, S., Vossel, K., Mucke, L., 2011. The Many Faces of Tau. Neuron 70, 410–426. https://doi.org/10.1016/j.neuron.2011.04.009

Mothes, T., Portal, B., Konstantinidis, E., Eltom, K., Libard, S., Streubel-Gallasch, L., Ingelsson, M., Rostami, J., Lindskog, M., Erlandsson, A., 2023. Astrocytic uptake of neuronal corpses promotes cell-to-cell spreading of tau pathology. Acta Neuropathol. Commun. 11, 97. https://doi.org/10.1186/s40478-023-01589-8

Mukrasch, M.D., Bibow, S., Korukottu, J., Jeganathan, S., Biernat, J., Griesinger, C., Mandelkow, E., Zweckstetter, M., 2009. Structural Polymorphism of 441-Residue Tau at Single Residue Resolution. PLoS Biol. 7, e1000034. https://doi.org/10.1371/journal.pbio.1000034

Mullard, A., 2024. Anti-tau antibody stumbles in phase II Alzheimer trial. Nat. Rev. Drug Discov. 23, 883–883. https://doi.org/10.1038/d41573-024-00180-7

Müller, U.C., Deller, T., Korte, M., 2017. Not just amyloid: physiological functions of the amyloid precursor protein family. Nat. Rev. Neurosci. 18, 281–298. https://doi.org/10.1038/nrn.2017.29

Mummery, C.J., Börjesson-Hanson, A., Blackburn, D.J., Vijverberg, E.G.B., Deyn, P.P.D., Ducharme, S., Jonsson, M., Schneider, A., Rinne, J.O., Ludolph, A.C., Bodenschatz, R., Kordasiewicz, H., Swayze, E.E., Fitzsimmons, B., Mignon, L., Moore, K.M., Yun, C., Baumann, T., Li, D., Norris, D.A., Crean, R., Graham, D.L., Huang, E., Ratti, E., Bennett, C.F., Junge, C., Lane, R.M., 2023. Tau-targeting antisense oligonucleotide MAPTRx in mild Alzheimer's disease: a phase 1b, randomized, placebo-controlled trial. Nat. Med. 29, 1437–1447. https://doi.org/10.1038/s41591-023-02326-3

Mungenast, A.E., Siegert, S., Tsai, L.-H., 2016. Modeling Alzheimer's disease with human induced pluripotent stem (iPS) cells. Mol. Cell. Neurosci. 73, 13–31. https://doi.org/10.1016/j.mcn.2015.11.010

Muntané, G., Dalfó, E., Martinez, A., Ferrer, I., 2008. Phosphorylation of tau and α-synuclein in synaptic-enriched fractions of the frontal cortex in Alzheimer's disease, and in Parkinson's disease and related α-synucleinopathies. Neuroscience 152, 913–923. https://doi.org/10.1016/j.neuroscience.2008.01.030

Neve, R.L., Harris, P., Kosik, K.S., Kurnit, D.M., Donlon, T.A., 1986. Identification of cDNA clones for the human microtubule-associated protein tau and chromosomal localization of the genes for tau and microtubule-associated protein 2. Mol. Brain Res. 1, 271–280. https://doi.org/10.1016/0169-328x(86)90033-1

Nishida, I., Yamada, K., Sakamoto, A., Wakabayashi, T., Iwatsubo, T., 2024. Chronic Neuronal Hyperexcitation Exacerbates Tau Propagation in a Mouse Model of Tauopathy. Int. J. Mol. Sci. 25, 9004. https://doi.org/10.3390/ijms25169004

Noble, M., Lewis, S.A., Cowan, N.J., 1989. The microtubule binding domain of microtubule-associated protein MAP1B contains a repeated sequence motif unrelated to that of MAP2 and tau. J. cell Biol. 109, 3367–3376. https://doi.org/10.1083/jcb.109.6.3367

Noda, N.N., Ohsumi, Y., Inagaki, F., 2010. Atg8-family interacting motif crucial for selective autophagy. FEBS Lett. 584, 1379–1385. https://doi.org/10.1016/j.febslet.2010.01.018

Ori-McKenney, K.M., McKenney, R.J., Huang, H.H., Li, T., Meltzer, S., Jan, L.Y., Vale, R.D., Wiita, A.P., Jan, Y.N., 2016. Phosphorylation of β-Tubulin by the Down Syndrome Kinase, Minibrain/DYRK1a, Regulates Microtubule Dynamics and Dendrite Morphogenesis. Neuron 90, 551–563. https://doi.org/10.1016/j.neuron.2016.03.027

Otvos, L., Feiner, L., Lang, E., Szendrei, G.I., Goedert, M., Lee, V.M., 1994. Monoclonal antibody PHF-1 recognizes tau protein phosphorylated at serine residues 396 and 404. J. Neurosci. Res. 39, 669–673. https://doi.org/10.1002/jnr.490390607

Pankiv, S., Clausen, T.H., Lamark, T., Brech, A., Bruun, J.-A., Outzen, H., Øvervatn, A., Bjørkøy, G., Johansen, T., 2007. p62/SQSTM1 Binds Directly to Atg8/LC3 to Facilitate Degradation of Ubiquitinated Protein Aggregates by Autophagy*. J. Biol. Chem. 282, 24131–24145. https://doi.org/10.1074/jbc.m702824200

Park, J., Song, W.-J., Chung, K.C., 2009. Function and regulation of Dyrk1A: towards understanding Down syndrome. Cell. Mol. Life Sci. 66, 3235–3240. https://doi.org/10.1007/s00018-009-0123-2

Paşca, A.M., Sloan, S.A., Clarke, L.E., Tian, Y., Makinson, C.D., Huber, N., Kim, C.H., Park, J.-Y., O'Rourke, N.A., Nguyen, K.D., Smith, S.J., Huguenard, J.R., Geschwind, D.H., Barres, B.A., Paşca, S.P., 2015. Functional cortical neurons and astrocytes from human pluripotent stem cells in 3D culture. Nat. Methods 12, 671–678. https://doi.org/10.1038/nmeth.3415

Patel, N.S., Paris, D., Mathura, V., Quadros, A.N., Crawford, F.C., Mullan, M.J., 2005. Inflammatory cytokine levels correlate with amyloid load in transgenic mouse models of Alzheimer's disease. J. Neuroinflammation 2, 9. https://doi.org/10.1186/1742-2094-2-9

Paudel, H.K., Li, W., 1999. Heparin-induced Conformational Change in Microtubule-associated Protein Tau as Detected by Chemical Cross-linking and Phosphopeptide Mapping*. J. Biol. Chem. 274, 8029–8038. https://doi.org/10.1074/jbc.274.12.8029

Pickett, E.K., Henstridge, C.M., Allison, E., Pitstick, R., Pooler, A., Wegmann, S., Carlson, G., Hyman, B.T., Spires-Jones, T.L., 2017. Spread of tau down neural circuits precedes synapse and neuronal loss in the rTgTauEC mouse model of early Alzheimer's disease. Synapse 71, e21965. https://doi.org/10.1002/syn.21965

Pierrot, N., Santos, S.F., Feyt, C., Morel, M., Brion, J.-P., Octave, J.-N., 2006. Calcium-mediated Transient Phosphorylation of Tau and Amyloid Precursor Protein Followed by Intraneuronal Amyloid-β Accumulation*. J. Biol. Chem. 281, 39907–39914. https://doi.org/10.1074/jbc.m606015200

Piras, A., Collin, L., Grüninger, F., Graff, C., Rönnbäck, A., 2016. Autophagic and lysosomal defects in human tauopathies: analysis of post-mortem brain from patients with familial Alzheimer disease, corticobasal degeneration and progressive supranuclear palsy. Acta Neuropathol. Commun. 4, 22. https://doi.org/10.1186/s40478-016-0292-9

Polydoro, M., Dzhala, V.I., Pooler, A.M., Nicholls, S.B., McKinney, A.P., Sanchez, L., Pitstick, R., Carlson, G.A., Staley, K.J., Spires-Jones, T.L., Hyman, B.T., 2014. Soluble pathological tau in the entorhinal cortex leads to presynaptic deficits in an early Alzheimer's disease model. Acta Neuropathol. 127, 257–270. https://doi.org/10.1007/s00401-013-1215-5

Pooler, A.M., Phillips, E.C., Lau, D.H.W., Noble, W., Hanger, D.P., 2013. Physiological release of endogenous tau is stimulated by neuronal activity. EMBO Rep. 14, 389–394. https://doi.org/10.1038/embor.2013.15

Portillo, M., Eremenko, E., Kaluski, S., Garcia-Venzor, A., Onn, L., Stein, D., Slobodnik, Z., Zaretsky, A., Ueberham, U., Einav, M., Brückner, M.K., Arendt, T., Toiber, D., 2021. SIRT6-CBP-dependent nuclear Tau accumulation and its role in protein synthesis. Cell Rep. 35, 109035. https://doi.org/10.1016/j.celrep.2021.109035

Prusiner, S.B., 1982. Novel Proteinaceous Infectious Particles Cause Scrapie. Science 216, 136–144. https://doi.org/10.1126/science.6801762

Qian, W., Liu, F., 2014. Regulation of alternative splicing of tau exon 10. Neurosci. Bull. 30, 367–377. https://doi.org/10.1007/s12264-013-1411-2

Rasmussen, N.L., Kournoutis, A., Lamark, T., Johansen, T., 2022a. NBR1: The archetypal selective autophagy receptor. J. Cell Biol. 221, e202208092. https://doi.org/10.1083/jcb.202208092

Rauch, J.N., Chen, J.J., Sorum, A.W., Miller, G.M., Sharf, T., See, S.K., Hsieh-Wilson, L.C., Kampmann, M., Kosik, K.S., 2018. Tau Internalization is Regulated by 6-O Sulfation on Heparan Sulfate Proteoglycans (HSPGs). Sci. Rep. 8, 6382. https://doi.org/10.1038/s41598-018-24904-z

Rauch, J.N., Luna, G., Guzman, E., Audouard, M., Challis, C., Sibih, Y.E., Leshuk, C., Hernandez, I., Wegmann, S., Hyman, B.T., Gradinaru, V., Kampmann, M., Kosik, K.S., 2020. LRP1 is a master regulator of tau uptake and spread. Nature 580, 381–385. https://doi.org/10.1038/s41586-020-2156-5

Redmann, M., Benavides, G.A., Berryhill, T.F., Wani, W.Y., Ouyang, X., Johnson, M.S., Ravi, S., Barnes, S., Darley-Usmar, V.M., Zhang, J., 2017. Inhibition of autophagy with bafilomycin and chloroquine decreases mitochondrial quality and bioenergetic function in primary neurons. Redox Biol. 11, 73–81. https://doi.org/10.1016/j.redox.2016.11.004

Reid, M.J., Beltran-Lobo, P., Johnson, L., Perez-Nievas, B.G., Noble, W., 2020. Astrocytes in Tauopathies. Front. Neurol. 11, 572850. https://doi.org/10.3389/fneur.2020.572850

Robbins, M., Clayton, E., Schierle, G.S.K., 2021. Synaptic tau: A pathological or physiological phenomenon? Acta Neuropathol. Commun. 9, 149. https://doi.org/10.1186/s40478-021-01246-y

Roberson, E.D., Scearce-Levie, K., Palop, J.J., Yan, F., Cheng, I.H., Wu, T., Gerstein, H., Yu, G.-Q., Mucke, L., 2007. Reducing endogenous tau ameliorates amyloid beta-induced deficits in an Alzheimer's disease mouse model. Sci. (N. York, NY) 316, 750–4. https://doi.org/10.1126/science.1141736

Roney, J.C., Li, S., Farfel-Becker, T., Huang, N., Sun, T., Xie, Y., Cheng, X.-T., Lin, M.-Y., Platt, F.M., Sheng, Z.-H., 2021. Lipid-mediated impairment of axonal lysosome transport contributing to autophagic stress. Autophagy 17, 1796–1798. https://doi.org/10.1080/15548627.2021.1938916

Rossi, R., Arjmand, S., Bærentzen, S.L., Gjedde, A., Landau, A.M., 2022. Synaptic Vesicle Glycoprotein 2A: Features and Functions. Front. Neurosci. 16, 864514. https://doi.org/10.3389/fnins.2022.864514

Roux, K.J., Kim, D.I., Burke, B., 2013. BioID: A Screen for Protein-Protein Interactions. Curr. Protoc. Protein Sci. 74, 19.23.1-19.23.14. https://doi.org/10.1002/0471140864.ps1923s74

Roux, K.J., Kim, D.I., Raida, M., Burke, B., 2012. A promiscuous biotin ligase fusion protein identifies proximal and interacting proteins in mammalian cells. J. Cell Biol. 196, 801–810. https://doi.org/10.1083/jcb.201112098

Ruan, Z., Pathak, D., Kalavai, S.V., Yoshii-Kitahara, A., Muraoka, S., Bhatt, N., Takamatsu-Yukawa, K., Hu, J., Wang, Y., Hersh, S., Ericsson, M., Gorantla, S., Gendelman, H.E., Kayed, R., Ikezu, S., Luebke, J.I., Ikezu, T., 2020. Alzheimer's disease brain-derived extracellular vesicles spread tau pathology in interneurons. Brain 144, 288–309. https://doi.org/10.1093/brain/awaa376

Rubinsztein, D.C., 2006. The roles of intracellular protein-degradation pathways in neurodegeneration. Nature 443, 780–786. https://doi.org/10.1038/nature05291

Rustom, A., Saffrich, R., Markovic, I., Walther, P., Gerdes, H.-H., 2004. Nanotubular Highways for Intercellular Organelle Transport. Science 303, 1007–1010. https://doi.org/10.1126/science.1093133

Ryoo, S.-R., Jeong, H.K., Radnaabazar, C., Yoo, J.-J., Cho, H.-J., Lee, H.-W., Kim, I.-S., Cheon, Y.-H., Ahn, Y.S., Chung, S.-H., Song, W.-J., 2007. DYRK1A-mediated hyperphosphorylation of Tau. A functional link between Down syndrome and Alzheimer disease. J. Biol. Chem. 282, 34850–7. https://doi.org/10.1074/jbc.m707358200

Ryter, S.W., Cloonan, S.M., Choi, A.M.K., 2013. Autophagy: A Critical Regulator of Cellular Metabolism and Homeostasis. Mol. Cells 36, 7–16. https://doi.org/10.1007/s10059-013-0140-8

Saman, Sudad, Kim, W., Raya, M., Visnick, Y., Miro, S., Saman, Sarmad, Jackson, B., McKee, A.C., Alvarez, V.E., Lee, N.C.Y., Hall, G.F., 2012. Exosome-associated Tau Is Secreted in Tauopathy Models and Is Selectively Phosphorylated in Cerebrospinal Fluid in Early Alzheimer Disease*. J. Biol. Chem. 287, 3842–3849. https://doi.org/10.1074/jbc.m111.277061

Sanchez, P.E., Zhu, L., Verret, L., Vossel, K.A., Orr, A.G., Cirrito, J.R., Devidze, N., Ho, K., Yu, G.-Q., Palop, J.J., Mucke, L., 2012. Levetiracetam suppresses neuronal network dysfunction and reverses synaptic and cognitive deficits in an Alzheimer's disease model. Proc. Natl. Acad. Sci. 109, E2895–E2903. https://doi.org/10.1073/pnas.1121081109

Sasaki, K., Shimura, H., Itaya, M., Tanaka, R., Mori, H., Mizuno, Y., Kosik, K.S., Tanaka, S., Hattori, N., 2009. Excitatory amino acid transporter 2 associates with phosphorylated tau and is localized in neurofibrillary tangles of tauopathic brains. FEBS Lett. 583, 2194–2200. https://doi.org/10.1016/j.febslet.2009.06.015

Savova, A., Romanov, J., Martens, S., 2020a. NBR1 directly promotes the formation of p62 – ubiquitin condensates via its PB1 and UBA domains. bioRxiv 2020.09.18.303552. https://doi.org/10.1101/2020.09.18.303552

Schlegel, K., Awwad, K., Heym, R.G., Holzinger, D., Doell, A., Barghorn, S., Jahn, T.R., Klein, C., Mordashova, Y., Schulz, M., Gasparini, L., 2019. N368-Tau fragments generated by legumain are detected

only in trace amount in the insoluble Tau aggregates isolated from AD brain. Acta Neuropathol. Commun. 7, 177. https://doi.org/10.1186/s40478-019-0831-2

Schreiber, A., Peter, M., 2014. Substrate recognition in selective autophagy and the ubiquitin–proteasome system. Biochim. Biophys. Acta (BBA) - Mol. Cell Res. 1843, 163–181. https://doi.org/10.1016/j.bbamcr.2013.03.019

Schweers, O., Schönbrunn-Hanebeck, E., Marx, A., Mandelkow, E., 1994. Structural studies of tau protein and Alzheimer paired helical filaments show no evidence for beta-structure. J. Biol. Chem. 269, 24290–24297. https://doi.org/10.1016/s0021-9258(19)51080-8

Selkoe, D.J., 2002. Alzheimer's Disease Is a Synaptic Failure. Science 298, 789–791. https://doi.org/10.1126/science.1074069

Selkoe, D.J., 2001. Alzheimer's Disease: Genes, Proteins, and Therapy. Physiol. Rev. 81, 741–766. https://doi.org/10.1152/physrev.2001.81.2.741

Serajee, F.J., Huq, A.M., 2015. Homozygous Mutation in Synaptic Vesicle Glycoprotein 2A Gene Results in Intractable Epilepsy, Involuntary Movements, Microcephaly, and Developmental and Growth Retardation. Pediatr. Neurol. 52, 642-646.e1. https://doi.org/10.1016/j.pediatrneurol.2015.02.011

Sergeant, N., Wattez, A., Delacourte, A., 1999. Neurofibrillary degeneration in progressive supranuclear palsy and corticobasal degeneration: tau pathologies with exclusively "exon 10" isoforms. J. Neurochem. 72, 1243–9. https://doi.org/10.1046/j.1471-4159.1999.0721243.x

Serrano-Pozo, A., Frosch, M.P., Masliah, E., Hyman, B.T., 2011. Neuropathological Alterations in Alzheimer Disease. Cold Spring Harb. Perspect. Med. 1, a006189. https://doi.org/10.1101/cshperspect.a006189

Shi, Y., Kirwan, P., Livesey, F.J., 2012. Directed differentiation of human pluripotent stem cells to cerebral cortex neurons and neural networks. Nat. Protoc. 7, 1836–1846. https://doi.org/10.1038/nprot.2012.116

Shi, Y., Zhang, W., Yang, Y., Murzin, A.G., Falcon, B., Kotecha, A., Beers, M. van, Tarutani, A., Kametani, F., Garringer, H.J., Vidal, R., Hallinan, G.I., Lashley, T., Saito, Y., Murayama, S., Yoshida, M., Tanaka, H., Kakita, A., Ikeuchi, T., Robinson, A.C., Mann, D.M.A., Kovacs, G.G., Revesz, T., Ghetti, B., Hasegawa, M., Goedert, M., Scheres, S.H.W., 2021. Structure-based classification of tauopathies. Nature 598, 359–363. https://doi.org/10.1038/s41586-021-03911-7

Shimojo, M., Takuwa, H., Takado, Y., Tokunaga, M., Tsukamoto, S., Minatohara, K., Ono, M., Seki, C., Maeda, J., Urushihata, T., Minamihisamatsu, T., Aoki, I., Kawamura, K., Zhang, M.-R., Suhara, T., Sahara, N., Higuchi, M., 2020. Selective Disruption of Inhibitory Synapses Leading to Neuronal Hyperexcitability at an Early Stage of Tau Pathogenesis in a Mouse Model. J. Neurosci. 40, 3491–3501. https://doi.org/10.1523/jneurosci.2880-19.2020

Shin, J., Nile, A., Oh, J.-W., 2021. Role of adaptin protein complexes in intracellular trafficking and their impact on diseases. Bioengineered 12, 8259–8278. https://doi.org/10.1080/21655979.2021.1982846

Shin, Y., Brangwynne, C.P., 2017. Liquid phase condensation in cell physiology and disease. Science 357. https://doi.org/10.1126/science.aaf4382

Sievers, S.A., Karanicolas, J., Chang, H.W., Zhao, A., Jiang, L., Zirafi, O., Stevens, J.T., Münch, J., Baker, D., Eisenberg, D., 2011. Structure-based design of non-natural amino-acid inhibitors of amyloid fibril formation. Nature 475, 96–100. https://doi.org/10.1038/nature10154

Sims, J. R., Zimmer, J. A., Evans, C. D., Lu, M., Ardayfio, P., Sparks, J., Wessels, A. M., Shcherbinin, S., Wang, H., Nery, E. S. M., Collins, E. C., Solomon, P., Salloway, S., Apostolova, L. G., Hansson, O., Ritchie, C., Brooks, D. A., Mintun, M., Skovronsky, D. M., … Zboch, M. (2023). Donanemab in Early Symptomatic Alzheimer Disease: The TRAILBLAZER-ALZ 2 Randomized Clinical Trial. *JAMA*, *330*(6), 512–527. https://doi.org/10.1001/jama.2023.13239

Slomski, A., 2022. Anti-Tau Antibody Semorinemab Fails to Slow Alzheimer Disease. JAMA 328, 415–415. https://doi.org/10.1001/jama.2022.12727

Sofroniew, M.V., Vinters, H.V., 2010. Astrocytes: biology and pathology. Acta Neuropathol. 119, 7–35. https://doi.org/10.1007/s00401-009-0619-8

Španić, E., Horvat, L.L., Hof, P.R., Šimić, G., 2019. Role of Microglial Cells in Alzheimer's Disease Tau Propagation. Front. Aging Neurosci. 11, 271. https://doi.org/10.3389/fnagi.2019.00271

Speicher, A.M., Wiendl, H., Meuth, S.G., Pawlowski, M., 2019. Generating microglia from human pluripotent stem cells: novel in vitro models for the study of neurodegeneration. Mol. Neurodegener. 14, 46. https://doi.org/10.1186/s13024-019-0347-z

Spillantini, M.G., Goedert, M., 1998. Tau protein pathology in neurodegenerative diseases. Trends Neurosci. 21, 428–433. https://doi.org/10.1016/s0166-2236(98)01337-x

Spires-Jones, T.L., Hyman, B.T., 2014. The Intersection of Amyloid Beta and Tau at Synapses in Alzheimer's Disease. Neuron 82, 756–771. https://doi.org/10.1016/j.neuron.2014.05.004

Sposito, T., Preza, E., Mahoney, C.J., Setó-Salvia, N., Ryan, N.S., Morris, H.R., Arber, C., Devine, M.J., Houlden, H., Warner, T.T., Bushell, T.J., Zagnoni, M., Kunath, T., Livesey, F.J., Fox, N.C., Rossor, M.N., Hardy, J., Wray, S., 2015. Developmental regulation of tau splicing is disrupted in stem cell-derived neurons from frontotemporal dementia patients with the 10 + 16 splice-site mutation in MAPT. Hum. Mol. Genet. 24, 5260–5269. https://doi.org/10.1093/hmg/ddv246

Stalder, M., Phinney, A., Probst, A., Sommer, B., Staufenbiel, M., Jucker, M., 1999. Association of Microglia with Amyloid Plaques in Brains of APP23 Transgenic Mice. Am. J. Pathol. 154, 1673–1684. https://doi.org/10.1016/s0002-9440(10)65423-5

Stamer, K., Vogel, R., Thies, E., Mandelkow, E., Mandelkow, E.-M., 2002. Tau blocks traffic of organelles, neurofilaments, and APP vesicles in neurons and enhances oxidative stress. J. Cell Biol. 156, 1051–1063. https://doi.org/10.1083/jcb.200108057

Stefanoska, K., Gajwani, M., Tan, A.R.P., Ahel, H.I., Asih, P.R., Volkerling, A., Poljak, A., Ittner, A., 2022. Alzheimer's disease: Ablating single master site abolishes tau hyperphosphorylation. Sci. Adv. 8, eabl8809. https://doi.org/10.1126/sciadv.abl8809

Steiner, H., Fukumori, A., Tagami, S., Okochi, M., 2018. Making the final cut: pathogenic amyloid-β peptide generation by γ-secretase. Cell Stress 2, 292–310. https://doi.org/10.15698/cst2018.11.162

Stokin, G.B., Lillo, C., Falzone, T.L., Brusch, R.G., Rockenstein, E., Mount, S.L., Raman, R., Davies, P., Masliah, E., Williams, D.S., Goldstein, L.S.B., 2005. Axonopathy and Transport Deficits Early in the Pathogenesis of Alzheimer's Disease. Science 307, 1282–1288. https://doi.org/10.1126/science.1105681

Sultan, A., Nesslany, F., Violet, M., Bégard, S., Loyens, A., Talahari, S., Mansuroglu, Z., Marzin, D., Sergeant, N., Humez, S., Colin, M., Bonnefoy, E., Buée, L., Galas, M.-C., 2011. Nuclear Tau, a Key Player in Neuronal DNA Protection*. J. Biol. Chem. 286, 4566–4575. https://doi.org/10.1074/jbc.m110.199976

Svenning, S., Lamark, T., Krause, K., Johansen, T., 2011. Plant NBR1 is a selective autophagy substrate and a functional hybrid of the mammalian autophagic adapters NBR1 and p62/SQSTM1. Autophagy 7, 993–1010. https://doi.org/10.4161/auto.7.9.16389

Takahashi, K., Foster, J.B., Lin, C.-L.G., 2015. Glutamate transporter EAAT2: regulation, function, and potential as a therapeutic target for neurological and psychiatric disease. Cell. Mol. Life Sci. 72, 3489–3506. https://doi.org/10.1007/s00018-015-1937-8

Takahashi, K., Tanabe, K., Ohnuki, M., Narita, M., Ichisaka, T., Tomoda, K., Yamanaka, S., 2007. Induction of Pluripotent Stem Cells from Adult Human Fibroblasts by Defined Factors. Cell 131, 861–872. https://doi.org/10.1016/j.cell.2007.11.019

Takahashi, K., Yamanaka, S., 2006. Induction of Pluripotent Stem Cells from Mouse Embryonic and Adult Fibroblast Cultures by Defined Factors. Cell 126, 663–676. https://doi.org/10.1016/j.cell.2006.07.024

Tanzi, R.E., 2012. The Genetics of Alzheimer Disease. Cold Spring Harb. Perspect. Med. 2, a006296. https://doi.org/10.1101/cshperspect.a006296

Tanzi, R.E., Bertram, L., 2005. Twenty Years of the Alzheimer's Disease Amyloid Hypothesis: A Genetic Perspective. Cell 120, 545–555. https://doi.org/10.1016/j.cell.2005.02.008

Tardivel, M., Bégard, S., Bousset, L., Dujardin, S., Coens, A., Melki, R., Buée, L., Colin, M., 2016. Tunneling nanotube (TNT)-mediated neuron-to neuron transfer of pathological Tau protein assemblies. Acta Neuropathol. Commun. 4, 117. https://doi.org/10.1186/s40478-016-0386-4

TCW, J., 2019. Human iPSC application in Alzheimer's disease and Tau-related neurodegenerative diseases. Neurosci. Lett. 699, 31–40. https://doi.org/10.1016/j.neulet.2019.01.043

TCW, J., Wang, M., Pimenova, A.A., Bowles, K.R., Hartley, B.J., Lacin, E., Machlovi, S.I., Abdelaal, R., Karch, C.M., Phatnani, H., Slesinger, P.A., Zhang, B., Goate, A.M., Brennand, K.J., 2017. An Efficient Platform for Astrocyte Differentiation from Human Induced Pluripotent Stem Cells. Stem Cell Rep. 9, 600–614. https://doi.org/10.1016/j.stemcr.2017.06.018

Tejedor, F., Zhu, X.R., Kaltenbach, E., Ackermann, A., Baumann, A., Canal, I., Heisenberg, M., Fischbach, K.F., Pongs, O., 1995. minibrain: A new protein kinase family involved in postembryonic neurogenesis in Drosophila. Neuron 14, 287–301. https://doi.org/10.1016/0896-6273(95)90286-4

Tejedor, F.J., Hämmerle, B., 2011. MNB/DYRK1A as a multiple regulator of neuronal development. FEBS J. 278, 223–235. https://doi.org/10.1111/j.1742-4658.2010.07954.x

Teng, E., Manser, P.T., Pickthorn, K., Brunstein, F., Blendstrup, M., Bohorquez, S.S., Wildsmith, K.R., Toth, B., Dolton, M., Ramakrishnan, V., Bobbala, A., Sikkes, S.A.M., Ward, M., Fuji, R.N., Kerchner, G.A., Investigators, T., Farnbach, P., Kyndt, C., O'Brien, T., Yassi, N., Schwartz, R., Lieten, S., Vandenberghe, R., Vanhee, F., Bergeron, R., Black, S., Cohen, S., Frank, A., Nisker, W., Tartaglia, M.C., Justesen, A., Alexandersen, P., Nielsen, S., Areovimata, A., Anthony, P., Belliard, S., Blanc, F., Ceccaldi, M., Dubois, B., Krolak-Salmon, P., Mollion, H., Pasquier, F., Grimmer, T., Kottke-Arbeiter, M.E., Laske, C., Peters, O., Polivka, D., Arnim, C. von, Bruno, G., Lena, C.D., Cassetta, E., Centonze, D., Logroscino, G., Dautzenberg, P., Rutgers, S., Prins, N., Czarnecki, M., Dobryniewski, J., Ilkowski, J., Klodowska, G., Krygowska-Wajs, A., Kucharski, R., Mickielewicz, A., Ratajczak, M., Zboch, M., Zielinski, T., Soler, P.A., Morales, E.A., Toledo, M.B., González, R.B., Rovira, M.B., Rodriguez, A.D.O., Krupinski, J., Cristobal, G.L., Arrieta, J.L., Fernandez, M.R., Diaz, R.S.D.V., Fernandez, F.V., Jonsson, M., Östlund, H., MacSweeney, J.E., Mummery, C., Agronin, M., Ala, T., Bond, W., Schaerf, F., Brody, M., Edwards, K., Forchetti, C., Sood, A., Geldmacher, D., Goldstein, M., Goodman, I., Hart, D., Honig, L., Justiz, W., Levey, A., Losk, S., Marshall, G., Martinez, W., McAllister, P., McElveen, W.A., Maldonado-Robles, O., Murphy, C., Nair, M., Nair, A., Omidvar, O., Oskooilar, N., Porsteinsson, A., Rosenbloom, M., Russell, D., Sajjadi, S.A., Pierce, A., Salloway, S., Sha, S., Shah, R., Sharma, S., Smith, W., Stein, L., Stoukides, J., Thein, S., Turner, R., Watson, D., Weisman, D., 2022. Safety and Efficacy of Semorinemab in Individuals With Prodromal to Mild Alzheimer Disease: A Randomized Clinical Trial. JAMA Neurol. 79, 758. https://doi.org/10.1001/jamaneurol.2022.1375

Terry, R.D., Masliah, E., Salmon, D.P., Butters, N., DeTeresa, R., Hill, R., Hansen, L.A., Katzman, R., 1991. Physical basis of cognitive alterations in alzheimer's disease: Synapse loss is the major correlate of cognitive impairment. Ann. Neurol. 30, 572–580. https://doi.org/10.1002/ana.410300410

Thies, E., Mandelkow, E.-M., 2007. Missorting of Tau in Neurons Causes Degeneration of Synapses That Can Be Rescued by the Kinase MARK2/Par-1. J. Neurosci. 27, 2896–2907. https://doi.org/10.1523/jneurosci.4674-06.2007

Thompson, J.C., Rabi, M.L., Novoa, M., Nash, K.R., Joly-Amado, A., 2024. Evaluating the Efficacy of Levetiracetam on Non-Cognitive Symptoms and Pathology in a Tau Mouse Model. Biomedicines 12, 2891. https://doi.org/10.3390/biomedicines12122891

Trabzuni, D., Wray, S., Vandrovcova, J., Ramasamy, A., Walker, R., Smith, C., Luk, C., Gibbs, J.R., Dillman, A., Hernandez, D.G., Arepalli, S., Singleton, A.B., Cookson, M.R., Pittman, A.M., Silva, R. de, Weale, M.E., Hardy, J., Ryten, M., 2012. MAPT expression and splicing is differentially regulated by brain region: relation to genotype and implication for tauopathies. Hum. Mol. Genet. 21, 4094–4103. https://doi.org/10.1093/hmg/dds238

Tracy, T.E., Madero-Pérez, J., Swaney, D.L., Chang, T.S., Moritz, M., Konrad, C., Ward, M.E., Stevenson, E., Hüttenhain, R., Kauwe, G., Mercedes, M., Sweetland-Martin, L., Chen, X., Mok, S.-A., Wong, M.Y., Telpoukhovskaia, M., Min, S.-W., Wang, C., Sohn, P.D., Martin, J., Zhou, Y., Luo, W., Trojanowski, J.Q., Lee, V.M.Y., Gong, S., Manfredi, G., Coppola, G., Krogan, N.J., Geschwind, D.H., Gan, L., 2022. Tau interactome maps synaptic and mitochondrial processes associated with neurodegeneration. Cell 185, 712-728.e14. https://doi.org/10.1016/j.cell.2021.12.041

Vanderlinden, G., Ceccarini, J., Casteele, T.V., Michiels, L., Lemmens, R., Triau, E., Serdons, K., Tournoy, J., Koole, M., Vandenbulcke, M., Laere, K.V., 2022. Spatial decrease of synaptic density in amnestic mild cognitive impairment follows the tau build-up pattern. Mol. Psychiatry 27, 4244–4251. https://doi.org/10.1038/s41380-022-01672-x

Vanderlinden, G., Koole, M., Michiels, L., Lemmens, R., Vandenbulcke, M., Laere, K.V., 2024. Longitudinal synaptic loss versus tau Braak staging in amnestic mild cognitive impairment. Alzheimer's Dement. https://doi.org/10.1002/alz.14412

Vanhaute, H., Ceccarini, J., Michiels, L., Koole, M., Sunaert, S., Lemmens, R., Triau, E., Emsell, L., Vandenbulcke, M., Laere, K.V., 2020. In vivo synaptic density loss is related to tau deposition in amnestic mild cognitive impairment. Neurology 95, e545–e553. https://doi.org/10.1212/wnl.0000000000009818

Vassar, R., Bennett, B.D., Babu-Khan, S., Kahn, S., Mendiaz, E.A., Denis, P., Teplow, D.B., Ross, S., Amarante, P., Loeloff, R., Luo, Y., Fisher, S., Fuller, J., Edenson, S., Lile, J., Jarosinski, M.A., Biere, A.L., Curran, E., Burgess, T., Louis, J.-C., Collins, F., Treanor, J., Rogers, G., Citron, M., 1999. β-Secretase Cleavage of Alzheimer's Amyloid Precursor Protein by the Transmembrane Aspartic Protease BACE. Science 286, 735–741. https://doi.org/10.1126/science.286.5440.735

Verheyen, A., Diels, A., Reumers, J., Hoorde, K.V., Wyngaert, I.V. den, d'Ydewalle, C. van O., Bondt, A.D., Kuijlaars, J., Muynck, L.D., Hoogt, R.D., Bretteville, A., Jaensch, S., Buist, A., Cabrera-Socorro, A., Wray, S., Ebneth, A., Roevens, P., Royaux, I., Peeters, P.J., 2018a. Genetically Engineered iPSC-Derived FTDP-17 MAPT Neurons Display Mutation-Specific Neurodegenerative and Neurodevelopmental Phenotypes. Stem Cell Rep. 11, 363–379. https://doi.org/10.1016/j.stemcr.2018.06.022

Verheyen, A., Diels, A., Reumers, J., Hoorde, K.V., Wyngaert, I.V. den, d'Ydewalle, C. van O., Bondt, A.D., Kuijlaars, J., Muynck, L.D., Hoogt, R.D., Bretteville, A., Jaensch, S., Buist, A., Cabrera-Socorro, A., Wray, S., Ebneth, A., Roevens, P., Royaux, I., Peeters, P.J., 2018b. Genetically Engineered iPSC-Derived FTDP-17 MAPT Neurons Display Mutation-Specific Neurodegenerative and Neurodevelopmental Phenotypes. Stem Cell Rep. 11, 363–379. https://doi.org/10.1016/j.stemcr.2018.06.022

Vitvitsky, V.M., Garg, S.K., Keep, R.F., Albin, R.L., Banerjee, R., 2012. Na+ and K+ ion imbalances in Alzheimer's disease. Biochim. Biophys. Acta (BBA) - Mol. Basis Dis. 1822, 1671–1681. https://doi.org/10.1016/j.bbadis.2012.07.004

Vos, K.J.D., Grierson, A.J., Ackerley, S., Miller, C.C.J., 2008. Role of Axonal Transport in Neurodegenerative Diseases*. Annu. Rev. Neurosci. 31, 151–173. https://doi.org/10.1146/annurev.neuro.31.061307.090711

Wahl, M.C., Will, C.L., Lührmann, R., 2009. The Spliceosome: Design Principles of a Dynamic RNP Machine. Cell 136, 701–718. https://doi.org/10.1016/j.cell.2009.02.009

Wang, D., Zhou, Q., Ren, L., Lin, Y., Gao, L., Du, J., Wang, Y., 2019. Levetiracetam-induced a new seizure type in a girl with a novel SV2A gene mutation. Clin. Neurol. Neurosurg. 181, 64–66. https://doi.org/10.1016/j.clineuro.2019.03.020

Wang, J., Huang, Q., Chen, X., You, Z., He, K., Guo, Q., Huang, Y., Yang, Y., Lin, Z., Guo, T., Zhao, J., Guan, Y., Li, B., Xie, F., 2024. Tau pathology is associated with synaptic density and longitudinal synaptic loss in Alzheimer's disease. Mol. Psychiatry 29, 2799–2809. https://doi.org/10.1038/s41380-024-02501-z

Wang, Y., Balaji, V., Kaniyappan, S., Krüger, L., Irsen, S., Tepper, K., Chandupatla, R., Maetzler, W., Schneider, A., Mandelkow, E., Mandelkow, E.-M., 2017. The release and trans-synaptic transmission of Tau via exosomes. Mol. Neurodegener. 12, 5. https://doi.org/10.1186/s13024-016-0143-y

Wang, Y., Mandelkow, E., 2016. Tau in physiology and pathology. Nat. Rev. Neurosci. 17, 22–35. https://doi.org/10.1038/nrn.2015.1

Wang, Y., Martinez-Vicente, M., Krüger, U., Kaushik, S., Wong, E., Mandelkow, E.-M., Cuervo, A.M., Mandelkow, E., 2009. Tau fragmentation, aggregation and clearance: the dual role of lysosomal processing. Hum. Mol. Genet. 18, 4153–4170. https://doi.org/10.1093/hmg/ddp367

Wang, Y., Wang, J., Gao, L., Stamm, S., Andreadis, A., 2011. An SRp75/hnRNPG complex interacting with hnRNPE2 regulates the 5′ splice site of tau exon 10, whose misregulation causes frontotemporal dementia. Gene 485, 130–138. https://doi.org/10.1016/j.gene.2011.06.020

Wegiel, J., Gong, C., Hwang, Y., 2011. The role of DYRK1A in neurodegenerative diseases. FEBS J. 278, 236–245. https://doi.org/10.1111/j.1742-4658.2010.07955.x

Wegmann, S., Biernat, J., Mandelkow, E., 2021. A current view on Tau protein phosphorylation in Alzheimer's disease. Curr. Opin. Neurobiol. 69, 131–138. https://doi.org/10.1016/j.conb.2021.03.003

Wegmann, S., Eftekharzadeh, B., Tepper, K., Zoltowska, K.M., Bennett, R.E., Dujardin, S., Laskowski, P.R., MacKenzie, D., Kamath, T., Commins, C., Vanderburg, C., Roe, A.D., Fan, Z., Molliex, A.M., Hernandez-Vega, A., Muller, D., Hyman, A.A., Mandelkow, E., Taylor, J.P., Hyman, B.T., 2018. Tau protein liquid–liquid phase separation can initiate tau aggregation. EMBO J. 37, EMBJ201798049. https://doi.org/10.15252/embj.201798049

Weingarten, M.D., Lockwood, A.H., Hwo, S.Y., Kirschner, M.W., 1975. A protein factor essential for microtubule assembly. Proc. Natl. Acad. Sci. 72, 1858–1862. https://doi.org/10.1073/pnas.72.5.1858

Wesseling, H., Mair, W., Kumar, M., Schlaffner, C.N., Tang, S., Beerepoot, P., Fatou, B., Guise, A.J., Cheng, L., Takeda, S., Muntel, J., Rotunno, M.S., Dujardin, S., Davies, P., Kosik, K.S., Miller, B.L., Berretta, S., Hedreen, J.C., Grinberg, L.T., Seeley, W.W., Hyman, B.T., Steen, H., Steen, J.A., 2020a. Tau PTM Profiles Identify Patient Heterogeneity and Stages of Alzheimer's Disease. Cell 183, 1699-1713.e13. https://doi.org/10.1016/j.cell.2020.10.029

Wilkin, M., Tongngok, P., Gensch, N., Clemence, S., Motoki, M., Yamada, K., Hori, K., Taniguchi-Kanai, M., Franklin, E., Matsuno, K., Baron, M., 2008. Drosophila HOPS and AP-3 Complex Genes Are Required for a Deltex-Regulated Activation of Notch in the Endosomal Trafficking Pathway. Dev. Cell 15, 762–772. https://doi.org/10.1016/j.devcel.2008.09.002

Will, C.L., Lührmann, R., 2011. Spliceosome Structure and Function. Cold Spring Harb. Perspect. Biol. 3, a003707. https://doi.org/10.1101/cshperspect.a003707

Williams, D.R., Holton, J.L., Strand, C., Pittman, A., Silva, R. de, Lees, A.J., Revesz, T., 2007. Pathological tau burden and distribution distinguishes progressive supranuclear palsy-parkinsonism from Richardson's syndrome. Brain 130, 1566–1576. https://doi.org/10.1093/brain/awm104

Wimo, A., Jönsson, L., Bond, J., Prince, M., Winblad, B., International, A.D., 2013. The worldwide economic impact of dementia 2010. Alzheimer's Dement. 9, 1-11.e3. https://doi.org/10.1016/j.jalz.2012.11.006

Winston, C.N., Aulston, B., Rockenstein, E.M., Adame, A., Prikhodko, O., Dave, K.N., Mishra, P., Rissman, R.A., Yuan, S.H., 2019. Neuronal Exosome-Derived Human Tau is Toxic to Recipient Mouse Neurons in vivo. J. Alzheimer's Dis. 67, 541–553. https://doi.org/10.3233/jad-180776

Wischik, C.M., Edwards, P.C., Lai, R.Y., Roth, M., Harrington, C.R., 1996. Selective inhibition of Alzheimer disease-like tau aggregation by phenothiazines. Proc. Natl. Acad. Sci. 93, 11213–11218. https://doi.org/10.1073/pnas.93.20.11213

Wojda, U., Salinska, E., Kuznicki, J., 2008. Calcium ions in neuronal degeneration. IUBMB Life 60, 575–590. https://doi.org/10.1002/iub.91

WOODS, Y.L., COHEN, P., BECKER, W., JAKES, R., GOEDERT, M., WANG, X., PROUD, C.G., 2001. The kinase DYRK phosphorylates protein-synthesis initiation factor eIF2Bε at Ser539 and the microtubule-associated protein tau at Thr212: potential role for DYRK as a glycogen synthase kinase 3-priming kinase. Biochem. J. 355, 609–615. https://doi.org/10.1042/bj3550609

Wortmann, M., 2012. Dementia: a global health priority - highlights from an ADI and World Health Organization report. Alzheimer's Res. Ther. 4, 40–40. https://doi.org/10.1186/alzrt143

Wu, J.W., Hussaini, S.A., Bastille, I.M., Rodriguez, G.A., Mrejeru, A., Rilett, K., Sanders, D.W., Cook, C., Fu, H., Boonen, R.A.C.M., Herman, M., Nahmani, E., Emrani, S., Figueroa, Y.H., Diamond, M.I., Clelland, C.L., Wray, S., Duff, K.E., 2016. Neuronal activity enhances tau propagation and tau pathology in vivo. Nat. Neurosci. 19, 1085–1092. https://doi.org/10.1038/nn.4328

Wu, J.Y., Kar, A., Kuo, D., Yu, B., Havlioglu, N., 2006. SRp54 (SFRS11), a Regulator for tau Exon 10 Alternative Splicing Identified by an Expression Cloning Strategy. Mol. Cell. Biol. 26, 6739–6747. https://doi.org/10.1128/mcb.00739-06

Xie, Z., Klionsky, D.J., 2007. Autophagosome formation: core machinery and adaptations. Nat. Cell Biol. 9, 1102–1109. https://doi.org/10.1038/ncb1007-1102

Xu, Y., Zhang, S., Zheng, H., 2019a. The cargo receptor SQSTM1 ameliorates neurofibrillary tangle pathology and spreading through selective targeting of pathological MAPT (microtubule associated protein tau). Autophagy 15, 583–598. https://doi.org/10.1080/15548627.2018.1532258

Yamamoto, H., Zhang, S., Mizushima, N., 2023. Autophagy genes in biology and disease. Nat. Rev. Genet. 24, 382–400. https://doi.org/10.1038/s41576-022-00562-w

Yanamandra, K., Kfoury, N., Jiang, H., Mahan, T.E., Ma, S., Maloney, S.E., Wozniak, D.F., Diamond, M.I., Holtzman, D.M., 2013. Anti-Tau Antibodies that Block Tau Aggregate Seeding In Vitro Markedly Decrease Pathology and Improve Cognition In Vivo. Neuron 80, 402–414. https://doi.org/10.1016/j.neuron.2013.07.046

Yang, L., Afroz, S., Valsamis, H.A., Michelson, H.B., Goodman, J.H., Ling, D.S.F., 2021. Early intervention with levetiracetam prevents the development of cortical hyperexcitability and spontaneous epileptiform activity in two models of neurotrauma in rats. Exp. Neurol. 337, 113571. https://doi.org/10.1016/j.expneurol.2020.113571

Yoshiyama, Y., Lee, V.M.Y., Trojanowski, J.Q., 2013. Therapeutic strategies for tau mediated neurodegeneration. J. Neurol., Neurosurg. Psychiatry 84, 784. https://doi.org/10.1136/jnnp-2012-303144

Yu, J., Vodyanik, M.A., Smuga-Otto, K., Antosiewicz-Bourget, J., Frane, J.L., Tian, S., Nie, J., Jonsdottir, G.A., Ruotti, V., Stewart, R., Slukvin, I.I., Thomson, J.A., 2007. Induced Pluripotent Stem Cell Lines Derived from Human Somatic Cells. Science 318, 1917–1920. https://doi.org/10.1126/science.1151526

Yu, Q., Guo, J., Zhou, J., 2004. A minimal length between tau exon 10 and 11 is required for correct splicing of exon 10. J. Neurochem. 90, 164–172. https://doi.org/10.1111/j.1471-4159.2004.02477.x

Yu, Y., Run, X., Liang, Z., Li, Y., Liu, F., Liu, Y., Iqbal, K., Grundke-Iqbal, I., Gong, C., 2009. Developmental regulation of tau phosphorylation, tau kinases, and tau phosphatases. J. Neurochem. 108, 1480–1494. https://doi.org/10.1111/j.1471-4159.2009.05882.x

Zempel, H., Dennissen, F.J.A., Kumar, Y., Luedtke, J., Biernat, J., Mandelkow, E.-M., Mandelkow, E., 2017. Axodendritic sorting and pathological missorting of Tau are isoform-specific and determined by axon initial segment architecture. J. Biol. Chem. 292, 12192–12207. https://doi.org/10.1074/jbc.m117.784702

Zhang, W., Xu, C., Sun, J., Shen, H.-M., Wang, J., Yang, C., 2022. Impairment of the autophagy–lysosomal pathway in Alzheimer's diseases: Pathogenic mechanisms and therapeutic potential. Acta Pharm. Sin. B 12, 1019–1040. https://doi.org/10.1016/j.apsb.2022.01.008

Zhang, X., Lin, Y., Eschmann, N.A., Zhou, H., Rauch, J.N., Hernandez, I., Guzman, E., Kosik, K.S., Han, S., 2017. RNA stores tau reversibly in complex coacervates. PLoS Biol. 15, e2002183. https://doi.org/10.1371/journal.pbio.2002183

Zhang, Y., Pak, C., Han, Y., Ahlenius, H., Zhang, Z., Chanda, S., Marro, S., Patzke, C., Acuna, C., Covy, J., Xu, W., Yang, N., Danko, T., Chen, L., Wernig, M., Südhof, T.C., 2013. Rapid Single-Step Induction of Functional Neurons from Human Pluripotent Stem Cells. Neuron 78, 785–798. https://doi.org/10.1016/j.neuron.2013.05.029

Zheng, H., Koo, E.H., 2011. Biology and pathophysiology of the amyloid precursor protein. Mol. Neurodegener. 6, 27–27. https://doi.org/10.1186/1750-1326-6-27

Zhou, L., McInnes, J., Wierda, K., Holt, M., Herrmann, A.G., Jackson, R.J., Wang, Y.-C., Swerts, J., Beyens, J., Miskiewicz, K., Vilain, S., Dewachter, I., Moechars, D., Strooper, B.D., Spires-Jones, T.L., Wit, J.D., Verstreken, P., 2017. Tau association with synaptic vesicles causes presynaptic dysfunction. Nat. Commun. 8, 15295. https://doi.org/10.1038/ncomms15295

Zhu, B., Liu, Y., Hwang, S., Archuleta, K., Huang, H., Campos, A., Murad, R., Piña-Crespo, J., Xu, H., Huang, T.Y., 2022. Trem2 deletion enhances tau dispersion and pathology through microglia exosomes. Mol. Neurodegener. 17, 58. https://doi.org/10.1186/s13024-022-00562-8